Understanding the role of anaerobic respiration in *Burkholderia thailandensis* and *B. pseudomallei* survival and virulence

Submitted by Clio Alexandra Martin Andreae to the University of Exeter as a thesis for the degree of Doctor of Philosophy in Biological Science

May 2014

I certify that all material in this thesis which is not my own work has been identified and that no material has previously been submitted and approved for the award of a degree by this or any other University.

Signature……

Abstract

Burkholderia pseudomallei is the causative agent of melioidosis, a disease endemic in Northern Australia and Southeast Asia. Melioidosis can present with acute, chronic and latent infections and can relapse several months or years after initial presentation. Currently not much is known about the ways in which *B. pseudomallei* can persist within the host, although it has been speculated that the ability to survive within an anaerobic environment will play some role. *B. pseudomallei* is able to survive anaerobically for extended periods of time but little is known about the molecular basis of anaerobic respiration in this pathogenic species.

Bioinformatic analysis was used to determine the respiratory flexibility of both *B. pseudomallei* and *B. thailandensis,* identifying multiple genes required for aerobic and anaerobic respiration, and molybdopterin biosynthesis. Using *B. thailandensis* as a model organism a transposon mutant library was created in order to identify genes required for anaerobic respiration. From this library one transposon mutant was identified to have disrupted *moeA*, a gene required for the molybdopterin biosynthetic pathway. This *B. thailandensis* transposon mutant (CA01) was unable to respire anaerobically on nitrate, exhibiting a significant reduction in nitrate reductase activity, altered motility and biofilm formation, but did not affect virulence in *Galleria mellonella*.

It was hypothesised that the reduction in nitrate reductase activity was contributing to the phenotypes exhibited by the *B. thailandensis moeA* transposon mutant. To determine whether this was true an in-frame *narG* deletion mutant was created in *B. pseudomallei.* Deletion of *B. pseudomallei narG* (Δ*narG*) resulted in a significant reduction in nitrate reductase activity, anaerobic growth, motility and altered persister cell formation, and but did not affect virulence in *G. mellonella* or intracellular survival within J774A.1 murine macrophages. This study has highlighted the importance of anaerobic respiration in the survival of *B. thailandensis* and *B. pseudomallei.*

Table of Contents

List of Figures

List of Tables

List of publications and poster presentations

Publications

Andreae, C. A., Titball, R. W., Butler, C. S. (2014) Influence of the molybdenum cofactor biosynthesis on anaerobic respiration, biofilm formation and motility in *Burkholderia thailandensis*. *Research in Microbiology.* 165 (1), 41-49

Wagley, S., Hemsley, C., Thomas, R., Moule, M., Vanaporn, M., Andreae, C. A., Robinson, M., Goldman, S., Wren, B. W., Butler, C. S., Titball, R. W., (2014) The twin arginine translocation system is essential for aerobic growth and full virulence of *Burkholderia thailandensis*. *Journal of Bacteriology.* 192 (2), 407-17

Hemsley, C. M., Luo, J. X., Andreae, C. A., Butler, C. S., Soyer, O. S., Titball, R. W. - Bacterial Drug Tolerance under Clinical Conditions is Governed by Anaerobic Adaptation, but not Anaerobic Respiration. *Article accepted for publication in Antimicrobial Agents and Chemotherapy* (July 2014).

NOTE: Both the Andreae *et al.* (2014) and Wagely *et al.* (2014) publications have been attached at the back of this thesis.

Poster presentations

Anaerobic respiration in *Burkholderia thailandensis* - Andreae, C., Titball, R. W., and Butler, C. S., – Poster presentation at the Melioidosis Networking meeting in Amsterdam (February 2012)

A role for nitrate reductase in *Burkholderia pseudomallei* – Andreae, C., Titball, R. W., and Butler, C. S., Poster presentation at the World Melioidosis Congress (WMC) in Bangkok Thailand (September 2013)

Declaration

Unless otherwise stated, the work presented in this thesis is solely the work of Clio Andreae.

The *Burkholderia thailandensis* E264 persister cell transcriptome dataset was performed and presented with permission by Dr. Claudia Hemsley.

The mouse infection model data was performed in collaboration with Dr. Gregory Bancroft group at the London School of Hygiene and & Tropical Medicine by Felipe Cia.

The J744A.1 macrophage experiment was performed with the aid of Dr. Rachael Thomas.

Transmission electron microscopy was performed with the aid of Peter Splatt.

Acknowledgements

I would like to thank both of my supervisors Dr. Clive Butler and Professor Richard Titball for their continued help and support throughout my PhD. I especially would like to thank Dr. Clive Butler for his continued encouragement, support and positive attitude throughout my PhD, especially during the long periods of failed cloning experiments. Without the continued help and support of my supervisors I don't think I would have successfully completed my PhD.

I wish also like to thank Dr. Steve Michell for training me to work in the BSL3 laboratory, and Dr. Rachael Thomas, Dr. Sariqa Wagely, Dr. Claudia Hemsley and Dr. Aaron Butt for all their help and advice throughout my PhD. I would like to thank everyone else I worked with on the 4th floor and the Biocatalysis center for their help and advice throughout my time here at the University of Exeter.

Finally I would like to thank my friends and family for all their support during my PhD, providing me with great times and laughs and never failing to keep me going when times got tough.

Abbreviations

% - Percent

Å - Angstrom

α - Alpha

β – Beta

γ – Gamma

λ – Lambda

n - Nano

µ - Micro

m – Milli

Δ – Delta

σ - Sigma

M – Molar

L- Litre

g – Grams

kDa – Kilo Daltons

Mb – Mega base pairs

kb – Kilo base

bp – Base pairs

^{o}C – Degree Centigrade

ATP – Adenosine triphosphate

AHLs - Acylhomoserine lactones

AMP – Adenosine monophosphate

Amp - Ampicillin

ANAMMOX – Anaerobic ammonium oxidation

ANOVA – Analysis of variants

BLAST – Basic Local Alignment Search Tool

BSL3 – Biological Safety Laboratory Class III

Cam – Chloramphenicol

CDC – Center for Disease Control

cPMP – Cyclic pyranopterin monophosphate

CFU – Colony forming units

CMP – Cytosine monophosphate

CPS – Capsular polysaccharide

DNA – Deoxyribonucleic acid

dNTPs - Deoxynucleotides

DMSO – Dimethyl sulfoxide

DMS – Dimethyl sulfide

EPS – Extracellular polysaccharide

$FADH_2$ – Flavin adenine dinucleotide

FNR – Fumarate/nitrate regulator

[Fe-S] – Iron-sulfur cluster

GMP – Guanosine monophosphate

GTP – Guanosine triphosphate

gDNA – Genomic DNA

H_2O_2 – Hydrogen peroxide

HF – High Fidelity

HK – Histidine kinase

HHS – Human and Health Service

K.E.G.G. – Kyoto Encyclopaedia of Genes and Genomes

Km - Kanamycin

IFN – Interferon

IL - Interleukin

IP - Intraperitoneal

IN - Intranasal

IH - Inhalation

IPTG - Isopropyl β-D-1-thiogalactopyranoside

LB – Luria Bertani

LPS – Lipopolysaccharide

LD_{50} – Lethal dose 50

LF – Left flank

Mb - Megabase

MCD – Molybdenum cytosine dinucleotide

MGD – Molybdenum guanine dinucleotide

MLD – Median lethal dose

MLST – Multi-locus sequence typing

MIC – Minimal inhibitory concentration

MNGCs – Multinucleate giant cells

MPT – Molybdopterin

MoO_4^- – Molybdate

Mo – Molybdenum

Moco – Molybdenum cofactor

min – Minute

mRNA – messenger ribonucleic acid

MV – Methyl-viologen

NCBI – National Center for Biotechnology Information

NADH – Nicotinamide adenine dinucleotide

NAR – Nitrate reductase

NIR – Nitrite reductase

NOR – Nitric oxide reductase

NOS – Nitrous oxide reductase

iNOS – Inducible nitric oxide synthase

NRP – Non-replicating persistence

NaOH – Sodium hydroxide

$NaNO_3^-$ –Sodium nitrate

$NaNO_2^-$ – Sodium nitrite

$NaWO_4^-$ – Sodium tungstate

NaCl – Sodium chloride

NH_4Cl – Ammonium chloride

N_2H_4 – Hydrazine

NO_3^- – Nitrate

NO_2^- – Nitrite

NO – Nitric oxide

N_2O – Nitrous oxide

N_2 – Dinitrogen (gas)

OD – Optical density

PAMPs – Pathogen associated molecular patterns

PBS – Phosphate buffer saline

PBP – Penicillin binding protein

PCR – Polymerase chain reaction

PDB – Protein Data Bank

PMF – Proton motive force

PMNs – Polymorphonuclear leukocytes

(p)ppGpp – Guanosine (penta) or tetraphosphate

Q – Quinone

QH_2 – Quinol

RNA – Ribonucleic acid

RT-PCR – Reverse transcriptase polymerase chain reaction

RNI – Reactive nitrogen intermediates

RF – Right flank

RR – Response regulator

ROS – Reaction oxygen species

SD – Standard deviation

secs – Seconds

TAE – Tris-acetate-EDTA buffer

TBE – Tris-borate-EDTA buffer

Tat – Twin-arginine translocation

Tet – Tetracycline

TLRs – Toll-like receptors

TMAO – Tri-methylamine N-oxide

TNF – Tumour necrosis factor

Tn - Transposon

Tp - Trimethoprim

UV – Ultraviolet

UQ - Ubiquinone

UQH_2 - Ubiquinol

VBNC – Viable but non-culturable

W – Tungsten

w/v – Weight per volume

WT – Wild-type

X-GAL - 5-bromo-4-chloro-3-indolyl-β-D-galactopyranoside

Chapter 1 – Introduction

1.1 Melioidosis

In 1911 Major Alfred Whitmore first identified a 'glanders-like' disease, known as Whitmore's disease, in morphia addicts in Rangoon, Burma (Whitmore A, 1912). This is now referred to as melioidosis, a tropical infection caused by pathogenic bacterium *Burkholderia pseudomallei.* The first and perhaps only fictional literary reference of this disease was provided in 1913 by Sir Arthur Conan Doyle, who incorporated a previously uncharacterised tropical infection (now thought to be melioidosis) as a murder weapon in Sherlock Holmes 'Adventures of a Dying Detective' (Sodeman, 1994). Not much was known about melioidosis until recently and research into pathogenesis of melioidosis is still on going and in much demand. *B. pseudomallei* has recently been characterised as a Tier 1 and category B bioterrorism agent by the Centre for Disease Control (CDC) and Health and Human Services (HHS), along with Anthrax and the Ebola virus (Butler, 2012).

B. pseudomallei survives environmentally and within the human body for extended periods of time, and is likely to experience oxygen limiting environments during the course of its life cycle. This ability to survive in a range of environments is likely to be partly due to the wide variety of respiratory and metabolic proteins encoded within the *B. pseudomallei* genome (Holden *et al.*, 2004). Determination of the respiratory flexibility exhibited by *B. pseudomallei* and identification of the role of anaerobic respiration in survival and virulence, will likely aid in understanding of the mechanisms of persistence exhibited by this pathogenic bacterium.

1.1.1 Global distribution and prevalence

B. pseudomallei is a Gram-negative soil dwelling saprophyte found environmentally within the soil, and often within rice paddy fields. *B. pseudomallei* is the causative agent of melioidosis, an emerging tropical infection endemic in Southeast Asia and Northern Australia. Melioidosis is becoming more a global problem with environmental isolates and cases seen in Asia, Central America,

Africa, the Middle East, and South America and Sri Lanka (Cheng & Currie, 2005; Currie *et al.*, 2008; Inglis & Sagripanti, 2006; Inglis *et al.*, 2008; Taweechaisupapong *et al.*, 2005) (Fig. 1.1). Sporadic cases of melioidosis have been reported in Europe (e.g. in France and Iceland), although many of these are imported cases from patients who have recently travelled abroad, for example to Southeast Asia (Cheng & Currie, 2005; Gudmundsdottir *et al.*, 2014). Increase in reported cases of melioidosis world-wide is likely to be due to better surveillance and identification of the disease.

1.1.2 Transmission and routes of infection

B. pseudomallei is known to survive environmentally, possessing mechanisms to ensure its survival and persistence under a range of different conditions (see *1.2.2 Environmental survival*). Melioidosis is thought be acquired via three different routes; inhalation, ingestion and inoculation (Cheng & Currie, 2005). Cases have been reported of acquisition of melioidosis directly from contaminated water sources, and near drowning experiences (Lee *et al.*, 1985; Limmathurotsakul *et al.*, 2014b; Pruekprasert & Jitsurong, 1991). The main route of infection is thought to be inoculation. Rice-paddy farmers or those from agricultural backgrounds are more at risk of acquiring a *B. pseudomallei* infection through cuts and abrasions in the skin, especially since many do not wear the appropriate protective foot-ware (Cheng & Currie, 2005; Hassan *et al.*, 2010). In Australia, 25 % of melioidosis cases in the Northern Territory have been associated with inoculation prior to presentation (Cheng & Currie, 2005; Currie *et al.*, 2000b).

Various environmental conditions have been described as risk factors for disease acquisition, with 407 patients out of 540 (75 %) in the Darwin study thought to have exposure to environmental *B. pseudomallei* (Currie *et al.*, 2010b). Environmental risk factors include heavy rainfall, agricultural activity, and consumption of contaminated food or untreated water, and soil or dust inhalation (Cheng & Currie, 2005; Currie *et al.*, 2004; Limmathurotsakul *et al.*, 2013b). Heavy rainfall is a significant environmental risk factor for melioidosis, with 81 % of patients in the 20 year Darwin study having presented with an infection during the monsoon season (Currie *et al.*, 2010b). On occasion, melioidosis has been acquired through unconventional manners, such as person to person spread in

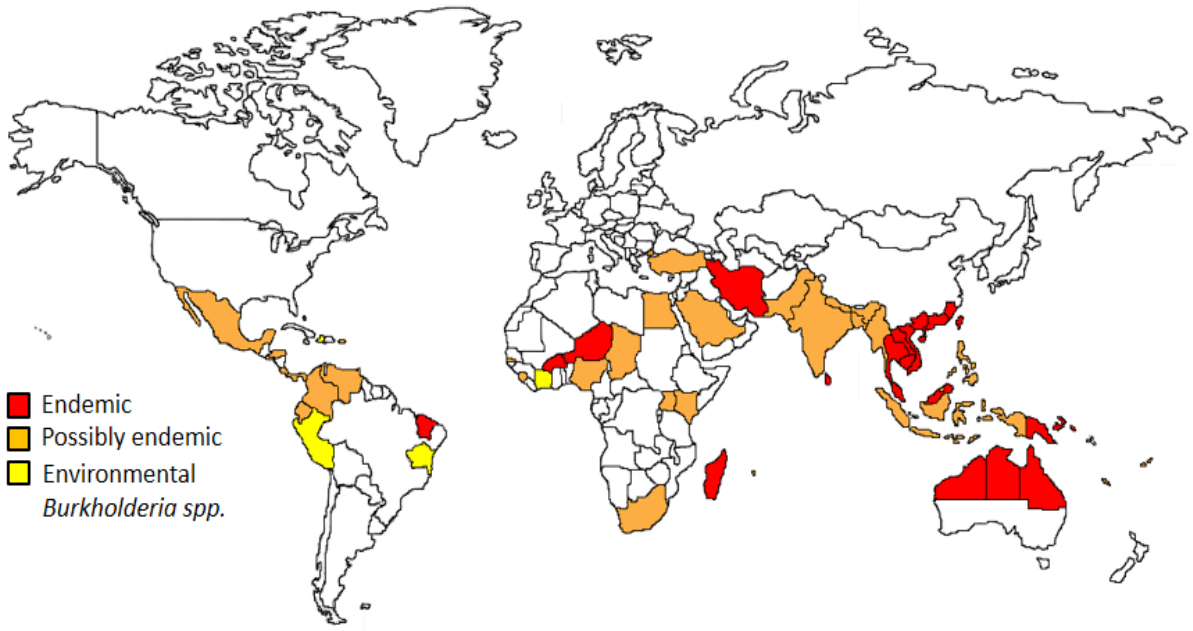

Figure 1.1 – Global distribution of melioidosis. The map shows the global distribution of *B. pseudomallei,* in reference to environmental sampling. Figure has been adapted from http://www.melioidosis.info/map.aspx using information from previously published literature (Limmathurotsakul *et al.*, 2013a). Regions shown in red indicate those endemic areas, where melioidosis cases have been reported, and environmental samples from soil or water have been isolated and confirmed using *B. pseudomallei* specific PCR. Regions shown in orange indicate those areas were melioidosis has been reported in the country but no environmental samples have been acquired. Regions in yellow are areas where *B. pseudomallei* has been isolated environmentally from soil or water, but the identification process was not sufficient to differentiate between different *Burkholderia* spp. (e.g. between *B. thailandensis*). The map does not include those cases reported in Europe.

patients with cystic fibrosis (Holland *et al.*, 2002), mother-to-child transmission through breast milk (Ralph *et al.*, 2004) and neonatal cases (Cheng & Currie, 2005).

1.1.3 Clinical presentations and associated risk factors

In Thailand melioidosis is one of the top three killers due to infectious disease, along with AIDS (acquired immunodeficiency syndrome) and tuberculosis (Limmathurotsakul *et al.*, 2010). The disease is endemic in Northeast Thailand and is often associated with a high mortality rate, reaching up to 40 % in some cases (White, 2003). Melioidosis is also endemic in Northern Australia, but the clinical outcome is much better for patients in Australia compared to those in Thailand, with the mortality rate being around 20 % (Currie *et al.*, 2000b; Currie *et al.*, 2010b). *B. pseudomallei* is a common cause of community-acquired bacteraemia, in both Ubon Ratchathani in Northeast Thailand (Chaowagul *et al.*, 1989) and Darwin in Northern Australia (Douglas *et al.*, 2004).

The annual incidence of melioidosis in Northern Australia is 19.6 cases per 100,000 of the population, with higher incidence seen per year in the diabetic population (260 cases per 100,000 per year) (Currie *et al.*, 2004). The incidence of melioidosis in Northeast Thailand has increased over the last few years from 8 culture confirmed cases per 100,000 in 2000, to 21.3 cases per 100,000 people per year in 2006, with an average incidence of 12.7 cases per 100,000 people (Limmathurotsakul *et al.*, 2010).

There are several risk factors and underlying conditions such as diabetes mellitus, excess alcoholism, heart conditions, steroid use, immunosuppression, cystic fibrosis, age (over 45 years), or renal failure which predispose a patient to an infection with *B. pseudomallei* (Cheng & Currie, 2005; Currie *et al.*, 2000b; Currie *et al.*, 2004; Currie *et al.*, 2010b). Patients with diabetes mellitus are at a greater risk of contracting melioidosis with 57 % of all primary diagnosed melioidosis cases, resulting in mortality, testing positive for diabetes (Hassan *et al.*, 2010; Suputtamongkol *et al.*, 1999).

Melioidosis can present with an array of clinical symptoms (Fig. 1.2), with *B. pseudomallei* causing either an acute, chronic or latent infection. *B. pseudomallei* unlike other pathogenic bacteria has the ability to infect almost every organ in the

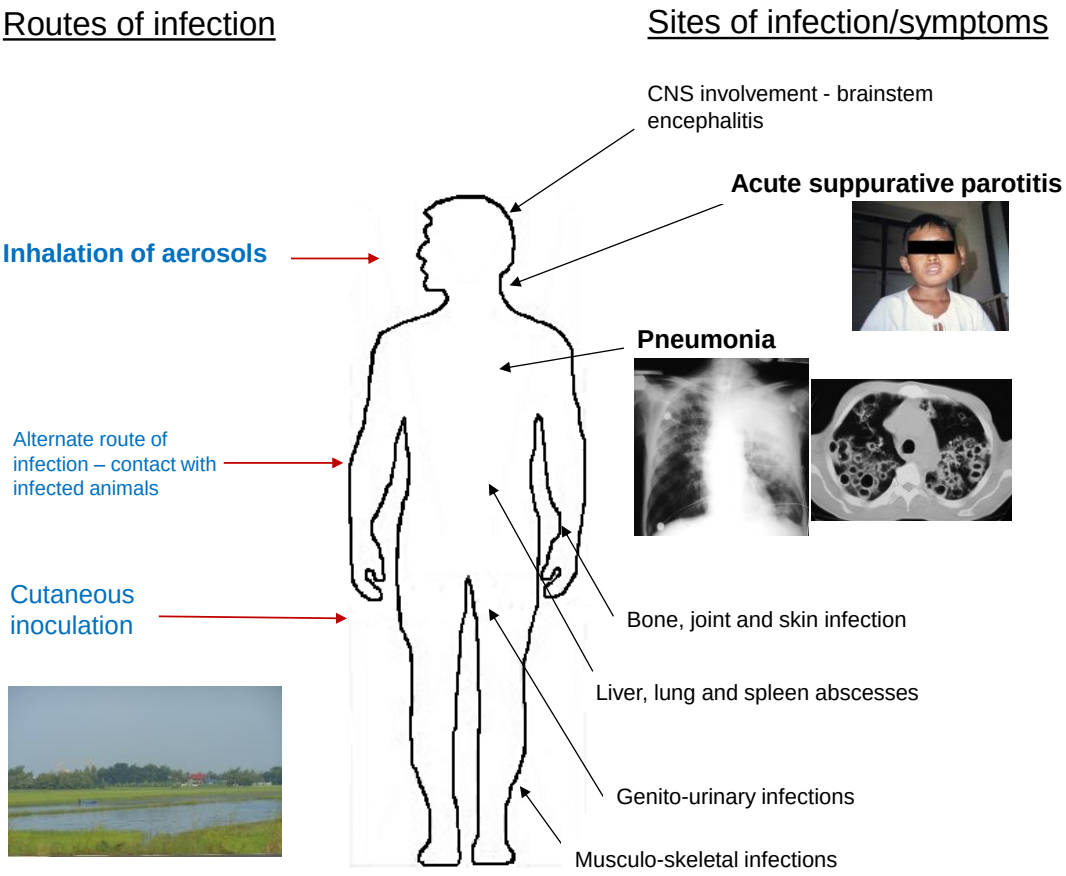

Figure 1.2 – Clinical presentations and sites of infection of melioidosis. Figure has been adapted from (Wiersinga *et al.*, 2006) using images from figure 2 in (Currie, 2003) and (White, 2003). Those highlighted in bold indicate the most common route of infection of disease presentation. Image of the rice paddy field (bottom left) is my own.

body. As a result clinical symptoms can range from pneumonia, sepsis, genitourinary tract infections, skin infection, acute suppurative parotitis, joint infections, brainstem encephalitis, central nervous system involvement (normally encephalomyelitis) and osteomyelitis (Currie *et al.*, 2000a; Currie *et al.*, 2004; Currie *et al.*, 2010b; White, 2003) (Fig. 1.2). Melioidosis most commonly presents with pneumonia, seen in 51 % of patients (Currie *et al.*, 2010b), with 55 % cases being bacteremic. Eighty five percent of cases during the 20 year Darwin study presented with acute disease from a recent infection, with 11 % presenting with chronic with symptoms lasting over 2 months (Currie *et al.*, 2010b). Septic shock, normally occurring within 24 hours of admission into hospital, was a major contributor to mortality with over 50 % of patients dying due to acute fulminant melioidosis (Currie *et al.*, 2010b). *B. pseudomallei* infections can cause the formation of abscess, for example in the lung, liver, spleen, kidney and prostate (Currie *et al.*, 2010b), which may have a microaerobic/anaerobic environment. The significance of this will be discussed later.

1.1.4 Recurrent melioidosis

One of the problems facing the treatment of melioidosis is the fact that the disease can relapse, often several months or years after treatment of the initial infection. Relapse is defined as a new presentation of acute culture confirmed melioidosis, with a repeat infection occurring after resolution of an initial infection by at least two weeks treatment with intravenous antibiotics (Currie *et al.*, 2000a). Relapse cases have been documented to have occurred between 10 and 62 years after initial exposure (Chen *et al.*, 2005; Frangoulidis *et al.*, 2008; Ngauy *et al.*, 2005).

Recurrent melioidosis is due to either re-infection or re-activation (relapse) of a latent infection. The majority of recurrent melioidosis cases are due to relapse of infection with the same strain, which is often genetically identical. This indicates that *B. pseudomallei* is likely to remain stable, residing within the body for months to years on end (Currie *et al.*, 2000a; Maharjan *et al.*, 2005; Vadivelu *et al.*, 1998). The rate of relapse can vary but tends to occur in around 4 to 13 % of melioidosis patients, and often occurs in those patients who have poorly adhered to their antibiotic regime (Chaowagul *et al.*, 1993; Currie *et al.*, 2000a; Limmathurotsakul *et al.*, 2006). Although not one risk factor has been identified for reinfection

(Limmathurotsakul *et al.*, 2006), individuals who are immunocompromised, have dietary deficiencies, or those who have poorly adhered to the appropriate antibiotic regime are more prone to relapse (Leelarasamee, 1998; Limmathurotsakul *et al.*, 2006; Limmathurotsakul *et al.*, 2008; Vadivelu *et al.*, 1998). Patients treated with a longer oral antibiotic regime, for 12 to 14 weeks, and those treated with initial parenteral ceftazidime treatment had a significant, reduced risk of relapse, a 1.6 and 2 fold reduction (or 90 % decreased risk), compared to those treated for 8 weeks (Chaowagul *et al.*, 1993; Limmathurotsakul *et al.*, 2006). Relapse cases occurs 4.7 times more frequently in patients with septicemic forms of meliodiosis to those who had localised disease (Chaowagul *et al.*, 1993). Re-infection, due to a repeat exposure to *B. pseudomallei* rather than relapse, has been associated with renal insufficiency or exposure to heavy rainfall (Limmathurotsakul *et al.*, 2008).

There are various explanations as to why *B. pseudomallei* can cause a relapse of infection. These include the ability of *B. pseudomallei* to produce glycocalyx, form micro-colonies in damaged tissues, presence of exopolysaccharides and finally its ability to survival within phagocytes (Leelarasamee, 1998; Vadivelu *et al.*, 1998).

1.1.5 Treatment and antibiotic resistance

Treatment of melioidosis is intensive and usually requires a 10 to 14 day intravenous administration of ceftazidime, followed by a prolonged antibiotic regime using a combination of antibiotics (Currie *et al.*, 2000a; Wiersinga *et al.*, 2012). Ceftazidime is frontline treatment for melioidosis, and has been shown to cut mortality rate of septicaemic melioidosis by around 35 to 45 % (Leelarasamee, 1998). Following intravenous treatment with ceftazidime melioidosis patients are often treated with a 12 to 20 week course of oral antibiotics either co-amoxiclav or a combination of chloramphenicol, doxycycline, and co-trimoxazole (Rajchanuvong *et al.*, 1995). Treatment of melioidosis with a single antibiotic, such as co-amoxiclav or doxycycline, in comparison to combination therapy, is known to result in a higher rate of relapse (Chaowagul *et al.*, 1999; Rajchanuvong *et al.*, 1995). Recently, prophylactic treatment of melioidosis with co-trimoxazole (trimethoprim/sulfamethoxazole) was shown to be an effective treatment in a murine model of inhalation melioidosis (Barnes *et al.*, 2013).

Antibiotic resistance is rapidly increasing in the clinical setting with *B. pseudomallei* being intrinsically resistant to many antibiotics such as gentamicin, rifampin, beta-lactams, penicillins, macrolides and cephalosporins (Wiersinga *et al.*, 2012). Recently *B. pseudomallei* has been shown to have developed resistance to ceftazidime due to mutations within *penA* (Rholl *et al.*, 2011; Tribuddharat *et al.*, 2003), a β-lactamase enzyme. This poses problems for the treatment of acute melioidosis infections, especially if the patient becomes infected with a resistant strain (Sarovich *et al.*, 2012). Loss of the penicillin binding protein (PBP-3 – BPSS1219) has also been seen in *B. pseudomallei* resistant variants isolated from a patient receiving prolonged ceftazidime treatment (Chantratita *et al.*, 2011).

1.1.6 Vaccine development

Currently there is no vaccine available for the prevention of melioidosis, and those currently under examination do not provide sterilising immunity. Current vaccine candidates include the capsular polysaccharide or LPS, heat-killed *B. pseudomallei* cells, and *B. thailandensis* E264 lipopolysaccharide (LPS) for use as a sub-unit vaccine (Ngugi *et al.*, 2010; Sarkar-Tyson *et al.*, 2007; Sarkar-Tyson *et al.*, 2009). Recently the *B. pseudomallei* outer membrane vesicle has been shown to provide effective protection against a septicaemic infection (Nieves *et al.*, 2014). All of these vaccine candidates have been shown to provide some form of protection, and induce an immune response against a wild-type *B. pseudomallei* infection when using a murine infection model.

1.2 *B. pseudomallei* and *B. thailandensis*

1.2.1 Genome and strain differences

B. pseudomallei is closely related to the generally avirulent *B. thailandensis* and the causative agent of glanders disease, *B.* mallei. All three of these *Burkholderia* species display a high degree of genetic similarity and close evolutionary lineage based on multi-locus sequence typing (MLST) analysis (Godoy *et al.*, 2003). *B. thailandensis* is often used as a surrogate for *B. pseudomallei* work, as it displays very similar biochemical, genetic properties, encoding many virulence factors found in *B. pseudomallei*, and does not require use of a containment level III laboratory. Unlike *B. pseudomallei, B. thailandensis*

possesses the ability to assimilate arabinose and displays different colony morphologies to those exhibited in *B. pseudomallei* (Brett *et al.*, 1998; Smith *et al.*, 1997). There are many different strains of *B. pseudomallei* and *B. thailandensis*, all of which exhibit slightly different virulence characteristics which vary depending on the route of infection and number of colony forming units (CFU) used in the study (Table 1.1 and Table 1.2). Differences in virulence seen for some *B. thailandensis* strains is thought to be due to the presence or absence of a capsular polysaccharide (CPS).

B. thailandensis is generally characterised as an avirulent species, not causing disease in humans. However there have been two documented cases of melioidosis caused by *B. thailandensis* strains (CDC2721121 and CDC3015869) in the United States, one of which was later shown to be due to the acquisition of a *B. pseudomallei*-like CPS (Glass *et al.*, 2006; Sim *et al.*, 2010). The acquisition of CPS-like genes has resulted in the strains becoming resistant to complement C3b deposition allowing the bacteria to avoid detection by the immune system. A CPS knockout strain of E555 exhibited the same phenotype seen with E264 which is not capable of blocking complement deposition (Sim *et al.*, 2010).

B. pseudomallei (K96243) has two chromosomes both encoding different genes involved in general cellular processes and those for virulence and pathogenicity. Chromosome 1 (4.07 Mb), the larger of the two chromosomes, encodes a higher proportion of genes (3,460) required for core functions, whereas chromosome 2 (3.17 Mb) encodes those genes involved in central metabolism, transcription and replication and amino acid biosynthesis (Holden *et al.*, 2004). Along with these genes the genome of *B. pseudomallei* also contains those that promote survival within the environment and the host, and those genes required to modulate pathogenicity (Holden *et al.*, 2004).

B. mallei is the causative agent of glanders disease in equines, and is related to *B. pseudomallei* but possess a smaller genome size (5.8 Mb) and is host restricted (Duan *et al.*, 2012b; Holden *et al.*, 2004). Unlike *B. pseudomallei* and *B. thailandensis B. mallei* has a host specific lifestyle, and struggles to persist in the environment. There is evidence to suggest that *B. mallei* has evolved from a *B. pseudomallei* strain, and was shown by MLST analysis to be a clone of *B. pseudomallei* (Godoy *et al.*, 2003) that has undergone a degree of genome down-

Table 1.1 - *B. pseudomallei* strains and characteristics

Strain	Description	Infection model - route of infection	Virulence - LD_{50} (CFU)	Reference
K96243[a]				
	Thailand isolate (1996) Isolated from a diabetic patient with a lethal infection	BALB/c – Intranasal (IN) BALB/c – Intraperitoneal (IP) BALB/c – Inhalation (IH) C57BL/6 – IN Marmoset Mouse – IN, IP, aerosol and intratracheal *G. mellonella*	226 262[d] 10[d] 1.5×10^4 10 5 to 3×10^7 100	(Nelson *et al.*, 2011; Tan *et al.*, 2008; Titball *et al.*, 2008; Van Zandt *et al.*, 2012; Wand *et al.*, 2010)
1710a	Thailand isolate (1996) Isolated from male rice paddy farmer	ND	ND	(Van Zandt *et al.*, 2012)
MSH305	Australian isolate Isolate from the brain of a fatal melioidosis encephalitis	Mouse	Highly virulent	(Van Zandt *et al.*, 2012)

1026b				
	Thailand isolate – (1993) Taken from patient with diabetes mellitus and disseminated disease	BALB/c – aerosol	10 ± 8	(Goodyear *et al.*, 2009; Jeddeloh *et al.*, 2003; Van Zandt *et al.*, 2012)
		C57BL/6 – aerosol	27 ± 20	
		BALB/c – IN (nose only)	2,772	
		BALB/c – IN (whole body)	1×10^3	
		C57BL/6	1×10^3	

[a] BALB/c infected mice are significantly more susceptible to infection with K96243

[b] 1026b LD_{50} varies depending on murine model and route of infection

[c] After 24 hours infection (100 % mortality)

[d] Median lethal dose - MLD_{50}

ND – not determined

BALB/c and C57BL/6 are murine models of infection

Infection route describe as either intraperitoneal (IP), intranasal (IN) or inhalation (IH)

Table 1.2 – *B. thailandensis* strains and characteristics

Strain	Description	Infection model - route of infection	Virulence - LD_{50} (CFU)	Reference
E264				
	Environmental isolate Avirulent clinically	Syrian hamster – IP C57BL/6 – IN BALB/c – IN *Galleria mellonella* *Caenorhabditis elegans*	1 x10^5 1 x 10^6 1 x 10^7 – only 16.7 % mortality after 13 days post infection 100 CFU – 50 % mortality[b] 100 % mortality after 3 days infection	(Brett *et al.*, 1998; Deshazer, 2007; Wand *et al.*, 2010)
E555				
	Cambodian isolate Contains *B. pseudomallei*-like CPS gene cluster	BALB/c - IN *C. elegans*	1 x 10^7 – 66.7% mortality after 13 days infection 100 % mortality after 3 days infection[c]	(Sim *et al.*, 2010)
Phuket 4W-1				
	Water isolate from water in Phuket Thailand (1965)	Syrian hamster - IP *G. mellonella*	1 x 10^5 100 CFU – 80 % mortality[b]	(Deshazer, 2007; Wand *et al.*, 2010)
CDC3015869				
	US isolate	Syrian hamster – IP	1x 10^5	

	Expresses CPS-like cluster Clinical blood isolate from 2 year-old-male with pneumonia and septicaemia	*G. mellonella*	100 % mortality[b]	(Deshazer, 2007; Glass *et al.*, 2006; Sim *et al.*, 2010; Wand *et al.*, 2010)
CDC2721121				
	US isolate Clinical isolate from pleural wound from a 76-year-old man	Syrian hamster – IP	Avirulent after 14 day challenge with 1 x 10^5 to 1 x 10^{7a}	(Deshazer, 2007; Wand *et al.*, 2010)
		G. mellonella	100	

[a] Compared to E264, CDC3015869 or Phuket 4W-1 (Deshazer, 2007)

[b] After 24 hours infection with 100 CFU. Challenge with 10,000 resulted in 100% mortality after 24 hours (Wand *et al.*, 2010)

[C] E555 exhibited a 2 day slower killing rate when compared to E264 (Sim *et al.*, 2010)

Infection route describe as either intraperitoneal (IP), intranasal (IN) or inhalation (IH)

sizing (Nierman *et al.*, 2004), resulting in the lack of genes allowing it to survive outside of the host.

1.2.2 Environmental survival

B. pseudomallei is a hardy bacterium, surviving and persisting under a wealth of different stresses encountered environmentally or within the host. *B. pseudomallei* has been previously shown to be able to cope with changes in pH, exposure to salt (NaCl), chlorine, changes in osmolarity, and can survive for up to three years within triple distilled water, and intracellularly within amoeba and professional and non-professional phagocytes (Dance, 2000; Inglis & Sagripanti, 2006; Moore *et al.*, 2008; Puthucheary & Nathan, 2006; White, 2003).

B. pseudomallei survival within nutrient deprived conditions and in water, requires an intact stable LPS core (Moore *et al.*, 2008), thought to aid in the natural dispersal and persistence within the environment (Robertson *et al.*, 2010). The number of culturable bacteria falls quite rapidly when exposed to stresses such as NaCl at concentrations above 2.5 % and pH 4.5 (Inglis & Sagripanti, 2006), with the bacteria entering a viable but non-culturable state (VBNC). *B. pseudomallei* is highly adaptable to growth in acidic environments both within the host and the unusually acidic soils of endemic regions of Northeast Thailand (Dejsirilert *et al.*, 1991; Inglis & Sagripanti, 2006). Survival of *B. pseudomallei* under various stresses such as high salt and acidic pH is known to cause a change in its morphology from a bacilli form to coccoid and spiral cells (Robertson *et al.*, 2010).

Use of fertilisers, containing nitrate may aid in the proliferation of *B. pseudomallei* in agricultural land, since it has been shown to be able to reduce nitrate (Dance, 2000). The ability for *B. pseudomallei* to reduce nitrate and survive under anaerobic conditions is likely to be a factor aiding in its persistence within the host and the environment.

1.2.3 Virulence factors

B. pseudomallei encodes a wide array of different virulence factors aiding in colonisation and pathogenesis. Many mutagenesis studies have been under taken to determine the role of various virulence factors in the pathogenesis of melioidosis. These include the type III secretion system, capsular polysaccharide, lipopolysaccharide, flagella, and many excreted extracellular proteins such as haemolysins (proteases, lecitinases and lipases) (Ashdown & Koehler, 1990), toxins, such as rhamnolipids (Haussler *et al.*, 2003), and possibly secondary metabolites such as syringolin A and glidobactin A (Groll *et al.*, 2008) (see Table 1.3 for details).

1.2.4 Intracellular survival

Macrophages are an important part of the immune response to invading bacteria. During phagocytosis, bacteria become enclosed within the phagosome which matures to form a phagolysosome, following phagosome-lysosome fusion. The phagolysosome possesses a highly acidic environment containing various proteins and enzymes to aid in the destruction of intracellular bacteria (Flannagan *et al.*, 2009). *B. pseudomallei* is an intracellular pathogen and can survive within a range of both professional and non-professional phagocytes, such as macrophages, epithelial cells, polymorphonuclear and mononuclear leukocytes, and alveolar macrophages (Ahmed *et al.*, 1999; Jones *et al.*, 1996; Pruksachartvuthi *et al.*, 1990). Entry into phagocytic cells requires the presence of a functional *bsa*-T3SS, which is required for the formation of membrane protrusions, actin tails and escape from endocytic vesicles (Wiersinga *et al.*, 2008). Following internalisation and subsequent release from endocytic vesicles, *B. pseudomallei* replicates intracellularly, avoiding various immune responses such as the induction of inducible nitric oxide synthase (iNOS), and forms actin based membrane protrusions required for cell-to-cell fusion/spreading and formation of multinucleate giant cells (MNGCs) (Kespichayawattana *et al.*, 2000; Wiersinga *et al.*, 2006) (Fig. 1.3). The formation of MNGCs is unique to *B. pseudomallei, B. mallei* and *B. thailandensis* infections. *B. pseudomallei* can cause apoptotic cell death of infected phagocytic and non-phagocytic cells lines, likely due to the induction of the caspase-1-dependent pathway (Kespichayawattana *et al.*, 2000).

Table 1.3 – *B. pseudomallei* virulence factors and mutant characteristics

Virulence factors	Role	Mutant characteristics	Reference
Capsular polysaccharide	Virulence Required for protection against host serum cidal activity and opsonophagocytosis Antigen recognised by Th1 immune system	*wcb* mutant attenuated for virulence in respiratory murine model and BALB/c mice Increased susceptibility to antimicrobials Susceptible to killing by polymorphonuclear neutrophils (PMNs)	(Reckseidler *et al.*, 2001; Warawa *et al.*, 2009; Wikraiphat *et al.*, 2009)
Lipopolysaccharide (O-antigenic polysaccharide moiety)	Serum resistance Virulence Modulation of host cell response and control of intracellular fate inside macrophages	Significant reduction in virulence in BALB/c mice Increased susceptibility to antimicrobials Susceptible to killing by PMNs and macrophages	(Arjcharoen *et al.*, 2007; DeShazer *et al.*, 1998; Wikraiphat *et al.*, 2009)
Flagella	Motility Adhesion	Aflagellate and non-motile Avirulent/reduced virulence during intranasal and intraperitoneal infection of BALB/c mice Retains virulence when using *C. elegans* or Syrian hamster models of infection Reduced bacterial load in lungs and spleens Still able to invade and replicate intracellularly	(Chua *et al.*, 2003; Inglis *et al.*, 2003; Tuanyok *et al.*, 2006; Wikraiphat *et al.*, 2009)

		fliC strongly down-regulated and *fliD* (flagella hook-associated protein) in acute model of infection (Syrian hamster model) *fliD* insertional mutant retains virulence in hamster infection model.	
Type III secretion system (T3SS-3)	Secretion of effector proteins e.g. BopA and BopE Required for full virulence and interaction with host cells	Significant attenuation of virulence in Syrian hamster model Reduced replication in J774A.2 macrophages Unable to escape from endocytic vacuoles due to disruption to the formation of membrane protrusions and actin tails Impaired intercellular spread and pathogenesis *bsaZ* mutant remains contained in vesicles during phagocytosis	(Stevens *et al.*, 2002; Warawa & Woods, 2005)
Type II secretion system	Secretion of exoproducts such as phospholipase C, protease, and lipase	Minor reduction in virulence in Syrian hamster	(DeShazer *et al.*, 1999)
Type VI secretion system	Virulence Injection of effector proteins into host cell cytosol Intracellular survival	Δ*hcp1* $LD_{50} > 10^3$ in Syrian hamster model of infection Δ*hcp1* mutant exhibits a growth defect, is weakly cytotoxic to RAW 264.7 macrophages and is unable to form multinucleated giant cells *tss-5* mutant exhibits a reduced ability to form plaques	(Burtnick *et al.*, 2011; Galyov *et al.*, 2010)

		Attenuated for virulence	
Quorum sensing	Cell density dependent signalling Synthesis of acylhomoserine lactones (AHLs) *B. pseudomallei* encodes three LuxI homologs and five LuxR	Quorum sensing mutants display increased time to death and reduced organ colonisation (seen in spleen but not liver) in an aerosolized BALB/c infection Increase in LD_{50} in intraperitoneal challenge of Syrian Hamster Reduced biofilm formation Reduced virulence in murine model for intraperitoneal, intranasal and subcutaneous challenge Regulation of MprA metalloprotease on entry to stationary phase	(Gamage *et al.*, 2011; Ulrich *et al.*, 2004; Valade *et al.*, 2004; Wiersinga *et al.*, 2006)
Type IV pili	Adherence	*pilA* deletion mutant displays reduced adherence to human epithelial cells and reduced virulence in *C. elegans* and murine models	(Essex-Lopresti *et al.*, 2005)
Isocitrate lyase	Persistence factor	Hypervirulent in murine model of infection	(van Schaik *et al.*, 2009)
Siderophore	Iron acquisition Known siderophores include malleobactin, pyochellin, cepaciachelin and cepabactin Acquire bound iron from lactoferrin and transferrin	Siderophore mutants remain fully lethal in BALB/c mice following acute intranasal challenge	(Kvitko *et al.*, 2012; Yang *et al.*, 1993)

		Lower organ burdens seen for lungs and spleens, but not liver, when mice were infected with quadruple iron acquisition mutant	
Secreted proteins (extracellular enzymes)	e.g. haemolysin, protease, lipase Putative virulence factors		(Ashdown & Koehler, 1990)
Phospholipase C	*B. pseudomallei* encodes three distinct phospholipase C enzymes (*plc-1, plc-2,* and *plc-3*) Role in cleavage of phospholipid phosphatidylinositol (PC) to produce phophorylcholine and diacylglycerol	*plc1* and *plc2* exhibit reduced plaque formation Reduction in plaque formation mainly due to loss of Plc-2 *plc2* mutant is significantly less cytotoxic *plc-3* is significantly upregulated in infected liver *plc-3* mutant exhibits a higher LD_{50} (4.5×10^3) when compared to the parental strain (< 10)	(Korbsrisate *et al.*, 2007; Tuanyok *et al.*, 2006)
Lactonase protein A (LfpA)	LfpA is similar to the eukaryotic protein regucalcin Regulates host cell response *in vitro* and virulence *in vivo* LfpA is upregulated when in contact with RAW26.47 macrophage-like cells *lfpA* is required for the expression of host osteoclast markers Required for optimal virulence	Δ*lfpA* displayed no difference in intracellular replication in RAW-264.7 cells Δ*lfpA* displays increased LD_{50} in Syrian hamster model and BALB/c mice inhalation model of acute melioidosis Δ*lfpA* infection resulted in reduced expression of most chemokines and all osteoclast markers	(Boddey *et al.*, 2007)

MviN	Member of the mouse virulence factor family Gene expression influence by free-iron availability	Increased LD_{50} in hamster model of infection and loss of ability to invade epithelial cells Slower growth rate	(Ling *et al.*, 2006)
RelA and SpoT	Involved in synthesis of (p)ppGpp required for signalling Role in global stress response and regulation of virulence genes	*relA* and *spoT* double mutant attenuated in *G. mellonella* and C57BL/6 black mice following intranasal challenge with either 2,500 CFU (acute infection) or 100 (chronic infection) CFU Double mutant displays a defect in stationary phase survival and intracellular replication within murine macrophages J774A.1	(Muller *et al.*, 2012)

Phagosome-lysosome fusion within *B. pseudomallei*-infected melioidosis macrophages is slow and inefficient, and leads to an increased number of surviving bacteria within monocytes (Puthucheary & Nathan, 2006). Slow formation of phagolysosomes ensures intracellular survival of *B. pseudomallei* and allows it to persist and become latent. This may enable a relapse of melioidosis to occur once the patient becomes immunocompromised.

Twenty two percent of *B. pseudomallei* genome undergoes a high amount of transcriptional adaptation to ensure its survival within macrophages. This includes the down-regulation of genes required for motility, aerobic respiration, amino acid and ion transport, replication and gene regulation. By contrast genes required for anaerobic metabolism show a degree of upregulation, highlighting the importance of anaerobic metabolism during intracellular survival (Chieng *et al.*, 2012). The significance of this will be discussed later.

1.2.5 Immune response

Internalisation of pathogenic bacteria by macrophage cells normally results in the induction of an immune response helping to clear the infection. Recognition of *B. pseudomallei* by the innate immune system is associated with recognition of 'pathogen associated molecular patterns' (PAMPs), by various toll-like receptors (TLRs) (Wiersinga *et al.*, 2012). TLR2 is known to recognise *B. pseudomallei* LPS allowing the host immune system to respond and clear the infection, reducing bacterial load on the infected organs (Wiersinga *et al.*, 2007). Both the innate and adaptive immune response are important for response to *B. pseudomallei,* with an infection often resulting in the induction of interferon gamma (IFN-γ), cytokines, interleukins (IL-6, IL-15 and IL-10) and the activation of the complement system (Wiersinga *et al.*, 2012). MyD88 has been shown to provide a protective response to *B. pseudomallei* infection, ensuring neutrophil recruitment to the site of infection (Wiersinga *et al.*, 2008).

Complement opsonisation has been shown to be required for efficient uptake and killing of *B. pseudomallei* by neutrophils. *In vitro* deposition of complement C3 deposits on *B. pseudomallei* was critical for efficient clearing of infection by neutrophils, with the killing of internalised *B. pseudomallei* largely due to the generation of reactive oxygen species (ROS) (Woodman *et al.*, 2012).

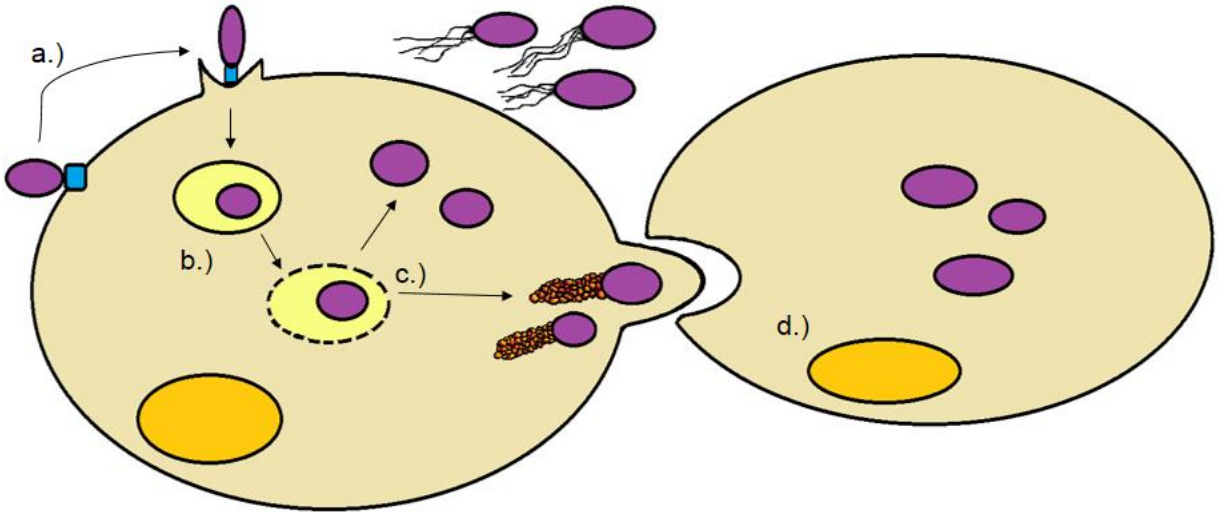

Figure 1.3 - Intracellular lifestyle of *B. pseudomallei*. a.) Invasion of host cells via a *bsa* type 3 secretion system (in blue); b.) Engulfment and subsequent lysis of endosomal membrane, along with the evasion of host defence mechanisms, such as iNOS, allows *B. pseudomallei* to survive and replicate intracellularly; c.) Formation of actin based protrusions, using BimA, allows cell to cell movement aiding in intracellular survival, spread and pathogenesis; d.) Formation of Giant Multinucleate cells (MNGC) (shown in orange), is regulated by RpoS and occurs via cell fusion which is unique to *B. pseudomallei*. Acute disseminated infection presents when the bacterium spreads to secondary sites such as organs and the blood. During chronic and latent infection *B. pseudomallei* persists within host cells. Figure is adapted from (Wiersinga *et al.*, 2006).

For pathogens to survive within macrophages they need to be able to cope with the production of ROS and reactive nitrogen species (RNS) produced directly or indirectly by NADPH oxidase or iNOS (Flannagan *et al.*, 2009). *B. pseudomallei* can evade the immune response by interfering with iNOS production, (Utaisincharoen *et al.*, 2001; Utaisincharoen *et al.*, 2003). *B. pseudomallei* fails to activate interferon regulatory factor-1, iNOS production, or stimulate IFN-β production in mouse macrophages. Macrophages activated, and to a lesser extent dendritic cells, with both IFN-β and IFN-γ enhances the production of iNOS and TNF-α release aiding in the destruction of intracellular *B. pseudomallei* (Charoensap *et al.*, 2009; Utaisincharoen *et al.*, 2003; Utaisincharoen *et al.*, 2006; Wiersinga *et al.*, 2012). The inability to stimulate IFN-β production is thought to be due to *B. pseudomallei* unique LPS, which in other species stimulates its production via TLR4 signalling.

1.3 Respiratory pathways in prokaryotes

Prokaryotes, unlike eukaryotic organisms, exhibit an extraordinary ability to utilise a diverse range of electron acceptors allowing for the colonisation of a range of different environments. This respiratory flexibility exhibited by bacteria allows for the use of a range of electron acceptors such as oxygen, nitrogen oxides (Gonzalez *et al.*, 2006), selenium oxyanions (Butler *et al.*, 2012), dimethyl-sulfoxide (DMSO) (Bilous & Weiner, 1985b), tetrathionate (Hensel *et al.*, 1999), iron (Richardson, 2000) and other sulfur oxyanions (Roychoudhury, 2004).

1.3.1 Aerobic respiration

The conservation of energy in the form of adenosine triphosphate (ATP) is fundamental to all life. Oxidative phosphorylation involves the transfer of electrons from energy donors such as NADH and $FADH_2$ to oxygen, generating a proton motive force (PMF), to allow for the release of ATP from ATP synthase. The mitochondrial and prokaryotic electron transport systems display some similarities. Under aerobic conditions NADH transfers its electrons to oxygen resulting in the generation of a PMF across the membrane. This is achieved using various different dehydrogenases, oxidoreductase enzymes and freely diffusible quinones, required for electron transfer. The respiratory chain, in the mitochondrion of eukaryotes and *Paracoccus denitrificans,* is composed of NADH dehydrogenase a proton pump which transfers electrons via the quinone pool to cytochrome bc_1 complex (ubiquinone: cytochrome *c* oxidoreductase), prior to electron transfer to cytochrome *c* oxidase using various *c*-type cytochromes (Fig. 1.4) (Richardson, 2000; Simon *et al.*, 2008). Succinate dehydrogenase (complex II) transfers electrons from succinate to the quinone pool, linking to the bc_1 complex. *E. coli,* unlike *P. denitrificans,* has a truncated electron transport chain and does not possess a cytochrome bc_1 complex, only transferring electrons through the Q-pool, to various terminal oxidoreductases.

1.3.2 The nitrogen cycle

Nitrogen is essential for all life and is a vital component of biomolecules including nucleic acids and proteins. The nitrogen cycle involves both reductive and oxidative reactions, requiring multiple different enzymes to allow for the use of nitrogen oxyanions in conservation of energy and the incorporation into biomolecules (Fig. 1.5).

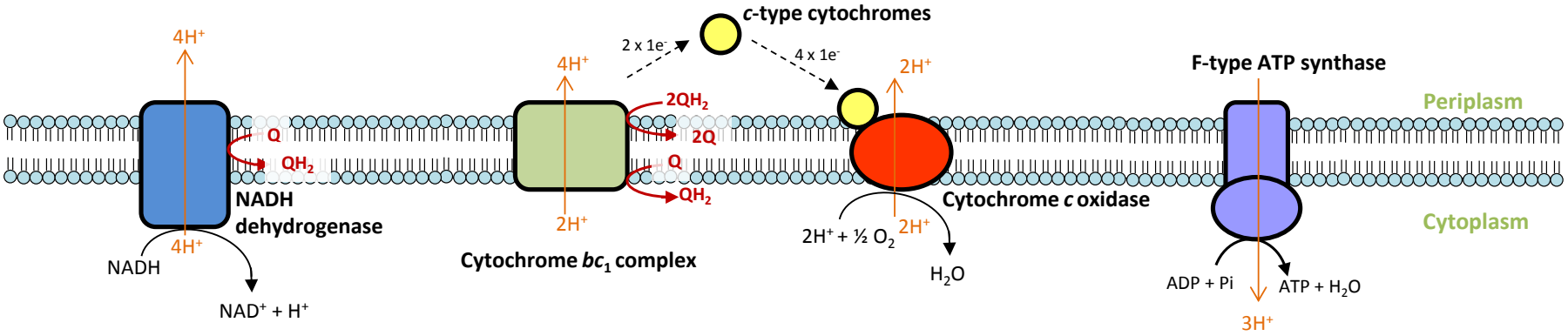

Figure 1.4 – Organisation of the aerobic respiratory pathway required for the generation of a proton motive force. Diagram is a representation of the aerobic respiratory pathway seen in the mitochondria and in some prokaryotic species such as *P. denitrificans.* Succinate dehydrogenase (complex II) is not included. The electron transport pathway shown above involves the electron transfer from NADH dehydrogenase (proton pump) via the cytochrome bc_1 complex to cytochrome *c* oxidase. Information from (Simon *et al.*, 2008).

Denitrification, or anaerobic nitrate respiration, utilises a series of reductase enzymes (nitrate reductase - NAR; nitrite reductase – NIR; nitric oxide reductase – NOR; and nitrous oxide reductase – NOS) to sequentially reduce nitrate (NO_3^-) to dinitrogen gas (N_2) (Berks *et al.*, 1995a; Richardson, 2000) (Fig. 1.6). The role of each reductase enzymes required for denitrification is detailed below (see sections *1.3.3* to *1.3.4*). This reaction predominately takes place under anaerobic conditions in the presence of nitrate and is found in many facultative or strict anaerobes. Nitrate reduction is coupled to proton translocation through a redox loop, involving electron transfer from formate dehydrogenase, via quinol oxidation and quinone reduction, to NAR, resulting in the generation of a PMF (Richardson & Sawers, 2002). The electrons during this reaction flow through a series of redox cofactors, for example various iron-sulfur clusters [Fe-S] and a molybdenum cofactor, generating energy to drive electron transfer across the membrane.

Respiratory nitrite ammonification (nitrate assimilation) allows organisms such as *Wollinella succinogenes, Salmonella, Campylobacter jejuni* and *Escherichia coli* to grow under anaerobic conditions via the reduction of nitrite to ammonia using the cytochrome *c* nitrite reductase (NrfA) (Simon, 2002). Anaerobic ammonium oxidation (ANAMMOX) is the second process in the nitrogen cycle that generates N_2, utilising nitrite as an electron acceptor and ammonia as an electron donor, producing NO and hydrazine (N_2H_4) as intermediates (Hu *et al.*, 2011; Kartal *et al.*, 2011). The ANAMMOX pathway, required for the conversion of nitrite and ammonia to dinitrogen gas, is a key part of the nitrogen cycle, found in *Planctomycete* bacteria isolated from marine environments (Hu *et al.*, 2011), and archae. Finally the conversion of ammonia to nitrate, via nitrification, is known to be primarily performed by soil dwelling bacteria such as *Nitrosomonas europaea* (Richardson, 2000).

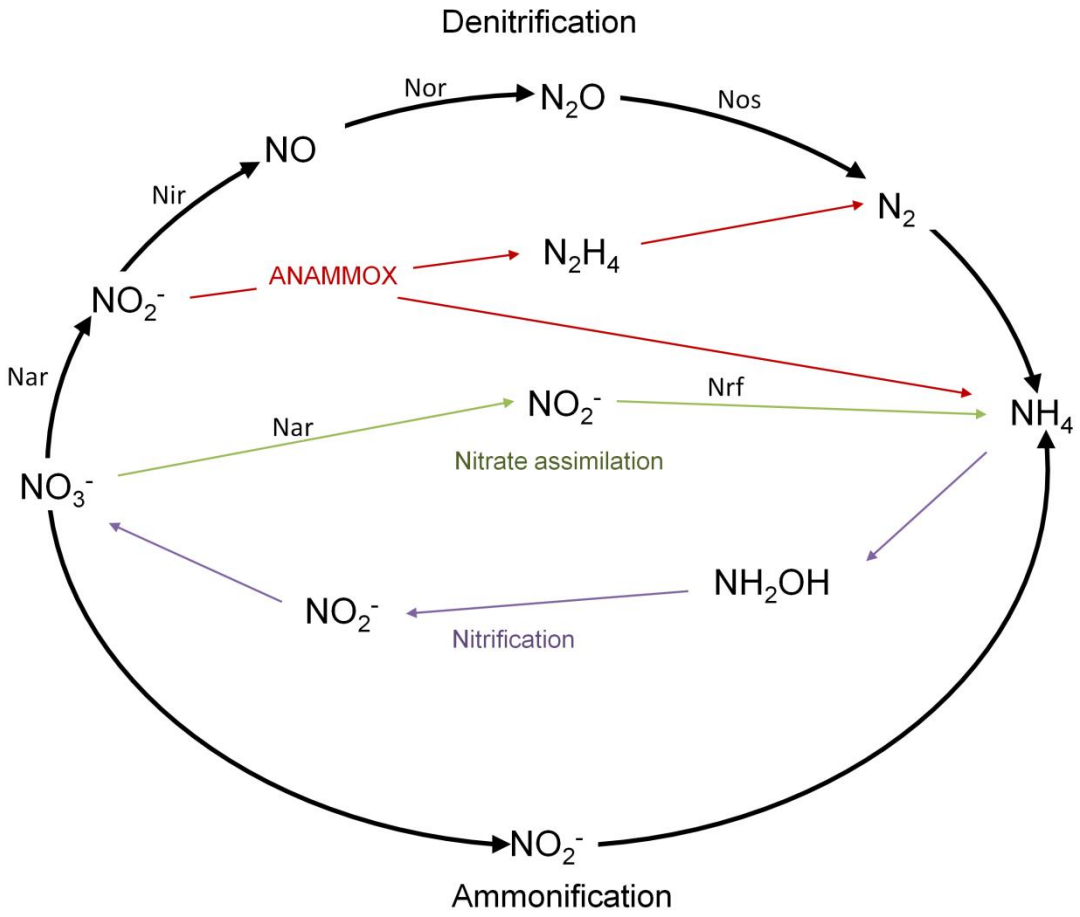

Figure 1.5 – The nitrogen cycle. Enzymes required for denitrification and nitrate assimilation are indicated on diagram; ANAMMOX (anaerobic ammonium oxidation) reactions shown in red, nitrate assimilation in green and nitrification in purple. Diagram altered from (Richardson, 2000; Moir, 2011a).

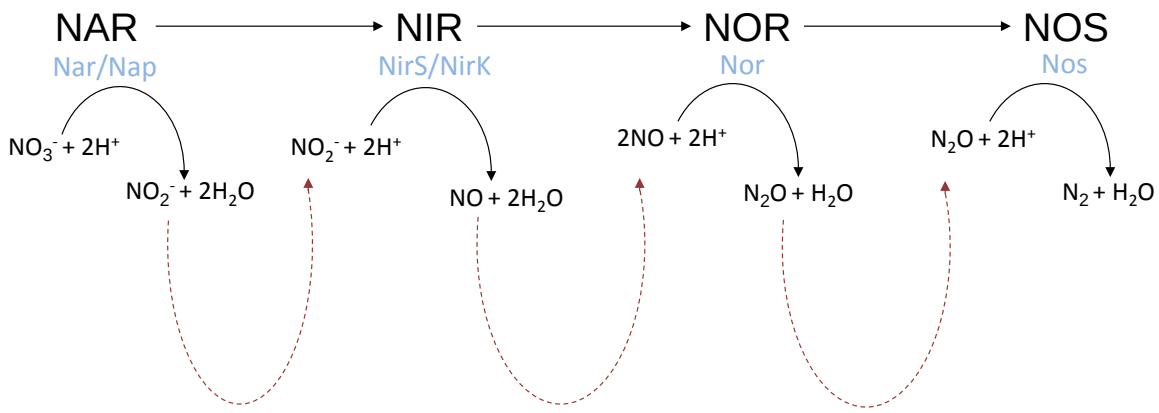

Figure 1.6 – Prokaryotic denitrification pathway. Schematic outlines the reactions that occur during denitrification, allowing for the reduction of nitrate (NO_3^-) to dinitrogen gas (N_2); using NAR, NIR, NOR and NOS. There are two different types of dissimilatory NAR, Nar and Nap, and two types of NIR, NirS and NirK, shown in blue. See text for details.

1.3.3 *Nitrate reductase*

There are three different types of nitrate reductases found in prokaryotes performing either assimilatory or dissimilatory functions, required for either the incorporation of nitrate into biomolecules or the generation of a PMF. A number of publications have demonstrated the importance of nitrate reductase in anaerobic respiration and virulence, and it is predicted that NAR will play some role in the pathogenesis of melioidosis. Therefore the structure and function of the different nitrate reductases will be discussed in more detail in sections 1.5 and 1.6.

1.3.4 Nitrite reductase

There are three distinct types of nitrite reductases (NIR), catalysing either the reduction of nitrite to nitric oxide or the reduction of nitrite to ammonia. The respiratory nitrite reductases are periplasmic enzymes that are structurally distinct and contain both *c*-type cytochromes and d_1 heme cofactors (cd_1-Nir - NirS) or multiple copper clusters (Cu-Nir - NirK). Prokaryotes also have an assimilatory Nir (NADH dependent) which reduces nitrite to ammonia, using NADH as its electron source.

E. coli, unlike some other facultative anaerobes, does not possess a full denitrification pathway, but is able to respire anaerobically by reducing nitrate to ammonia, using formate as an electron donor. *E. coli* requires a periplasmic penta-heme cytochrome *c* nitrite reductase (NrfA) to reduce nitrite to ammonia, utilising a soluble penta-heme cytochrome (NrfB) as its redox partner (Bamford *et al.*, 2002; Clarke *et al.*, 2008). NrfA can utilise both nitrite and nitric oxide as substrates and is required for respiratory reduction of nitrite to ammonia, nitric oxide detoxification, electron transport and energy conservation (Cole, 1996; Kemp *et al.*, 2010; Mills *et al.*, 2008; Poock *et al.*, 2002).

The second step in the denitrification pathway is catalysed by either a cytochrome cd_1-type nitrite reductase (NirS) or copper containing nitrite reductase (NirK/Cu-Nir). Both NirS and Cu-Nir take electrons from the cytochrome bc_1 complex via various *c*-type cytochromes or cupredoxins, and catalyse the reduction of nitrite to nitric oxide. No prokaryotic species is known to encode both the cd_1-Nir and the Cu-Nir within their genome. Both respiratory nitrite reductases are evolutionarily unrelated and the fact that no known prokaryote encodes both cd_1-type and copper containing NIR indicates

that the presence of one type excludes the acquisition of the other (Jones *et al.*, 2008; Moir, 2011a).

The structure and function of the cytochrome cd_1-type nitrite reductase (NirS) is known for *P. denitrificans, Pseudomonas aeruginosa* and *Thiosphaera pantotropha.* This enzyme is a functional dimer composed of two subunits containing either a *c*-type heme domain required for electron uptake and electron transfer, or a d_1-heme required for the reduction of nitrite to nitric oxide (Baker *et al.*, 1997; Silvestrini *et al.*, 1994; Timkovich *et al.*, 1982). The *P. aeruginosa* cd_1-type NIR is known to exhibit both reductase and oxidase activity, being capable of the reduction of NO_2^- to NO and the reduction of O_2 to H_2O (Rinaldo *et al.*, 2008). The cytochrome *c* domain in one of the dimers is required for the formation of a complex with *c*-type cytochromes or cupredoxin. Nitrite binds to *P. aeruginosa* cd_1-type heme when in the reduced state ($cd^{2+}d_1{}^{2+}$), and is dehydrated to give oxidised d_1 heme and nitric oxide (Rinaldo *et al.*, 2008). Variations in electron transfer rate between cd_1-type NIR from *P. stutzeri* and *P. aeruginosa* have been noted due to differences in nitrosyl d_1-heme complex and altered solvent accessibility, with faster electron transfer rates seen with *P. stutzeri* cd_1-type NIR (Radoul *et al.*, 2012). The formation of a functional NirS in *P. aeruginosa* requires the successful incorporation of both *c* type and d_1-type hemes, the incorporation of which is thought to occur using a transient membrane associated complex composed of NirF, NirN and NirS (Nicke *et al.*, 2013)

The copper nitrite reductase is sub-divided into different groups based on their colour (blue or green) and the structure is known for a number of species; such as *Alcaligenes xylosoxidans* (blue Cu-Nir)*, A. faecalis* (green Cu-Nir)*, Achromobacter cycloclastes* (green Cu-Nir) and *Neisseria gonorrhoeae* (Abraham *et al.*, 1993; Adman *et al.*, 1995; Boulanger & Murphy, 2002; Murphy *et al.*, 1995; Prudencio *et al.*, 1999). The copper nitrite reductase is a periplasmic enzyme composed of three identical monomers, which form a trimer containing type I and type II copper ligands. Type I copper is required for electron transfer from pseudoazurin, cupredoxins, or azurin, whereas the type II copper is required for the one electron reduction of nitrite to nitric oxide (Boulanger & Murphy, 2002; Kukimoto *et al.*, 1994; Murphy *et al.*, 2002). In comparison to other Cu-Nir the *Neisseria* AniA accepts electrons from a string of *c*-type cytochromes (c_4, c_2 and c_5) via the cbb_3 cytochrome oxidase, which mediates electron transfer from the bc_1 complex (Boulanger & Murphy, 2002; Hopper *et al.*, 2009; Hopper *et al.*, 2013).The orientation of the methionine (Met150) side chain in

the type I copper structure is known to contribute to the different coloured nitrite reductases, either blue or green (Inoue *et al.*, 1998).

Recently a different type of Cu-Nir has been characterised in both *Ralstonia picketti* and *Pseudoalteromonas haloplanktis.* These Cu-Nir possess a tethered cytochrome *c* domain allowing for self-electron transfer from cytochrome *c* to the type I copper ligand (Antonyuk *et al.*, 2013; Tsuda *et al.*, 2013). In comparison to most other species *Hyphomicrobium denitrificans* encodes a hexameric, rather than trimeric, Cu-Nir containing twelve type I and six type II copper atoms (Nojiri *et al.*, 2007).

N. meningitidis and *N. gonorrhoeae* are obligate human pathogens that have a truncated denitrification pathway containing only AniA (a Cu-Nir) and NorB, lacking both NAR and NOS, both of which are found in other *Neisseria* species. (Barth *et al.*, 2009). The *Neisseria* AniA is classified as a class II Cu-Nir along with the archaebacteria *Haloarcula marismortui*, and is phylogenetically related to the predicited class II *B. pseudomallei* Cu-Nir (Boulanger & Murphy, 2002; Fig. 2). Unlike other Cu-Nir, AniA is an outer-membrane lipoprotein required for anaerobic growth on nitrite, removal of oxidative radicals, and is known to play a role in evasion of the immune response and human serum resistance by interacting with the complement system (Cardinale & Clark, 2000; Hoehn & Clark, 1992; Mellies *et al.*, 1997). The crystal structure is known for the soluble domain of AniA (sAniA) from *N. gonorrhoeae,* lacking the N-terminal palmityl group required for binding to the outer-membrane. AniA like other Cu-Nir is trimeric in structure and contains all key residues for binding of the type I and type II copper atoms (Boulanger & Murphy, 2002).

The expression of *Neisseria* AniA is tightly regulated by FNR, FUR, NarP and NsrR on the switch between aerobic and anaerobic respiration (Edwards *et al.*, 2012). The *aniA* from *N. gonorrhoeae* and *N. meningitidis,* although very similar, exhibits different levels of expression in the presence of FNR, due a single nucleotide polymorphism (SNP) in the promoter region. This SNP in the *aniA* promoter region of *N. gonorrhoeae* results in a weaker FNR binding, compensated for by an increased *aniA* promoter affinity of NarP (Edwards *et al.*, 2012). This differential tuning of *aniA* expression by both *Neisseria* species is thought to be due to the different lifestyles that they lead. Interestingly, although *N. meningitidis* encodes an *aniA,* many mutations have been noted to occur in a number of isolates resulting in the premature stop codon, large deletion or amino acid replacement (Moir, 2011b; Stefanelli *et al.*, 2008). The loss of a functional AniA from *N. meningitidis* indicates AniA is not required

for meningococcal survival and *N. meningitidis* may be switching to a solely aerobic lifestyle (Moir, 2011b). In comparison to *N. meningitidis* strains*, N. gonorrhoeae* is a facultative anaerobe and the majority of strains are thought to maintain the capacity to respire anaerobically on nitrite via AniA. Recently evidence has pointed towards *N. gonorrhoeae* AniA to be expressed on the cell surface, with a modified form of AniA being able of eliciting an immune response, pointing towards its potential use as a vaccine candidate (Shewell *et al.*, 2013).

1.3.5 Nitric oxide reductase

Bacterial nitric oxide reductases (NOR) are required for the two electron reduction of nitric oxide (NO) to nitrous oxide (N_2O). There are two subclasses of NOR defined by their electron transfer centres and electron donors, either *c*-type cytochrome (for cNOR) or quinol (for qNOR) (Tavares *et al.*, 2006).

NOR from *P. denitrificans* and *P. aeruginosa* is an integral membrane iron containing heterodimeric enzyme composed of a large catalytic cytochrome *c* subunit (NorB) and small membrane anchor subunit (NorC) (Hendriks *et al.*, 1998; Hino *et al.*, 2010). The NorB subunit displays similarities to heme-copper oxidases family proteins. However unlike members of the heme-copper oxidase family NorB does not contain a copper (Cu_B) dinuclear center but instead possesses two heme irons (heme *b* and heme b_3) and a non-heme iron (Fe_B) (Hendriks *et al.*, 1998; Hino *et al.*, 2010; Watmough *et al.*, 2009). NorC is a membrane-anchor cytochrome *c* containing a heme *c*, which serves as an intermediate electron acceptor for the periplasmic electron donors pseudoazurin, cytochrome c_{555} or cytochrome c_{552} (Duarte *et al.*, 2014; Hendriks *et al.*, 1998; Hino *et al.*, 2010; Watmough *et al.*, 2009). When in the fully reduced active form *Pseudomonas nautica* NOR reduces NO to N_2O, following the formation of a non-iron heme Fe_B-mononitrosyl catalytic intermediate, resulting in the formation of the N-N bond (Duarte *et al.*, 2014).

NorBC, unlike heme-copper oxidase family members (e.g. cytochrome *c* oxidase), is not a proton pump, but transfers electrons from the periplasm to the active site of NorB found within the inner membrane (ter Beek *et al.*, 2013). Recent structural analysis on the cytochrome *c* dependent NOR from *P. aeruginosa* has shown that, in comparison to cytochrome *c* oxidase, cNOR exhibits no structural changes on ligand binding, other than a small change to the Fe-Fe distance in the active site that allows

for efficient formation of the N-N bond (Sato *et al.*, 2013). This lack of a conformational change in cNOR on ligand binding is thought to explain the lack of a role of NOR in proton translocation (Sato *et al.*, 2013).

Unlike *P. denitrificans* and *P. aeruginosa, Alcaligenes eutrophus* genome encodes two iso-functional *norB* and *norZ* genes, both of which are required for anaerobic growth and denitrification (Cramm *et al.*, 1997). Neither *A. eutrophus norB* or *norZ* genes have an adjacent *norC* homolog, however both contain an extra amino-terminal extension not seen in other prokaryotic NOR (Cramm *et al.*, 1997).

1.3.6 Nitrous oxide reductase

Nitrous oxide reductase (NOS) catalyses the final step in the denitrification pathway, reducing nitrous oxide (N_2O) to dinitrogen gas (N_2). The NOS from *P. denitrificans* and *P. nautica* are homodimers of monomers containing two redox active copper centres, Cu_A and Cu_Z (Brown *et al.*, 2000; Haltia *et al.*, 2003). The NOS Cu_A is the electron transfer and entry site, which is known to share structural homology with the Cu_A site found in cytochrome oxidase. The Cu_Z site is the active site of NOS required for N_2O binding and contains four copper ions coordinated by several histidine residues in a tetrahedral orientation (Brown *et al.*, 2000; Haltia *et al.*, 2003). Recently the NOS tetranuclear copper active site (Cu_Z) has been shown to have two structural forms; the fully reduced 4CuS Cu_Z^* form, required for catalysis, and a 4Cu2S Cu_Z form (Johnston *et al.*, 2014).

Biogenesis of NosZ Cu_Z occurs within the periplasm and requires NosFYD (ABC transporter) and the Tat translocated NosL (copper periplasmic chaperone protein), both of which are encoded on an operon with *nosZ* (Zumft, 2005). The function of NosZ is dependent on NosR (a membrane-bound iron sulfur flavoprotein) and NosX (FAD-containing protein) which are thought to function during electron transport recruiting electrons from quinol to NOS to help maintain Cu_Z in its active state (Zumft, 2005). The expression of *P. denitrificans nosRZDFYLX* (encoding NosZ), mediated by NosR and NosC, is dependent on the presence of copper, with a reduction in expression and increased abundance of N_2O in copper limited medium (Sullivan *et al.*, 2013).

The NOS from *Pseudomonas stutzeri* is transcribed in three transcriptional units; *nosZ* (main enzyme), *nosR* and *nosDFY.* These are under the control of six different promoter regions which required for transcriptional response to denitrifying conditions,

aerobosis and the maintenance of a low level of transcription to ensure the constitutive expression of *nosZ* (Cuypers *et al.*, 1995). Electron transfer to NOS in *P. denitrificans* occurs via the cytochrome bc_1 complex through pseudoazurin and *c-type* cytochromes. In comparison *Wolinella succinogenes* electron transport to NosZ occurs directly through the quinol pool from Nap, as like *E. coli, W. succinogenes* lacks a cytochrome bc_1 complex (Kern & Simon, 2009).

1.4 Molybdopterin biosynthesis and molybdoenzymes

Molybdenum (Mo), an essential trace element, is found in a wide range of different proteins. The majority of molybdoproteins are oxo-transferases catalysing reactions involving the transfer of oxygen to a donor/acceptor molecule (Hille, 1996). Molybdenum dependent enzymes fall into two distinct categories; bacterial nitrogenase containing an iron based molybdenum cofactor (Fe-Moco) in their active site and pterin based molybdoenzymes. This second group of molybdoenzymes contains three different subfamilies each with distinct active site structures. These include xanthine oxidase, sulfite oxidase family proteins and the dimethyl sulfoxide (DMSO) reductase family proteins (Gonzalez *et al.*, 2006; Hille, 2002; Schwarz *et al.*, 2009) (see Fig. 1.7 and 1.8).

Tungsten has been shown to be able to perform a similar biochemical function to molybdenum and has been found in replacement of Mo in various molybdoenzymes. For example under microaerobic conditions *C. jejuni* formate dehydrogenase activity was shown to be enhanced in the presence of 1 mM sodium tungstate, suggesting it to use tungsten rather than molybdenum for its catalytic activity (Smart *et al.*, 2009). The same study also indicated that *C. jejuni* tri-methylamine N-oxide (TMAO) reductase was able to utilise both molybdenum and tungsten as catalytic cofactors, suggesting *C. jejuni* to have a branched pterin biosynthesis pathway allowing for the synthesis of both molybdopterin and tungstopterin cofactors (Smart *et al.*, 2009). Similarly, tungsten has been shown to be able to substitute molybdenum in *E. coli* TMAO reductase (Buc *et al.*, 1999). Tungstate is also known to inhibit molybdoprotein function by replacing molybdenum in the active site. This inhibition of catalytic activity on addition of tungstate is known to occur *in vitro,* as seen with *Paracoccus pantotrophus* periplasmic nitrate reductase and the formate dehydrogenase from *Methanobacterium formicicum* (Gates *et al.*, 2003; May *et al.*, 1988).

1.4.1 Molybdopterin cofactor biosynthetic pathway

The molybdopterin cofactor (Moco) is synthesised via a conserved pathway found in both eukaryotic and prokaryotic organisms. The *E. coli* molybdopterin biosynthetic pathway is a four step enzymatic pathway involving various molybdate dependent biosynthetic proteins and transport systems (Fig. 1.7) (Leimkuhler *et al.*, 2011; Schwarz *et al.*, 2009). The first step in the pathway is catalysed by MoaA and MoaC and involves the conversion of guanosine triphosphate (GTP) to the pterin intermediate cyclic pyranopterin monophosphate (cPMP). Following this reaction MPT synthase converts cPMP to molybdopterin (MPT), adding on the dithiolene ligands essential for the function of the cofactor (Leimkuhler *et al.*, 2011). MPT synthase is a heterotetramer composed of two MoaE and one MoaD subunit ($MoaE_2MoaD$). MPT synthase is activated by MoeB (a sulfurase) in an ATP dependent manner, following the formation of a MoaD-MoeB complex (Leimkuhler *et al.*, 2011). During this activation reaction MoeB is used to help regenerate the active MPT synthase, catalysing the adenylation of the C-terminal glycine residue of MoaD (Schwarz *et al.*, 2009). *Mycobacterium tuberculosis* is known to encode multiple gene homologs required for the first two steps of molybdopterin biosynthesis (e.g. *moaA, moaC, moaE, moaD* and *moeB*). Along with these *M. tuberculosis* encodes a fused MPT synthase (MoaX), thought to display both *moaD* and *moaE* activities (Williams *et al.*, 2011). Expression of *M. tuberculosis* MoaX was able to fully restore Moco biosynthesis in a *M. smegmatis moaD2-moaE2* mutant.

The third step requires transport of molybdate (MoO_4^-) into the cell, using a high affinity transport system (ModABC) (Grunden & Shanmugam, 1997), and MogA and MoeA, required for the conversion of MPT to the molybdenum cofactor (Mo-MPT – Moco). MogA is required to activate MPT, using an adenylation reaction, to allow for MoeA to efficiently ligate Mo to MPT (Leimkuhler *et al.*, 2011). The sulfite oxidase family of molybdoproteins is the only known member to bind Mo-MPT (Brokx *et al.*, 2005), requiring no final modifications of Moco as seen for other molybdoenzymes. The final step in the pathway is catalysed by MobA or MocA and involves the addition of various nucleotides (such as GMP and CMP) to Moco, to form the cofactor required for either the DMSO reductase family (Mo-*bis*MGD) or the xanthine oxidase family

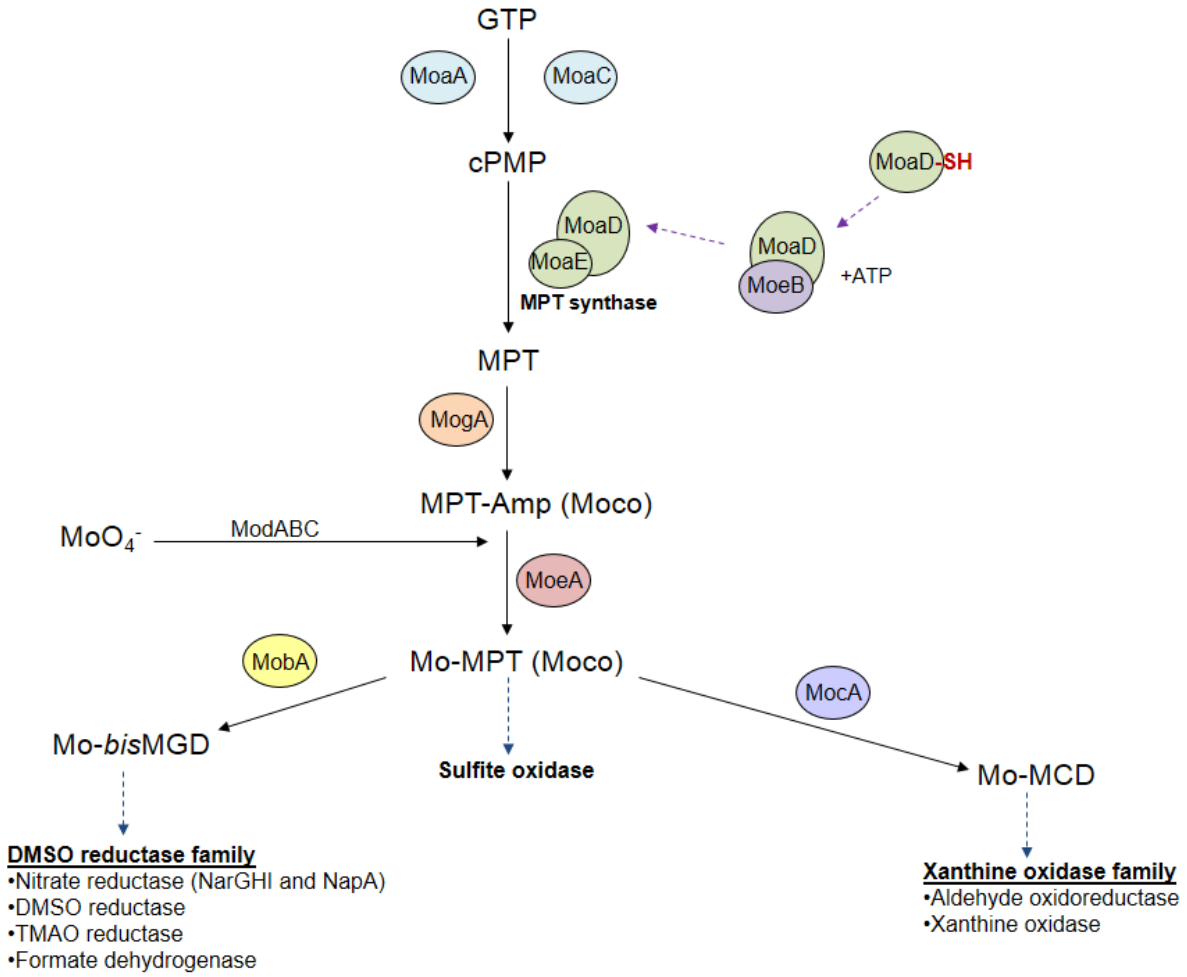

Figure 1.7 – Molybdopterin biosynthesis pathway in *E. coli*. The *E. coli* molybdopterin biosynthetic pathway is a four step enzymatic pathway involving multiple biosynthetic and transport proteins, required for the generation of the molybdenum cofactor (Moco). Different types of molybdoenzymes require different forms of the molybdenum cofactor (Moco) (Fig. 1.8), modified by the addition of a nucleotide in the final steps of the pathway using either MobA or MocA. For the DMSO reductase family Moco is modified via the addition of GMP, generating the Mo-*bis*MGD cofactor. In comparison the xanthine oxidase family Moco is modified by the covalent attachment of cytosine nucleotide (CMP), generating Mo-MCD. The sulfite oxidase family is the only molybdoenzyme that does not have a modified form of Moco. See text for more details on the pathway and function of different molybdoenzymes. Diagram generated using information from Leimkuhler *et al.* (2011).

(Mo-MCD) (Leimkuhler *et al.*, 2011; Xi *et al.*, 2000). The final stage of Moco biosynthesis is known to occur on a complex made up of MogA, MoeA, MobA and MobB. This complex is required for the efficient delivery of Mo-*bis*MGD cofactor to apo-nitrate reductase and occurs in a NarJ assisted manner (Vergnes *et al.*, 2004).

1.4.2 Nitrogenases

Bacterial nitrogenase is the only molybdoenzyme that contains a non-pterin based molybdenum cofactor. Nitrogenases require both an iron based molybdenum cofactor (Fe-Moco; Mo-3Fe-3S) and an iron-sulfur cluster [4Fe-3S] for electron transfer (Schwarz *et al.*, 2009). Nitrogenases are found in various nitrogen-fixing bacteria and are required for the reduction of dinitrogen to ammonia, a reaction which occurs in an ATP dependent manner (Burgess & Lowe, 1996; Seefeldt *et al.*, 2009).

1.4.3 DMSO reductase family

All DMSO reductase family members require a Mo-*bis*MGD as their catalytic cofactor (Kisker *et al.*, 1997). The molybdenum atom in this cofactor is coordinated by two pterin moieties each with a guanine monophosphate (GMP), which together form the molybdenum guanine dinucleotide (MGD) (Fig. 1.8 b) (Schwarz *et al.*, 2009). DMSO reductase family members are diverse in their structure and function but share similarities in their organisation and cofactors they contain; often being bound to the inner membrane or cytoplasmically orientated. DMSO reductase family members include the dissimilatory nitrate reductase, formate dehydrogenase, DMSO reductase, biotin-sulfoxide reductase and TMAO reductase (Kisker *et al.*, 1997; Leimkuhler *et al.*, 2011). The majority of these enzymes function in oxygen limiting environments and are required for the generation of a PMF.

Rhodobacter capsulatus and *E. coli* DMSO reductases have been studied in detail (Cheng *et al.*, 2005; McAlpine *et al.*, 1998; Sambasivarao & Weiner, 1991). *E. coli* DMSO reductase is composed of catalytic subunit (DmsA) containing a Mo-*bis*MGD cofactor linked to a high spin Fe-S cluster (FS0) (Tang *et al.*, 2011), DmsB subunit containing four [4Fe-4S] clusters required for electron transfer, and an integral membrane subunit (DmsC) allowing transfer of electrons from the menaquinol pool in the inner membrane (Weiner *et al.*, 1992) . *E. coli* DMSO reductase is encoded by the

a.)

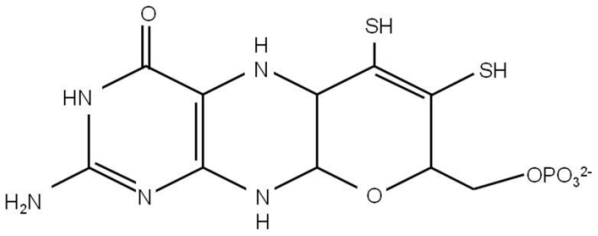

b.)

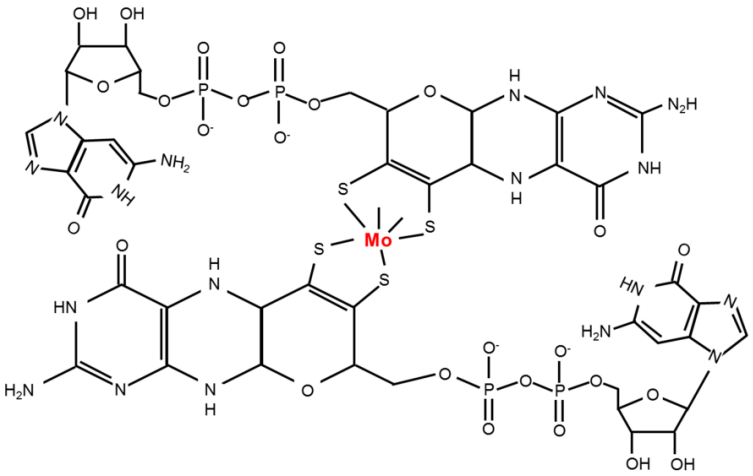

c.)

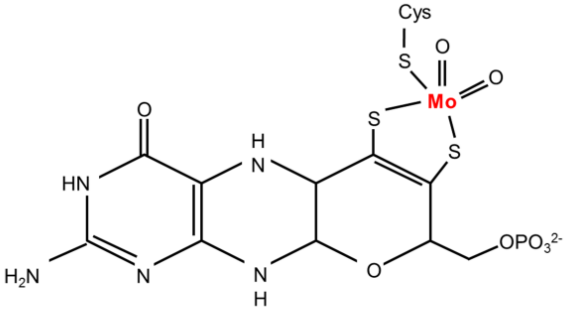

d.)

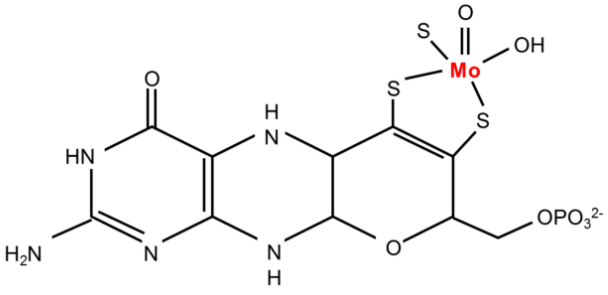

Figure 1.8 – Chemical structure of different molybdenum cofactors. a.) molybdopterin; b.) Mo-*bis*MGD; c.) Sulfite oxidase family cofactor; d.) Xanthine oxidase family cofactor. Molybdenum ion is shown in red. Figure altered from (Schwarz *et al.*, 2009).

dmsABC operon and is required for anaerobic growth on DMSO (Bilous & Weiner, 1985b; Sambasivarao & Weiner, 1991). DMSO reductase catalyses the reduction of DMSO to DMS, in a reaction linked to oxygen atom transfer and electron transfer via the oxidation of Mo (IV) to Mo (V) (McAlpine *et al.*, 1998). The DMSO reductase from *R. capsulatus* is known to bind either tungsten (W) or molybdenum (Mo) within its catalytic site (Stewart *et al.*, 2000). *R. capsulatus* W-DMSO reductase, a tungstoenzyme, displays higher levels of activity compared to Mo-DMSO, but does not catalyse the oxidation of DMS (Stewart *et al.*, 2000).

DmsAB are Tat-translocated into the periplasm by the Tat secretion system, prior to binding to DmsC (Stanley *et al.*, 2002). Functional assembly and maturation of the DMSO reductase enzyme requires the DmsD chaperone protein (Ray *et al.*, 2003). The DmsD chaperon has recently been shown to specifically recognise the hydrophobic leader peptide of DmsA, containing a twin arginine (RR) leader sequence (Winstone *et al.*, 2013). Recent analysis of an *E. coli* DmsABC variant (DmsA-Cys59Ser) has revealed a link between FS0 and the Mo-*bis*MGD cofactor (Tang *et al.*, 2013). This same study also revealed Mo-*bis*MGD to act as a chemical chaperone, ensuring correct assembly for DmsABC (Tang *et al.*, 2013).

E. coli encodes two structurally related but distinct formate dehydrogenase isoenzymes; formate dehydrogenase-N (Fdh-N) and formate dehydrogenase–O (Fdh-O/FdoGHI) that are known to act as electron transfer sinks (Abaibou *et al.*, 1995; Jormakka *et al.*, 2003). Formate dehydrogenase is required for the oxidation of formate to carbon dioxide (CO_2) and H^+ and plays a role in the electron transfer to nitrate reductase (Richardson & Sawers, 2002). FdoGHI contains a selenomolybdenum polypeptide in the catalytic site for formate oxidation (Benoit *et al.*, 1998). FdoGHI is required for the transition from aerobic to anaerobic growth, along with NarZYV, both being expressed under aerobic conditions (Abaibou *et al.*, 1995). In comparison Fdh-N is the major electron donor for anaerobic nitrate respiration, mediating electron transfer via menaquinone to NarGHI (Jormakka *et al.*, 2002a; Jormakka *et al.*, 2002b; Jormakka *et al.*, 2003).

R. capsulatus encodes an *fdsGBACD* operon, required for the formation of the oxygen tolerant NAD^+-dependent formate dehydrogenase, that contains a Mo-*bis*MGD cofactor, FMN-cofactor and various iron-sulfur clusters ([4Fe-4S] and [2Fe-2S]) (Hartmann & Leimkuhler, 2013). The *fdsGBACD* operon is located downstream of *moaD2* and *moaE*, and encodes FdsC and FdsD which do not form part of the

mature formate dehydrogenase complex (Hartmann & Leimkuhler, 2013). FdsC is a chaperone protein that has recently been shown to bind specifically with Mo-*bis*MGD cofactor and interact with molybdopterin biosynthesis proteins, prior to cofactor insertion (Bohmer *et al.*, 2014).

Nitrate reductase is a member of the DMSO reductase family, requiring a Mo-*bis*MGD cofactor for the reduction of nitrate to nitrite. The structure and function of nitrate reductase required for the assimilation or dissimilation of nitrate will be discussed in more detail in section 1.5.

1.4.4 Sulfite oxidase family

Unlike other molybdoenzymes, the sulfite oxidase is structurally distinct and is the only molybdoprotein containing an unmodified Mo-MPT cofactor (Fig. 1.7 c). *E. coli* sulfite oxidase (YedYZ) is a heterodimer, composed of YedY and YedZ subunits. YedY is the catalytic subunit containing a Tat leader signal sequence and Mo-MPT cofactor. YedZ a membrane-intrinsic cytochrome *b* subunit acting to anchor the protein to the membrane and provide YedY with a redox partner (Brokx *et al.*, 2005; Loschi *et al.*, 2004). Kinetic analysis has shown YedY to possess no detectable sulfite oxidase activity, exhibiting instead reductase function in response to TMAO, dimethyl sulfide (DMS), and methionine sulfoxide (Loschi *et al.*, 2004). YedY from *E. coli* is thought to function as an oxidoreductase, exhibiting catalytic activity towards S- and N-oxides (Iobbi-Nivol & Leimkuhler, 2013).

1.4.5 Xanthine oxidase family

Xanthine oxidase family members include xanthine oxidase (XdhABC), xanthine dehydrogenase and aldehyde oxidoreductase (PaoABC), which are characterised by the presence of a Mo-MPT cofactor (Iobbi-Nivol & Leimkuhler, 2013; Kisker *et al.*, 1997) (Fig. 1.8 d). Xanthine oxidase and xanthine dehydrogenase are required for purine metabolism. XdhABC is required for the conversion of xanthine to hypoxanthine and uric acid. *E. coli* aldehyde oxidoreductase is required for the detoxification of aromatic aldehydes under certain growth conditions (Iobbi-Nivol & Leimkuhler, 2013). The structure of *Desulfovibrio gigas* aldehyde oxidoreductase was solved and shown to contain a molybdenum cytosine dinucleotide and a [2Fe-2S] center (Romao *et al.*, 1995). In comparison the aldehyde oxidoreductase from archaeon *Pyrococcus*

furiosus contains a tungsto-bispterin cofactor, containing tungsten rather than molybdenum as its catalytic cofactor (Sevcenco *et al.*, 2010).

1.5 Nitrate reductase

There are three types of nitrate reductase enzymes required for assimilation (Nas) or the dissimilation of nitrate (NapA and NarGHI) (Table 1.4). All nitrate reductase enzymes require a Mo-*bis*MGD cofactor, associated with nitrate binding, and a [4Fe-4S] cluster to facilitate electron transfer to molybdenum. Nitrate reductase enzymes, such as the NarGH from *P. pantotrophus* and assimilatory nitrate reductase (NarB) from *Synechococcus elongates* (Jepson et al., 2004), are known require reductive activation for catalysis (Field *et al.*, 2005). During catalysis the molybdenum ion cycles between oxidation states, Mo (VI), Mo (V) and Mo (IV). Nar catalyses an oxo-transferase reaction were the oxidised Mo (VI) is reduced to Mo (IV) on the reduction of nitrate to nitrite; with the intermediate Mo (V) state thought to be associated with NO_3^- binding (Jepson *et al.*, 2004; Jormakka *et al.*, 2004).

1.5.1 Membrane-bound nitrate reductase

The crystal structure of *E. coli* membrane-bound quinol-nitrate oxidoreductase, also referred to as NarGHI, has been solved to a 1.9 Å resolution (Bertero *et al.*, 2003) (Fig.1.9). NarGHI is a heterotrimeric enzyme composed of two NarGHI homodimers. NarG (140 kDa) is the catalytic subunit of the enzyme, containing a high spin [4Fe-4S] cluster (FS0), coordinated by one histidine and three cysteine residues (amino acid sequence – HxxxCxxxC$(x)_n$C) (Jormakka *et al.*, 2004; Rothery *et al.*, 2004) and a Mo-*bis*MGD cofactor required for the two electron reduction of nitrate to nitrite (Bertero *et al.*, 2003). The N-terminus of NarG, forms a ‘tail’ (an extended β hairpin structure) which forms tight hydrogen bonds with the electron transfer subunit NarH. NarH (58 kDa) contains three [4Fe-4S] clusters (FS1-3) and one [3Fe-4S] cluster (FS4), providing an efficient electron transport link between NarI and NarG (Fig. 1.7 c) (Bertero *et al.*, 2003; Jormakka *et al.*, 2004). NarGH are anchored to the cytoplasmic side of the inner membrane by the transmembrane subunit NarI (Bertero *et al.*, 2003). NarI (20 kDa) contains two heme prosthetic groups, heme b_P/b_D, and provides a quinol binding and oxidation site to link the electron transfer from menaquinol or ubiquinol to the iron-sulfur clusters in NarH and Mo-*bis*MGD in NarG (Bertero *et al.*, 2003). The

heme b_D of NarI is part of the quinol binding and oxidation site that exhibits heterogeneity depending on the occupancy of the Q-site, either bound to quinone or quinone-free (Fedor *et al.*, 2014).

The Mo-*bis*MGD cofactor in NarG is coordinated by the four *cis*-thiolate groups from Mo-*bis*MGD and either a monodentate or bidentate interaction with the oxygen atom(s) from the carboxylate ligand from asparagine, Asp^{222} (Bertero *et al.*, 2003; Jormakka *et al.*, 2004). This difference was thought to reflect potential structural flexibilities in the Mo active site (Jormakka *et al.*, 2004).

Unlike other members of the DMSO reductase family, the Mo in NarGHI is coordinated by an Asp (D) residue. This alternative coordination of Mo lead to the structural classification of NarGHI as a type II (D-group) molybdoenzyme, distinct from type I molybdoenzymes, such as formate dehydrogenase (Jormakka *et al.*, 2004). These different classes of molybdoenzymes often differ in the coordination of FS0. In NarGHI the iron sulfur cluster is coordinated by one histidine and three cysteine residues ($HxxxCxxxC(x)_nC$), whereas the Fe-S cluster in formate dehydrogenase, periplasmic nitrate reductase and assimilatory nitrate reductase is coordinated by three cysteine residues, $CxxxCxxxC(x)_nC$ (Jormakka *et al.*, 2004; Magalon *et al.*, 1998).

The unique coordination of the molybdenum cofactor by an Asp residue is seen in bacterial NarGHI and a number of archael nitrate reductases and selenate reductases (Martinez-Espinosa *et al.*, 2007). Unlike most NarGHI, a number of archael nitrate reductase enzymes are periplasmically orientated, due to the presence of a twin arginine motif (RR) which allows for translocation through the Tat apparatus (Martinez-Espinosa *et al.*, 2007). This periplasmic orientation of the catalytic subunit is also seen for *Thauera selenatis* SerA (Martinez-Espinosa *et al.*, 2007). SerA is the catalytic subunit of the selenate reductase (SerABC), a molybdoenzyme required for the reduction of selenate to selenite under anaerobic conditions (Butler *et al.*, 2012).

NarGHI is encoded on an operon containing a chaperone protein (NarJ), nitrate/nitrite antiporter (NarK) and a two component system (NarXL), involved in its regulation. NarJ is critical for the proper folding, assembly and incorporation of the molybdenum cofactor, and the formation of a functional NarGHI protein (Blasco *et al.*, 1998). The N-terminal region of NarJ specifically recognises the N-terminus of NarG (1-15 peptide), and upon binding causes a conformational change allowing for efficient

Table 1.4 – Prokaryotic nitrate reductases

	Nas	**Nar**	**Nap**
Function	NO_3^- assimilation	NO_3^- respiration	NO_3^- reduction
Location	Cytoplasm	Membrane-bound	Periplasm
Structural gene operon	*nasFEDCBA*[b]	*narGHJI*[a] *narZYWV*	*napFDAGHBC*[a]
Function	Biosynthesis of N compounds	PMF generation	Denitrification and redox balancing
Prosthetic groups	Mo-*bis*MGD, Fe-S clusters, FAD	Mo-*bis*MGD, Fe-S clusters, *b*-type cytochrome	Mo-*bis*MGD, Fe-S clusters, *c*-type cytochrome
Regulation[d]		***narXL***[c]	***narQP***[c]
Response to: nitrate/nitrite	Yes	Yes	Yes
		Fnr[e]	**Fnr**
Absence of O_2	Yes	Yes	No/Yes

[a] in *Escherichia coli* K12 (Gonzalez *et al.*, 2006)

[b] in *Bacillus subtilis* (Gonzalez *et al.*, 2006)

[c] Two component system regulation (Gonzalez *et al.*, 2006; Stewart, 1993)

[d] Differences have been reported in different bacterial species

[e] Senses cellular oxidation status.

Table has been altered from (Moreno-Vivian *et al.*, 1999)

a.) Structure of *E. coli* NarGHI b.) Ligands c.) Redox cofactors

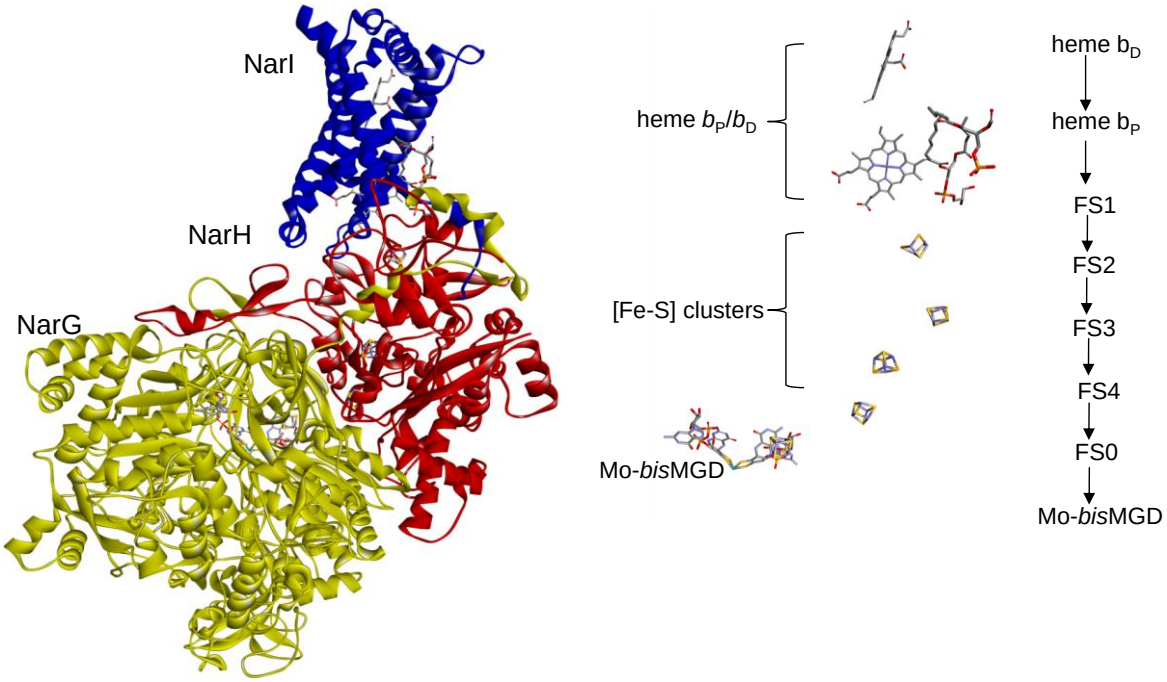

Figure 1.9 – Structure of *E. coli* NarGHI (PDB: 1Q16). a.) Structure of *E. coli* NarGHI (PDB number: 1Q16) (Bertero *et al.*, 2003). Each subunit is individually coloured; NarI (blue), NarH (red) and NarG (yellow). b.) NarGHI ligands (heme b_P/b_D, [Fe-S] clusters and Mo-*bis*MGD) required for both electron transfer and nitrate reduction, shown in the same orientation as the full protein structure in (a.). c.) Redox cofactors and electron transfer through NarGHI. Image created using DS Visualizer 3.5 software. See text for details.

folding and assembly of NarGHI (Lorenzi *et al.*, 2012; Zakian *et al.*, 2010). NarJ binds to two distinct sites on NarG, one for membrane anchoring of the apo-enzyme and one involved in the incorporation of the molybdenum cofactor (Vergnes *et al.*, 2006). Once Moco is formed a MobA, MobB, MogA and MoeA complex interact with NarGH in a NarJ assisted manner transferring Moco forming the mature nitrate reductase (Vergnes *et al.*, 2004).

The crystal structure for NarK (nitrate/nitrite exchanger) has recently been solved, showing it to contain a nitrate signature motif (Zheng *et al.*, 2013). The substrate translocation pathway of NarK contains positively charged amino acid residues allowing for efficient translocation of NO_3^- and NO_2^- across the membrane via a proposed 'Rocker Switch' mechanism for ion exchange (Zheng *et al.*, 2013).

E. coli and *Salmonella typhimurium* are known to encode a second membrane-bound NAR known as the cryptic nitrate reductase (NarZYWV). *E. coli* NarZYWV unlike NarGHI is constitutively expressed under aerobic conditions, and is regulated on the onset of stationary phase by RpoS and repressed under anaerobic conditions by FNR (Chang *et al.*, 1999; Moreno-Vivian *et al.*, 1999). *S. typhimurium* NarZYV is positively regulated by carbon starvation, and is required for carbon-starvation-inducible thermo-tolerance, hydrogen peroxide resistance and acid tolerance (Spector *et al.*, 1999).

The control of the nitrate reductase operon (*narKGHJI*) has been studied in detail in a number of bacterial species. These regulatory systems range from the cAMP-dependent regulator GlxR in *Corynebacterium glutamicium* (Nishimura *et al.*, 2010), ArcAB, Fur in *Salmonella* (Teixido *et al.*, 2010), the Res system in *Bacillus subtilis,* NarXL and FNR (fumarate and nitrate reductase regulator) in a number of proteobacteria including *P. aeruginosa, B. subtilis, E. coli, Salmonella spp.,* and *Paracoccus* (Bonnefoy & Demoss, 1994; Egan & Stewart, 1990; Fink *et al.*, 2007; Hartig *et al.*, 1999; Nakano & Zuber, 1998; Stewart, 1993).

1.5.2 Periplasmic nitrate reductase

Many proteobacteria species contain both a membrane-bound and periplasmic nitrate reductase (Nap) required for dissimilation of nitrate. The crystal structure for the heterodimeric periplasmic nitrate reductase (NapAB) from *Rhodobacter sphaeroides* and *Desulfovibrio desulfuricans,* and monomeric NapA from *E. coli* have

been solved (Arnoux *et al.*, 2003; Dias *et al.*, 1999; Jepson *et al.*, 2007). The catalytic subunit, NapA, contains Mo-*bis*MGD cofactor and [4Fe-4S] (Arnoux *et al.*, 2003; Jepson *et al.*, 2007) and is linked to the di-heme cytochrome electron transfer subunit NapB (Arnoux *et al.*, 2003), which together form a dimeric complex in *R. sphaeroides*. In comparison to *R. sphaeroides* and *P. pantotrophus* Nap, the *E. coli* NapA does not form a tight association with NapB, and is generally found to be a monomeric enzyme located within the periplasm (Jepson *et al.*, 2007). It was been recently been shown that the pyranopterin of the molybdenum cofactor, and not the Mo metal ion, is required for the reductive activation of NapAB from *R. sphaeroides* (Jacques *et al.*, 2014). This pyranopterin is proximally located to the [4Fe-4S] cluster allowing for efficient electron transfer (Jacques *et al.*, 2014).The Mo ion in Nap is coordinated by six sulfur ligands, which aid in the reduction of nitrate via a 'sulfur-switch' mechanism (Cerqueira *et al.*, 2013; Grimaldi *et al.*, 2013)

NapAB is often found to be linked to the membrane, on the periplasmic side by the membrane-anchor protein NapC, required for menaquinol oxidation (Potter *et al.*, 2001). NapA is exported to the periplasm by the Tat translocation pathway, allowing for the reduction of nitrate to occur outside on the inner-membrane aiding in its role in denitrification, redox balancing and nitrate scavenging (Potter *et al.*, 2001).

Like all of the nitrate reductase enzymes NapABC is encoded on an operon (e.g. *napFDAGHBC* in *E. coli* and *napEDABC* in *Thiosphaera pantotropha* and *P. aeruginosa*) containing genes that play a direct role in NO_3^- reduction (NapA and NapB) and those which play accessory functions, encoding chaperone-like proteins (NapD) and cytoplasmic iron-sulphur proteins (NapG and NapH) (Berks *et al.*, 1995b; Gonzalez *et al.*, 2006; Stewart *et al.*, 2002; Van Alst *et al.*, 2009). The NapD chaperone protein is crucial for the folding and insertion of the molybdenum cofactor into NapA, forming a NapDA complex on binding to the NapA Tat signal peptide (Dow *et al.*, 2014).

The Nap from *P. denitrificans,* in contrast to NarGHI, is predominately expressed under aerobic conditions, whereas NarGHI is expressed anaerobically. This difference in expression is thought to be partly due to the cellular location of both Nap and Nar (Richardson *et al.*, 2001). In Nap, quinol is oxidised at the periplasmic face of the cytoplasmic membrane by NapC, where the electrons are shuttled to the periplasm to be used in the reduction of nitrate to nitrite, resulting in a dissipation of energy. In contrast Nar reduces nitrate to nitrite in the cytoplasm, conserving the free energy

produced in the QH_2/nitrate loop as a PMF (Richardson *et al.*, 2001). This conservation of energy is bioenergetically favourable and would allow for efficient respiration under anaerobic conditions in the presence of nitrate (Richardson *et al.* 2001). *P. pantotrophus* Nap plays a role in cellular redox balancing and displays differential transcription in response to various carbon sources, with butyrate resulting in a high level of *nap* expression and Nap enzyme activity seen under aerobic conditions (Ellington *et al.*, 2003).

E. coli and *P. aeruginosa* uses both Nap and NarGHI to support anaerobic growth, using Nap to support growth, when the levels of nitrate are low, prior to the induction of NarGHI (Gonzalez *et al.*, 2006; Moreno-Vivian *et al.*, 1999; Stewart *et al.*, 2002; Van Alst *et al.*, 2009).

1.5.3 Assimilatory nitrate reductase

The assimilatory nitrate reductase (Nas) is involved in the incorporation of nitrogen into organic molecules, catalysing the two electron reduction of nitrate to nitrite (Gonzalez *et al.*, 2006). Like both Nar and Nap, Nas requires both a Mo-*bis*MGD cofactor and [4Fe-4S] for its activity (Moreno-Vivian *et al.*, 1999). *Klebsiella oxytoca* can use both nitrate and nitrite as sole sources of nitrogen, using Nas encoded by *nasFEDCBA* (Lin *et al.*, 1994). The catalytic subunit (NasA – 92 kDa) contains [4Fe-4S] cluster and Mo-*bis*MGD, and is likely to take electrons from the electron transfer subunit NasC, a predicted flavoprotein exhibiting homology to NADH-dependent reductases. Both *Bacillus subtilis* and *K. oxytoca nasFEDCBA* have additional genes for electron transport (*nasB*), a siroheme-FeS nitrite reductase (*nasD*), and *nasFED* genes required for nitrate transport and uptake (Lin *et al.*, 1994; Lin & Stewart, 1998; Richardson *et al.*, 2001).

P. denitrificans encodes a NADH-dependent assimilatory NAR, containing a ferredoxin subunit (NasG) required for electron transfer to the NADH-oxidising site in the nitrite reductase (NasB) to the nitrate/nitrite reduction site in NasC (Gates *et al.*, 2011). *P. denitrificans* Nas is regulated by the nitrogen oxyanion binding sensor (NasS) and RNA-binding protein (NasT) in response to nitrate/nitrite, allowing for the assimilation of nitrate (Luque-Almagro *et al.*, 2013).

1.6 Role of anaerobic respiratory proteins in pathogenesis

B. pseudomallei has the capacity to survive and persist for extended periods of time within the host and environment, likely to be partly due to its ability to respire anaerobically (Hamad *et al.*, 2011). It is thought that *B. pseudomallei* is likely to encounter oxygen limiting environments during the course of its life cycle, either within the rice paddy fields or *in vivo*. A genome wide analysis has shown an upregulation of nitrate reductase, the outer membrane nitrite reductase and formate dehydrogenase in the liver and spleen of a mouse infected with *B. mallei,* pointing towards a role for anaerobic respiration in these organs (Kim *et al.*, 2005). Currently little is known about what role anaerobic respiration will play in virulence of *B. pseudomallei*. However there is evidence in the literature for a role of anaerobic respiration and molybdopterin biosynthesis, and more specifically nitrate reductase, in pathogenesis of various bacterial species, such as *M. tuberculosis, Neisseria,* and *P. aeruginosa.*

M. tuberculosis, the causative agent of tuberculosis, displays very similar clinical presentations to those seen with a *B. pseudomallei* infection, both displaying chronic and latent infections. Because of this melioidosis is often referred to as the great mimicker or 'Vietnamese tuberculosis' (van Schaik *et al.*, 2009). Both *M. tuberculosis* and *B. pseudomallei* chronic infections are known to produce granulomas within infected organs and tissue (Conejero *et al.*, 2011; Saunders & Britton, 2007). Granulomas are thought to be limiting in both nutrients and oxygen, highlighting the potential importance for anaerobic respiration in survival within this structured environment.

1.6.1 Wayne's model for hypoxic shift down

In 1996 Wayne and Hayes developed an *in vitro* model to study *M. tuberculosis* mechanisms of persistence and adaptation to anaerobiosis (Wayne & Hayes, 1996). This is now referred to the Wayne's model for hypoxic shift down, which is characterised by two stages of non-replicating persistence (NRP); NRP-1 and NRP-2. NRP-1 is characterised as a shift to microaerophilic growth, displaying an increase in NAR activity, increase in glycine dehydrogenase activity, DNA synthesis and number of colony forming units (CFU) (Wayne & Hayes, 1996; Wayne & Hayes, 1998). The increase in NAR activity seen during NRP-1 is due to an increase in the expression of the *narK2* transport protein (Sohaskey & Wayne, 2003). NRP-1 and NAR activity are

important for the adaptation to non-replicating persistence seen in NRP-2, which is characterised by a further reduction in oxygen levels to hypoxia, reduction in NAR activity and decrease in glycine dehydrogenase activity (Wayne & Hayes, 1996; Wayne & Hayes, 1998). Although an increase in NAR activity is seen during NRP-1, nitrate reductase is not required for shift-down to non-replicating persistence (Sohaskey, 2008).

1.6.2 A role for the membrane-bound nitrate reductase in virulence

The main source of nitrate in the human body is obtained as a dietary source, or is produced through the L-arginine-NO pathway (Lundberg *et al.*, 2004). Nitrate and nitrite can be found circulating within the blood, saliva and in various organs and are produced, along with NO, as part of the immune response (Kelm, 1999; Lundberg *et al.*, 2004). Commensal organisms naturally found within the gut unlike some pathogenic species do not, almost without exception denitrify, with most species reducing nitrate to ammonia as seen in *E. coli* (Moir, 2011a). However many pathogenic bacteria are known to utilise the denitrification to aid survival within the host, with roles for both nitrate and nitrite reductase in virulence being described for various different pathogenic species such as *Mycobacterium spp., Neisseria spp* and *P. aeruginosa* (Moir, 2011a).

M. tuberculosis has been described as an obligate aerobe, but like other members of its genus it possess a NAR within its genome. *M. tuberculosis* is the strongest denitrifier out of all the *Mycobacterium spp. M. tuberculosis* encodes a fused nitrate reductase (NarX), a NarGHI, responsible for the majority of NAR activity, and various NarK transport proteins (Sohaskey & Wayne, 2003). The *M. tuberculosis* NarK2, a proposed Type I H (+)/nitrate symporter required for nitrate import into the cytoplasm, has been recently shown to be inactive in the presence of oxygen (Giffin *et al.*, 2012). *M. tuberculosis narGHJI* is constitutively expressed under aerobic and microaerobic conditions during NRP-1, with its expression being independent of both nitrate and nitrite (Sohaskey & Wayne, 2003). The survival of both *M. smegmatis* (non-pathogenic) and *M. tuberculosis* (pathogenic) declines dramatically on sudden switch to anaerobiosis (Dick *et al.*, 1998; Wayne & Hayes, 1996). However, gradual acclimatisation to anaerobiosis and the addition of nitrate have been shown to significantly enhance long-term survival and entry into a non-replicating persistent state (Dick *et al.*, 1998; Sohaskey, 2008).

The role of *M. bovis* BCG Δ*narG* mutant in virulence has been assessed using both immune competent BALB/c and immune deficient SCID mice. Deletion of the nitrate reductase (Δ*narG*) in *M. bovis* BCG prevented the reduction of nitrate under anaerobic conditions, but did not affect survival *in vitro* under anaerobic conditions, with both the wild-type and mutant displaying similar viability after 15 week incubation (Fritz *et al.*, 2002; Weber *et al.*, 2000). In a study by Weber *et al.* (2000) a *narG* mutant displayed a difference in virulence using SCID mice, with fewer bacteria seen in granulomas of the liver and lungs, and no outward signs of clinical infection were seen when compared to wild-type infected mice (Weber *et al.*, 2000). In comparison a study by Fritz *et al.* (2002) did not show a role for *narG* in chronic infection in SCID even though bacilli loads in the liver, kidney and lungs were reduced in comparison to the wild-type (Fritz *et al.*, 2002).

Fritz *et al.* (2002) studied the histopathology of the lungs of SCID and BALB/c infected mice with either wild-type *M. bovis* BCG or the Δ*narG* mutant. After 14 weeks wild-type infected SCID mice displayed large lesions containing acid-fast bacilli, with infected individuals suffering a severe pulmonary infection. In comparison mice infected with Δ*narG* mutant, although displaying smaller lesions, succumbed to a fatal infection after 37 weeks. This indicated that although deletion of *narG* does not cause avirulence, the presence of a functional NarGHI affects survival of *M. bovis* within infected SCID mice (Fritz *et al.*, 2002). Similarly although the deletion *M. tuberculosis narG* (Δ*narG*) resulted in failure to persist under anaerobic conditions *in vitro*, infection of C57BL/6 mice with the Δ*narG* mutant resulted in characteristic growth patterns within the lungs and both wild-type *M. tuberculosis* and mutant mice succumbing to infection after 400 days (Aly *et al.*, 2006). By contrast, *M. bovis* NarG was shown to play a role in virulence when using BALB/c as an infection model. In the BALB/c (immune competent) murine model deletion of *narG* resulted in avirulence, with substantially lower lung tissue destruction and clearing of infected lungs, liver and kidney seen when infected with the mutant when compared to the wild-type *M. bovis* BCG (Fritz *et al.*, 2002). These results taken together suggest that the role of *Mycobacterium* NarG in virulence is tissue specific and depends on the immune status of the host.

The difference in virulence levels seen in different infection models may also be due to the oxygen status of the lungs. For example although the lungs of C57BL/6 mice infected with *M. tuberculosis* were shown to have a reduced level of oxygen,

compared to uninfected mice, the levels did not quite reach that of severe hypoxia or anoxia (Aly *et al.*, 2006). By contrast to mice infected with *M. tuberculosis,* infection with *M. avium* displayed necrotizing lesions that were severely hypoxic (Aly *et al.*, 2006). Although lungs of mice infected with *M. tuberculosis* are not anaerobic (Aly *et al.*, 2006; Tsai *et al.*, 2006), tuberculosis infected guinea pigs, rabbits and non-human primates models display highly structured necrotic lesions with a hypoxic microenvironment, allowing entry into non-replicating persistent state (Via *et al.*, 2008). Clinical samples obtained from patients with a tuberculosis infection have revealed an upregulation of genes required for anaerobic respiration such as *narG, narX,* and *frdA* within granulomas indicating a role for nitrate reductase in human pulmonary tuberculosis (Fenhalls *et al.*, 2002; Rachman *et al.*, 2006).

P. aeruginosa is an opportunistic, nosocomial pathogen known to cause lung infections in patients who are immunocompromised or have cystic fibrosis (CF). *P. aeruginosa* encodes both a NapA and NarGHI, required for anaerobic respiration and growth within CF sputum (Palmer *et al.*, 2007). *P. aeruginosa narG* mutants demonstrated a severe anaerobic growth defect, significantly affecting growth within the CF sputum, whereas the *napA* mutant showed no growth defect growing at wild-type levels (Palmer *et al.*, 2007). The wild-type *P. aeruginosa* and the *napA* mutant were able to reduce the same amounts of nitrate, but the *narG* mutant was deficient in anaerobic nitrate reduction. Deletion of *narGH* is known to cause avirulence in *C. elegans,* and affect swarming motility and biofilm formation (Van Alst *et al.*, 2007).

Brucella suis resides and multiplies within phagocytic vacuoles of macrophages, requiring various genes required for stress response, nitrogen reduction, sugar and lipid metabolism oxidoreduction and DNA/RNA metabolism (Kohler *et al.*, 2002). Interestingly mutations within the cytochrome *bd* oxidase and *narG* caused a 2-fold attenuation 48 hours post infection, indication a role for nitrate reductase in growth within a macrophage (Kohler *et al.*, 2002).

1.6.3 Role of the molybdopterin biosynthetic pathway and molybdoproteins in pathogenesis

The molybdopterin biosynthetic pathway and molybdopterin containing proteins, other than NarGHI, have also been implicated in playing a role in *in vivo* survival.

Genes required for Moco biosynthesis are enriched in pathogenic *Mycobacteria* species, and show a degree of upregulation within macaque primate lungs (Dutta *et al.*, 2010; McGuire *et al.*, 2012). *M. tuberculosis moeB*1::Tn transposon mutant shown to exhibit an intracellular growth defect, attributed to a trafficking deficiency, and sensitivity to macrophage effector mechanisms (MacGurn & Cox, 2007). Indeed a link between various proteins required for Moco synthesis and pathogenesis has been found for *M. tuberculosis.* A *moaC1* mutant, among other genes required for metabolism, DNA repair and stress responses, was shown to be attenuated for growth in macaque lungs following aerolised infection (Dutta *et al.*, 2010). In this same study *narX* (a fused nitrate reductase), along with other genes required for hypoxia, was not attenuated for survival and growth in primate lungs (Dutta *et al.*, 2010).

C. jejuni, an obligate microaerophile and human gastrointestinal pathogen, encodes a periplasmic sulfite reductase encoded by a monohaem cytochrome *c* (cj004c) and molybdopterin oxidoreductase (cj005c), required for the utilisation of sulfite as a respiratory electron donor (Myers & Kelly, 2005). Mutations within cj005c caused a significant reduction in invasion and adherence to Caco2 cells, reduced motility and reduction in growth in the presence of sodium sulfite (Tareen *et al.*, 2011).

DMSO reductase has also been implicated in virulence and persistence. *Actinobacillus pleuropneumonia,* the causative agent of porcine pleuropneumonia (Bosse *et al.*, 2002), is known to persist within the oxygen limiting environment of necrotic lung tissue. *A. pleuropneumonia* is known to respire anaerobically using DMSO as an alternative electron acceptor. Both DMSO reductase and asparate ammonium lyase have been shown to be upregulated during infection, playing a role in *A. pleuropneumonia* virulence (Baltes *et al.*, 2003; Baltes *et al.*, 2005). An *A. pleuropneumonia dmsA* deletion mutant was created and assessed for its role in virulence using pigs as an infection model. Pigs infected with Δ*dmsA* displayed fewer symptoms to wild-type infected animals, but both the mutant and wild-type could persist within host tissues, indicating DMSO reductase plays a role during the acute but not chronic stage of infection (Baltes *et al.*, 2003; Baltes *et al.*, 2005; Jacobsen *et al.*, 2005).

Recently the assimilatory nitrate reductase from the plant pathogen *Ralstonia solanacearum* (NasA) was shown to aid in plant root colonisation, with a *nasA* mutant displaying inability to utilise nitrate as a sole nitrogen source, reduced virulence and

delayed tomato stem colonisation (Dalsing & Allen, 2014). The NasA was also shown to affect the production of extracellular polysaccharide, a key virulence factor in *R. solanacearum* (Dalsing & Allen, 2014).

Finally, *E. coli* nitrate reductase (*narG*) and fumarate reductase (*frdA*) mutants have been shown to exhibit severe intestinal colonisation defects (Jones *et al.*, 2011) *E. coli* was shown to utilise nitrate and fumarate as alternative electron donors, preferentially using fumarate reductase as a terminal oxidase in the intestine as nitrate is often limiting (Jones *et al.*, 2011). Fumarate reductase was shown to provide *E. coli* with a colonisation advantage, with nitrate reductase being required for long term persistence (Jones *et al.*, 2011).

1.7 Aims of this project

The ability for bacteria to respire under aerobic and anaerobic conditions is likely to provide a distinct advantage aiding in environmental and *in vivo* survival. Currently little is known about the respiratory flexibility exhibited by *B. thailandensis* and *B. pseudomallei*, although it is speculated that the ability to respire aerobically and anaerobically will contribute to the pathogenesis of melioidosis. The aim of this PhD is to determine what role anaerobic respiration has to play in the survival and virulence of *B. pseudomallei.* Work will first be conducted on *B. thailandensis* in order to identify anaerobic respiratory genes that may play a role in survival and virulence of *B. pseudomallei.*

This PhD aims to:

- Use bioinformatic analysis to determine the respiratory flexibility exhibited by *B. thailandensis, B. pseudomallei* and *B. mallei*
- Identify genes required for anaerobic respiration, by creation of a random transposon mutant library in *B. thailandensis* E264
- Characterise the transposon mutants for their role in aerobic and anaerobic respiration, *in vitro* survival, nitrate reductase activity and role in motility, biofilm formation and virulence.
- Create clean deletion mutants in *B. pseudomallei* K96243 using the pDM4 suicide vector bearing a chloramphenicol resistance cassette
- Characterise the role of the *B. pseudomallei* deletion mutants using various *in vitro* and *in vivo* assays including - anaerobic respiration, persistence, motility and virulence

Chapter 2 - Materials and methods

2.1 Bioinformatics

2.1.1 NCBI BLAST and K.E.G.G. analysis

NCBI (http://www.ncbi.nlm.nih.gov/) BLAST analysis and the *Burkholderia* Genome Database (Winsor *et al.*, 2008) were used to identify genes required for anaerobic respiration in *B. thailandensis* E264, *B. pseudomallei* K96243 and *B. mallei* ATCC 23344. A Kyoto Encyclopaedia of Genes and Genomes (K.E.G.G. - http://www.kegg.jp/) ortholog analysis was carried out to determine the degree of amino acid sequence conservation and orthology between various proteobacteria species.

Softberry promoter analysis (http://linux1.softberry.com/berry.phtml) was used to predict bacterial gene promoters to identify potential regulatory networks.

2.1.2 Sequence alignments

Clustal Omega (https://www.ebi.ac.uk/Tools/msa/clustalo/), an online multiple sequence alignment tool, was used when performing nucleotide or protein sequence alignments (Higgins *et al.*, 1996). The TMHMM server v. 2.0 (Krogh *et al.*, 2001) was used to predict potential transmembrane helices in the putative copper nitrite reductases.

2.1.3 Structure prediction

The online platform for protein structure prediction, the I-TASSER server (Zhang, 2008) was used in order to determine the degree of structural conservation between *B. pseudomallei* K96243 NarG (BPSL2309) and *E. coli* K-12 NarG (b1224) based on an amino acid sequence alignment. The sequence alignment generated was based on the *E. coli* NarGHI protein sequence (PDB: 1Q16) (Bertero *et al.*, 2003). Discovery Studios (DS Visualizer 3.5 and DS Visualizer ActiveX Control 3.5) was used to visualise the predicted protein structures created by the I-TASSER server. SWISS-MODEL (Kumar *et al.*, 2012; Minch *et al.*, 2012) was also used to determine the degree

of structural homology of the putative copper nitrite reductases encoded by *B. thailandensis* and *B. pseudomallei,* based on previous published structures.

***2.2 B. thailandensis* work – transposon mutagenesis, PCR and enzymatic assays**

2.2.1 Media, growth conditions and bacterial strains

All bacterial strains were routinely grown in Luria Bertani broth (L-broth), solidified when required using 1.5 % bacteriological agar. *B. thailandensis* (strain E264) was routinely grown at 37 ^{o}C in a shaking incubator (220 rpm) or statically for all procedures unless otherwise stated. *E. coli* strain 19851 (*pir*$^{+}$), used for direct mating during transposon mutagenesis, was maintained in LB media supplemented with kanamycin (30 µg/mL) and ampicillin (100 µg/mL) to ensure the maintenance of the modified *pir*-dependent plasmid pUTminiTn5Km2, encoding kanamycin resistance cassette (Cuccui *et al.*, 2007; de Lorenzo *et al.*, 1990). Where appropriate the growth media was supplemented with the appropriate antibiotic to maintain selection of the antibiotic resistance cassette (ampicillin – 100 µg/mL; chloramphenicol 35-50 µg/mL; gentamicin 100 µg/mL; kanamycin 50-250 µg/mL; tetracycline – 50 µg/mL).

B. thailandensis anaerobic growth studies were conducted in medical flat bottomed flasks, or within an anaerobic chamber (10 % CO_2, 80 % N_2 and 10 % H_2) using L-broth or M9 minimal media. M9 minimal media was supplemented with or without sodium nitrate ($NaNO_3^-$) or sodium nitrite ($NaNO_2^-$) (0-20 mM) and 20 mM of a carbon source (succinate or glucose). Sodium succinate was used for the majority of experiments as it is a non-fermentable carbon source capable of sustaining good aerobic and anaerobic growth, when in the presence of an electron acceptor. When using medical flat bottomed flasks the media was sparged for 20 minutes with oxygen free nitrogen. M9 media contained 2 mM $MgSO_4$, 0.1 mM $CaCl_2$, 20 % M9 salts (5 x stock solution; 85.5 gL^{-1} Na_2HPO_4, 15 gL^{-1} KH_2PO_4, 2.5 gL^{-1} NaCl, 5 gL-1 NH_4Cl). When needed the M9 minimal media plates were solidified using 1.5 % agar and placed into an anaerobic chamber for 2 to 4 days.

All frozen stocks of mutants or wild-type bacterial strains were made using a final glycerol concentration of 30 % and stored at -80 ^{o}C.

Table 2.1 - Bacterial strains and plasmids used for *B. thailandensis* transposon mutagenesis and complementation

Bacterial strain	Characteristics	Reference
Burkholderia thailandensis		
B. thailandensis E264	Wild-type Gram negative saprophyte, isolated from soil in 1995 (Thailand)	(Brett *et al.*, 1998)
CA01	*B. thailandensis* BTH_I1704 Tn5Km2 transposon mutant, Km^{Ra}	This study
CA01_pDA-17::BTH_I1704	CA01, pDA-17::BTH_I1704, Km^{R}, Tet^{R}	This study
Escherichia coli		
JM109	Chemically competent cells *end*A1, *rec*A1, *gyr*A96, *thi, hsd*R17 (r_k^-, m_k^+), *rel*A1, *sup*E44, Δ(*lac-pro*AB), [F´ *tra*D36, *pro*AB, *laq*I^qZΔM15]	Promega
E. coli strain 19851	*pir*$^+$, pUTminiTn5Km2, Km^{Ra}	(Cuccui *et al.*, 2007; de Lorenzo *et al.*, 1990)
GT115	Chemically competent cells *Δdcm, uidA::pir-116, sbcCD*	Invivogen
DH5α lamda (λ) *pir*	Chemically competent cells F– Φ80*lac*ZΔM15 Δ(*lac*ZYA-*arg*F) U169 *rec*A1 *end*A1 *hsd*R17 (rK–, mK+) *pho*A *sup*E44 λ– *thi*-1 *gyr*A96 *rel*A1	Laboratory stock
S17 λ *pir*	TpR SmR recA, thi, pro, hsdR-M$^+$RP4: 2-Tc:Mu: Km Tn7 λ*pir*	Laboratory stock
pRK2013	Kan^{R}, helper strain	Clontech

Plasmids		
pJET1.2/blunt	rep (pMB1), replication start, *bla* (Amp^{Ra}), *eco47IR,* $P_{lacUV5'}$, T7 promoter, multiple cloning site (MCS), insertion site, primer binding sites	Thermo-Scientific
pUTminiTn5Km2	Mini-Tn5Km2 (Kan^{R}), oriR6K *mob*RP4, *tnp**	(Cuccui *et al.*, 2007; de Lorenzo *et al.*, 1990)
pJET-Tn#1	pJET1.2/blunt containing Tn#1 arbitrary PCR product (approximately 200 bp) Maintained in JM109 competent cells	This study
pJET-Tn#2	pJET1.2/blunt containing Tn#2 arbitrary PCR product (approximately 200 bp) Maintained in JM109 competent cells	This study
pJET-Tn#3	pJET1.2/blunt containing Tn#3 arbitrary PCR product (approximately 180 bp) Maintained in JM109 competent cells	This study
pDA-17	ori_{pBBR1}, Tet^{Ra}, mob^{+}, P_{dhfr}, FLAG epitope Maintained in DH5α competent cells	(Flannagan *et al.*, 2007)
pDA-17::BTH_I1704	ori_{pBBR1}, Tet^{Ra}, mob^{+}, P_{dhfr}, BTH_I1704 gene Maintained in DH5α competent cells	This study

[a]Km^{R} – Kanamycin resistance cassette; Tet^{R} -Tetracycline resistance cassette; Amp^{R} – Ampicillin resistance cassette

2.2.2 Genomic DNA and plasmid extraction

B. thailandensis E264 and mutant genomic DNA was extracted using Sigma Aldrich GenElute Genomic DNA extraction kit. All plasmids were extracted using either GeneJet Miniprep (Thermo Scientific) or QIAprep spin Miniprep kit (Qiagen). DNA concentration was determined using a nanodrop (ng/µL) (Thermo Scientific Nanodrop 2000c).

2.2.3 Transposon mutagenesis

B. thailandensis E264 was screened on solid M9 minimal media plates supplemented with various concentrations of nitrate (0-30 mM) and succinate (0-30 mM) to determine the lowest concentration of nitrate best able to support anaerobic growth. The results of this were then used to screen the transposon mutant library for mutants unable to grow anaerobically in the presence of nitrate. Each plate was streaked in triplicate with one colony of *B. thailandensis* and left either to grow at 37 ^{o}C within an anaerobic chamber for three days or within a static aerobic incubator overnight.

A transposon mutant library was created by conjugation using *E. coli* strain 19851 *pir*$^{+}$ containing the transposon delivery vector pUTminiTn5Km2, to allow for identification of those genes required for anaerobic growth (Table 2.1). *E. coli* 19851 and *B. thailandensis* cultures were grown in the appropriate media overnight in a shaking incubator at 225 rpm set at 37 ^{o}C. A 100 µl aliquot of an overnight culture of *E. coli* (19851) carrying pUTminiTn5Km2 plasmid was sub-cultured into sterile L-broth supplemented with 100 µg/mL ampicillin and 30 µg/mL kanamycin, and left to grow for 3 hours until exponential phase (absorbance at 600 nm of 0.5 to 0.6). This *E. coli* culture was then mixed at a 1:3 ratio with wild-type *B. thailandensis* prior to centrifugation for 10 minutes at 3,000 x g. The supernatant was decanted and the remaining cells where resuspended in 100 µl L-broth, plated out onto LB agar and left in the 37 ^{o}C incubator for 6 hours. Bacterial cells were then collected by scraping and resuspended cells in 1 mL L-broth, prior to plating out a 1 in 100 dilution onto antibiotic selective plates (containing 250 µg/mL kanamycin, to select for the mutants, and 100 µg/mL gentamicin used to kill off any remaining *E. coli* cells) and incubating at 37 ^{o}C for 48 hours. The resulting transposon mutant colonies were re-picked into 96 well micro-titre plates containing 200 µL of L-broth supplemented with 100 µg/mL

gentamicin and 250 µg/mL kanamycin and left to grow overnight at 37 ^{o}C. The random transposon mutant library was then screened on M9 minimal media plates, containing 5 mM nitrate and 10 mM succinate, and left to grow at 37 ^{o}C within in an anaerobic chamber for three days or within an aerobic incubator overnight.

2.2.4 Agarose gel electrophoresis and DNA visualisation.

Agarose gel electrophoresis was used to separate DNA products based on size. All gel electrophoresis was performed using a 0.75 % to 1.5 % TAE agarose gel and a 1 x TAE buffer, run at 110 volts for 30 to 90 minutes. PCR products were run with the appropriate volume of 6 x loading dye (Thermo Scientific) (2 µL per 10 µL DNA sample). Gels contained 5 % (v/v) ethidium bromide for visualisation of DNA fragments and DNA ladders. All gels were visualised under ultra-violet light. When required restriction digested products or PCR products were gel purified using either Qiagen Gel extraction kit (Qiagen) or the GeneJet gel extraction kit protocol (Thermo Scientific).

2.2.5 Transposon mutagenesis - Polymerase chain reaction (PCR)

All PCR reactions used to confirm transposon insertion were conducted using Fishers Thermostart master mix (2 X concentration), containing a heat active *Taq* DNA polymerase (requiring an initial 95 ^{o}C denaturation step of 15 minutes), 1.5 mM $MgCl_2$ and dNTPs, unless otherwise stated; reaction mix contained 12.5 µL Thermostart 2 X PCR master mix, 8.5 µL nuclease free water, 1 µL template (genomic DNA or a colony) and on occasion 1 µL DMSO. Primer sequences are listed in Table 2.2.

2.2.6 PCR confirmation of the transposon mutants

To confirm the transposon mutant contained the kanamycin resistance cassette and were in fact *B. thailandensis* and not *E. coli,* two separate PCR reactions were performed. PCR reactions used primers either binding to the kanamycin resistance gene (KanR and KanF) or those specific for *B. thailandensis* (S7 and S12). The PCR conditions to amplify the kanamycin resistance gene were 95 ^{o}C for 15 minutes, then 34 cycles of 94 ^{o}C for 30 seconds (secs), 55 ^{o}C for S7 and S12 primers or 48 ^{o}C for

KanF and KanR for 30 seconds, 72 ^{o}C for 1 minute, finally followed by a 10 minute 72 ^{o}C steps.

2.2.7 Nested PCR using arbitrary and transposon specific primers

Nested PCR was used to identify the site of insertion of the transposon (Tn5Km2) into the genome of *B. thailandensis* using the AmpliTaq Gold 360 master mix and 360 GC enhancer. Arbitrary primers (Arb1, 3, 4, or Arb5) and transposon specific primer P7M1 were used for the first round of PCR under the following conditions; 95 ^{o}C for 10 minutes, then 6 cycles of 95 ^{o}C for 30 seconds (secs), 30 ^{o}C for 30 secs, 72 ^{o}C for 1.5 minutes, followed by 30 cycles of 95 ^{o}C for 30 secs, 45 ^{o}C for 30 secs, and finally 72 ^{o}C for 2 minutes. The resultant PCR product was subsequently used for a second round of PCR with Arb2 and P7U under the following cycle; 35 cycles of 30 seconds (secs) at 95 ^{o}C, 30 secs 45 ^{o}C and 1 minute at 72 ^{o}C. Those arbitrary primers giving PCR fragments (150 to 300 bp) where then gel excised and purified.

The purified PCR product was then cloned into pJET1.2/blunt following Thermo Scientific CloneJET protocol. To effectively ligate the PCR products into the pJET1.2/blunt cloning vector a blunting reaction was carried out to remove the 3' A (adenine) nucleotides generated by the *Taq* polymerase. The resultant product was then transformed into *E. coli* JM109 competent cells (see section 2.2.10). Any successful transformants were verified using colony PCR and the plasmid was extracted sent off for sequencing using the supplied pJET1.2 forward primer. Once the sequencing was successful NCBI BLAST analysis was used to determine where in the genome the transposon had inserted.

2.2.8 Transposon mutant (CA01) complementation

To ensure that the phenotypes exhibited by CA01 were due to transposon insertion into BTH_I1704 and not pleiotropic effects on genes within the same cluster, a mutant complement was created, using the constitutive expression vector pDA-17 (7,360 bp) encoding a tetracycline resistance cassette. BTH_I1704 (1,299 bp) was cloned into pDA-17 in front of the *dhfr* promoter region via *Nde*I and *Xba*I restriction sites. Primers were designed to bind to the start and end of BTH_I1704 (see Table 2.2). BTH_I1704 (1,299 bp) was amplified using Phusion PCR master mix with 5 x GC

Table 2.2 - Primers used in *B. thailandensis* E264 mutagenesis, complementation and RT-PCR

Primer name	Sequence (5'- 3')	Characteristics/reference
Transposon mutagenesis		
KanF	CGACTGAATCCGGTGAGAAT	Binds within Km^R cassette
KanR	CCGCGATTAAATTCCAACAT	Binds within Km^R cassette
Arb1	GGCCACGCGTCGACTAGTACNNNNNNNNNNGATAT	(Cuccui *et al.*, 2007)
Arb2	GGCCACGCGTCGACTAGTAC	(Cuccui *et al.*, 2007)
Arb3	GGCCACGCGTCGACTAGTACNNNNNNNNNNTGACG	(Cuccui *et al.*, 2007)
Arb4	GGCCACGCGTCGACTAGTACNNNNNNNNNNACGCC	(Cuccui *et al.*, 2007)
Arb5	GGCCACGCGTCGACTAGTACNNNNNNNNNNTACNG	(Cuccui *et al.*, 2007)
P7M1	GTCATTAAACGCGTATTCAGGCTGAC	(Cuccui *et al.*, 2007)
P7U	CTGCAGGCATGCAAGCTTCG	(Cuccui *et al.*, 2007)
P7M	GCCGAACTTGTGTATAAGAGTC	(Cuccui *et al.*, 2007)
Complementation		
moeA1704_fwd	GCCTCTAGATCAGATGGCGCCGTCG	*Nde*I restriction site
moeA-1704_rv	GCCTCTAGATCAGATGGCGCCGTCG	*Xba*I restriction site
Southern Blot		
SB1	CACGCCCACGCCATCCGCCA	Binds within BTH_I1704
SB2	TCTTTCGCGACGCGGGGGCCG	Binds within BTH_I1704

Reverse transcriptase PCR		
16s-RT1	GCCAGTCACCAATGCAGTTC	Binds within 16s rRNA gene
16s-RT2	ACCAAGGCGACGATCAGTAG	Binds within 16s rRNA gene
RT-1704_fwd	CACGCCCACGCCATCCGCCA	Binds within BTH_I1704
RT-1704_rv	TCTTTCGCGACGCGGGGGCCG	Binds within BTH_I1704
RT-2200_fwd	CGGCCTGACCGGACAGCCCG	Binds within BTH_I2200
RT-2200_rv	GGGGGTTGGGGTGGGACATCG	Binds within BTH_I2200

master mix and purified using GeneJet Gel extraction kit (Thermo Scientific). PCR reaction cycle included an initial denaturation step of 98 ^{o}C for 30 secs, and 30 cycles of 98 ^{o}C for 10 secs, 66 ^{o}C for 30 secs, 72 ^{o}C for 45 secs, and a final extension cycle of 72 ^{o}C for 7 minutes. DMSO was added to all PCRs when using moeA-1704_fwd and moeA-1704_rv primers to prevent formation of any undesired secondary structures. Purified PCR product and pDA-17 vector were both digested using *Nde*I and *Xba*I, ligated together using T4 DNA ligase, and transformed into DH5α competent cells as described in sections 2.2.10 to 2.2.12. Transformants were plated out on to LB agar plates containing tetracycline 50 µg/mL. Successful DH5α pDA-17::BTH_I1704 transformants were confirmed using PCR and sequencing.

2.2.9 Tri-parental mating

Tri-parental mating was performed to conjugate pDA-17::BTH_I1704 into CA01. CA01 (recipient), DH5α pDA-17::BTH_I1704 (donor), and *E. coli* pKR2013 (helper strain) were grown overnight in L-broth supplemented with the appropriate antibiotics; kanamycin 30-50 µg/mL, or tetracycline 50 µg/mL. All 10 mL overnight cultures were centrifuged for 15 minutes at 5,000 x g at 4 ^{o}C, and both donor and helper cell pellets were resuspended in 2 mL sterile PBS. 1 mL donor and helper bacterial suspension was added to the CA01 cell pellet to give a final 1:1:2 mating mix ratio. The bacterial suspension was then re-centrifuged and resuspended in 2 mL sterile PBS. 100 µL of the mating mix was plated out on SOB agar plates onto three nitrocellulose membranes. As a control 100 µL of recipient, donor and helper cells were also plated out onto a nitrocellulose membrane as controls and the plates were incubated overnight. The next day the mating mix and controls were resuspended in 1 mL of sterile L-broth, plated out onto LB plates containing tetracycline 100 µg/mL, gentamicin 100 µg/mL and kanamycin 50 µg/mL and incubated for 2 days at 37 ^{o}C. Tetracycline was used to select for the pDA-17::BTH_I1704 plasmid, gentamicin to kill off any remaining *E. coli* and kanamycin to maintain the transposon selection in CA01. Any potential complements were re-streaked onto the same antibiotic plates prior to PCR screening using crude DNA lysates. Crude DNA lysates were made by resuspending on colony in 20 µL lysis solution (0.05 M NaOH, 0.25 % SDS), incubating at 95 ^{o}C for 15 minutes and resuspending the crude lysate in 180 µL nuclease free

water. Qiagen HotStar Taq master mix, with Q-solution, was used in order to verify presence of pDA-17::BTH_I1704 in CA01 using moeA1704-fwd and moeA1704-rv primers. The PCR reaction cycle for involved an initial denaturation step of 95 ^{o}C for 15 minutes, then 30 cycles of 94 ^{o}C for 1 minute, 56 ^{o}C for 45 seconds, 72 ^{o}C for 2 minutes, with a final extension at 72 ^{o}C for 10 minutes.

2.2.10 Competent cell preparation

Chemically competent cells were made using buffers TFB1 and TFB2 (see Chapter 8 – Appendix for buffer composition), both containing calcium chloride and glycerol. Competent cell preparation was carried out on ice at all times to ensure the bacterial cells remained stable. An overnight culture (25 to 50 mL L-broth) was inoculated with the desired bacterial strain and incubated overnight at 37 ^{o}C with shaking (220 rpm). The next day 200 mL of sterile LB supplemented with 20 mM $MgSO_4^-$ was inoculated with 2 mL of the overnight culture and incubated at 37 ^{o}C until the absorbance (600 nm) reached 0.4 to 0.6. Cells were harvested via centrifugation at 6,800 x g for 10 minutes. The cell pellet was resuspended in two 50 mL volumes of ice cold TFB1 and left to incubate on ice for 5 minutes. The culture was then re-centrifuged and resuspended gently in 10 mL of ice cold TFB2. This then was incubated on ice for over an hour before 200 µL aliquots were made and snap frozen in liquid nitrogen. The competent cells were stored at -80 ^{o}C until required.

2.2.11 Digestion and Ligation

Restriction enzyme digests were performed using Fast Digest restriction enzymes (RE) at 37 ^{o}C for 5 to 10 minutes (Thermo Scientific). RE digests were performed in a final reaction volume of 20 µL using 1 µL each RE, 2 µL 10 x fast digest buffer, 2-15 µL vector or 10 µL PCR product. When required the digested vectors were treated with 1 µL FastAP alkaline phosphatase (Thermo-Scientific) for 10 minutes at 37 ^{o}C to remove the 5’ and 3’ phosphate groups and prevent self-ligation. Digested DNA fragments were run on a 1 % agarose gel, gel excised and purified.

All ligations were performed at 22 ^{o}C for 1 to 2 hours, or overnight at 15 ^{o}C, using T4 DNA ligase (Thermo-Scientific). Ligation reactions were performed using different vector to insert ratios (1:1, 1:3, 1:5, 3:1 or 5:1) using 1 µL T4 DNA ligase, 2 µL T4 DNA

ligase buffer, with the final reaction volume made up to 10 or 20 µL using nuclease free water.

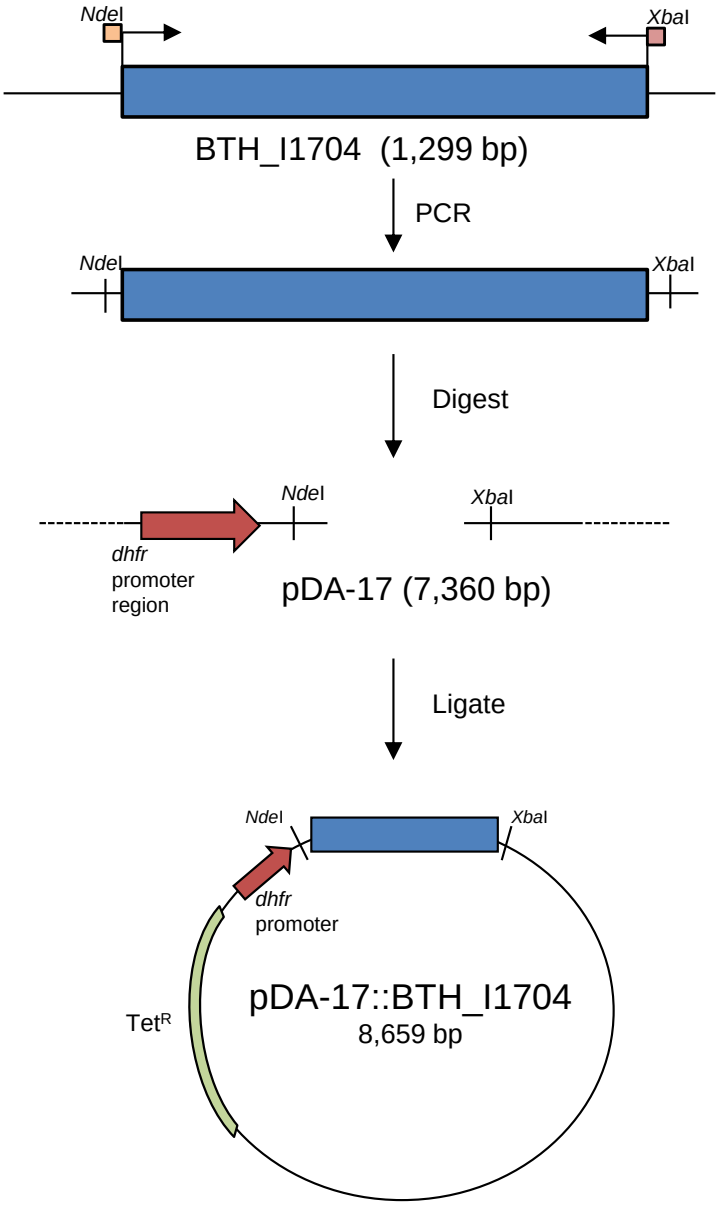

Figure 2.1 – Cloning strategy for pDA-17::BTH_I1704 vector construction for transposon mutant (CA01) confirmation. See methods section 2.2.7 for more details. Briefly BTH_I1704 (in blue) was amplified by PCR, digested using *Nde*I and *Xba*I restriction enzymes prior to ligation into digested pDA-17. pDA-17 encodes a tetracycline resistance gene cassette (Tet^R – in green) and a *dhfr* promoter region to allow for constitutive expression of BTH_I1704.

2.2.12 Transformation

All ligation reactions were transformed into the appropriate competent cells (*E. coli* JM109, DH5α, High efficiency 5α or S17 λ *pir*) and plated out on to antibiotic selective plates. 5 μL of the ligation reaction was added to 50 μL of competent cells and incubated on ice for 20 to 30 minutes. The reaction mixture was then heat shocked at 42 ^{o}C for 45 seconds and immediately placed back on ice for 2 minutes. L-broth or SOB medium (450 μL) was then added and left in a 37 ^{o}C incubator for 90 minutes. The transformants where then plated out on the appropriate antibiotic selective plates. To increase the number of transformants the cells were centrifuged at 13,000 rpm, in a table top centrifuge (MiniSpin®, Eppendorf), for 4 minutes prior to resuspension in 100 µL sterile L-broth and plating out on to antibiotic selective plates.

2.2.13 Isolation of chromosomal DNA

Chromosomal DNA was isolated from *B. thailandensis* and CA01 using buffers TNE (10 mM Tris, 10 mM NaCl, and 10 mM EDTA - pH 8) and TNE-X (TNE and 1 % Triton X-100 mL). One mL of an overnight bacterial culture was harvested via centrifugation for 4 minutes at 13,000 rpm and resuspended in 1 mL TNE. The suspension was then re-centrifuged and the supernatant was discarded. The pelleted bacterial cell culture was then resuspended in 270 µL TNE-X, and 30 µL lysozyme (5 mg/mL) was then added and left to incubate for 20 minutes at 37 ^{o}C to ensure efficient cell lysis. 15 µL of proteinase K (20 mg/mL) was then added, gently mixed by inversion and incubated at 65 ^{o}C for 2 hours until the suspension became clear, ensuring all proteins were degraded. The chromosomal DNA was precipitated out of solution using 15 µL of NaCl and 500 µL 100 % ethanol, fished out or the eppendorf tube with a sterile loop and then transferred into a fresh tube containing 500 µL 70 % ethanol. This was then spun down at room temperature for 10 minutes (13,000 rpm), supernatant removed and the DNA pellet air dried prior to resuspension in 100 µL nuclease free water.

2.2.14 Southern blot

A southern blot was performed using Amersham ECL Direct nucleic acid labelling and detection system and Hybond N^+ positively charged nylon membrane (Amersham; GE Healthcare), to confirm the site transposon insertion in CA01. The ECL direct labelling and detection system is based on chemiluminescence allowing for visualisation of bound DNA using high-performance chemiluminescent film (Amersham Hyperfilm ECL). Briefly the system involved direct labelling of probe DNA with horseradish peroxidase (complex with a positively charged polymer), achieved through complete probe denaturation at 100 ^oC. Prior to hybridisation of the blot the peroxidase is linked to the DNA probe via the addition of glutaraldehyde. The DNA probe once bound then becomes immobilised to the membrane, and once washed can be visualised on a chemiluminescent film after the addition of detection reagents. The detection reagents provided in the kit couple the production of hydrogen peroxide with a light production reaction generated via the oxidation of luminal. The presence of an enhancer within the detection reagent helps to prolong the output and allow for detection on a blue-light sensitive film. The protocol is briefly described below. For more information please refer to the manufacturer's instructions (Amersham; GE Healthcare).

Labelled DNA probes were created using 300 bp purified PCR products, generated using primers binding within BTH_I1704 (SB1 and SB2), for the wild-type probe, or primers binding within the kanamycin resistance cassette (KanF and KanR), for the mutant probe (see Table 2.2). The DNA probes were generated using PCR using the Phusion *Pfu* polymerase and High Fidelity (HF) master mix. The PCR reaction cycles included an initial denaturation step of 98 ^oC for 30 secs, then 30 cycle of denaturation 98 ^oC for 10 secs, annealing 64 ^oC (for primers SB1 and SB2) or 48 ^oC (for KanR and KanF) for 30 secs, extension 72 ^oC for 20 seconds, and a final extension of 7 minutes at 72 ^oC. The PCR product was run on a 1 % agarose gel, gel extracted and purified using Qiagen Gel extraction kit

B. thailandensis E264 and CA01 (BTH_I1704-Tn5Km2) chromosomal DNA were digested for an hour with *Xho*I prior to electrophoresis overnight on a 1 % TAE agarose gel. The gel was then washed using depurination solution (250 mM HCl), denaturation solution (1.5 NaCl, 0.5 M NaOH) and finally neutralisation solution (1.5

M NaCl, 0.5 M Tris-HCl – pH adjusted to 7.5) prior to performing capillary blotting. DNA was transferred overnight onto a Hybond N^+ nylon membrane using Whatman 3 MM filter paper soaked in 20 x SSC. Individual blots were used for either the wild-type or mutant DNA probes.

The blots were pre-hybridised at 42 ^oC for one hour using ECL gold hybridisation buffer containing 5 % (w/v) blocking reagent and 0.5 M NaCl (0.125 mL/cm^2). 100 ng of the DNA probes were labelled with glutaraldehyde solution prior to addition to the hybridisation solution and incubation with the blots overnight at 42 ^oC. The hybridised blots were then washed in primary wash buffer (6 M urea, 0.4 % SDS, 0.5 x SSC) at 42 ^oC for 20 minutes, and then in secondary wash buffer (2 x SSC) for 5 minutes at room temperature. An equal volume of both detection 1 and detection 2 reagents were mixed together and added to the hybridised blots and incubated at room temperature for 1 minute. The southern blot was then visualised and imaged using high performance chemiluminescent film (Amersham ECL).

2.2.15 Griess reaction

The concentration of nitrite produced throughout aerobic and anaerobic growth, in M9 minimal media was measured following an established Griess Reagent system protocol (Promega). The Griess Reagent System is based on the chemical reaction using sulfanilamide and *N*-1-napthylethylenediamine dihydrochloride (NED) used to detect nitrite levels in culture medium through the generation of a pink coloured azo compound. A nitrite standard curve was generated for each experiment to ensure accurate estimations of nitrite concentration in the sample medium.

2.2.16 Methyl-viologen assay on cell membrane fractions

In order to confirm the lack of NAR activity in CA01, a methyl-viologen assay was performed on cell membrane fractions, isolated from cultures acclimatised to anaerobic conditions. Both wild-type *B. thailandensis* and CA01 were grown aerobically overnight (37 ^oC, 200 rpm) in 100 mL of L-broth to obtain biomass. The entire culture was centrifuged at 4,000 x g for 20 minutes at 4 ^oC, and the cell pellet was washed in sterile PBS prior to re-centrifugation and resuspended in 30 mL M9 minimal media, supplemented with 20 mM sodium succinate and 20 mM sodium

nitrate. The cultures were then incubated for four hours within an anaerobic chamber to ensure expression of the nitrate reductase. After 4 hour incubation the cells were harvested following centrifugation at 5,000 x g for 30 minutes. The cells were resuspended in 50 mM phosphate buffer (pH 7.5) and sonicated for 3 minutes (10 seconds on, 10 seconds off at an amplitude of 10 – 15 microns in a Soniprep 150 Sonicator) to lyse the cells. Sonicated cells were then centrifuged at a low speed (3,000 x g) for 30 minutes (4 ^{o}C) to remove any cellular debris, the supernatant was decanted and centrifuged at 20,000 x g for 20 minutes (4 ^{o}C) to separate out the soluble and cell membrane fractions.

An anaerobic quartz-cuvette viologen assay, using methyl-viologen as the artificial electron donor and NO_3^- as the electron acceptor, was then performed in triplicate cell membrane fractions (Craske & Ferguson, 1986; Jones & Garland, 1977). Nitrate reductase activity was measured spectrophometrically (absorbance 600 nm), via the re-oxidation of viologen, following the addition of sodium dithionite.

$$2[\text{Me-viologen}]^{o+} + NO_3^- + 2H^+ \rightarrow 2[\text{Me-viologen}]^{2+} + NO_2^- + H_2O^+$$

Each 3 mL quartz cuvette contained 2.8 mL 50 mM phosphate buffer (pH 7.5), 30 µL 100 mM methyl-viologen, and 150 µL cell membrane fraction to give a final concentration of 1 mg/mL. Using a Hamilton syringe 100 mM sodium dithionite was titrated until the absorbance (600 nm) was approximately 2.5 units. After a stable base line was reached, normally after 130 seconds, 20 mM sodium nitrate was added and the change in absorbance was monitored until the reaction was complete. A no cell membrane control was used to monitor any spontaneous re-oxidation of viologen, when in the absence of nitrate reductase.

2.2.17 Reverse Transcriptase PCR

Reverse transcriptase PCR (RT-PCR) was performed to determine the expression of both putative *moeA* genes (*moeA1* - BTH_I1704 and *moeA2* - BTH_I2200) during anaerobic growth. A starter culture of 50 mL *B. thailandensis* was grown aerobically in L-broth for 16 hours overnight, centrifuged at 6,000 x g, for 15 minutes (4 ^{o}C), and resuspended in M9 minimal media. The next day 150 mL of anaerobic M9 minimal media, supplemented with succinate and nitrate, was

inoculated with *B. thailandensis* at an absorbance of 0.1 (600 nm). Cultures were then incubated at 37 ^{o}C and when required 10-30 mL culture was extracted, centrifuged and resuspended in 500 µL M9 minimal media prior to RNA extraction.

RNA samples were extracted using Qiagen RNeasy Protect mini kit which includes an RNA protect Bacterial reagent for efficient stabilisation of RNA prior to extraction (Qiagen). RNA samples were extracted at various points during the anaerobic growth cycle (lag phase, early, mid and late exponential and stationary phase). RNA was also extracted from aerobic LB *B. thailandensis* overnight cultures (16 hours) grown in the presence of absence of nitrate. All RNA samples were eluted using 30 µL RNase-free water and quantified using a nanodrop, used to determine level of purity and concentration of RNA. Once the RNA had been extracted all samples were treated with Ambion DNase-free kit (Applied Biosystems) to remove any contaminating DNA. The concentration of RNA was standardised to 50 ng/µL prior to performing RT-PCR to ensure level of band intensity seen on the agarose gel would reflect the relative expression level of each gene (*moeA1, moeA2* or 16s RNA).

To confirm all RNA samples were free of DNA contamination, a PCR was performed using Phusion polymerase with the 5 x HF master mix and RT-1704-fwd and RT-1704-rv primers (Table 2.2). Phusion PCR reaction mix consisted of 4 µL 5 x HF, 0.4 µL dNTPS, 1 µL each primer, 1 µL DMSO, 11.4 µL nuclease free water, 0.2 µL Phusion polymerase, and 1 µL template (RNA sample or gDNA). Genomic *B. thailandensis* DNA was used as a positive control. PCR cycle; 98 ^{o}C for 30 secs, then 35 cycles of 98 ^{o}C for 10 secs, 62 ^{o}C for 30 secs, 72 ^{o}C for 30 secs, and a final extension of 72^{o}C for 7 minutes.

RT-PCR performed using Invitrogen SuperScript III One-step RT-PCR mix with Platinum *Taq* polymerase. Superscript III One step RT-PCR (Invitrogen) mix allows for generation of complementary DNA (using reverse transcriptase), and PCR in one reaction. Primers amplifying an approximate 700 bp region of 16s rRNA (16S-RT1 and 16S-RT2) and an approximate 300 bp region of BTH_I1704 (RT-1704-fwd and RT-1704-rv) and BTH_I2200 (RT-2200-fwd and RT-2200-rv) were used in separate reactions (see Table 2.2). RT-PCR reaction mix (per 25 µL) consisted of 12.5 µL 2 x reaction mix, 0.5 µL of each primer, 1 µL Superscript III RT/platinum *Taq,* 9.5 µL nuclease-free water, 1 µL RNA (50 ng/µL) or gDNA (100 ng/µL). DMSO was added to

the reaction mix when using RT-2200-fwd and RT-2200-rv primers. Reaction cycle; cDNA synthesis 1 x 60 ^{o}C for 30 minutes; PCR reaction initial denaturation at 94 ^{o}C for 2 minutes, then 40 cycles of 94 ^{o}C 15 seconds, 62 ^{o}C for 30 seconds, 68 ^{o}C 20 seconds and a final extension of 68 ^{o}C for 5 minutes.

2.2.18 Anaerobic viability assay

To determine whether the ability to grow under anaerobic conditions affects the viability of *B. thailandensis,* wild-type and CA01 were grown anaerobically in a static 37 ^{o}C incubator in medical flat bottomed flasks (initially sparged with nitrogen) for up to one year. The experiment was performed using L-broth supplemented with or without 20 mM $NaNO_3$ or 6 mM $NaNO_2$. Every few weeks the number of viable cells was enumerated by spot plating 10 µl of a 10 fold serial dilutions onto LB agar and incubating the plates aerobically at 37 ^{o}C.

***2.3 B. thailandensis in vitro* and *in vivo* virulence assays**

2.3.1 Swimming motility

Motility assays were performed using nutrient broth supplement with 0.5 % glucose solidified using 0.3 % (w/v) bacteriological agar, supplemented with 20 mM sodium nitrate when required. Cultures, grown overnight with shaking at 37 ^{o}C (220 rpm), were spun down and resuspended in fresh L-broth and standardised to an absorbance (600 nm) of 0.5. The centre of the motility plates were inoculated with 2 µL of the standardised cell suspension and incubated at 37 ^{o}C for 18 hours to 24 hours. The zone of swimming was measured (mm) and recorded. Each biological replicate was assayed in triplicate.

2.3.2 *Biofilm formation*

Bacterial cultures were grown overnight in L-broth at 37 ^{o}C with shaking (220 rpm) and standardised to an absorbance (600 nm) of 0.1 in either M9 minimal media or L-broth. The biofilm formation assays were conducted using Griener polystyrene flat bottomed 96 well plates. A 96 well plate was set up containing 200 µL bacterial

cultures supplemented with or without 20 mM sodium nitrate. The 96 well plates were then incubated for 3 days in a static aerobic or anaerobic chamber. Final growth readings (absorbance – 600 nm) were recorded prior to staining with crystal violet. After 3 days growth aerobically or anaerobically all planktonic cells were carefully removed and the biofilm was washed twice in 200 µL of sterile phosphate buffer saline solution (PBS). The cells were then heat fixed at 80 ^{o}C for one hour, prior to staining with 0.1 % crystal violet for 15 minutes. Once the biofilm was stained the crystal violet solution was gently removed and the crystal violet dye was solubilised using 200 µL of 70 % ethanol and the absorbance was measured in a plate reader at 570 nm. Three biological replicate were used, each with five technical replicates.

2.3.3 Galleria mellonella *infection assay*

Wax moth larvae (*Galleria mellonella*) have previously been used as a model organism for virulence studies on *B. thailandensis* and *B. pseudomallei*, as it has been shown to reflect the observed differences in virulence in murine infection models (Wand *et al.* 2011). *G. mellonella* were purchased from Exeter Exotics (Exeter, Devon, UK) and maintained on wood chips at 15 ^{o}C until required. Bacterial overnight cultures adjusted to give 450 to 500 CFU/10 µL, and 10 µL of either bacterial cell culture or sterile PBS was injected into the uppermost proleg using a Hamilton syringe. Each challenge was performed using 10 larvae and the numbers of surviving/dead *G. mellonella* were measured periodically. PBS was used as a control to measure any potential lethal effects of the infection process. The larvae were considered dead when no movement was displayed after gentle prodding. All experiments were carried out in triplicate.

2.4 ***Burkholderia pseudomallei*** **mutagenesis work**

2.4.1 *Growth media and conditions used for B. pseudomallei work*

All work with *B. pseudomallei* (strain K96243) was carried out in a BSL3 laboratory in a Class I/III safety cabinet. All media was prepared outside of the BSL3 lab and all work was carried out on a mat soaked with 5 to 10 % Biocleanse. *B. pseudomallei* was routinely grown, aerobically with shaking 200 rpm, in universal tubes containing 4 mL L-broth based media or M9 minimal media. *E. coli* strains DH5α

and S17, used for the maintenance of pDM4 suicide vector and deletion constructs, were grown in the presence of 50 µg/mL chloramphenicol. Chloramphenicol stocks of 50 mg/mL were made using 70 % ethanol and kept in the freezer until required.

All centrifugation steps were performed in a table top centrifuge (MiniSpin®, Eppendorf) within the Class I/III safety cabinet.

2.4.2 *pDM4 deletion mutagenesis*

2.4.2.1 *Creation of a knockout cassette*

The pDM4 suicide vector was used for the creation of *B. pseudomallei* deletion mutants (Logue *et al.*, 2009). To create a knockout cassette 600 bp of both up and down stream flanking regions of the target gene were amplified using the appropriate primer set; primers 1 and 2 or primers 3 and 4 (Table 2.3 and Fig. 2.2). Each 600 bp 5' and 3' flanking regions (left and right flanks) was amplified using Phusion *Pfu* polymerase with 5 x HF or 5 x GC master mix, dNTPs and DMSO. 0.5 µL of *B. pseudomallei* K96243 gDNA was used per 20 µL PCR reaction. Reaction cycles for each 600 bp flanking region were an initial denaturation of 98 ^{o}C for 30 seconds, denaturation 98 ^{o}C for 10 seconds, annealing X ^{o}C (X = 54 ^{o}C for p1159_1/p1159_2; 68 ^{o}C for p2309_1/p2309_2, p2309_3/4, p1159_3/p1159_4, and p2299_1/p2299_2; 65 for ^{o}C p2455_1/p2455_2; 70 ^{o}C for p2299_3/p2299_4; 71 ^{o}C p2455_3/p2455_4 and p1479_1/p1479_2 and p1479_3/p1479_4 primer sets) for 30 secs, extension 72 ^{o}C for 45 secs, and a final extension of 72 ^{o}C for 7 minutes. PCR products were electrophoresed and gel purified (see section 2.2.4).

To create the knockout cassette both 5' and 3' flanking regions were fused together using a second 'fusion' PCR. Primers 2 and 3 contain homologous regions allowing for efficient ligation of both flanking regions together in a PCR reaction. Primers 1 and 4 were used together in a second fusion PCR reaction using purified 600 bp PCR products of both left and right flanks as templates. Reaction cycles for each fusion PCR products included an initial denaturation of 98 ^{o}C for 30 seconds, denaturation 98 ^{o}C for 10 secs, annealing X ^{o}C (71 ^{o}C for p2455_1/p2455_4 and p1479_1/p1479_4; 68 ^{o}C p2309_1/p2309_4; and 66 ^{o}C for p2299_1/p2299_4) for 2 minutes, extension 72 ^{o}C for 45 secs, and a final extension of 72 ^{o}C for 10 minutes. An extended extension time was used to ensure effective ligation of complementary

ends corresponding to the start codon, *Hind*III site, and stop codon (see Table 2.3). Fusion PCR for creation of a BPSS1159 proved difficult to optimise so further construction of a BPSS1159 pDM4 deletion construct was put on hold. The fusion PCR products were run on a 1 % agarose gel and the 1.2 kb PCR product was gel excised and purified.

Table 2.3 - Bacterial strains and plasmids used for *B. pseudomallei* mutagenesis and complementation

Bacterial strain	Characteristics	Reference
Burkholderia pseudomallei		
B. pseudomallei K96243	Wild-type Gram-negative saprophyte. Thailand patient isolate (1996)	(Sarkar-Tyson *et al.*, 2007)
Δ*narG*	K96243 BPSL2309 pDM4 deletion mutant	This study
Δ*narG*_pBHR-2309native	K96243 BPSL2309 pDM4 deletion mutant, pBHR-BPSL2309native, Cam^{Ra}	This study
Δ*narG*::pBH01	K96243 BPSL2309 pDM4 deletion mutant, pBHR-BPSL2309-2312native, Cam^{R}	
Escherichia coli		
S17 λ pir	Conjugal transfer of pDM4-deletion constructs	(Sarkar-Tyson *et al.*, 2007) Laboratory stock
DH5α λ pir	Chemically competent cloning strain F– Φ80*lac*ZΔM15 Δ(*lac*ZYA-*arg*F) U169 *rec*A1 *end*A1 *hsd*R17 (rK–, mK+) *pho*A *sup*E44 λ– *thi*-1 *gyr*A96 *rel*A1	Laboratory stock
5 α	DH5α derivative – *fhuA2 Δ(argF-lacZ)U169 phoA glnV44 Φ80 Δ(lacZ)M15 gyrA96 recA1 relA1 endA1 thi-1 hsdR17* High efficiency chemically competent cloning strain	NEB
DH5α pDM4-2309	DH5α λ *pir*, pDM4 BPSL2309 deletion construct, Cam^{R}	This study
DH5α pDM4-2455	DH5α λ *pir*, pDM4 BPSL2455 deletion construct, Cam^{R}	This study
DH5α pDM4-2299	DH5α λ *pir*, pDM4 BPSS2299 deletion construct, Cam^{R}	This study
DH5α pDM4-1479	DH5α λ *pir,* pDM4 BPSL1479 deletion construct, Cam^{R}	This study

S17 pDM4-2309	S17 λ *pir*, pDM4 BPSL2309 deletion construct, Cam^R	This study
S17 pDM4-2455	S17 λ *pir*, pDM4 BPSL2455 deletion construct, Cam^R	This study
S17 pDM4-2299	S17 λ *pir*, pDM4 BPSS2299 deletion construct, Cam^R	This study
S17 pDM4-1479	S17 λ *pir*, pDM4 BPSL1479 deletion construct, Cam^R	This study
5α pBH01	5α, pBHR-MCS-1::BPSL2309-2312native construct, Cam^R	This study
Plasmids		
pDM4	Suicide vector carrying *sacB* for sucrose counter selection Cam^{Ra}, Tet^{Ra}, Amp^{Ra}, *RP4 Mob, oriR6K, sacB, insB*	(Anand *et al.*, 2004), (Logue *et al.*, 2009)
pDM4-2309	pDM4, BPSL2309 deletion cassette, Cam^R	This study
pDM4-2455	pDM4, BPSL2455 deletion cassette, Cam^R	This study
pDM4-1479	pDM4, BPSL1479 deletion cassette, Cam^R	This study
pDM4-2299	pDM4, BPSS2299 deletion cassette, Cam^R	This study
pBHR::BPSL2309native	pBHR-MCS-1 vector, BPSL2309 with its native promoter, Cam^R	This study
pJ01	pJET1.2/blunt, BPSL2309-2312 operon with native promoter (BPSL2309-2312native), Amp^R	This study
pBH01	pBHR-MCS-1, BPSL2309-2312 operon with native promoter, Cam^R	This study

[a] Amp^R – Ampicillin resistance cassette; Cam^R – Chloramphenicol resistance cassette; Tet^R – Tetracycline resistance cassette

2.4.2.2 *Ligation of knockout cassettes into pDM4*

Once gel extracted and purified the 1.2 kb knockout cassettes and pDM4 plasmid were digested using appropriate Fast Digest restriction enzymes; *Xba*I and *Spe*I (for BPSS1159, BPSS2299, BPSL2455 and BPSL1479) or *Nhe*I and *Xba*I (for BPSL2309) and ligated together using T4 DNA ligase (see *2.2.11 Digestion and ligation*, and Fig. 2.2.). Once ligation was complete the plasmid was transformed into DH5α competent cells (see *2.2.12 Transformation*) and plated out on to LB agar plates containing 35 µg/mL chloramphenicol. Successful transformants were isolated using colony PCR using primer 1 (p2309-1, p2299-1, p2455-1, or p1479-1) and primer 4 (p2309-4, p2299-4, p2455-4, or p1479-4). Frozen stocks of successful transformants were made and plasmids (pDM4 deletion constructs – see Table 2.3) were extracted and sent for sequencing. Once confirmed the recombinant plasmids were then transformed into S17 λ *pir* competent cells, and verified using colony PCR.

2.4.2.3 *Conjugation into B. pseudomallei*

Once the pDM4 deletion construct was successfully created the recombinant plasmid (e.g. pD2309) was conjugated into wild-type *B. pseudomallei* in order to create an in-frame deletion mutant. *B. pseudomallei* K96243 and *E. coli* S17 λ *pir* strains containing the appropriate pDM4 recombinant plasmid were grown overnight in L-broth, supplemented with 35 µg/mL chloramphenicol when required. The next day both *B. pseudomallei* and S17 pD2309 cultures were centrifuged at 13,000 rpm and the supernatant was carefully removed. Control *B. pseudomallei* and S17 cell pellets were resuspended in 500 µL sterile LB broth and 10 µL was plated out onto nitrocellulose membranes. The S17 cell pellet (containing the pDM4 recombinant plasmid; pD2309) was then resuspended in 100 µL L-broth and added to the *B. pseudomallei* cell pellet to give a 1:1 mating mix ratio. 400 µL L-broth was then added and mating mix was re-centrifuged, supernatant discarded and the pellet was resuspended in 100 µL L-broth. 10 µL of the mating mix was plated out on to 3 separate nitrocellulose membrane on a LB agar plate incubated at 37 ^{o}C overnight.

The next day the entire bacterial growth from both the controls and mating mix were then scraped off and resuspended in 1 mL sterile PBS. 100 µL of each controls (S17 containing pDM4 recombinant plasmid) or *B. pseudomallei* of undiluted (neat) culture was then plated out onto LB agar plates containing 100 µg/mL chloramphenicol

Table 2.4 – Primers used for *B. pseudomallei* pDM4 mutagenesis, mutant confirmation and complementation

Primer name	Sequence (5'- 3')	Characteristics
pDM4 mutagenesis [a]		
p2309-1	CGAGCTAGCTCGCGATGTTCATCGTGCTG	*Nhe*I site
p2309-2	GGATCT**TAC**AAGCTT**CAT**CGTGTGTTTCTCCAAGGG	*Hind*III site, start and stop codons
p2309-3	CACACG**ATG**AAGCTT**TGA**AGATCCGCGCACAAGTGG	*Hind*III site, start and stop codons
p2309-4	CGCTCTAGATGTAGACCGAGCCCGACGGG	*Xba*I site
p2455-1	CAGACTAGTCGGCTCGCGCCGCAGGTCGAC	*Spe*I site
p2455-2	ACGGAT**TCA**AAGCTT**CAT**CGGTGACGAGGCGCCGCT	*Hind*III site, start and stop codons
p2455-3	TCACCG**ATG**AAGCTT**TGA**ATCCGTACTCAGCACTTC	*Hind*III site, start and stop codons
p2455-4	CGCTCTAGACGTACAGATCCTCGAGATAC	*Xba*I site
p1479-1	GTCACTAGTTCGGCGGGCAGGCGGCACGC	*Spe*I site
p1479-2	CGGCTT**TCA**AAGCTT**CAT**CGTCGATTGAAATGTTGA	*Hind*III site, start and stop codons
p1479-3	TCGACG**ATG**AAGCTT**TGA**AAGCCGGGCGGCGTAGCG	*Hind*III site, start and stop codons
p1479-4	CAGTCTAGACCGCGGTGCGCGGACACGGT	*Xba*I site
p1159-1	GGCACTAGTTTGCGTGATTCCCGCCATTTTC	*Spe*I site
p1159-2	GGATCT**TCA**AAGCTT**CAT**GGCTATCCTTGCGGGGAG	*Hind*III site, start and stop codons

p1159-3	ATAGCC **ATG** AAGCTT **TGA** AGATCCGCGCGCAGATCG	*Hind*III site, start and stop codons
p1159-4	CAG TCTAGA TGTAGATCGAGCCCGACGGG	*Xba*I site
p2299-1	GAT ACTAGT GCGGCTGCCGCGAACGACG	*Spe*I site
p2299-2	TCCTCG **TCA** AAGCTT **CAT** CTTCACTTCGCGTGGTTC	*Hind*III site, start and stop codons
p2299-3	GTGAAG **ATG** AAGCTT **TGA** CGAGGAGGACGCGATGACGC	*Hind*III site, start and stop codons
p2299-4	CAG TCTAGA GCG GGC CGC GTT CCC CAT TC	*Xba*I site
pDM4 mutant confirmation		
2309-fwd-1	CTACGTGTCGTGCGTCGCGATC	Binds 300 bp upstream of BPSL2309
2309-rv-2	CGATCGCGGGCAGGTTCGGATTC	Binds 300 bp downstream of BPSL2309
2309_check_fwd	CATCTGGCCGCTTCGCTGAGCG	Binds within BPSL2309
2309_check_rv	GACGCGCTTCGCGGGCACGC	Binds within BPSL2309
pBHR-MCS-1 complementation		
narG_fwd(2)	TTAGGATCCTGACGCCTCCCGCCTCTTTG	*Bam*HI site, binds approximately upstream of

		BPSL2309 to amplify gene with its native promoter
narG_rv(2)	GGCGTCTAGACATTGTTCTGCTCCTTCG	*Xba*I site, binds at the end of BPSL2309
comp_rv(2)	TAATCTAGAGCTGCGACATTCGAGCACGTGAG	*Xba*I site, binds downstream of BPSL2312

[a] Number denote primer number 1, 2, 3 or 4. See section 2.4.4 for more details.

Restriction sites are highlighted in blue

Those nucleotides in bold highlight the start and stop codons of each respective gene to be amplified

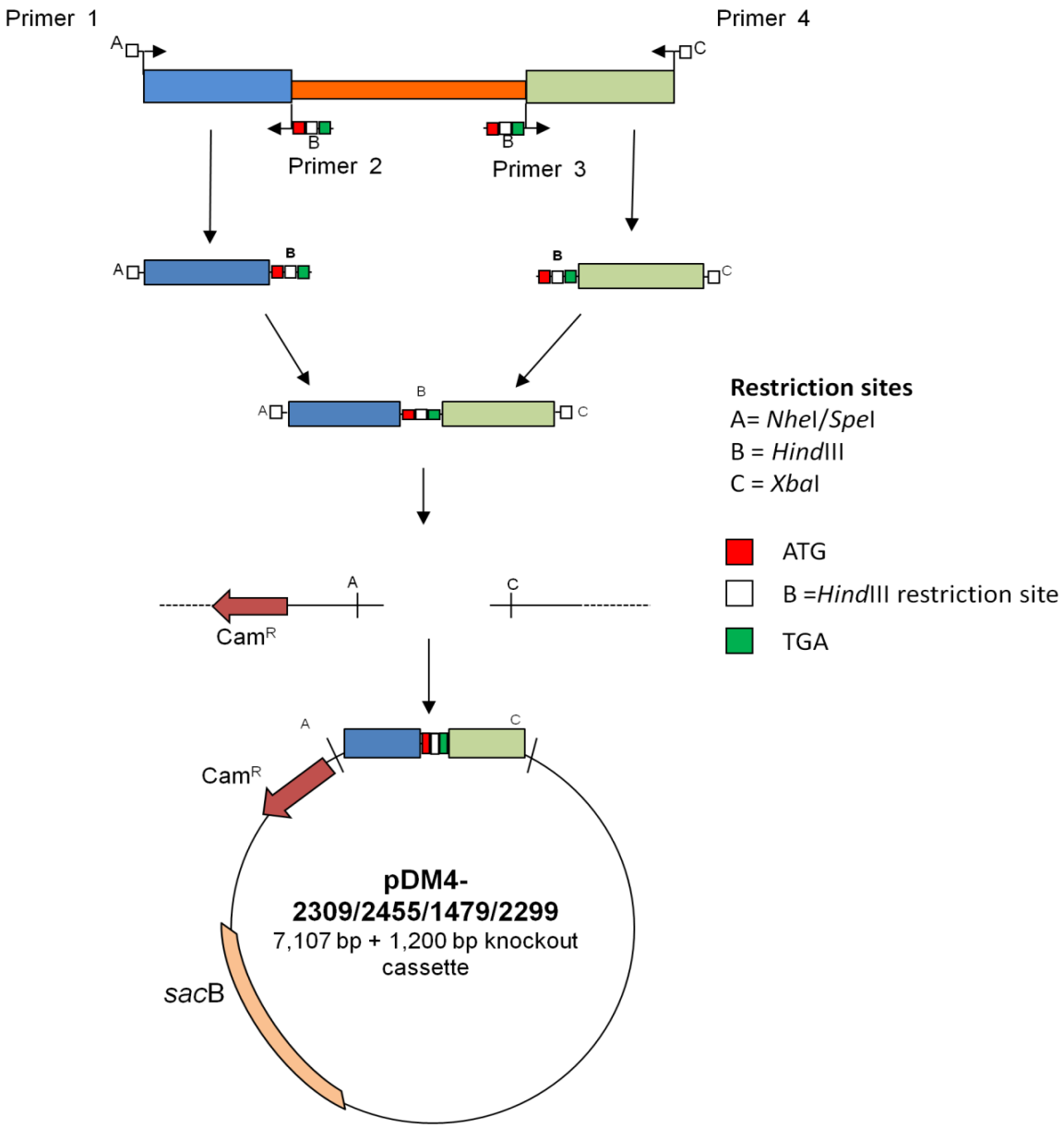

Figure 2.2 – Schematic of the work through for creation of a pDM4 suicide vector containing a knockout cassette. The 600 bp flanking regions, left (blue) and right (green) of the target gene (BPSL2309, BPSL2455, BPSL1479 or BPSS2299) were amplified by PCR, purified and fused together using second PCR reaction to create the knockout cassette (1,200 bp). Both the knockout cassette and pDM4 were digested with the appropriate restriction enzymes and ligated together to create pDM4-2309/2455/1479/2299, maintained in either DH5α or S17 λ pir competent cells. See section 2.4.2 for more details.

and 100 µg/mL gentamicin. A 10 fold serial dilution series to 10^{-2} was performed on the mating mix in PBS and 100 µL of each dilution (neat, 10^{-1}, and 10^{-2}) was plated out onto LB agar plates containing chloramphenicol (100 µg/mL) and gentamicin (100 µg/mL). Addition of chloramphenicol was used to select for the pDM4 recombinant plasmid and gentamicin to select against *E. coli* S17 ʎ *pir*. Plates were incubated for two days at 37 ^{o}C.

Selection for a *B. pseudomallei* merodiploid (*B. pseudomallei* containing integrated pDM4 deletion construct into target gene – 1st crossovers) was the performed by re-streaking colonies onto LB agar plates containing 100 µg/mL chloramphenicol and 100 µg/mL gentamicin. Frozen stocks were made of any successful merodiploids, and stored at -80 ^{o}C.

2.4.2.4 *Sucrose counter selection*

The pDM4 suicide vector contains a *sacB* gene allowing for efficient sucrose counter selection. Selection for the second crossover was achieved through selection for sucrose-resistance followed by a screening for chloramphenicol sensitivity to confirm excision of the suicide vector. *B. pseudomallei* strains have been shown to be resistant to sucrose, allowing for efficient use of sucrose counter selection to create deletion mutants (Logue *et al.*, 2009) (Fig. 2.3).

B. pseudomallei merodiploids were grown in L-broth overnight and standardised to an absorbance (590 nm) of 0.4 in 1 mL media. A 10 fold serial dilution was then performed and 100 µL of undiluted, 10^{-2} and 10^{-4} diluted cultures were plated LB agar (no NaCl) supplemented with 10 % sucrose plates and left to incubate for 3 to 5 days at 24 ^{o}C. Excision of the integrated pDM4 in the target gene via sucrose counter selection can results in either allelic exchange resulting in a deletion mutant or reversion to the wild-type form of the gene (Fig. 2.3) (Logue *et al.*, 2009). Colonies growing on the 10 % sucrose plates were then re-streaked onto LB agar plates and LB agar plates supplemented with 35 µg/mL chloramphenicol, to check for excision of the suicide vector. Any colonies exhibiting chloramphenicol sensitivity were then screened for deletion of the target gene using PCR.

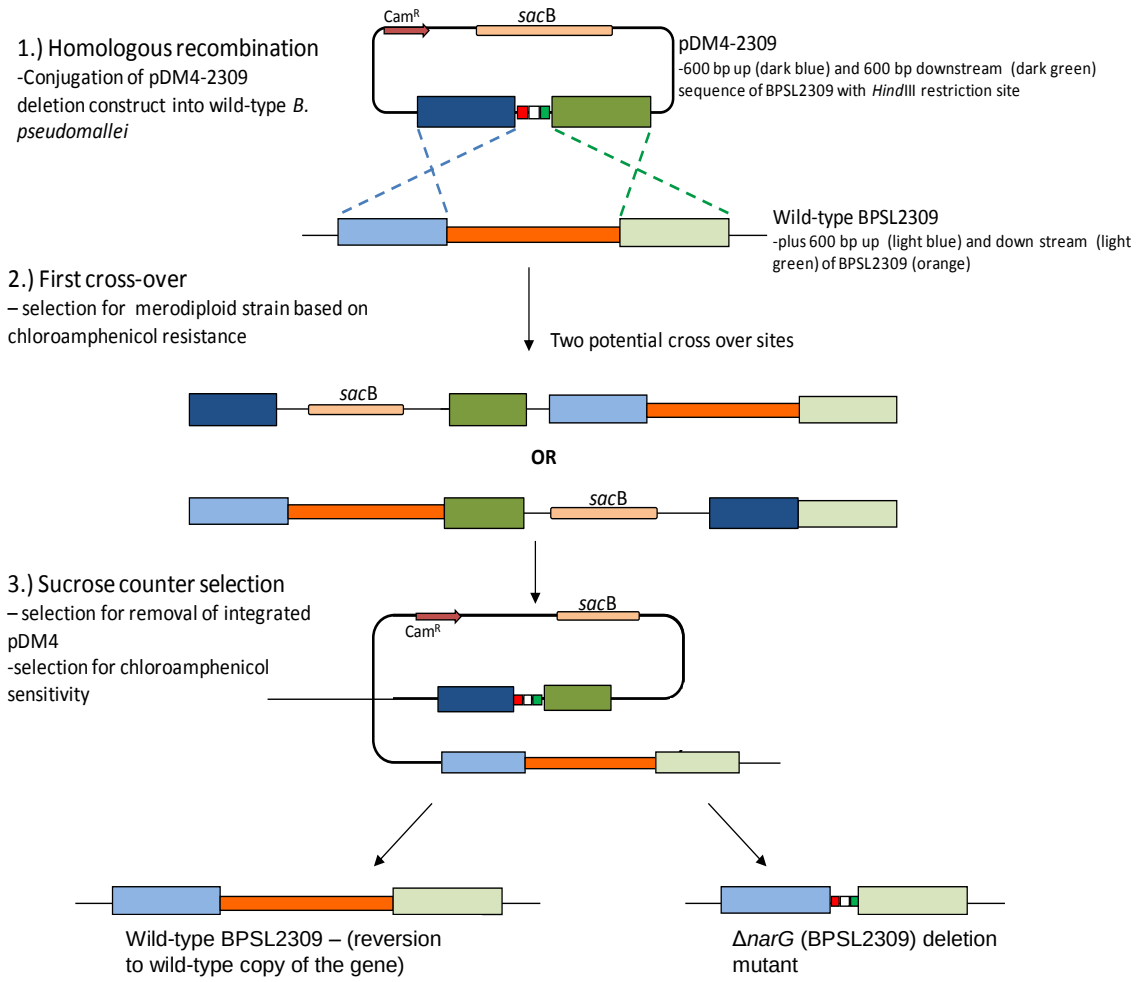

Figure 2.3 - Procedure for creation of a deletion mutant in *B. pseudomallei.* pDM4-2309 was conjugated into *B. pseudomallei* to create a *ΔnarG* deletion mutant. Diagram altered from Logue *et al.* (2009). 1.) Conjugation of pD2309 into the wild-type caused its integration into the genome by homologous recombination. 2.) Integration of the deletion construct into the genome could result in two potential first crossover events (generating what is known as a merodiploid), selected for based on chloramphenicol resistance. Merodiploids, containing the integrated plasmid are chloramphenicol resistant and sucrose sensitive due to the presence of *sacB.* 3.) The integrated plasmid encoding *sacB* was then removed by sucrose counter selection and subsequent screening for chloramphenicol sensitivity. Deletion construct 600 bp up (dark blue) or down (dark green) stream sequence with start codon ATG (red box), *Hind*III site (white box) and stop codon TGA (green box). Wild-type BPSL2309 gene shown in orange; wild-type 600 bp up (light blue) and 600 bp downstream sequences (light green), are represented with lighter colours for clarity. See sections 1.22.3 and 1.22.4 for experimental details.

2.4.3 *Boiled PCR lysates*

Boiled *B. pseudomallei* PCR lysates were used in all PCR reactions for confirmation of deletion mutants and complements. PCR lysates were created by boiling one colony in 150 µL of sterile water for 1 hour at 100 ^{o}C. 5 µL of the boiled PCR lysates were used in any subsequent PCR reaction.

2.4.4 *PCR to confirm deletion of target gene*

Two sets of PCR reactions were used to confirm deletion of BPSL2309, one using primers binding within the wild-type gene, generating a 300 bp product and one using primers binding outside BPSL2309, generating a 600 bp product. Primers binding to a 300 bp internal region of the gene (2309-check_fwd and 2309-check_rv) were used to verify the loss of BPSL2309 in the deletion mutant. Phusion PCR reaction mix with 5 x HF buffer and DMSO) was used with a reaction cycle of; initial denaturation 98 ^{o}C for 30 seconds, then cycles of 98 ^{o}C for 10 secs, 65 ^{o}C for 30 secs, 72 ^{o}C for 30 secs with a final extension of 72 ^{o}C for 7 minutes.

Primers binding 300 bp outside of the target gene (2309-fwd-1 and 2309-rv-2) were used to further confirm the deletion mutant. The Qiagen HotStar Taq with Q solution and 10 x PCR buffer was used for this primer set. PCR reaction cycle consisted of an initial denaturation step of 95 ^{o}C 15 for minutes, then 30 cycles of denaturation at 94 ^{o}C for 1 minute, annealing at 63 ^{o}C for 1 minute 30 secs, extension 72 ^{o}C for 5 minutes and a final extension time of 72 ^{o}C for 7 minutes.

2.4.5 *Complementation using pBHR-MCS-1*

In order to complement the phenotype exhibited by the Δ*narG* deletion mutant, BPSL2309 (*narG*) or BPSL2309-2312 (*narGHJI*) were separately cloned into pBHR-MCS-1 with the native promoter. The pBHR-MCS-1 vector encodes a chloramphenicol resistance cassette and *lacZ* gene found within the multiple cloning site allowing for efficient blue/white screening to identify any successful transformants. The pBHR-MCS-1 vector was selected as it lacked any promoter site so would allow for use of the genes native promoter.

BPSL2309 (*narG*) was amplified with its predicted native promoter by PCR using primers narG_fwd(2) and narG_rv(2) and Phusion polymerase (Thermo-Scientific) with 5 x HF master mix. DMSO was added to the PCR mix to prevent the formation of any unwanted secondary structures. PCR reaction cycle included an initial denaturation of 98 ^{o}C for 30 secs then 35 cycles of 98 ^{o}C for 10 secs, 64 ^{o}C for 30 secs, 72 for 2 minutes 30 secs and a final extension of 72 ^{o}C for 7 minutes. The resultant 3,966 bp product was purified using Qiagen PCR purification kit and eluted into 30-50 µL nuclease free water. Both the PCR product and pBHR-MCS-1 vector were digested with *Bam*HI and *Xba*I and ligated together using T4 DNA ligase, prior to transformation into DH5α competent cells (see section 1.9 and 1.10). Transformants were plated out onto LB agar plates containing chloramphenicol 50 µg/mL, X-GAL (20 µg/mL) and IPTG (100 µg/mL) to allow for blue/white screening. Any successful transformants (DH5α pBHR-MCS::BPSL2309native) were confirmed using PCR and DNA sequencing and were maintained in LB medium containing chloramphenicol 50 µg/mL.

The *narGHJI* operon and the native promoter (BPSL2309-2312native) was amplified using KOD Xtreme HotStart DNA polymerase, optimised for use in amplification of large PCR products and GC-rich templates. Each 25 µL PCR reaction contained 12.5 µL 2 x Xtreme buffer, 1 µL 10 mM dNTPs, 7.5 µL nuclease free water, 0.75 µL each forward and reverse primer, 0.5 µL KOD Xtreme HotStart DNA polymerase and 1 µL 50 ng/µL K96243 genomic DNA. Primers used to amplify the entire *narGHJI* (BPSL2309-2312) operon bound upstream of the native promoter and slightly downstream of the end of BPSL2312 (see primer sequences narG_fwd(2) and comp_rv(2) in Table 2.4). PCR cycling conditions were 94 ^{o}C for 2 minutes then 35 cycles of 98 ^{o}C for 10 secs, 65 ^{o}C for 30 secs and 68 ^{o}C for 7 minutes 30 secs. Initially the 6,632 bp PCR (BPSL2309-2312 with native promoter) product was purified, digested using *Bam*HI and *Xba*I and ligated into pJET1.2/blunt, and transformed into High Efficiency 5α competent cells following the same protocol as described previously. Any successful transformants containing pJET1.2::BPSL2309-2312native (pJ01) were confirmed using PCR, restriction digest and DNA sequencing.

Next BPSL2309-2312 was sub-cloned into the pBHR-MCS-1 vector following a *Bam*HI and *Xba*I restriction digest. Both the digested pBHR-MCS-1 vector and pJ01 vectors were run on an agarose gel, and the appropriate products were gel excised

using GeneJet Gel Extraction kit (Thermo-Scientific). Once gel excised and purified the digested products, pBHR-MCS-1 and BPSL2309-2312native, were ligated together using T4 DNA ligase and transformed into 5α High efficiency competent cells. Successful constructs, pBHR::BPSL2309-2312native (pBH01) were confirmed with restriction digest, PCR (using 2309check_fwd/2309check_rv primers and narG_fwd(2)/comp_rv(2)) and DNA sequencing.

2.4.6 *Conjugation of pBHR vector constructs into the Δ*narG *mutant– Tri-parental mating*

Tri-parental mating was performed to conjugate pBHR-MCS::BPSL2309native or pBH01 into the Δ*narG* mutant. Overnight cultures of the Δ*narG* mutant (recipient), DH5α pBHR-MCS::BPSL2309native (donor) or 5α pBH01, and *E. coli* pKR2013 (helper strain), were grown in 4 mL LB broth supplemented when required with appropriate antibiotic; chloramphenicol 50 µg/mL (donor), or kanamycin 30 µg/mL (helper). One mL of the overnight cultures was centrifuged for 5 minutes at 13,400 rpm and both donor and helper cell pellets were resuspended in 200 µL sterile PBS. 100 µL of each donor and helper bacterial suspension was added to the Δ*narG* cell pellet to give a final 1:1:2 mating mix ratio. The bacterial suspension was resuspended in 800 µL PBS prior to centrifugation and resuspended in 1 mL sterile PBS. 100 µL of the mating mix or controls were plated out onto nitrocellulose membranes placed onto a SOB agar plate and incubated at 37 ^{o}C overnight. The next day the mating mix and controls were resuspended in 1 mL of sterile L-broth and plated out onto LB plates containing gentamicin (100 µg/mL) and chloramphenicol (100 µg/mL) and plates were incubated for 2 days at 37 ^{o}C. Any potential complements were re-streaked onto antibiotic selective LB agar plates and confirmed with PCR using 2309check_fwd/rv primers.

2.5 ***B. pseudomallei in vitro and in vivo experiments***

2.5.1 Anaerobic growth of B. pseudomallei

Due to the safety constraints when working in the BSL3 lab all the anaerobic experiments were performed using an anaerobic box, rather than medical flat bottles sparged with nitrogen. All anaerobic growth experiments were carried out in the BD GasPak EZ Incubation container with two GasPak EZ anaerobic container system sachets with indicator. The level of anaerobiosis was monitored with an anaerobic indicator provided with the GasPak Anaerobic system sachets (white = anaerobic; blue = aerobic). The GasPak EZ Anaerobe Container System Sachets produced an anaerobic atmosphere within 2.5 hour with less than 1.0 % oxygen, and greater than or equal to 13 % carbon dioxide within 24 hours. Due to the constraints of only being able to take one time point for an experiment (due to loss of anaerobiosis when the container is opened), anaerobic growth experiments were conducted as end point experiments in a 24 well plate or on solid agar medium. Bacterial overnight cultures were standardised to an absorbance of 0.1 (600 nm). 500 µL of the standardised culture was then added to 500 µL of the desired medium (LB or M9 minimal media supplemented with or without 20 mM sodium nitrate). 100 µL of the standardised overnight culture was retained to determine the input CFU/mL. Both input and output CFU counts were performed in a 96 well plate using a 10 fold dilution series, with 10 µL spots plated out onto LB agar plates incubated aerobically at 37 ^{o}C. Input CFU/mL cell counts were divided by two to give the number of cells in the assay. Anaerobic growth of *B. pseudomallei* was determined by dividing output CFU/mL by the number of cells in the assay (input CFU per mL divided by 2).

2.5.2 Determination of NAR activity under aerobic conditions

To determine the effect of deletion of BPSL2309 on *B. pseudomallei* nitrate reductase activity both the wild-type and mutant (Δ*narG*) were grown aerobically in M9 minimal media supplemented with 20 mM sodium succinate, and a Griess reaction was performed in triplicate, as before (section 2.2.15). Samples were taken throughout aerobic growth and 1 mL samples were frozen at -80 ^{o}C. Three independent biological replicates were used per experiment, each with three technical replicates.

2.5.3 Motility

Motility experiments were performed as described previously (section 2.3.1) using nutrient broth, L-broth or M9 minimal media solidified using 0.3 % bacteriological agar. Overnight cultures (16 to 18 hour) were grown in 4 mL L-broth at 37 ^{o}C with shaking at 200 rpm. Motility plates were incubated at 37 ^{o}C for 24 to 48 hours. When appropriate the motility was supplemented with 20 mM sodium nitrate or 5 mM sodium nitrite

2.5.4 G. mellonella *challenge*

A *G. mellonella* challenge was performed in a similar manner to that seen in section 2.3.3, with overnight cultures grown in L-broth overnight at 37 ^{o}C (200 rpm) The only difference in the protocol was the use of a hands-free injection method requiring the user to pin down the galleria using two sterile 1 mL pipettes and a blunted Hamilton syringe, used to reduce the risk of accidental injection.

2.5.5 Sensitivity to acidified nitrite (pH 5)

To test whether the Δ*narG* mutant displayed altered sensitivity to RNIs both the wild-type *B. pseudomallei* and deletion mutant were grown in acidified L-broth (pH 5) containing varying concentrations of sodium nitrite (0 mM, 0.1 mM, 1 mM, 2 mM and 4 mM). Overnight cultures (grown in L-broth at 37 ^{o}C with shaking at 200 rpm) were standardised to absorbance (590 nm) of 1, and 4 mL of the acidified LB nitrite medium was inoculated with 10 % of the standardised culture prior to incubation at 37 ^{o}C for 6 to 24 hours. Input and output cell counts were performed using a 10-fold dilution series, spot plating onto LB agar plates and incubating overnight at 37 ^{o}C.

2.5.6 Persister cell assay

To test whether anaerobic respiration played a role in persister cell formation *B. pseudomallei* was treated with 400 µg/mL ceftazidime, in L-broth supplemented with or without nitrate. The persister cell assay was performed statically in a 24 well plate under conditions designed to mimic oxygen limiting conditions likely to be

experienced *in vivo* (Hemsley et al. unpublished data). *B. pseudomallei* was grown aerobically overnight (to late exponential/stationary phase – for 16 to 18 hours) in 4 mL L-broth and standardised to an optical density of 0.2 (corresponding to approximately 2 x 10^8 CFU/mL). Overnight *B. pseudomallei* cultures were also sub-cultured into fresh L-broth and grown for 6 hours to mid-log phase at 37 ^oC in 4 mL L-broth. A ceftazidime stock (10 mg/mL) was freshly prepared prior to each experiment in 0.1 M NaOH. A working stock of 800 µg/mL ceftazidime was prepared in L-broth. 500 µL of the ceftazidime working stock and 500 µL of the standardised bacterial suspension were mixed at a 1:1 ratio, to give a 400 µg/mL final concentration of ceftazidime and 1 x 10^8 CFU/mL. When appropriate 20 mM sodium nitrate was added to the 24 well plate assay wells prior to static incubation at 37 ^oC for 24 hours. After 24 hours the persister assay mixture was centrifuged for 7 minutes at 13,400 rpm and the supernatant was removed. The persister cell pellets was then resuspended in 1mL sterile L-broth and a 10 fold serial dilution and spot plating was performed to determine the output persister counts. Persister cell frequency was calculated by dividing the output CFU/mL by the number of cells in the assay (input CFU/mL divided by 2). All experiments were repeated in triplicate using at least three biological replicates.

An antibiotic kill curve was performed in the same manner as the persister cell assay, taking CFU/mL counts after 0, 2, 4, 6, 8, 10, 24 and 30 hours post antibiotic (ceftazidime) treatment.

2.5.7 Antibiotic minimal inhibitory concentration determination

An antibiotic MIC experiment was performed on *B. pseudomallei* and Δ*narG* mutant bacterial cultures in a 96 well plate in the presence or absence of 20 mM $NaNO_3$ to determine whether nitrate addition affected susceptibility of *B. pseudomallei* to various antibiotics. Overnight cultures (grown in 4 mL L-broth with shaking at 200 rpm, at 37 ^oC) were standardised to an optical density (OD) of 0.1 (absorbance 590 nm) to give 1 x 10^8 CFU/mL prior to performing a 100 x fold serial fold dilution in L-broth. 10 mg/mL antibiotic stocks were made in the appropriate media for ceftazidime hydrate (0.1 M NaOH), ciprofloxacin (0.1 M NaOH), trimethoprim (DMSO) and chloramphenicol (70 % ethanol), prior to preparation of a 1,024 µg/mL working stock in 1 mL L-broth. 100 µL of the antibiotic solution was added to the first well of a 96 well plate and a subsequent 1:1 dilution series was performed prior to addition of 100 µL

standardised bacterial culture. Experiment was performed using two independent biological replicates.

2.5.8 Hydrogen peroxide sensitivity

B. pseudomallei sensitivity to hydrogen peroxide was tested by treating standardised cultures with varying concentrations of hydrogen peroxide (H_2O_2) for 15 minutes. Overnight bacterial cultures were standardised to give 1 x 10^8 CFU/mL (OD = 0.1; absorbance 600 nm) and treated with 0 mM to 15 mM H_2O_2 for 15 minutes, in a final volume of 1 mL. After 15 minutes treatment the cultures were centrifuged and resuspended in fresh medium prior to performing a 10 fold serial dilution series and spot plating. Percentage survival was determined by comparing number of CFU from 0 mM treatment with those cells treated with hydrogen peroxide (2.5 mM, 5 mM, 10 mM and 15 mM H_2O_2). Experiment was performed using three biological replicates.

2.5.9 Murine infection model

The role of *B. pseudomallei* NarGHI in virulence was determine using a murine infection model, C56BL/6, performed in collaboration with Dr. Gregory Bancroft's group at the London School of Tropical Hygiene and Medicine. Female C57BL/6 mice (6-8 week-old; Harlan Laboratories, Bicester, Oxon, UK) were used throughout the studies. Groups of 8-10 mice were given free access to food and water and subjected to a 12 h light/dark cycle. For challenge the animals were handled under bio-safety level III containment conditions. All animal experiments were performed in accordance with the guidelines of the Animals (Scientific Procedures) Act of 1986 and were approved by the local ethical review committee at the London School of Hygiene and Tropical Medicine. For each infection, aliquots were thawed from frozen bacteria stocks and diluted in pyrogen-free saline (PFS). Prior to intranasal (IN) infection, mice were anesthetized intraperitoneally with ketamine (50 mg/kg; Ketaset; Fort Dodge Animal, Iowa, USA) and xylazine (10 mg/kg; Rompur; Bayer, Leverkusen, Germany) diluted in PFS. Challenge was performed administering a total volume of 50 µL IN containing 2000 CFU (high dose model) or 400 CFU (low dose model) of *B. pseudomallei* K96243 wild type or isogenic mutant. Control uninfected mice received 50 µL of PFS. The animals were observed twice daily for up to 150 days. Humane

endpoints were strictly observed and animals deemed incapable of survival were humanely killed by cervical dislocation.

2.5.10 Macrophage infection

To determine whether deletion of BPSL2309 affect intracellular replication J774A.1 murine macrophages were infected with either wild-type *B. pseudomallei* or the Δ*narG* mutant following a similar protocol to that seen in (Wand *et al.*, 2010). Cell culture was performed with the aid of Dr. Rachael Thomas. J774A.1 murine macrophage cell lines were maintained in DMEM medium supplemented with 10 % foetal bovine serum and 1 % L-glutamine (Hyclone) in a 37 ^{o}C 5 % CO_2^- incubator.

J774A.1 murine macrophages were seeded at a cell density of 1.5 x 10^5, resulting in a multiplicity of infection (MOI) 10:1, and cells were maintained overnight at 37 ^{o}C in a 5 % CO_2^- incubator. The next day the macrophages were washed three times in warmed modified DPBS and once with Leibovitz L-15 medium supplemented with L-glutamine and L-amino acids (Gibco). *B. pseudomallei* overnight cultures were standardised, to an optical density of 0.0015 (absorbance 590 nm) to give 1 x 10^6 CFU/mL, in L-15 media. The standardised bacterial suspension was carefully added to macrophage monolayers and incubated at 37 ^{o}C for 2 hours to allow for bacterial internalisation. Input cell counts were performed using standardised bacterial suspensions. After two hours cells were washed with DPBS and L-15 medium containing 1 mg/mL kanamycin, added to suppress the growth of extracellular bacteria. At appropriate time points (2, 4, 6 and 8 hours) cells were washed three times with warm PBS and cells were scraped off the bottom of the 24 well plate and lysed using purite water for 5 minutes. All cell counts were performed using a 10 fold dilution series and spot plating 10 µL onto LB agar plates, incubated overnight at 37 ^{o}C. The experiment was performed using three technical replicates.

2.5.11 Transmission electron microscopy

Transmission electron microscopy (TEM) was performed on samples taken from *B. pseudomallei* overnight cultures to determine whether the Δ*narG* mutant displayed any difference in flagella. TEM was performed with the aid of Peter Splatt, using TEM grids prepared by myself under containment level three conditions. Wild-type and

mutant cultures were grown aerobically overnight in LB medium. Cultures were fixed for 10 minutes using 4 % formaldehyde. Fixed samples were then centrifuged for 8 minutes at 3,000 rpm prior to resuspension in purite water and 2 µL of the fixed sample was placed onto a 3 mm TEM grid. Uranyl-acetate, a radioactive label and negative stain was added to the TEM grids prior to imaging. Three TEM grids were used per fixed bacterial samples, and a total of 15 images were taken.

Chapter 3 – Bioinformatic analysis of the respiratory flexibility exhibited by *B. thailandensis, B. pseudomallei* and *B. mallei*

3.1 Introduction

The ability to respire using a variety of diverse electron acceptors provides prokaryotic species with a distinct advantage, aiding the colonisation of a wide range of environments. Prokaryotic species possessing respiratory proteins that act under aerobic and anaerobic conditions are likely to have the greatest survival advantage, when compared to obligate aerobic or anaerobic respirers.

The respiratory flexibility of number of prokaryotes (such as *E. coli,* and *P. denitrificans*) have been well described, but currently little is known about the diversity of respiratory proteins encoded by *B. pseudomallei* and *B. thailandensis.* Prokaryotes are known to encode a range of primary dehydrogenases (such as NADH dehydrogenase, formate dehydrogenase, formate hydrogen-lyase, hydrogenase, succinate dehydrogenase and glycerol-3-phosphate dehydrogenase) and terminal oxidoreductases (e.g. NAR, quinol oxidases, NIR, and DMSO reductase), allowing for growth on a number of electron donors (formate, succinate, NADH and glycerol-3-phosphate) and electron acceptors (nitrate, nitrite and DMSO) (Unden & Bongaerts, 1997). There are multiple different types of cytochrome *c* oxidases, known to display varying affinities for oxygen concentrations. The cytochrome *bd* oxidase displays a high affinity for oxygen and is induced in the presence of low oxygen concentrations. By comparison the aa_3-type predominates under aerobic conditions, whereas the cbb_3-type functions in a micro-aerophilic environment (Garcia-Horsman *et al.*, 1994; Pitcher & Watmough, 2004).

The structure of prokaryotic electron transport chains is highly diverse and varies in different species depending on the lifestyles that they lead. Denitrification is often associated with free-living prokaryotic species (e.g. *P. denitrificans*) and those with clinical relevance (e.g. *P. aeruginosa* and *N. gonorrhoeae*). *E. coli* does not encode a cytochrome bc_1 complex and it cannot denitrify, as it lacks dissimilatory NIR, NOR and

NOS. In comparison to *E. coli, R. sphaeroides* can take electrons from both the cytochrome bc_1 complex (ubiquinol cytochrome *c* oxidoreductase) and quinone (Garcia-Horsman *et al.*, 1994). *P. denitrificans* and *P. aeruginosa* both encode a full denitrification pathway, possessing all genes required for the reduction of nitrate to dinitrogen gas. Although *E. coli* does not encode a full denitrification pathway it can grow anaerobically via respiratory ammonification, reducing nitrate to ammonia via Nar and Nrf (Cole, 1996). The capacity for *E. coli* to only grow via respiratory ammonification is likely to be partly due to the lack of a cytochrome bc_1 complex, required for electron transfer to NIR and NOR in the denitrification pathway.

Nitrate, nitrite, DMSO and TMAO can be utilised as alternative terminal electron acceptors to power growth in oxygen limiting environments (Richardson, 2000). Denitrification (anaerobic nitrate respiration) utilises a series of reductase enzymes, NAR, NIR, NOR, and NOS, to sequentially reduce nitrate to dinitrogen gas. Many of the enzymes required for anaerobic respiration, such as formate dehydrogenase and NarGHI, require a molybdenum cofactor for catalysis, synthesised via the molybdopterin biosynthetic pathway (Schwarz *et al.*, 2009).

B. pseudomallei, the causative agent of melioidosis is closely related to the avirulent *B. thailandensis* and *B. mallei* (Galyov *et al.*, 2010). All three of these *Burkholderia spp.* possess two chromosomes encoding genes required for core metabolic functions and virulence. The *B. pseudomallei* genome is composed of two chromosomes, one of 4.07 megabase pairs (chromosome 1) and one of 3.17 megabase pairs (chromosome 2) (Holden *et al.*, 2004). *B. pseudomallei* genome exhibits gene partitioning, with chromosome 1 encoding genes required for core metabolic function and cell growth, and chromosome 2 encoding genes required for accessory functions, virulence and adaptation (Holden *et al.*, 2004). *B. mallei* is an obligate pathogen and has a smaller genome (5.8 Mb) to that seen in *B. pseudomallei* (7.2 Mb) and *B. thailandensis* (6.7 Mb) (Nierman *et al.*, 2004). *B. thailandensis* is a very close, but generally avirulent, relative of *B. pseudomallei* encoding a large majority of the same genes seen in the pathogenic *B. pseudomallei* and *B. mallei.* This high degree of genetic similarity of *B. thailandensis* to *B. pseudomallei* allows *B. thailandensis* to be utilised as a model organism to identify genes required for survival and virulence.

B. pseudomallei is a facultative anaerobe, and is known to survive for extended periods of time under both aerobic and anaerobic conditions (Dance, 2000; Hamad *et al.*, 2011). Previous studies have shown *B. pseudomallei* to be able to respire anaerobically using nitrate (Hamad *et al.*, 2011), but currently no studies have been done into identifying the molecular mechanisms required for anaerobic growth. This next chapter will present bioinformatic data used to determine the respiratory flexibility of *B. thailandensis, B. pseudomallei* and *B. mallei.* Genome wide searches, using NCBI, K.E.G.G. and the *Burkholderia* genome database, were undertaken in order to identify genes in *B. thailandensis, B. pseudomallei* and *B. mallei* required for aerobic respiration, anaerobic respiration and molybdopterin biosynthesis based on what is known in other prokaryotes.

Results

3.2 Identification of genes required for aerobic and anaerobic respiration

3.2.1 *Identification of respiratory proteins required for the* B. thailandensis *E264,* B. pseudomallei *K96243,* and B. mallei *ATCC 23344 electron transport chain*

Bioinformatic searches, using K.E.G.G and the *Burkholderia* genome database, were used to determine the respiratory flexibility of *B. pseudomallei* K96243*, B. mallei* ATCC 23344 and *B. thailandensis* E264*,* based on similarities with other prokaryotic species (Unden & Bongaerts, 1997). *B. thailandensis, B. pseudomallei* and *B. mallei* were shown to encode an array of different primary dehydrogenases (e.g. NADH dehydrogenase, succinate dehydrogenase, formate dehydrogenase, and formate hydrogen-lyase), and wide range of different cytochrome *c* oxidases and terminal oxidoreductases (Table 3.1). This diversity of respiratory proteins is likely to allow for growth under a wide range of conditions using multiple different carbon sources (e.g. succinate, formate, and glucose) and electron acceptors, (e.g. oxygen or nitrate). *B. thailandensis* and *B. pseudomallei* also encode a wide array of different *c*-type cytochromes, required for the electron transport chain during aerobic and anaerobic growth (see Chapter 8 – Appendix Table 1).

A putative *cbb*$_3$-type cytochrome *c* oxidase was identified in *B. thailandensis* E264*.* Intriguingly, no ortholog of the putative *B. thailandensis cbb*$_3$-type cytochrome

c oxidase (BTH_II1618-1619) was identified in any other *Burkholderia* species, apart from *B. ambifaria* MC40-6 (BamMC406_4623-4624). *B. ambifaria* is an environmental species and part of the *B. cepacia* complex (Coenye *et al.*, 2001). BTH_II1618-1619 displays around 70 % identity to BamMC406_4623-4624 found in *B. ambifaria* and around 55 to 60 % identity with CMR15_mp20073-20074 from *R. solanacearum. B. thailandensis, B. ambifaria* and *R. solanacearum* are found environmentally within the soil, often associated with plant roots. The significance of the putative *cbb*$_3$-type cytochrome *B. thailandensis* and *B. ambifaria* alone and its absence in any pathogenic *Burkholderia* species is currently unknown. However, one could speculate that *B. thailandensis,* unlike *B. pseudomallei* or *B. mallei,* requires this putative *cbb*$_3$-type cytochrome *c* oxidase specifically for environmental survival, and not colonisation of the host.

All three *Burkholderia* species, unlike *E. coli* and other prokaryotic species, encode a cytochrome *bc*$_1$ complex and two ATP synthases, one on each chromosome (Table 3.1). Possession of two separate ATP synthases may indicate that they are differentially expressed, and may be required for either aerobic or anaerobic respiration. Interestingly the ATP synthase encoded on chromosome 2 of *B. pseudomallei* (BPSS1945-1953) has been shown to be induced under hypoxic conditions (Hamad *et al.*, 2011). This indicates that BPSS1945-1953 may be required for ATP synthesis under anaerobic conditions, whereas the ATP synthase encoded on chromosome 1 (BPSL3395-3404) may function during aerobic respiration.

3.2.2 *Identification of genes required for denitrification*

A genome wide search using the NCBI database was successfully used to identify genes required for denitrification in *B. pseudomallei* K96243 (Fig. 3.1). Following the identification of a full predicted denitrification pathway in *B. pseudomallei* K96243 and *B. thailandensis* E264 a K.E.G.G ortholog analysis and NCBI BLAST analysis were used to determine the degree of sequence conservation and orthology with other *Burkholderia* spp. (Table 3.2).

Both *B. thailandensis* E264 and *B. pseudomallei* K96243 encode two membrane-bound NAR, two putative multi-copper oxidases thought to be copper

Table 3.1 - Predicted respiratory proteins encoded by *B. thailandensis, B. pseudomallei* and *B. mallei.*

	Genes	*B. thailandensis* (E264)	*B. pseudomallei* (K96243)	*B. mallei* (ATCC 23344)	Sequence identity (%)[a]
Primary dehydrogenases					
NADH dehydrogenase	*nuoA-N*	BTH_I1061-1074	BPSL1211-1224	BMA1819-1829	97 – 100
	ndh	BTH_I0660	BPSS1769	BMA0320	94
NAD^+ formate dehydrogenase	*fdsGBAD*	BTH_I1621-1624	BPSL2528-2531	BMA0448-0451	93 –100
Formate dehydrogenase-N	*fdoGHI*	BTH_II0707-0710	BPSS1665-1667	BMA1680-1682	94 – 98
Succinate dehydrogenase	*sdhCDAB*	BTH_II0660-0663	BPSS1717-1720	BMAA1746-1749	98.6 - 100
Putative formate hydrogen-lyase	-	BTH_II1261-1266	BPSS1142-1147	-	95
Glycerol-3-phosphate dehydrogenase	*glpD*	BTH_I0600	BPSL0688	BMA0241	96
Pyruvate dehydrogenase	*poxB*	-	BPSS1636	BMAA1650	99.5
Cytochrome bc_1 complex	*petABC*	BTH_I2975-2977	BPSL3121-3123	BMA2696-2698	95 – 99
ATP synthase		BTH_I3307-3315	BPSL3395-3404	BMA2950-2958	95-99
		BTH_II0419-0426	BPSS1945-1953	BMAA0123-0131	90-100
Terminal oxidases					
aa_3 type cytochrome *c* oxidase	*coxABC*	BTH_I0426-0430	BPSL0453-0458	BMA3193-3197	96 - 99
Cytochrome *c* oxidase(s)	*coxAB*	BTH_I2874-2875	BPSL1259-1260	-	97

	-	BTH_I2175	BPSL1454	BMA1408	90.8
		-	BPSL0722-0723	-	-
Cytochrome *bd* ubiquinol oxidase(s)	*cydAB*	BTH_I0453-0454	BPSL0501-0502	BMA3177-3178	96-100
		BTH_II2148-2149	BPSS0234-0235	BMAA1835-1836	97-99
		-	BPSS1376-1377	-	
Cytochrome *bo*$_3$ ubiquinol oxidase	*cyoABCD*	BTH_I1785-1788	BPSL2378-2381	BMA0600[b]	96-97
		BTH_II0479-0482	BPSS1894-1897	BMAA0194-0197	95-100
Putative *cbb*$_3$-type cytochrome *c* oxidase	*ccoNOP*	BTH_II1618-1620	-	-	-
Nitrate reductase	*narGHJI*	BTH_I1851-1854	BPSL2309-2312	BMA1731-1734	90-99
Nitrate reductase	*narZYWV*	BTH_II1249-1252	BPSS1156-1159	-	90-99
Putative DMSO reductase	*dmsABC*	-	BPSS2299-2301	BMAA2047-2049	98-100

[a] Sequence identity of *B. pseudomallei* K96243 and *B. mallei* ATCC 23344 genes to those orthologous genes found in *B. thailandensis* E264; according to a K.E.G.G ortholog search

[b] Only one gene was identified in gene cluster for *B. mallei* ATCC 23344 (BMA0600), which appears to be missing two subunits required for formation of the cytochrome *bo*$_3$ ubiquinol oxidase

- marked in the table indicate absence of homolog or the absence of gene cluster in the respective *Burkholderia* species.

nitrite reductases (Cu-NIR), a NADH-dependent nitrite reductase (an assimilatory nitrite reductase not required for respiration), NOR and NOS (Table 3.2 and Figure 3.1). Unlike *B. thailandensis* and *B. pseudomallei*, *B. mallei* ATCC 23344 only encodes one membrane-bound NAR and one NOS. All the genes predicted to be involved in denitrification in *B. thailandensis* display around 91 % to 99 % sequence identity with those seen in pathogenic *B. pseudomallei* and *B. mallei.* This high degree of percentage identity suggests *B. thailandensis* to be a good model for identification of those genes required for anaerobic nitrate respiration and determination of their role in virulence (see Chapter 4).

3.2.3 *Nitric oxide reductase and nitrous oxide reductase in* B. thailandensis *E264 and* B. pseudomallei *K96243*

All three *Burkholderia* species analysed encode two separate *norZ* genes (Table 3.2), predicted to encode a single subunit nitric oxide reductase. BTH_I1813 shares 71.7 % identity with *norB* from *R. solanacearum* (RSp1505) and 48.2 % identity with *norB* from *N. gonorrhoeae* (NGO1275). The second *norZ* in *B. thailandensis,* BTH_II0945, shares 64.4 % identity with the *norB* from *Legionella pneumonia* (lpa_03215).

B. pseudomallei and *B. thailandensis* encode a multicopper nitrous oxide reductase composed of *nosZ* (catalytic subunit), *nosD* (periplasmic copper processing gene), *nosF* (cytoplasmic protein; related to ABC transporters), *nosY* (transmembrane protein) and *nosL* (Philippot, 2002) (Fig. 3.1 and Table 3.2) sharing around 90 to 97 % identity. The *nosZ* gene in *B. thailandensis* shares 51 % identity with *P. aeruginosa* PA3392, and 47 % identity with Pden_4219 from *P. denitrificans.*

The majority of studies in to the role of anaerobic respiratory genes in virulence has concentrated on NAR and NIR, and not NOS or NOR. Because of this detailed bioinformatic analysis was not conducted on the nitric oxide and nitrous oxide reductases encoded by both *B. thailandensis* E264 and *B. pseudomallei* K96243.

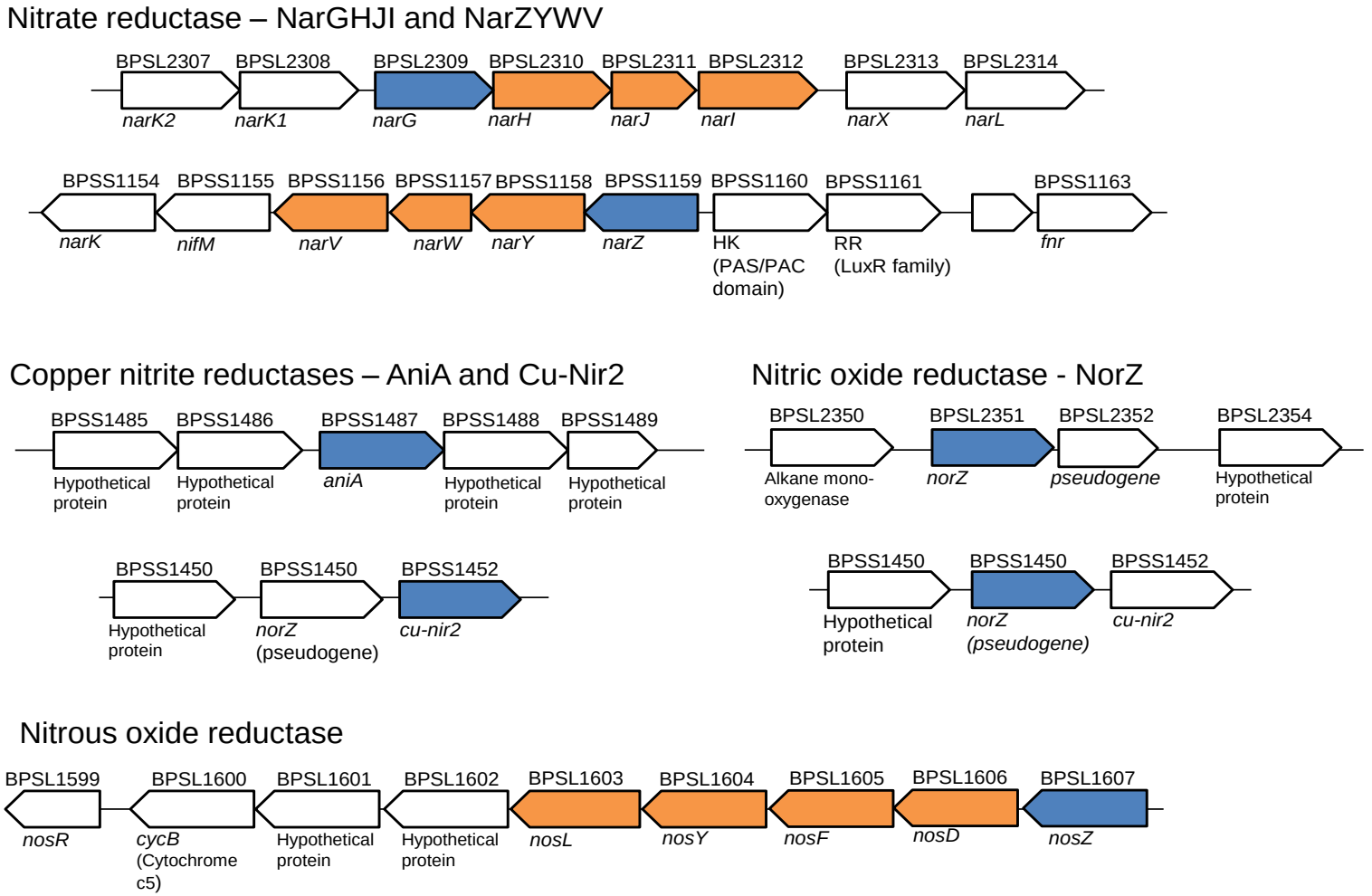

Figure 3.1 – **Organisation of gene clusters encoding genes required for denitrification in *B. pseudomallei* K96243.** Arrows denote direction of transcription. Genes encoding the catalytic subunits are shown in blue and those genes in orange indicate those required for the function of the enzyme. BPSS1154-BPSS1161 gene operon encodes a HK – histidine kinase; RR – response regulator. The nitrous oxide reductase gene cluster includes a *cycB encoding* a cytochrome c_5. Gene clusters have been previously identified in (Philippot, 2002).

Table 3.2 - Putative genes required for denitrification in *B. thailandensis, B. pseudomallei* and *B. mallei*

	Gene name(s)	***B. thailandensis*** **(E264)**	***B. pseudomallei*** **(K96243)**	***B. mallei*** **(ATCC 23344)**	**Sequence identity (%)[a]**
Chromosome 1					
Nitrate reductase	*narGHJI*	BTH_I1851-1854	BPSL2309-2312	BMA1731-1734	95 - 99
NADH-dependent NIR[b]	*nirBD*	BTH_I0463-0464	BPSL0511-0512	BMA3130-3131	95 - 96
Nitric oxide reductase	*norZ*	BTH_I1813	BPSL2351	BMA0633	96
Nitrous oxide reductase	*nosZDFYL*	BTH_I2317-2325	BPSL1599-1607	BMA09885-0995	90- 97
Chromosome 2					
Nitrate reductase	*narZYWV*	BTH_II1249-1252	BPSS1159-1156	-	91 – 97
Copper-nitrite reductase(s)	*aniA*	BTH_II0881	BPSS1487	BMAA0755	94
	cu-nir2[c]	BTH_II0944	BPSS1452	BMAA0798	86
Nitric oxide reductase	*norZ*	BTH_II0945	BPSS1450 (pseudogene)	BMA0799	98
NADH-dependent NIR[b]	*nirBD-2*	BTH_II1170-1171	BPSS1242-1243	BMAA1085-1086	94

[a] Sequence identity (%) relates to gene orthology (K.E.G.G) of *B. pseudomallei* and *B. mallei* genes to those orthologous genes found in *B. thailandensis* E264

[b] NADH-dependent nitrite reductase (NADH-dependent-NIR) are not required for anaerobic respiration, but is likely to play a role in nitrate assimilation

- Denotes absence of homologous gene cluster in the respective *Burkholderia* spp.

[c] Annotated as *cu-nir*2 in this study

3.3 *Bioinformatic analysis of the NAR and NIR genes encoded by* B. pseudomallei *and* B. thailandensis

3.3.1 *Both* B. pseudomallei *K96243 and* B. thailandensis *E264 encode two membrane-bound nitrate reductases*

Both *B. thailandensis* and *B. pseudomallei* encode two membrane-bound nitrate reductases (Table 3.2), which display similarity to either the *narGHJI* or *narZYWV* operons found in other prokaryotic species. All genes encoded within the *narGHJI* and *narZYWV* operons in *B. thailandensis* E264 share between 90 and 100 % sequence identity with the orthologous gene clusters in *B. pseudomallei* K92643 and *B. mallei* ATCC 23344 (Fig. 3.2 a and c). *B. mallei,* in comparison to *B. thailandensis* and *B. pseudomallei,* does not encode a *narZYWV* operon within its genome. A K.E.G.G. ortholog analysis was performed on both the NAR operons to determine the degree of sequence identity of those *B. thailandensis* genes (BTH_I1849-BTH_I1856 or BTH_II1249-1252) in *E. coli, P. aeruginosa* and *Salmonella*. (Fig. 3.2 b and d). The genes encoding NAR are organised into operons, which in the case of *narGHJI* includes genes coding for a nitrate/nitrite transporters (*narK*1 and *narK*2) and a NarXL two component system (TCS), likely to be involved in its regulation (Fig. 3.1). The *B. thailandensis narG/narZ* and *narH/narY* genes share between 60 to 70 % identity with those orthologous genes in *E. coli, P. aeruginosa* and *Salmonella.* In comparison the membrane anchor subunits (*narI/narV*) and the chaperone proteins involved in the assembly of NAR (*narJ/narW*), are less well conserved, and show only between 30 to 40 % and 40 to 50 % identity (Fig. 3.2).

Like *P. aeruginosa* and *E. coli,* the *B. thailandensis* and *B. pseudomallei narGHJI* operon also encodes a NarK nitrate/nitrite transporter and a NarXL TCS. Most published *narGHJI* gene clusters exhibit the sequence order <*narXL-narK>narGHJI*> (arrows indicate transcriptional direction), whereas the gene cluster in *R. solancearaum* and *Burkholderia spp. narK>narGHJI>narXL*> (Stewart, 2003) (Fig. 3.2). The significance of this gene rearrangement in the *Burkholderia* spp is currently unknown. Softberry promoter analysis has revealed the presence of an *rpoD* (a housekeeping sigma factor - σ^{70}) recognition site in the predicted *narG* promoters of NarG encoded by *B. pseudomallei* (BPSL2309) and *B. thailandensis* (BTH_I1854). A putative NarL binding domain, similar to that seen in *P. aeruginosa* was also found

upstream of both BPSL2309 and BTH_I1854, within the promoter region. This pointed towards the potential role of NarXL in the regulation of the *narGHJI* operon in *B. pseudomallei* K96243 and *B. thailandensis* E264*.*

B. thailandensis E264 and *B. pseudomallei* K96243*,* unlike *B. mallei* ATCC 23344*,* encode a second nitrate reductase on chromosome 2 (BTH_II1249-1252 or BPSS1156-1159). This NAR displays a high degree of similarity (40-70 %) with the cryptic nitrate reductase, *narZYWV*, seen in *E. coli* and *Salmonella.* This gene cluster was annotated in this study as a cryptic Nar due to the lack of a NarXL TCS within the operon and the fact that this cluster is not found in *B. mallei.* This second Nar (BTH_II1249-1252 or BPSS1156-1159) is thought to play a secondary role in adaptation to hypoxia or environmental survival rather than anaerobic respiration. Softberry promoter analysis has revealed the presence of a putative FNR binding site upstream of BPSS1159 (*narZ*), and *argR* and *argR2* binding sites upstream of BTH_I1854.

Sequence alignment and comparison with published NarG sequences has revealed that both nitrate reductases in *Burkholderia* to be part of the D-group of molybdoenzymes, containing the conserved aspartate (D) ligand, found within the substrate entry channel (Fig. 3.3 b.) (Jormakka *et al.*, 2004; Martinez-Espinosa *et al.*, 2007). The N-terminal region of NarG in *E. coli* contains conserved cysteine residues and histidine residue ($HxxxCxxxC(x)_nC$), involved in coordination of the high-spin [4Fe-4S] cluster (Fig. 3.3 a.) (Bertero *et al.*, 2003; Jormakka *et al.*, 2004; Magalon *et al.*, 1998; Rothery *et al.*, 2004). These same residues are also found in both nitrate reductase of all three *Burkholderia spp.* (Fig. 3.3).

Along with the identification of the amino acid residues involved in the coordination of the [4Fe-4S] cluster, a second signature relating to the substrate binding pocket (Martinez-Espinosa *et al.*, 2007) was identified (Fig. 3.3 b). This signature relates to a the potential substrate entry site designated by tyrosine (Y), aspartate (D), glutamine (Q) and threonine (T) residues, as seen in *E. coli* and *P. denitrificans* (Martinez-Espinosa *et al.*, 2007).

a.) *narGHJI* operon in *B. thailandensis, B. pseudomallei* and *B. mallei*

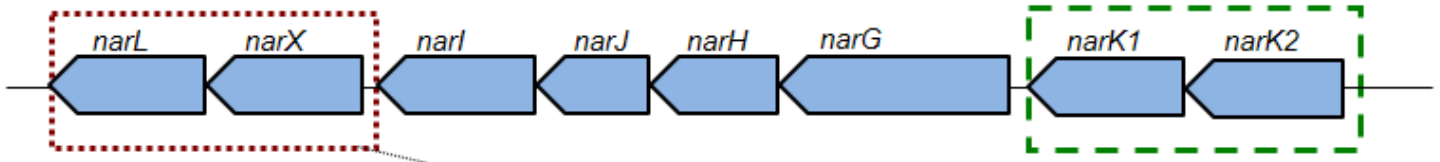

b.) *narGHJI* operon in *P. aeruginosa, E. coli* and *Salmonella* spp.

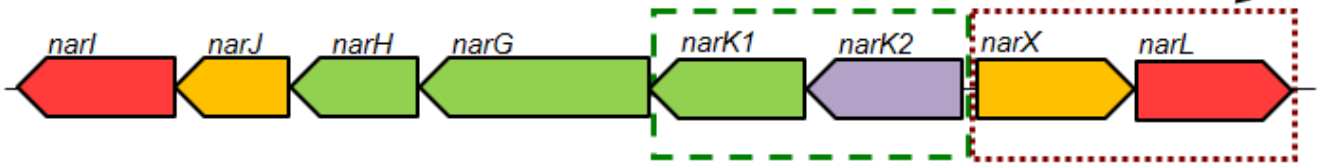

c.) *narZYWV* operon in *B. thailandensis* and *B. pseudomallei*

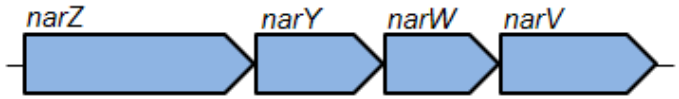

d.) *narZYWV* operon in *E. coli* and *Salmonella spp.*

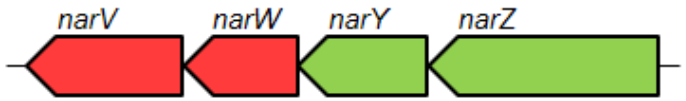

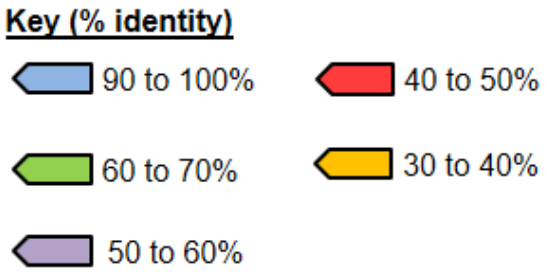

Figure 3.2 – K.E.G.G. ortholog analysis on both the nitrate reductase operons in *B. thailandensis* E264*.*** K.E.G.G. ortholog analysis (diagram on the previous page) is based on the gene clusters BTH_I1849-1854 and BTH_II1249-1252 from *B. thailandensis* E264. Diagram represents transcriptional direction of *B. thailandensis* genes. Percentage sequence identity of each of the *B. thailandensis* E264 genes with orthologs in other prokaryotes (such as *B. pseudomallei* K96243 and *B. mallei* ATCC 23344, or *P. aeruginosa, E. coli* and *Salmonella*), is shown with different colours (see key). a.) Similarities of the NarGHJI operon encoded on chromosome 1 in *B. thailandensis, B. pseudomallei* and *B. mallei.* All the genes encoded in the operon, including *narK1* and *narK2* and the *narX/narL*, share between 90 and 100 % sequence identity. b.) NarGHJI operon in *P. aeruginosa, E. coli* and *Salmonella* spp. Colours relate to percentage identity to the corresponding *B. thailandensis* genes. Please note only *P. aeruginosa* encodes two NarK genes (*narK1* and *narK2*), whereas *Salmonella* and *E. coli* only one NarK (*narK2*). The sequence identity for *B. thailandensis narK2* therefore only refers to its identity with the *P. aeruginosa* ortholog. c.) Second nitrate reductase encoded only in the genome of *B. thailandensis* and *B. pseudomallei.* This gene cluster is not found in *B. mallei.* d.) NarZYWV operon in *E. coli* and *Salmonella* spp. *B. pseudomallei* and *B. mallei narGHJI* and *narZYWV* operons are encoded on the opposite strand to *B. thailandensis.* See text for details.

a.) Iron sulfur cluster signature

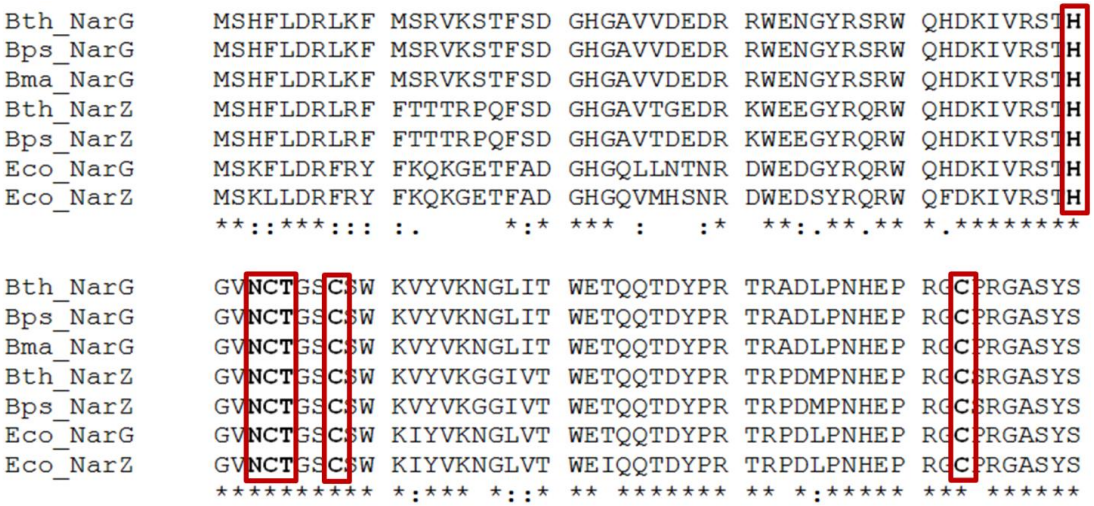

b.) Substrate pocket signature

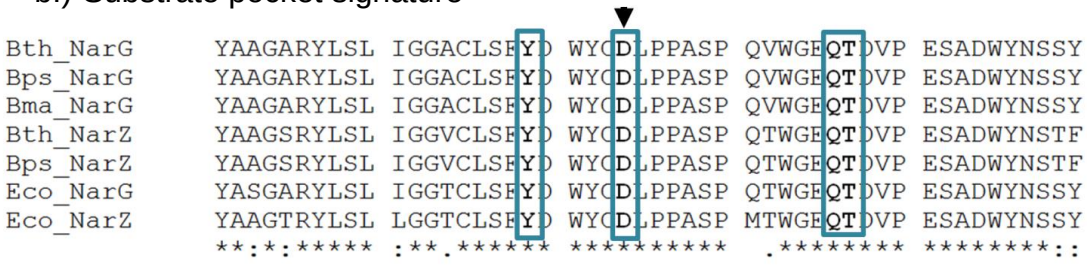

Figure 3.3 – *Burkholderia* nitrate reductases are part of the D-group of molybdoenzymes. Figure shows a sequence alignment of the N–terminal region of NarG and NarZ from *B. thailandensis* E264 (Bth_NarG/Bth_NarZ), *B. pseudomallei* K96243 (Bps_NarG/Bps_NarZ), *B. mallei* ATCC 23344 (Bma_NarG), and *E. coli* (Eco_NarG/Eco_NarZ). a.) Iron-sulphur cluster signature, highlighting potential cysteine and histidine residues involved in coordination of the high spin [4Fe-4S] cluster found in the *E. coli* NarG (Jormakka *et al.*, 2004). b.) Potential substrate binding pocket signature in NarG. Arrow points towards the conserved Asp (D), within the substrate entry channel required for the coordination of Mo-*bis*MGD. Highlighted residues in the sequence alignment are based on similarity to the NarG sequences annotated in (Martinez-Espinosa *et al.*, 2007; Rothery *et al.*, 2004). Alignment was performed by Clustal Omega. Asterisks (*) denote conserved amino acid residues in all sequences analysed. See text for details.

3.3.2 B. pseudomallei *K96243 NarG (BPSL2309) structural model*

B. pseudomallei NarG shares 67.8% sequence identity with *E. coli* NarG. *B. pseudomallei* K96243 NarG (BPSL2309) was modelled against the *E. coli* NarGHI (PDB: 1Q16; (Bertero *et al.*, 2003)) to determine the degree of structural homology. Structural analysis was performed using the online I-TASSER service. The *B. pseudomallei* NarG structure was shown to be almost identical to that seen in *E. coli* NarG (Fig. 3.4), both displaying a loop required for binding to the NarH subunit.

3.3.3 B. thailandensis, B. pseudomallei, *and* B. mallei *are predicted to encode two putative copper nitrite reductases*

B. thailandensis E264*, B. pseudomallei* K96243 and *B. mallei* ATCC 23344 encode two putative copper nitrite reductases (annotated as multicopper oxidase domain containing proteins) on chromosome 2, sharing between 86 to 94 % sequence identity (Table 3.2).

The crystal structure of the soluble domain of *N. gonorrhoeae* AniA (sAniA) has been solved and has revealed it to be part of the class II copper nitrite reductases (Boulanger & Murphy, 2002). BTH_II0881, BPSS1487 and BMAA0755 (referred to as AniA in Table 3.2) share around 60 % sequence identity with the outer membrane copper nitrite reductase (AniA) found in *N. gonorrhoeae* and *N. meningitidis.* Due to the high degree of similarity exhibited by BTH_II0881, BPSS1487 and BMAA0755 to the *N. gonorrhoeae* AniA an amino acid sequence alignment was performed, using Clustal Omega, to identity potential catalytic residues (Fig. 3.5). The N-terminus of BTH_II0881, BPSS1487 and BMAA0755 proteins were shown to contain all the key amino acid residues required for binding of the type I and type II copper atoms. The amino acid residues denoted with the arrows in figure 3.5 (His140, Cys181, His189 and Met194) correspond to those involved in the coordination of the type I copper atom as seen in *Neisseria* sAniA (Boulanger & Murphy, 2002). Residues required for the binding of the type II (His145, His180 and His335), are required for catalytic activity and substrate binding in *N. gonorrhoeae* sAniA (Boulanger & Murphy, 2002), are shown with the ball and stick in figure 3.5. The Asp (D) and His (H) residues highlighted in green indicate those predicted to be

Figure 3.4 - *B. pseudomallei* NarG structural model. *B. pseudomallei* NarG (BPSL2309) was modelled against the NarG from *E. coli* using *E. coli* NarGHI (1Q16) as a template. *B. pseudomallei* NarG (query) structure is shown in red; *E. coli* NarG (template) is shown in blue. Analysis was performed using the online I-TASSER structural modelling service, with the image created using DS Visualizer 3.5.

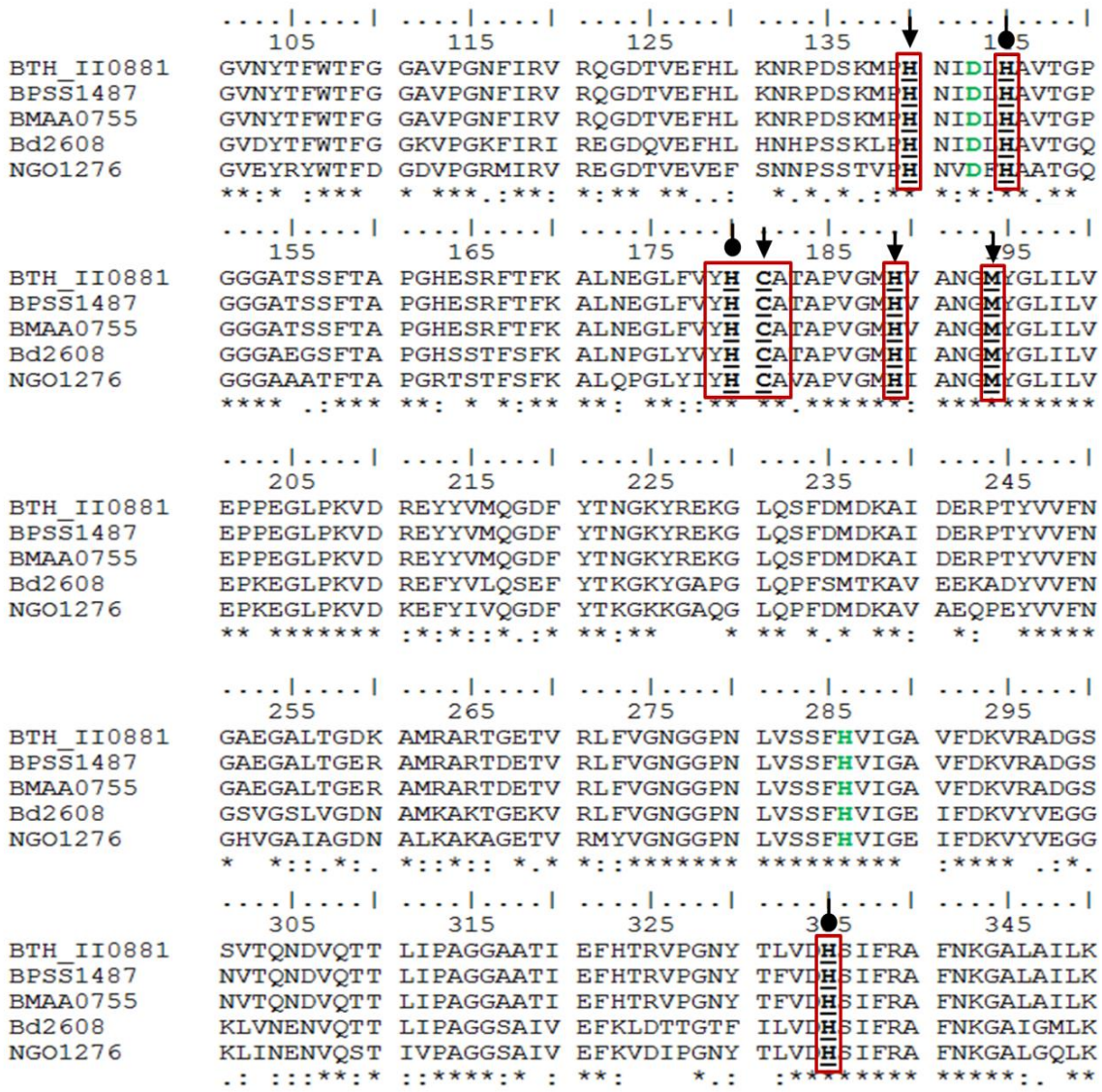

Figure 3.5 – Sequence alignment of the putative anaerobic outer membrane copper nitrite reductase from *Burkholderia* spp. with *Neisseria* AniA. Amino acid sequences the putative copper nitrite reductases (AniA) from *B. thailandensis* E264 (BTH_II0881), *B. pseudomallei* K96243 (BPSS1487), *B. mallei* ATCC 23344 (BMAA0755), were aligned with AniA from *N. gonorrhoeae* (NGO1276), and *Bdellovibrio bacteriovorus* (Bd2608) using Clustal Omega. Potential type I and type II copper ligands denoted by an arrow (type I) or ball and stick (type II). The Asp (D) and His (H) residues highlighted in green indicate those required for nitrite reduction, in sAniA. The asterisks (*) indicate conserved residues between all amino acid sequences. See text for more details

required for nitrite reduction, in sAniA.

The second putative copper nitrite reductase (Cu-Nir2) in *B. thailandensis* E264 (BTH_II0944) shares around 85 % sequence identity with orthologous genes in various *B. pseudomallei* and *B. mallei* strains. By comparison, BTH_II0944 only exhibits around 47.6 % sequence identity with other characterised copper nitrite reductase, such as that found in *Idiomarina loihiensis* (IL0762), sharing only 35 % identity with AniA from *N. gonorrhoeae* (NGO1276).

Preliminary sequence alignment BTH_II0944 and BPSS1452 with NGO1276 identified a difference in the highly conserved consensus YHCA sequence. To identify whether this difference was seen in other *Burkholderia* strains, the Cu-Nir2 amino acid sequences from a range of different *B. pseudomallei* (K96243 – BPSS1452; 668 - BURPS668_A2061; 1710b – BURPS1710b_A047; MSHR305 – BDL_4759) and *B. mallei* strains (ATCC 23344 – BMAA0798; NCTC 10247 – BMA10247_A1613) were aligned against BTH_II0944 using Clustal Omega (Fig. 3.6). The sequence alignment revealed all strains to have residues required for type I copper binding and Asp200 (D) required for nitrite reduction. Interestingly several of the *B. pseudomallei* (1710b, K96234 and MSHR305) and *B. mallei* (NCTC 10247) strains analysed displayed a difference in the generally conserved YHCx consensus sequence, having an arginine replacement for a key His residue (His236) implicated in type II copper binding (highlighted in red in Fig. 3.6). This amino acid replacement is not seen in *B. thailandensis* E264 (BTH_II0944), *B. pseudomallei* 668 (BURPS668_A2061) or *B. mallei* ATCC 23344 (BMAA0798). The replacement of His236 for an Arg residue at the same position could have implications of nitrite reduction since this His residue is likely to be required for the coordination of the type II copper atom required for nitrite reduction (Fig. 3.6). Whether or not Cu-Nir2 in these *B. pseudomallei* and *B. mallei* strains is in fact a true copper nitrite reductase remains to be determined.

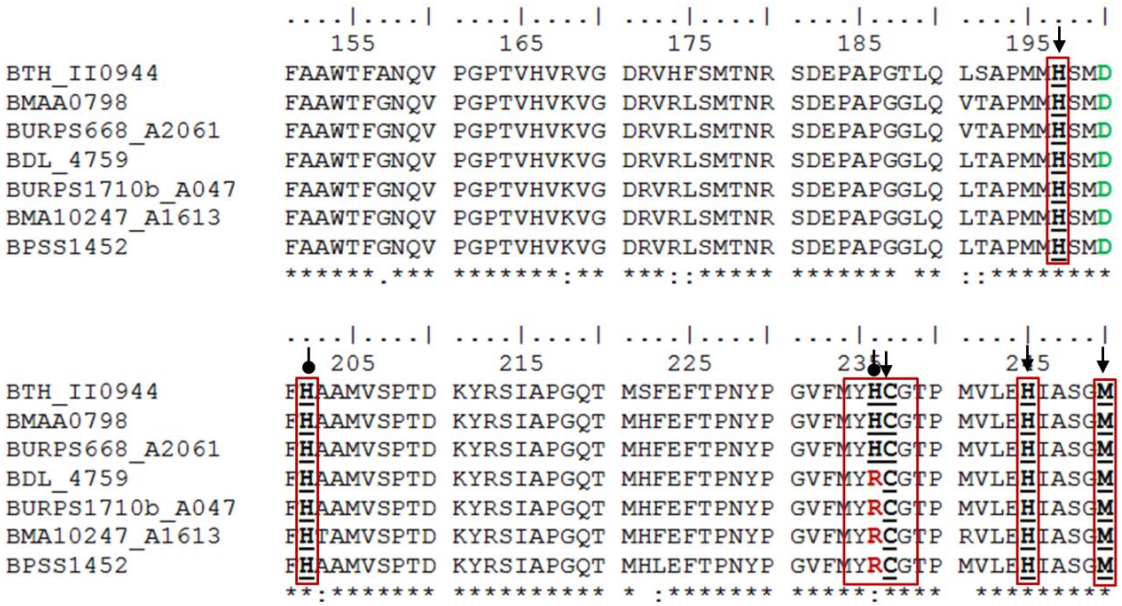

Figure 3.6 - Sequence alignment of BTH_II0944 orthologs in different *B. pseudomallei* and *B. mallei* strains. The second putative copper nitrite reductase (Cu-Nir2), annotated as a multicopper oxidase domain-containing protein, in *B. thailandensis* E264 (BTH_II0944) was aligned with its orthologs in different *B. pseudomallei* (K96243 – BPSS1452; 668 – BURPS668_A2061; 1710b – BURPS1710b_A047; MSHR305 – BDL_4759) and *B. mallei* (ATCC 23344 – BMAA0798; NCTC 10247 – BMA10247_A1613) strains using Clustal Omega. Differences in amino acid residue, required for the coordination of the type II copper atom, between the strains are marked in red (see text for details). Potential type I and type II copper ligands denoted by an arrow (type I) or ball and stick (type II). The asterisks (*) indicate conserved residues between all amino acid sequences.

3.3.4 *Prediction of transmembrane helices in both putative copper nitrite reductases*

AniA from *N. gonorrhoeae* is known to be bound to the outer-membrane (Boulanger & Murphy, 2002; Hoehn & Clark, 1992). Due to the high degree of homology of BPSS1487 and BTH_II0881 with the AniA from *N. gonorrhoeae* (Fig. 3.5) the TMHMM server v. 2.0 (Krogh *et al.*, 2001; Sonnhammer *et al.*, 1998) was used to predict potential transmembrane helices in both putative copper nitrite reductases (BTH_II0881/BPSS1487 and BPSS1452/BTH_II0944) to determine their potential cellular location (Fig. 3.7). The TMHMM server v. 2.0 flagged up a predicted transmembrane helix in BTH_II0881 and BPSS1487 (AniA) in the N-terminus of the protein. In comparison, no transmembrane helices were identified in either BTH_II0944 or BPSS1452 (Cu-Nir2). Caution must be executed when interpreting these results as the TMHMM 2.0 program is known to also pick up N-terminal signal peptides. The TMHMM2.0 program was only used to help predict the potential location of the putative Cu-Nirs in *B. thailandensis* E264 and *B. pseudomallei* K96243 within the periplasmic space, either being associated with the outer-membrane (for BTH_II0881 and BPSS1487) or found freely within the periplasmic space (for BTH_II0994 and BPSS1452). Both the putative copper nitrite reductases from *B. thailandensis* and *B. pseudomallei* were predicted to contain Sec signal peptides (predicted using the SignalP 4.1 server) in the N-terminus, indicating both are likely to be translocated into the periplasmic space.

3.3.5 *Structural prediction of both putative copper nitrite reductases in* B. pseudomallei

SWISS-MODEL (Bordoli *et al.*, 2009; Bordoli & Schwede, 2012) was used to determine whether both copper nitrite reductases encoded by *B. pseudomallei* K96243 and *B. thailandensis* E264 exhibited structural homology to published NIRs. Both BTH_II0881 and BPSS1487 were successfully modelled against sAniA from *N. gonorrhoeae* (PDB: 1kbv; (Boulanger & Murphy, 2002)), showing it to have the same quaternary structure (Fig. 3.8). All the residues required for the interaction with copper ligands were completely conserved and the model was successfully built (displaying a QMEAN Z-score of -0.012) as a trimer with all six copper ligands predicted to be required for catalysis (Fig. 3.8). This confirms that BTH_II0881 and BPSS1487 encode

an AniA like protein containing copper binding ligands required for the reduction of nitrite to nitric oxide.

a.) BTH_II0881/BPSS1487

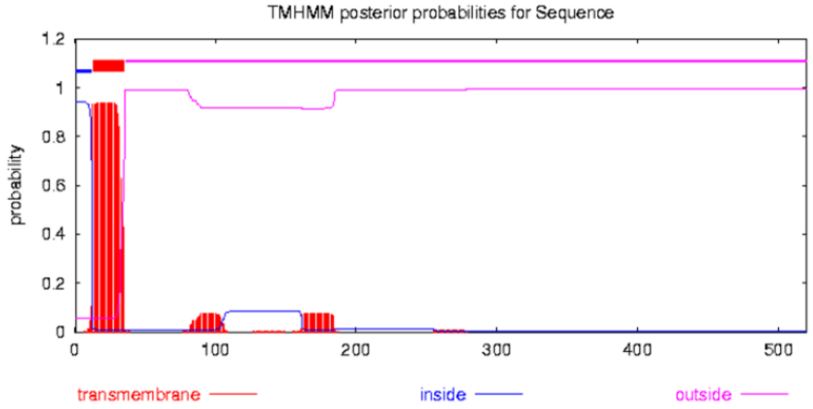

b.) BTH_II0944/BPSS1452

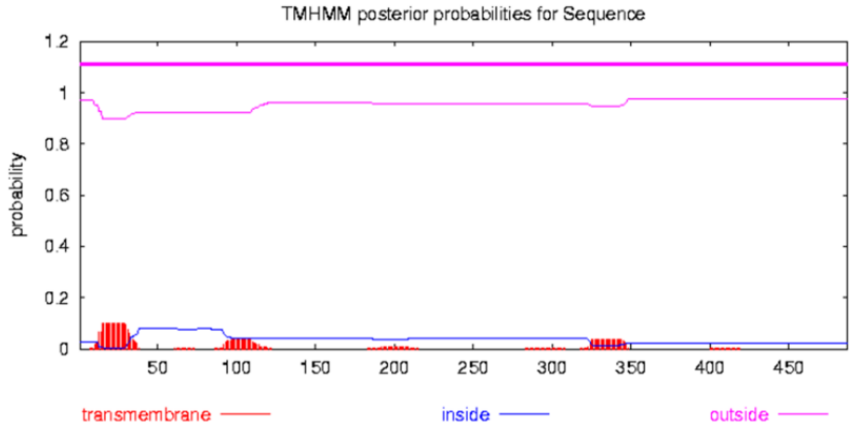

Figure 3.7 - *Burkholderia* copper nitrite reductase transmembrane helices prediction. The TMHMM server v. 2.0 was used to predict the presence of transmembrane helices in the putative copper nitrite reductases from *B. thailandensis* E264 and *B. pseudomallei* K96243. a.) Predicted transmembrane helices in BTH_II0881 and BPSS1487 containing one predicted transmembrane helix in N-terminal sequence. This and their similarity with the membrane-bound nitrite reductase (AniA) from *N. gonorrhoeae* could indicate BTH_II0881 and BPSS1487 are associated with the outer-membrane. b.) No transmembrane helices predicted for BTH_II0944 or BPSS1452 (Cu-Nir2), corresponding with its predicted periplasmic location.

Structural models for BPSS1452 and BTH_II0944 were also constructed based on several different template structures, but little structural homology was seen with other published nitrite reductases. As an example BPSS1452 was modelled, as a single chain, against the hexameric copper-containing nitrite reductase from *H. denitrificans* (PDB: 2dv6E) (Nojiri *et al.*, 2007), but only displayed 33.4 % sequence identity. This structural model had a low QMEAN Z-score of -5.56, as the sequences were too diverse to infer a conservation of the oligomeric state, and not all the copper ligands were conserved. BTH_II0944 and BPSS1452 share little structural homology with any published copper nitrite reductase and no successful models could be made using either the amino acid sequence. This indicates, along with the sequence alignment (Fig. 3.5), that BTH_II0944 and BPSS1452 may not encode a true copper nitrite reductase, and may potentially be redundant in function. Further characterisation will be required to determine whether BTH_II0944 and BPSL1452 play a role in either *B. thailandensis* or *B. pseudomallei.*

3.4 Molybdopterin biosynthetic pathway in *Burkholderia*

Many proteins involved in anaerobic respiration (such as formate dehydrogenase, NAR and DMSO reductase) require the formation of a molybdopterin cofactor (Moco), synthesised via the molybdopterin biosynthetic pathway. Disruption of a gene cluster encoding *moaA1-moaB1-moaC1-moaD1* and a *moaD2* derivative, required for molybdopterin biosynthesis, in *Mycobacterium* was shown to cause an impairment of growth on nitrate leading to the accumulation of nitrite (Williams *et al.*, 2011). The function of the denitrification pathway is known to be dependent on the formation of various metal cofactors, with NarGHI requiring [Fe-S] clusters and an active Mo-*bis*MGD cofactor for the reduction of nitrate to nitrite (Gonzalez *et al.*, 2006). Because a full denitrification pathway was identified in *B. thailandensis* and *B. pseudomallei* it seemed logical that these species would also encode genes required for the synthesis of the molybdenum cofactor. Therefore a bioinformatics analysis, using K.E.G.G. and NCBI searches, was performed to identify genes required for the molybdopterin biosynthetic pathway. Bioinformatic analysis successfully identified the presence of a full molybdopterin biosynthetic pathway in *B. thailandensis* E264*, B. pseudomallei* K96243 and *B. mallei* ATCC 23344, with all genes sharing between 88 and 99 % identity (Table 3.3). All three *Burkholderia* species, unlike some other prokaryotes,

a.)

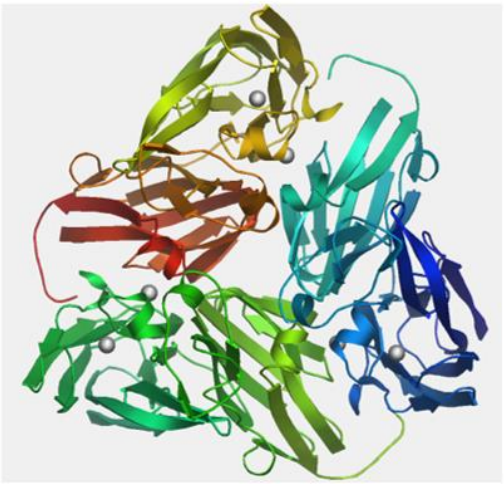

b.)

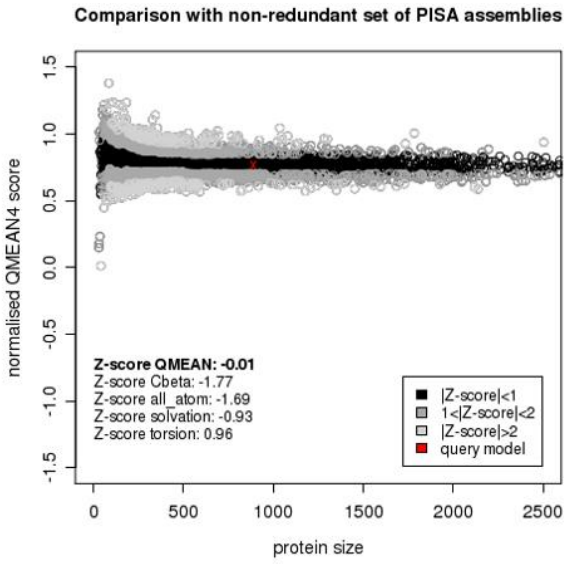

Figure 3.8 – Predicted structure of *B. pseudomallei* AniA (BPSS1487). The structure of BPSS1487 was predicted using SWIS-MODEL and modelled on *N. gonorrhoeae* sAniA (PDB: 1kbv) (Boulanger & Murphy, 2002). a.) Predicted model for BPSS1487 showing copper ligands (grey balls), found within each subunit of the trimeric enzyme. b.) Global model quality estimation showing QMEAN Z-score of -0.012 (Benkert *et al.*, 2011). A structural model was also constructed for BTH_II0881, showing it to display the same degree of homology to sAniA (1kbv) from *N. gonorrhoeae.*

encode two putative *moeA* genes (see Chapter 4 for more details). No MobB homolog was identified in any of the three *Burkholderia spp.* However *E. coli* MobB was shown not to be essential molybdopterin biosynthesis (Palmer *et al.*, 1996).

The predicted *Burkholderia* molybdopterin biosynthetic pathway is identical to that seen in other prokaryotic species (Fig. 3.9) (Schwarz *et al.*, 2009). The molybdopterin biosynthetic pathway is a highly conserved four step enzymatic pathway. This pathway initially involves the conversion of GTP to cPMP, which is then converted to molybdopterin, following molybdenum uptake, and finally Mo-*bis*MGD (see Chapter 1 – *1.4.1 Molybdopterin biosynthetic pathway*). This pathway involves many different transport and biosynthetic proteins (Schwarz *et al.*, 2009), all of which are found in *B. thailandensis, B. pseudomallei* and *B. mallei* (Table 3.3 and Fig. 3.9).

3.5 Discussion

Bioinformatic analysis has shown *B. thailandensis* E264, *B. pseudomallei* K96243, and *B. mallei* ATCC 23344 to encode multiple types of primary dehydrogenases, terminal oxidases and anaerobic respiratory proteins (Fig. 3.10). This respiratory flexibility exhibited by all three *Burkholderia* spp. is likely to contribute to their environmental survival and virulence.

Bioinformatic analysis revealed *B. pseudomallei* K96243 to encode the widest range of primary dehydrogenases and oxidoreductases, possessing gene clusters that were not identified in either *B. thailandensis* E264 or *B. mallei* ATCC 23344 (Table 3.1). For example *B. mallei* seems to lack a number of terminal oxidoreductases found in *B. thailandensis* or *B. pseudomallei.* This difference could be due to the fact that the *B. mallei* genome is thought to have undergone a degree of genome downsizing (Nierman *et al.*, 2004). Although majority of *B. mallei* genome is around 90 % identical to that seen in *B. pseudomallei, B. mallei* is known to either lack genes or encode gene variants of 627 genes encoded on chromosome 1 and 819 on chromosome 2 in *B. pseudomallei* (Nierman *et al.*, 2004). This difference is likely to reflect the fact that *B. mallei,* unlike *B. pseudomallei* and *B. thailandensis,* is an obligate pathogen, surviving poorly within the environment. The differences in respiratory flexibility between *B. pseudomallei* and *B. thailandensis*, may indicate that *B. pseudomallei* requires a

Table 3.3 - Genes required for molybdopterin biosynthesis in *B. thailandensis, B. pseudomallei* and *B. mallei*

Gene name	Function	*B. thailandensis* (E264)	*B. pseudomallei* (K96243)	*B. mallei* (ATCC 23344)	Sequence similarity[a] (%)
moaA	molybdenum cofactor biosynthesis protein A	BTH_I1706	BPSL2453	BMA0519	95
moaC	molybdenum cofactor biosynthesis protein C	BTH_I0653	BPSL0786	BMA0283	88 - 95.7
moaD	molybdopterin converting factor subunit 1 and 2	BTH_I2201-2202	BPSL1480-1481	BMA1380-1381	92 - 98.8
mogA	molybdenum cofactor biosynthesis protein	BTH_I1671	BPSL2480	BMA0391	96
moeA1	molybdopterin biosynthesis protein A	BTH_I1704	BPSL2455	BMA0517	89-90
moeA2	molybdopterin biosynthesis protein A	BTH_I2200	BPSL1479	BMA1382	92.5
modABC	molybdate specific transport system	BTH_II0591-0593	BPSS1786-1788	BMAA0297-0299	95 – 96
modE	molybdate transport system transcriptional regulator	BTH_II0590	BPSS1789	BMAA0294	93 - 94
mobA	molybdopterin-guanine dinucleotide biosynthesis protein	BTH_I1705	BPSL2454	BMA0518	90
moeB	Molybdopterin biosynthesis protein	BTH_I0414	BPSL0441	BMA3210	95 - 100
moaE	molybdenum converting factor subunit 2	BTH_I2202	BPSL1481	BMA1381	92 - 99

[a] Sequence identity (%) relates to gene orthology (K.E.G.G) of *B. pseudomallei* and *B. mallei* genes to those found in *B. thailandensis*

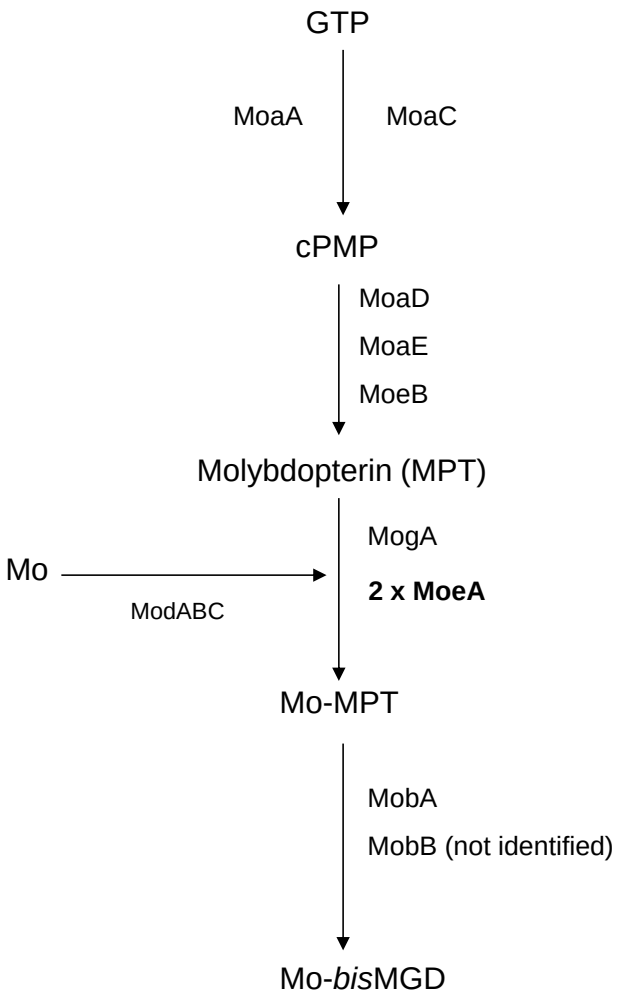

Figure 3.9 - Molybdopterin biosynthetic pathway in *Burkholderia* spp. Predicted pathway based bioinformatic searches (NCBI BLAST and KEGG) and published literature (Schwarz *et al.*, 2009; Vergnes *et al.*, 2004). All genes are present in *B. pseudomallei* and *B. thailandensis* (see Table 3.3). A homologue of MobB has not yet been identified in *B. thailandensis* or *B. pseudomallei.* Both *B. pseudomallei* and *B. thailandensis* encode two putative *moeA* genes as shown in bold (Table 3.3).

greater array of different cytochrome *c* oxidases to survive and persist within the human body.

Cytochrome *c* oxidase couples electron transfer from *c*-type cytochromes to proton translocation, via the conversion of oxygen to water, pumping protons into the periplasm. There are various types of cytochrome *c* oxidases that are known to function under different oxygen concentrations. The *aa*$_3$-type cytochrome *c* oxidase predominates under aerobic conditions and is similar to the mitochondrial cytochrome *c* oxidase (complex III) (Kishikawa *et al.*, 2010; Richter & Ludwig, 2009). The cytochrome *bd* oxidase displays a high affinity for oxygen and is generally induced under microaerobic conditions, often replacing the *bo*$_3$-type which displays a lower affinity for oxygen (Garcia-Horsman *et al.*, 1994). *B. thailandensis* E264*, B. pseudomallei* K96243 and *B. mallei* ATCC 23344 encode a putative *aa*$_3$-type oxidase, cytochrome *bd* oxidase and *bo*$_3$-type oxidase (Table 3.1 and Fig. 3.10) similar to that seen in other prokaryotic species. *B. thailandensis,* but not *B. pseudomallei,* encodes a putative *cbb*$_3$-type oxidase, *ccoNOP*. The *cbb*$_3$-type oxidases are expressed specifically under microaerobic conditions, under the control of FNR, to allow for colonisation of oxygen limited environments (Pitcher & Watmough, 2004). Although no homolog of the *cbb*$_3$-type oxidase was found in *B. pseudomallei, B. pseudomallei* seems to encode an extra copy of a cytochrome *bd* oxidase not found in *B. thailandensis* (Table 3.1). The significance of these findings is currently unknown. However, one can speculate the absence of a putative *cbb*$_3$-type cytochrome oxidase in pathogenic *Burkholderia* spp. may point to a role for that gene cluster in *B. thailandensis* (BTH_II1618-1619) in environmental survival. The extra copy of cytochrome *bd* oxidase may provide a compensatory role in *B. pseudomallei,* allowing for both environmental and in host survival, considering it does not encode a putative *cbb*$_3$-type cytochrome *c* oxidase.

B. thailandensis, B. pseudomallei and *B. mallei* encode a cytochrome *bc*$_1$ complex, required for aerobic and anaerobic respiration. All three *Burkholderia* spp. possess multiple types of cytochrome *c* oxidase proteins which are likely to take electrons either straight from the quinol pool (for cytochrome *bd* oxidase, cytochrome *bo*$_3$ oxidase) or from *c*-type cytochromes via the *bc*$_1$ complex (for *aa*$_3$-type and *cbb*$_3$-type cytochrome oxidases), similar to that seen in *R. sphaeroides* (Garcia-Horsman *et al.*, 1994) (Fig. 3.11).

a.) Primary Dehydrogenases

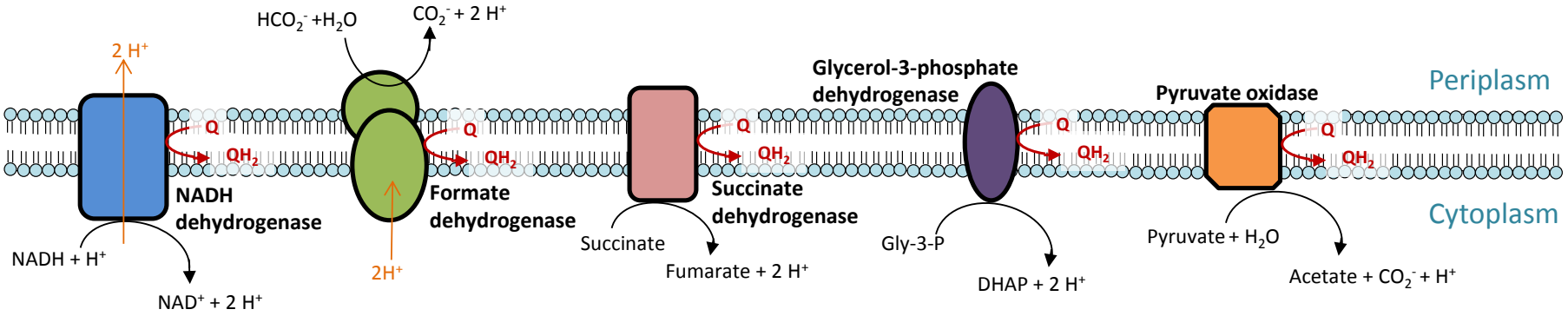

b.) Terminal oxidases

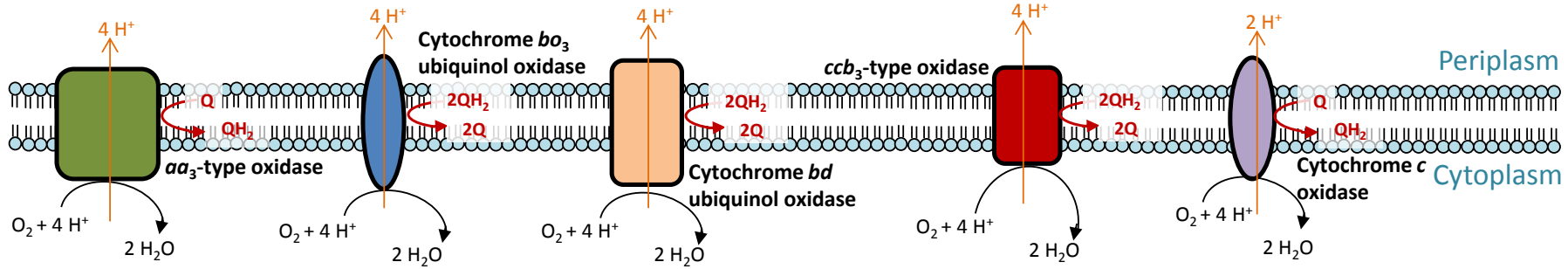

Figure 3.10 - Diagrammatic representation of predicted primary dehydrogenases and terminal oxidases found in *B. thailandensis* E264 and *B. pseudomallei* K96243. Topology and reaction cycles are derived from previous published literature (Unden & Bongaerts, 1997). a.) Primary dehydrogenases found in both *B. thailandensis* and *B. pseudomallei;* b.) Terminal oxidases found in both *B. thailandensis* and *B. pseudomallei*. *B. pseudomallei* does not encode a predicted *cbb*$_3$-type oxidase (see Table 3.1). Q and QH (in red) refer to quinones which may be in ubiquinone or menaquinone.

The Tat-secretion system is required for the export of proteins across the cytoplasmic membrane (Berks *et al.*, 2000). Recently the Tat-system in *B. thailandensis* has been shown to be required for the export of a number of different proteins required for respiration, including the Rieske iron-sulfur protein PetA, and BTH_I2175/BTH_I1276 containing Ser/Thr phosphatase and cytochrome *c* oxidase subunit II PFAM domain matches (Wagley *et al.*, 2013). PetA is part of the cytochrome bc_1 complex (Table 3.1) required for aerobic respiration. Insertion of a rhamnose inducible gene in front of *petA* (E264-P*rhaB*::petA) and BTH_I2175 (E264-P*rhaB*::BTH_I1275-1276) identified BTH_I2175/BTH_I2176, and not *petA,* as being required for aerobic, but not anaerobic respiration. BTH_I2175 was shown not to be Tat- exported, whereas BTH_I2176 was (Wagley *et al.*, 2013). Because deletion of *petA* did not cause a growth defect aerobically it is likely that *B. thailandensis* can by-pass this enzyme to transfer electrons directly to the terminal oxidases from the quinol pool, as seen in *E. coli* (Fig. 3.11). BTH_I2175 is annotated as a cytochrome *c* oxidase and is part of a gene cluster encoding a predicted Ser/Thr phosphatase. Currently it is not completely understood why disruption of this gene cluster would prevent aerobic growth but not affect anaerobic respiration (Wagley *et al.*, 2013).

B. thailandensis E264*, B. pseudomallei* K96243 and *B. mallei* ATCC 23344 encode a full denitrification pathway, encoding membrane-bound NAR (NarGHI and/or NarZYV), Cu-Nir (AniA), NOR and NOS, all required for the reduction of nitrate to dinitrogen gas (Table 3.2 and Fig. 3.1). The presence of the full denitrification pathway is likely to allow for generation of a PMF in the presence of nitrate to allow for growth within a hypoxic environment. *B. thailandensis* and *B. pseudomallei,* unlike *B. mallei* encode two membrane-bound nitrate reductases, one on each chromosome. The NAR encoded on chromosome 2 (BTH_II1249-1252 or BPSS1156-1159) exhibits similarity to the cryptic nitrate reductase (*narZYWV*) seen in *E. coli* and *Salmonella.* NarZYWV in *S. typhimurium* has been shown play a role in response to carbon starvation and was negatively regulated under anaerobic conditions by FNR (Spector *et al.*, 1999). Due to the similarity with the cryptic nitrate reductase *narZYWV,* BTH_II1249-1252/BPSS1156-1159 are predicted to be required for adaptation to hypoxia, whereas the other nitrate reductase encoded on chromosome 1 (found in all three *Burkholderia* spp.) is likely to be the main nitrate reductase required for anaerobic growth (Fig. 3.12).

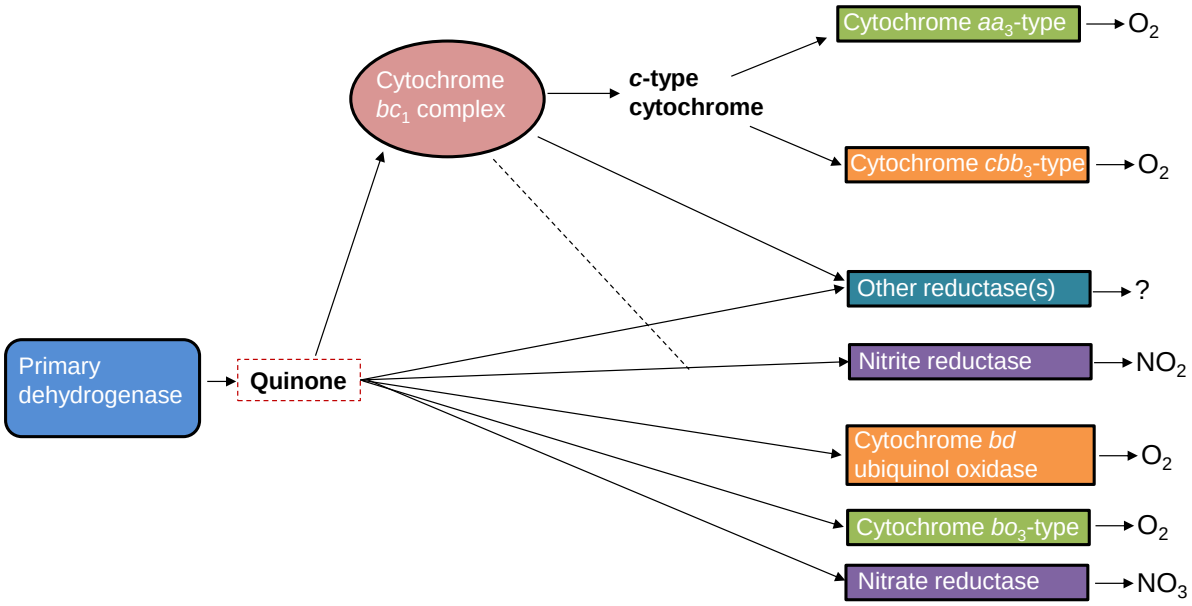

Figure 3.11 – Proposed respiratory and electron transport pathways in *B. pseudomallei* and *B. thailandensis*. Diagram represents the predicted electron transfer pathways in *B. thailandensis* E264 and *B. pseudomallei* K96243, based on respiratory pathways seen in other prokaryotic species (Garcia-Horsman *et al.*, 1994). Terminal oxidases shown in green are predicted to function either under aerobic conditions, microaerobically (orange) or anaerobically (purple). Only *B. thailandensis* encodes a predicted *cbb*$_3$-type oxidase. Electrons are transferred from primary dehydrogenase(s) (see Table 3.1) through the quinol pool and either directly to the terminal oxidases or via the cytochrome bc_1 complex. Various different cytochromes thought to transfer electrons to the other three reductase enzymes and cytochrome *c* oxidase.

The regulation of the switch to anaerobiosis and regulation of nitrate reductase, involves multiple different mechanisms. These range from the relatively conserved NarXL and FNR family members (Fnr, Anr, Dnr) (Benkert *et al.*, 2008; Bouchal *et al.*, 2010; Gonzalez *et al.*, 2006; Hartig *et al.*, 1999; Lonetto *et al.*, 1998; Schreiber *et al.*, 2007; Trunk *et al.*, 2010; Whitehead & Cole, 2006), the cAMP-dependent regulator GlxR (Nishimura *et al.*, 2010), ArcAB, Fur (Teixido *et al.*, 2010), the Res system, and quorum sensing (Toyofuku *et al.*, 2007; Toyofuku *et al.*, 2008).

Both the nitrate reductase operons in *B. pseudomallei* K96243 encode genes required for the formation of a TCS; either NarXL (BPSL2313-2314) encoded within the *narGHJIKXL* gene cluster, or a PAS/PAC sensor and LuxR regulator protein (BPSS1160-1161) found upstream of the *narZYWV* gene cluster (Fig. 3.1). Prokaryotic TCS are composed of a histidine kinase (HK), which senses environmental stimuli, and a cognate response regulator, which on phosphorylation by its respective HK can cause transcriptional change allowing the bacteria to response quickly to changes in the surrounding environment (Chang & Stewart, 1998). NarXL has been well characterised and is known to play a key role in regulating *narGHJI* in response to low oxygen levels and nitrate (Hartig *et al.*, 1999; Schreiber *et al.*, 2007; Stewart, 1993). Both *B. pseudomallei* and *B. thailandensis* encode a FNR gene (BPSS1163/BTH_II1244), which along with NarXL is likely to be required for transcriptional regulation in response to anaerobiosis. Unsurprisingly the BPSL2309 promoter region contains a NarL response regulator binding region, indicating the likely involvement of NarXL in the regulation of *narGHJI* in *B. pseudomallei* and *B. thailandensis.*

Upstream of the *narZYWV* operon in *B. pseudomallei* are genes encoding a predicted TCS; BPSS1160 encoding a sensor kinase similar to the PAS/PAC sensor signal transduction kinase and BPSS1161 encoding a response regulator exhibiting similarity to LuxR family regulatory proteins. PAS domain signal transduction kinase have been shown to sense oxygen, redox potential and light (Taylor & Zhulin, 1999). PAS sensors are thought to sense changes in the electron transport chain, serving as an early warning signal to allow for adaptation to response to changes in internal energy levels (Taylor & Zhulin, 1999). Whether or not this predicted PAS/PAC TCS is involved in the regulation of BPSS1156-1159, or other genes required for the electron

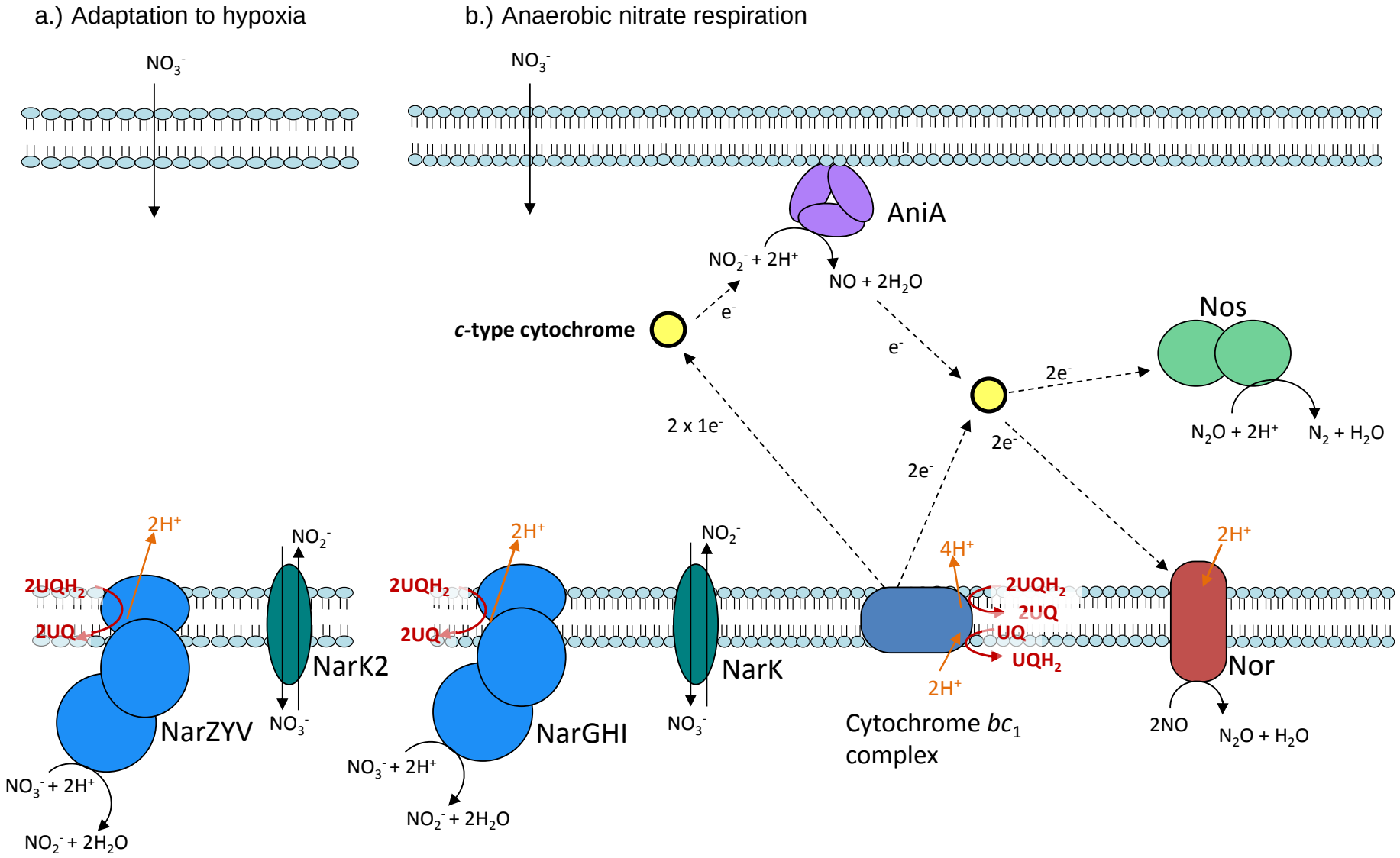
a.) Adaptation to hypoxia
b.) Anaerobic nitrate respiration
NO3-
AniA
NO2- + 2H+
NO + 2H2O
c-type cytochrome
e-
2 x 1e-
2e-
Nos
N2O + 2H+
N2 + H2O
2H+
2UQH2
2UQ
NO2-
NO3-
NarK2
NarZYV
NO3- + 2H+
NO2- + 2H2O
NarK
NarGHI
4H+
UQH2
UQ
Cytochrome bc1 complex
Nor
2NO
N2O + H2O

Figure 3.12 - **Predicted denitrification pathway in *B. thailandensis* E264, *B. pseudomallei* K96243 and *B. mallei* ATCC 23344.** Bacterial denitrification starts with the reduction of nitrate (NO_3^-) to nitrite (NO_2^-), releasing two protons to the periplasmic side of the membrane were NO_2^- is reduced to nitric oxide (NO), then nitrous oxide (N_2O) and finally dinitrogen gas (N_2). Abbreviations - NAR (NarGHI/NarZYV), NarK (nitrate/nitrite antiporter), Cu-Nir (AniA), NO reductase (Nor), and N_2O reductase (Nos). Cytochromes involved in electron transfer are shown in yellow. a.) Adaptation to hypoxia. Putative cryptic nitrate reductase (NarZYV; BTH_II1249-1252; BPSS1159-1156), absent in *B. mallei,* potentially required for adaptation to growth in a hypoxic environment prior the induction of the NarGHI (BTH_I1851-1854/BPSL2309-2314). b.) Anaerobic nitrate respiration. Main proposed denitrification pathway for *B. thailandensis* and *B. pseudomallei.* Includes predicted electron transport chain, based on known pathways known in other prokaryotes, e.g. *P. denitrificans.* QH_2 could potentially come from a range of primary dehydrogenases. Diagram on previous page.

transport chain remains to be determined.

The second step in the anaerobic respiratory pathway is catalysed by nitrite reductase, reducing nitrite to nitric oxide. There are two different types of NIR (reducing NO_2^- to NO) found in the periplasm of different prokaryotic species; *cd*$_1$-type containing *c* and *d*-type hemes (Silvestrini *et al.*, 1994), and copper containing nitrite reductase (Abraham *et al.*, 1993; Boulanger & Murphy, 2002; Nojiri *et al.*, 2007). An alternative NIR, required for the respiratory reduction of nitrite to ammonia, is found in *E. coli* and is known as the cytochrome *c* nitrite reductase NrfA (Bamford *et al.*, 2002; Clarke *et al.*, 2008). *B. thailandensis, B. pseudomallei* and *B. mallei* are predicted to encode two copper NIRs, one of which showing homology to the anaerobically induced outer-membrane AniA from *N. gonorrhoeae* (Boulanger & Murphy, 2002). Presence of a transmembrane helix within BPSS1487 and BTH_II0881 provides evidence that they may also be bound to the outer-membrane (Fig. 3.7), as shown in figure 3.12. Bioinformatic analysis has indicated that the second copper nitrite reductase (Cu-Nir2) may not function as a nitrite reductase, at least in some *B. pseudomallei* and *B. mallei* strains, considering it lacks key catalytic residues required for copper binding and seems to show little homology to published nitrite reductases.

The final two steps in the anaerobic respiratory pathway are catalysed by the membrane-bound NOR and periplasmic NOS, required for the reduction of nitric oxide (NO) to nitrous oxide (N_2O) and then finally dinitrogen gas (N_2) (Fig. 3.12). All three *Burkholderia* species encode two nitric oxide reductase (*norZ*) and one nitrous oxide reductase (*nosZDFYL*) (Table 3.2). NOR in *A. eutrophus* and *N. gonorrhoeae* is encoded a single subunit NorB/NorZ, which is induced under anaerobic conditions by nitric oxide (Cramm *et al.*, 1997; Householder *et al.*, 2000). Like *N. gonorrhoeae* and *A. eutrophus,* all three *Burkholderia* spp. encode a single subunit NOR (NorZ). By contrast *P. denitrificans* NOR (NorBC) is heme-copper oxidase family protein composed of two subunits, a membrane anchor with heme ligands for catalysis and a water soluble subunit required for electron transfer (Flock *et al.*, 2006; Watmough *et al.*, 2009).

The NOS found in *Burkholderia* is similar to other characterised copper containing NOS enzymes, such as that from *P. stutzeri*. NosZ, structural component of nitrous oxide reductase containing Cu_A and Cu_Z copper centres, is found on a large operon containing genes required for regulation (*nosR*) and those required for copper

incorporation (*nosDFY*) (Brown *et al.*, 2000; Cuypers *et al.*, 1995; Zumft *et al.*, 1990). All these genes are found in *B. thailandensis, B. pseudomallei* and *B. mallei.*

Many of the proteins required for anaerobic respiration and electron transport in *B. pseudomallei, B. thailandensis,* and *B. mallei* are likely to require molybdenum cofactor for catalysis. It was therefore unsurprising then that all three species encoded a full molybdopterin biosynthetic pathway similar to that seen in other prokaryotic species (see Chapter 4 for more details).

3.6 Conclusions

B. pseudomallei K96243*, B. thailandensis* E264 and *B. mallei* ATCC 23344 encode a wealth of genes required for aerobic or anaerobic respiration likely to allow for colonisation of a range of different environments. Differences between these three *Burkholderia* spp*.* in terms of the number and variety of respiratory proteins that they encode may reflect their differing abilities to survive within the environment and/or the host. Currently little has been done to characterise these pathways on a molecular level. Using *B. thailandensis* as a model system, the role of anaerobic respiration will be initially characterised to determine whether it is likely be important for *B. pseudomallei* survival and virulence (see Chapters 4, 5 and 6).

Chapter 4 – Role of the molybdopterin biosynthetic pathway in anaerobic growth and survival of *B. thailandensis*

NOTE: Results and discussion presented in this chapter have been published previously in Research in Microbiology (Andreae *et al.*, 2014)

4.1 Introduction

The anaerobic respiratory pathway is important for survival and virulence of multiple pathogenic bacteria. Under oxygen limiting conditions a number of alternative electron acceptors (such as nitrate, nitrite or DMSO), can be utilised to generate a PMF via a series of reductase enzymes (Richardson, 2000). Bioinformatic analyses have revealed that both *B. thailandensis* E264 and *B. pseudomallei* K96243 encode a full denitrification pathway encoding NAR, NIR, NOR and NOS, allowing for the sequential reduction of nitrate to dinitrogen gas (see Chapter 3).

NarGHI requires an active molybdenum cofactor (Mo-*bis*MGD) for the reduction of nitrate (NO_3^-) to nitrite (NO_2^-) (Gonzalez *et al.*, 2006; Jormakka *et al.*, 2004). The Mo-*bis*MGD cofactor is generated by a four step enzymatic pathway known as molybdopterin biosynthesis, and requires a variety of molybdenum transport and biosynthetic proteins. The first step in the enzymatic pathway involves the conversion of guanosine triphosphate (GTP) to the pterin intermediate cPMP using MoaA and MoaC. Next MPT synthase ($MoaD_2MoaE$) converts cPMP to MPT dithiolate (Schwarz *et al.*, 2009), prior to the ligation of molybdenum (Mo) to MPT, using MogA and MoeA, to generate Moco. Molybdenum is transported into the cell by the high affinity Mo transport proteins (Grunden & Shanmugam, 1997). Finally for pyranopterin based molybdo-cofactors Moco is converted to its various derivatives, such as Mo-*bis*MGD, using MobA or MocA (Leimkuhler *et al.*, 2011; Schwarz *et al.*, 2009) (see Chapter 1 section 1.4.1 *Molybdopterin biosynthetic pathway* for more information).

As described previously, disruption of anaerobic respiration, through mutation in NAR or lack of Moco biosynthesis, causes defects in intracellular growth, virulence, persistence, motility, biofilm formation, invasion and proliferation within Hep-2 epithelial cells in a number of pathogenic species (Fritz *et al.*, 2002; Kohler *et al.*, 2002; MacGurn & Cox, 2007; Sohaskey, 2008; Van Alst *et al.*, 2007; Weber *et al.*, 2000).

B. thailandensis, a Gram-negative soil dwelling saprophyte (Brett *et al.*, 1998) is closely related to *B. pseudomallei,* the causative agent of melioidosis (Wiersinga *et al.*, 2012). *B. thailandensis*, although displaying a very high degree of genetic similarity to *B. pseudomallei*, is avirulent rarely causing disease in humans (Deshazer, 2007; Glass *et al.*, 2006). Due to the high degree of genetic similarity, ability to survive and replicate intracellularily and lower risk associated with handling, *B. thailandensis* is often used as a surrogate for *B. pseudomallei* (Chandler *et al.*, 2009; French *et al.*, 2011; Haraga *et al.*, 2008; Horton *et al.*, 2012; West *et al.*, 2008).

Although *B. pseudomallei* has been shown to respire anaerobically on nitrate, and survive within a hypoxic environment for one year (Hamad *et al.*, 2011), currently little is known about the role anaerobic respiration plays in *Burkholderia* spp*.* pathogenesis*.* In this chapter work will be presented on the generation of a *B. thailandensis* E264 transposon library. The transposon mutant library was constructed in order to identify genes required for anaerobic respiration/molybdopterin biosynthesis, and determine the role of anaerobic respiration in nitrate reductase activity, virulence, biofilm formation and motility (Andreae *et al.*, 2014)

4.2 Results

4.2.1 B. thailandensis *E264 is an obligate respirer, only growing anaerobically in the presence of an alternative electron acceptor*

Bioinformatic analysis presented in Chapter 3 identified the presence of a full denitrification pathway in *B. thailandensis* E264*, B. pseudomallei* K96243 and *B. mallei* ATCC 23344 (Table 3.2)*.* To verify this *B. thailandensis* was grown within either medical flat bottomed flasks or an anaerobic chamber in the presence or absence of nitrate or nitrite, in M9 minimal media or L-broth. The majority of anaerobic studies were conducted using M9 minimal media supplemented with sodium succinate as a

carbon source to ensure growth was due to generation of a PMF via the denitrification pathway rather than carbon fermentation.

B. thailandensis was grown anaerobically in M9 minimal media containing either 20 mM sodium succinate or 20 mM glucose, in the presence or absence of 20 mM sodium nitrate. *B. thailandensis* could only grow under anaerobic conditions in the presence of nitrate (Fig. 4.1) or nitrite. *B. thailandensis* anaerobic growth using either glucose or succinate as a carbon source was not significantly different.

To determine when *B. thailandensis* NAR was active during anaerobic growth a Griess reaction was performed on samples taken throughout the growth cycle. During the lag phase *B. thailandensis* displayed an increase in the concentration of nitrite (NO_2^-), reaching around 120-140 µM after 25 to 30 hours incubation (Fig. 4.2). This increase in NO_2^- is likely due to an increase in NAR activity and/or expression. The drop in NO_2^- at the end of lag phase/early exponential phase indicates the increase in expression (or activity) of the copper nitrite reductase (AniA), NOS and NOR enzymes encoded within the *B. thailandensis* E264 genome (see Chapter 3).

To validate that the anaerobic growth exhibited by wild-type *B. thailandensis* E264 was due to NAR, sodium tungstate, an analogue of molybdenum, was added to the anaerobic growth medium. Sodium tungstate has been used to inhibit the activity of molybdoenzymes, such as NarGHI, as tungsten (W) can either replace the molybdenum cofactor inhibiting catalytic activity or prevent the formation of Moco (Deng *et al.*, 1989; Seki-Chiba & Ishimoto, 1977). Addition of increasing concentrations of sodium tungstate (1 mM to 10 mM) to the anaerobic growth media caused severe inhibition of growth anaerobically (Fig. 4.3). No growth inhibition was seen when the same experiment was performed under aerobic growth conditions (see Chapter 8 – Appendix figure 8.1). This confirms the role of NarGHI in anaerobic growth of *B. thailandensis.*

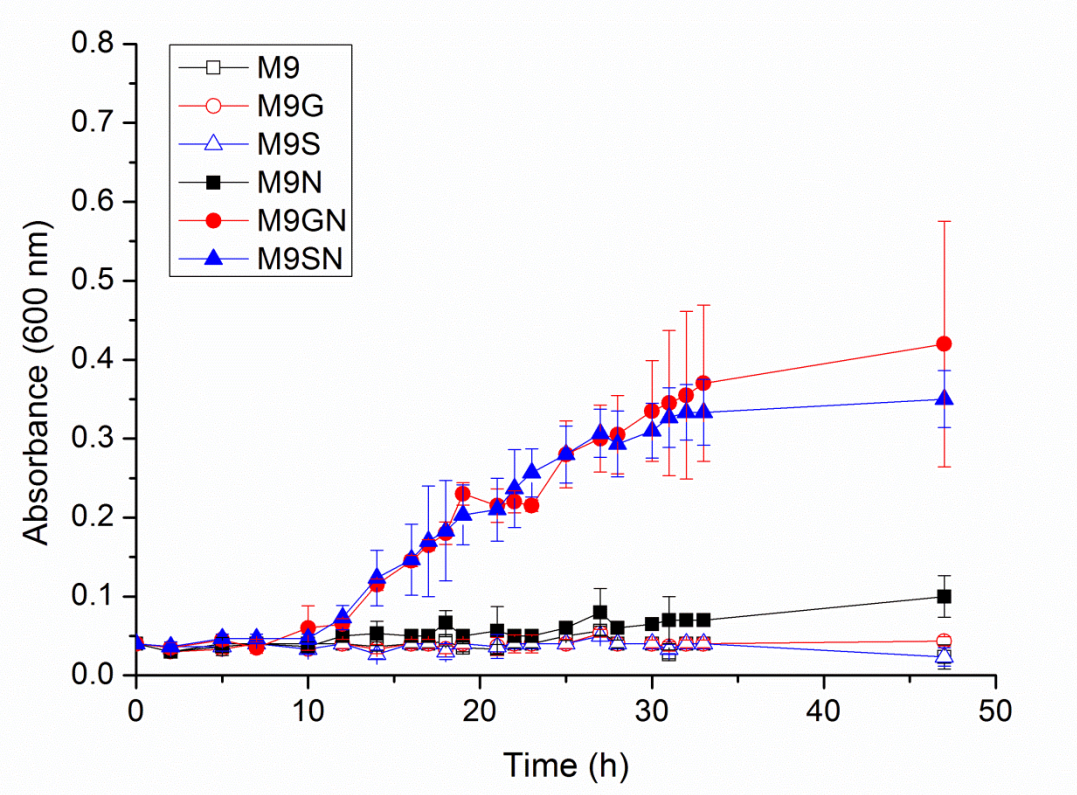

Figure 4.1 - **Anaerobic growth of *B. thailandensis* E264.** *B. thailandensis* was acclimatised to growth within an anaerobic environment prior to inoculation into anaerobic M9 minimal media. The experiment was performed in medical flat bottom flasks sparged with nitrogen and sealed with a rubber bung. *B. thailandensis* was grown in the presence (filled shapes) or absence (empty shapes) of 20 mM sodium nitrate (N) with various carbon sources; 20 mM glucose (red circles – M9G/M9GN), 20 mM sodium succinate (blue triangles – M9S/M9SN) or no carbon source (black squares – M9/M9N). Data is the representation of two (for glucose and nitrate only) or three biological replicates (all other experiments). Error bars ± standard deviation (SD).

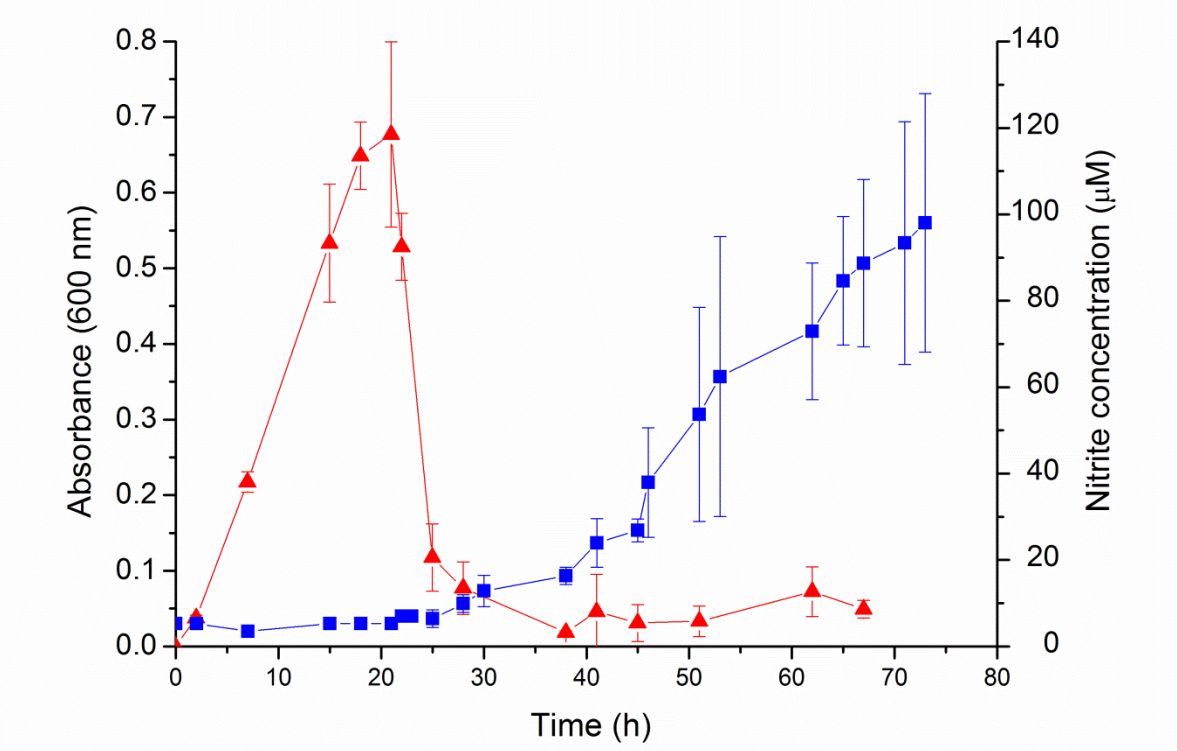

Figure 4.2 - *B. thailandensis* anaerobic growth and nitrate reductase activity. *B. thailandensis* was grown anaerobically in M9 minimal media in the presence of 20 mM sodium nitrate and 20 mM sodium succinate (blue squares). The production nitrite, and therefore relative nitrate reductase (NAR) activity, was monitored throughout anaerobic growth cycle using the Griess reagent (red triangles). Nitrite concentration (μM) was determined using a nitrite standard curve. Three biological replicates each with three technical replicates used when conducting the Griess reaction. Error bars ± SD.

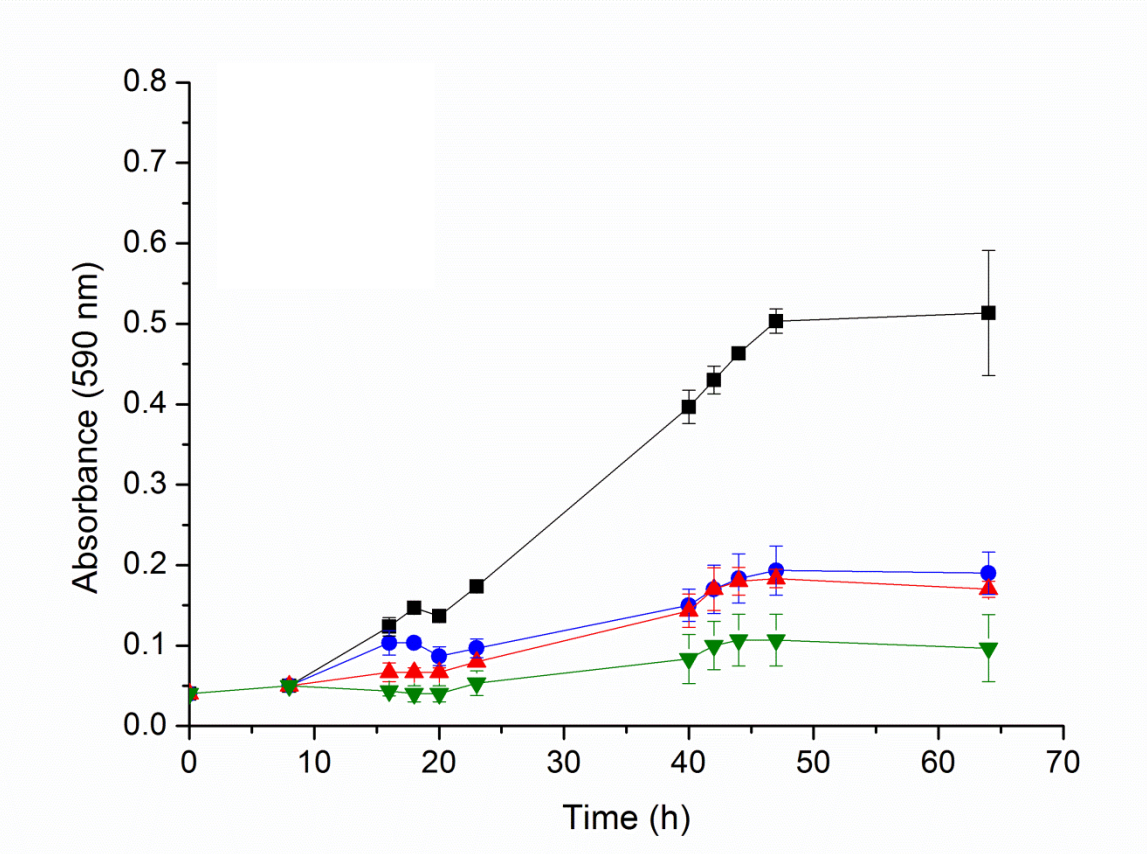

Figure 4.3 - Anaerobic growth of *B. thailandensis* E264 in the presence of sodium tungstate. Anaerobic growth of *B. thailandensis* in M9 minimal media supplemented with 20 mM sodium succinate, 20 mM sodium nitrate and varying concentrations of sodium tungstate (Na_2WO_4); 0 mM (black squares), 1 mM (blue circles), 5 mM (red triangles) 10 mM (green inverted triangle). Results are the average of three biological replicates. Error bars ± SD.

4.2.2 Construction of a B. thailandensis *E264 transposon mutant library and identification of miniTn5Km2 insertion into BTH_I1704*

B. thailandensis E264 encodes a wide range of genes required for anaerobic respiration. In order to determine which genes were important for anaerobic growth, a random transposon mutant library was created using the pUTminiTn5Km2 vector, encoding a kanamycin resistance cassette. The library of 1,344 random transposon mutants was screened on M9 minimal media containing 10 mM sodium succinate and 5 mM sodium nitrate, supplemented with gentamicin (100 µg/mL) and kanamycin (250 µg/mL). Insertion of the transposon into *B. thailandensis* was confirmed for three transposon mutants using primers specific for *B. thailandensis* and those specific for the kanamycin resistance cassette. Three transposon mutants (initially referred to as Tn #1, Tn #2, Tn #3) displayed a lack of growth anaerobically (Fig. 4.4). No growth defect was seen for any of the three transposon mutants when grown aerobically in rich or minimal media.

Nested PCR was performed, using both arbitrary and transposon specific primers, in order to identity the site of transposon insertion into the *B. thailandensis* E264 genome (Fig. 4.5 a and b). The nested PCR products were cloned into pJET1.2/blunt, transformed into JM109 competent cells (Fig. 4.5 c) and the resultant plasmid construct was sent for sequencing. The site of miniTn5Km2 insertion was successfully identified for one of the three transposon mutants (Tn #3 - now referred to as CA01), as having inserted into BTH_I1704 encoding *moeA1,* a gene required for the molybdopterin biosynthetic pathway.

B. thailandensis E264 is predicted to encode two *moeA* genes (BTH_I1704 and BTH_I2200) required for the second to last step of the molybdopterin biosynthetic pathway (Table 3.3 and Fig. 3.9). Transposon insertion into BTH_I1704 was confirmed with a southern blot using labelled DNA probes that would bind to either a 300 bp region within the kanamycin resistance (Km^R) cassette (Δ probe), or to an undisrupted 300 bp region within BTH_I1704 (wild-type probe). Both wild-type *B. thailandensis* and transposon mutant (CA01) genomic DNA were digested using *Xho*I and the DNA fragments were run on a 1 % TAE agarose gel. *XhoI* restriction sites, found outside of BTH_I1704 and within the transposon, generated either a 2,927 bp band for the wild-type or an approximately 2,000 bp band for the mutant with the wild-type probe (Fig.

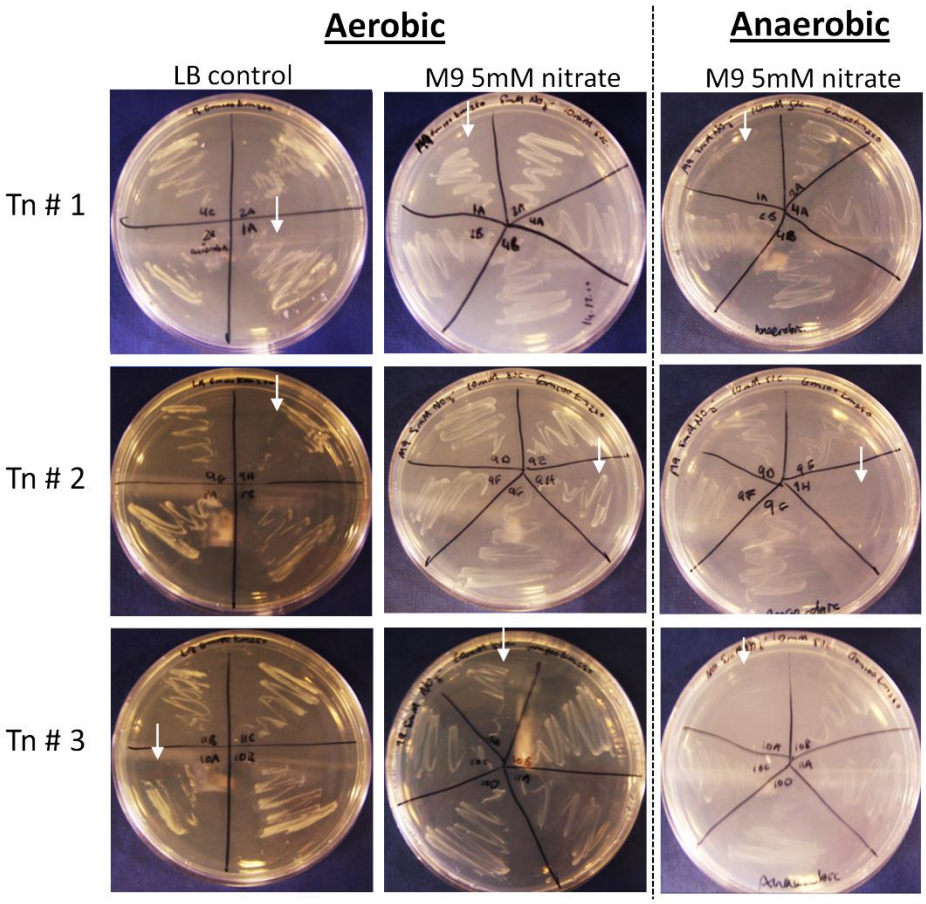

Figure 4.4 – Screening of *B. thailandensis* E264 transposon (mini-Tn5Km2) mutants to identify those defective in anaerobic respiration. *B. thailandensis* transposon mutants displaying initial anaerobic growth deficiency on the M9 minimal media selection plates (supplemented with 10 mM sodium succinate) were re-streaked onto LB agar plates (control) and M9 minimal media agar plates supplemented with 5 mM sodium nitrate. Plates were incubated at 37 ^{o}C either aerobically (left and middle columns) or anaerobically (right column). Both the M9 minimal and LB agar plates were supplemented with gentamicin (100 µg/mL) and kanamycin (250 µg/mL). Three transposon mutants (Tn #1-3) displayed no growth when incubated anaerobically but could grow under aerobic conditions, shown with white arrows.

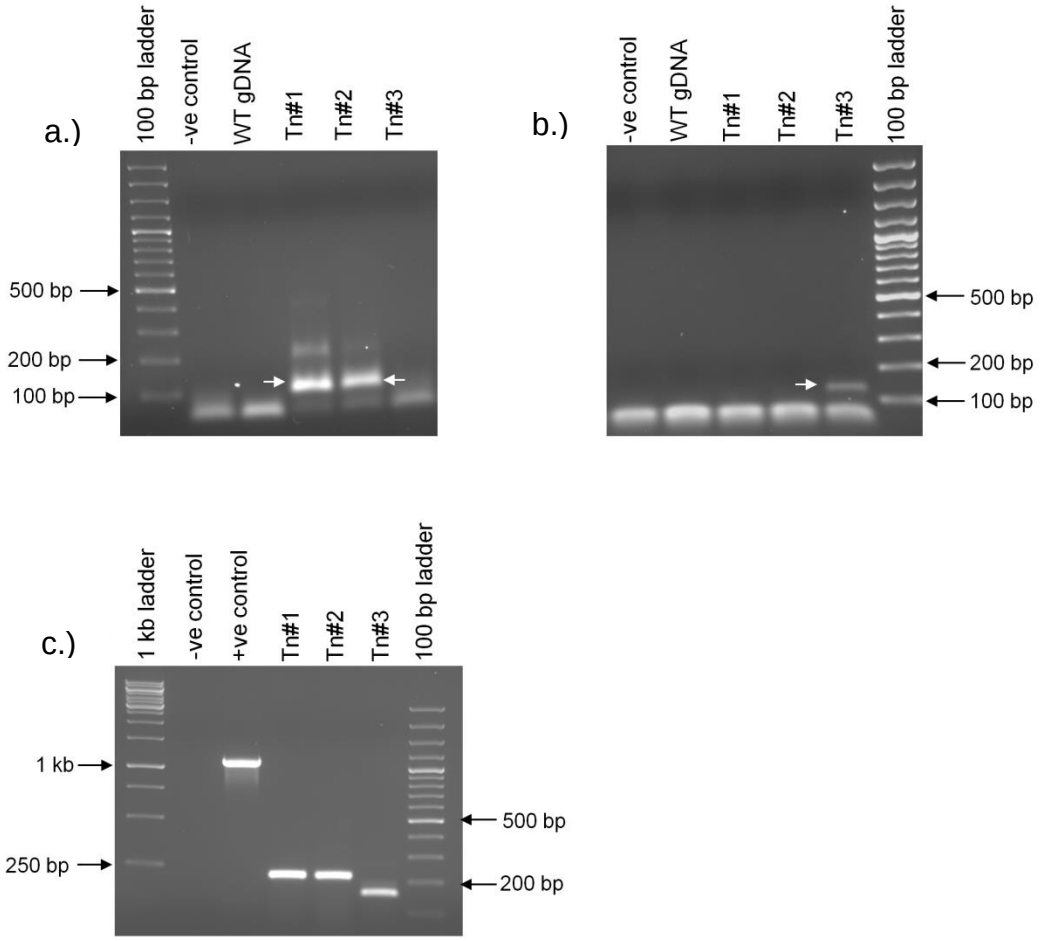

Figure 4.5 – Cloning of the *B. thailandensis* transposon mutant nested PCR products into pJET1.2/blunt. Top gels are the result of the nested PCR reaction using (a.) Arb4 or (b.) Arb3 and P7M1. Wild-type (WT) *B. thailandensis* (E264) genomic DNA, Tn#1-3 DNA or H_20 (negative (–ve) control) were used as templates in the first round of nested PCR, the products of which were then used as templates for another PCR reaction using Arb2 and P7U primers. PCR products (100 to 200 bp) from nested PCR using Arb4 (Tn #1 and Tn #2) or Arb3 (Tn #3) were purified and ligated into the pJET1.2/blunt cloning vector. c.) PCR confirmation using pJET1.2 forward and reverse primers, of successful cloning of arbitrary PCR ligation into pJET1.2/blunt. Positive control (+ve control) - PCR control product (976 bp) into pJET1.2/blunt.

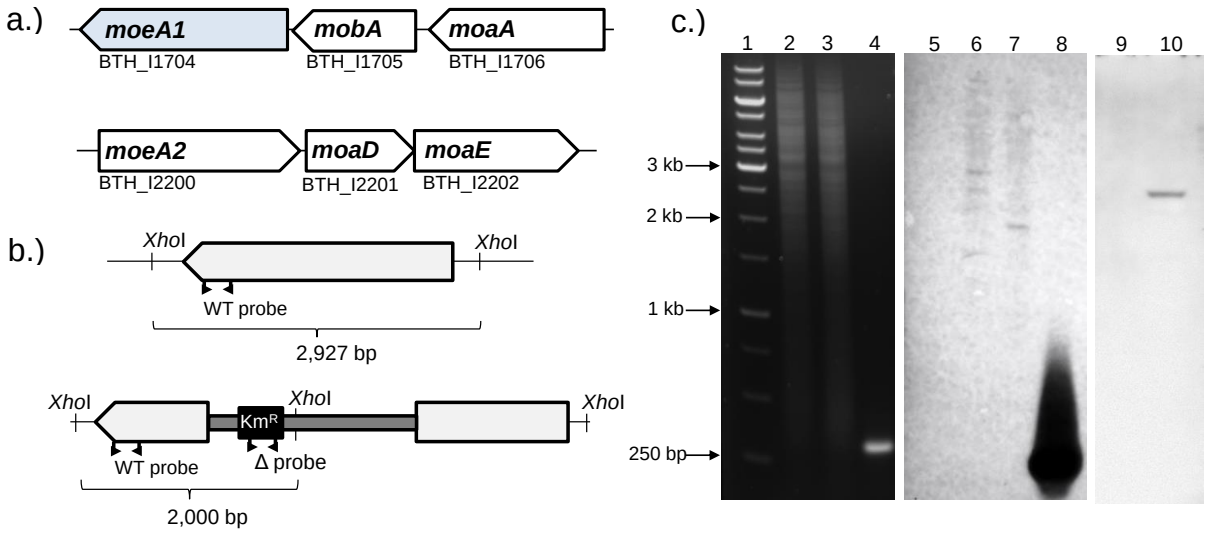

Figure 4.6 - Schematic representation of the *moeA* gene clusters in *B. thailandensis* and southern blot confirmation of site of the insertion in CA01. a.) *B. thailandensis* E264 encodes two *moeA* encoded on gene clusters with other genes required for the molybdopterin biosynthetic pathway; BTH_I1704 (*moeA1*), BTH_I1705 (*mobA*) and BTH_I1706 (*moaA*) and a second gene cluster encoding BTH_I2200 (*moeA2*), BTH_I2201 (*moaD*) and BTH_I2202 (*moaE*). b.) Southern blot *Xho*I restriction sites and primer binding regions for the wild-type and mutant probes (small black arrows) found in BTH_I1704 (top – highlighted in blue) and CA01 (BTH_I1704-Tn5Km2 - bottom). CA01 was previously referred to as Tn #3 prior to identification of site of transposon insertion. Both wild-type (WT) and CA01 gDNA were digested with *Xho*I, as *Xho*I restriction sites were found outside BTH_I1704, generating a 2,927 bp product, and within Tn5Km2, generating gene fragment of approximately 2,000 bp. c.) Southern blots (lanes 5-8 and lanes 9-10), and agarose gel (lanes 1-4) used to confirm Tn5Km2 insertion into BTH_I1704. Lane 1, 1 kb GeneRuler DNA ladder (Thermo-Scientific); lane 2, *B. thailandensis* digested DNA; lane 3, CA01 digested DNA; lane 4, 300 bp WT DNA probe. Lanes 5-8 – southern blot hybridised with WT probe; lane 5, 1 kb GeneRuler DNA ladder; lane 6, wild-type *B. thailandensis* digested DNA; lane 7, digested CA01; lane 8, 300 bp WT probe DNA. Lanes 9-10 – southern blot hybridised with mutant (Δ) probe; lane 9, digested *B. thailandensis* DNA; lane 10, digested CA01 DNA.

4.6 b and c). This and the absence of a band in wild-type digest DNA, when using the Δ probe, confirmed the site of transposon insertion in CA01 (Fig.4.6 c).

4.2.3 BTH_I1704 is required for anaerobic growth and nitrate reductase activity

Transposon insertion into BTH_I1704 in CA01 prevented anaerobic growth on nitrate (Fig. 4.7 a) but did not significantly affect aerobic growth in either M9 minimal media or L-broth. Addition of molybdate did not affect anaerobic growth of either the wild-type of mutant. Both wild-type *B. thailandensis* and CA01 are able to utilise nitrite anaerobically as an alternative electron acceptor, by-passing the need for the molybdenum dependent nitrate reductase required for anaerobic respiration.

The lack of anaerobic growth seen in CA01 is likely due to a reduction in NAR activity. To confirm a lack of NAR activity in the mutant both the wild-type and CA01 were grown aerobically in M9 minimal media supplemented with 20 mM sodium nitrate (Fig. 4.7 b) and samples were taken at various time-points to determine the concentration of nitrite produced using the Griess reaction. Only wild-type *B. thailandensis* displayed an accumulation of nitrite during aerobic growth on nitrate, indicating NAR is active during late exponential and stationary phase of growth (Fig. 4.7 c). To further confirm the lack of NAR activity in CA01 a spectrophotometric methyl-viologen assay was performed on cell membrane fractions. Wild-type and CA01 cultures were grown aerobically to generate biomass prior to incubation under anaerobic conditions for 4 hours in the presence of nitrate, to ensure expression of NAR. CA01 displayed a significant difference in NAR activity (T-test; p-value < 0.05) displaying 0.04 μmol [NO_3^-]/min/g (ww) compared to 0.134 μmol [NO_3^-]/min/g (ww) NAR activity seen in the wild-type (Fig. 4.7 d). These results together confirm the inability of CA01 to respire on nitrate is due to a reduction in NAR activity (Fig. 4.7).

4.2.4 The B. thailandensis *genome encodes two putative* moeA *genes*

Two putative *moeA* genes have been identified in *B. thailandensis* E264 (BTH_I1704 and BTH_I2200) and *B. pseudomallei* K96243 (BPSL2455 and BPSL1479) sharing around 39.5 % sequence identity and displaying 40 % homology to the MoeA found in *E. coli* K-12 (b0827). The *moeA* genes from *B. thailandensis* E264*, B. pseudomallei* K96243*, B. mallei* ATCC 23344 and *E. coli* were aligned using

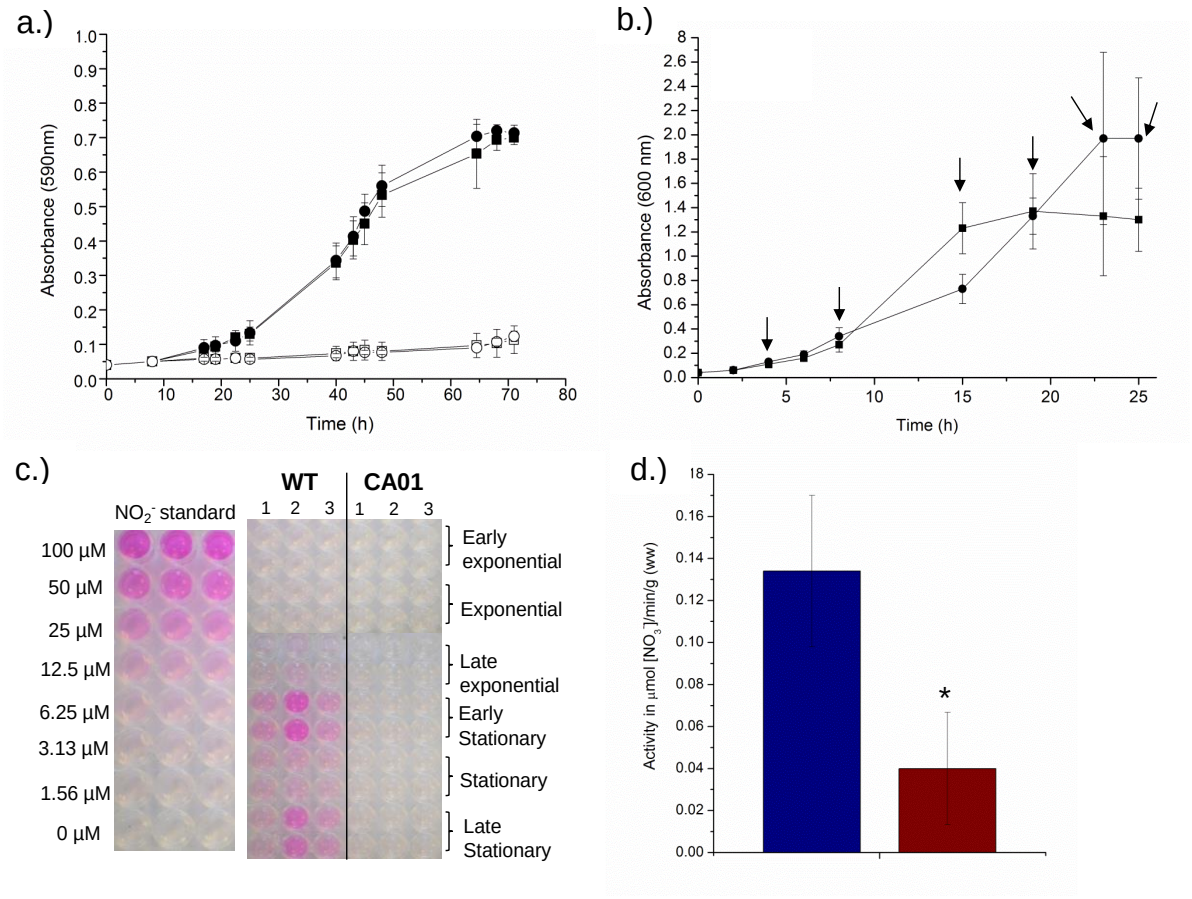

Figure 4.7 - Nitrate-dependent growth and NAR activity of *B. thailandensis* E264 and CA01. *B. thailandensis* was grown in M9 minimal medium aerobically or anaerobically in the presence or absence of nitrate. a.) Anaerobic growth of *B. thailandensis* (filled) and CA01 (open) in the presence (squares) or absence (circles) of 1 mM molybdate. b.) Aerobic growth in M9 minimal media supplemented with 20 mM sodium nitrate of WT (filled squares) and CA01 (filled circles). Samples were taken at various intervals (shown with the arrows) and used in a Griess reaction shown in (c.). c.) Nitrite production measured using the Griess reaction during aerobic growth – 4 hours (h), early exponential; 8 h, exponential; 15 h, late exponential; 19 h, early stationary; 24 h, stationary; 27 h late stationary phase. No nitrite was detected in CA01 at any time point tested. Time points are not from a sequential culture. Columns of the 96 well plate represents three technical replicates from one biological replicate. d.) Nitrate reductase activity (in µmol [NO_3^-]/min/g (ww)) of membrane fractions from anaerobically acclimatised wild-type (blue) and CA01 (red) cultures. Results are the average of three biological replicates. Statistically significant results (p-values ≤ 0.05) are shown with asterisk (*). Error bars ± SD.

Clustal Omega to determine the degree of sequence conservation and identify conserved residues required for MoeA function. *E. coli* MoeA contains a highly conserved sequence SSGGVSVG required for catalytic activity (Schrag *et al.*, 2001). All *Burkholderia* spp*. moeA* genes analysed in (Fig. 4.8) contained highly conserved residues, Thr319 (T), Glu322 (E), Asp362 (D) and Gly390 (G) (residue numbers corresponding to BTH_I2200 amino acid sequence), predicted to be required for binding an coordination of the magnesium (Mg^{2+}) hexahydrate ion, as seen in the *E. coli* MoeA (Schrag *et al.*, 2001). In comparison to *E. coli* MoeA, all the *Burkholderia* MoeA have a threonine residue in replacement of serine residue, giving **T**SGGVSVG (Fig. 4.8), instead of SSGGVSVG seen in the *E. coli* MoeA. A point mutation within this conserved cluster in *Anabaena*, causing a replacement a key guanine residue for an asparate (SSG**D**VSVG), prevented MoeA function, and consequently disrupted nitrate reductase activity (Ramaswamy *et al.*, 1996). BTH_I2200, BTH_I1704, BPSL2455, BPSL1479, BMA0517 and BMA1382 all contain the highly conserved Gly390 (G) found within TSG**G**VSVG, and the conserved Thr319, Glu322 and Asp362 it is unlikely that the replacement of S for T in *Burkholderia* would prevent MoeA activity.

BTH_I1704 (*moeA1*) is located within a gene cluster encoding *moaA* (BTH_I1706) and *mobA* (BTH_I1705), required for initial and final steps of Mo-*bis*MGD cofactor biosynthesis. A second *moeA* (BTH_I2200; *moeA2*), encoded within a gene cluster which included *moaD* and *moaE* required for MPT synthase, was also identified. Because the transposon insertion into BTH_I1704 (in CA01) prevented anaerobic growth and NAR activity, the function of BTH_I2200 was brought into question. To determine whether BTH_I2200 was expressed during aerobic and anaerobic growth RT-PCR was performed on mRNA extracted from wild-type *B. thailandensis* cultures grown anaerobically in minimal media and aerobically overnight. BTH_I1704 was shown to be constitutively expressed under anaerobic conditions in the presence of nitrate and was expressed to a similar degree after aerobic overnight growth in L-broth supplemented with or without nitrate (Fig. 4.9). No expression was seen for BTH_I2200 under the conditions tested in this study. The significance of BTH_I2200 is currently unknown.

Figure 4.8 – Sequence alignment of putative *moeA* proteins in *Burkholderia* spp. highlighting potential catalytic residues. Putative *moeA* genes from *B. thailandensis* E264 (BTH_I1704 and BTH_I2200), *B. pseudomallei* K96243 (BPSL2455 and BPSL1479) and *B. mallei* ATCC 23344 (BMA1382 and BMA0517) were aligned against the *moeA* gene found in *E. coli* (b0827), using Clustal Omega. Highlighted residues correspond to those seen in Schrag *et al*. (2001) highlighting part of domain 1 = blue and domain 3 = green. Residues in bold in the red box are the potential conserved Mg^{2+} hexahydrate binding site and the active site of MoeA. Both putative MoeA proteins in *Burkholderia* spp. have the residues implicated in binding of Mg^{2+} hexahydrate, in the active site of the protein. The rest of the sequence is less well conserved between *Burkholderia* and the *E. coli* MoeA. Arrows denote conserved Thr319 (T), Glu322 (E), Asp362 (D) and Gly390 (G) residues required for MoeA activity (see text for details). Asterisks (*) denote conserved resides in all amino acid sequences analysed.

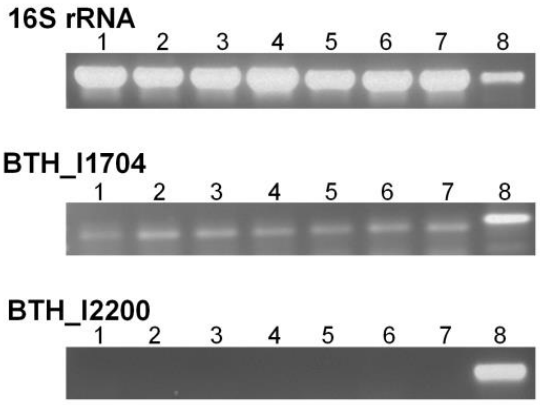

Figure 4.9 – **Expression of *B. thailandensis* BTH_I1704 (*moeA1*) and BTH_I2200 (*moeA2*) during anaerobic growth**. Reverse transcriptase PCR (RT-PCR) was used to determine the expression of putative *moeA* genes in wild-type *B. thailandensis* E264 when grown aerobically or anaerobically using nitrate as a sole electron acceptor. Primers amplifying regions within 16s rRNA, BTH_I1704 and BTH_I2200 were used in separate reactions. Lane 1 – aerobic LB overnight culture; lane 2 – aerobic LB overnight culture supplemented with nitrate; lane 3 - 2 h (lag phase); lane 4 - 24 h (early exponential); lane 5 - 47 h (mid-exponential); lane 6 - 54 h (late exponential); lane 7 - 72 h (stationary phase); lane 8 – *B. thailandensis* gDNA. *B. thailandensis* gDNA was used as a positive control. Images are the representative of two independent biological replicates.

4.2.5 B. thailandensis *E264 can remain viable for up to one year within an anaerobic environment*

B. pseudomallei has been shown to persist within an anaerobic environment for up to one year, when cultured in a modified version of the Wayne's model for hypoxic shift down, in the absence of a terminal electron acceptor (Hamad *et al.*, 2011). The Wayne's model allows for a gradual acclimatisation to an anaerobic environment. Initial growth of *B. pseudomallei* seen in the Hamad *et al.* (2011) study was likely due to aerobic/microaerobic respiration rather than denitrification. To determine whether anaerobic growth in the presence of an electron acceptor affects entry into dormancy wild-type *B. thailandensis* E264 and CA01 were grown in the presence or absence of nitrate or nitrite (Fig. 4.10). Under anaerobic conditions, *B. thailandensis* could only grow in the presence of either nitrate or nitrite, displaying the best growth seen when cultured with nitrate (Fig. 4.10 a). Considering CA01 cannot grow anaerobically in the presence of nitrate, CA01 was only grown in L-broth or L-broth supplemented with 6 mM nitrite. CA01 initially displayed a slower anaerobic growth rate to the wild-type in the presence of nitrite, but reach a similar density to the wild-type after 40 hours anaerobic incubation. After around 14 days a sub-population (1×10^5 CFU/mL) of both wild-type and mutant cells entered a dormant/persistent state, lasting for up to one year. This entry into a dormant/persistent state occurred regardless of *B. thailandensis* ability to grow under anaerobic conditions, with similar CFU/mL seen for wild-type *B. thailandensis* and CA01 when grown in L-broth alone or L-broth supplemented with nitrate or nitrite (Fig. 4.10). Growth of dormant *B. thailandensis* and CA01 cells could be restored when transferred to fresh medium aerobically, but as expected only the only wild-type *B. thailandensis* could be revived for anaerobically on nitrate. Entry of *B. thailandensis* into a non-replicating persistent state under anaerobic conditions is consistent with what was seen for *B. pseudomallei* (Hamad *et al.*, 2011).

a.)

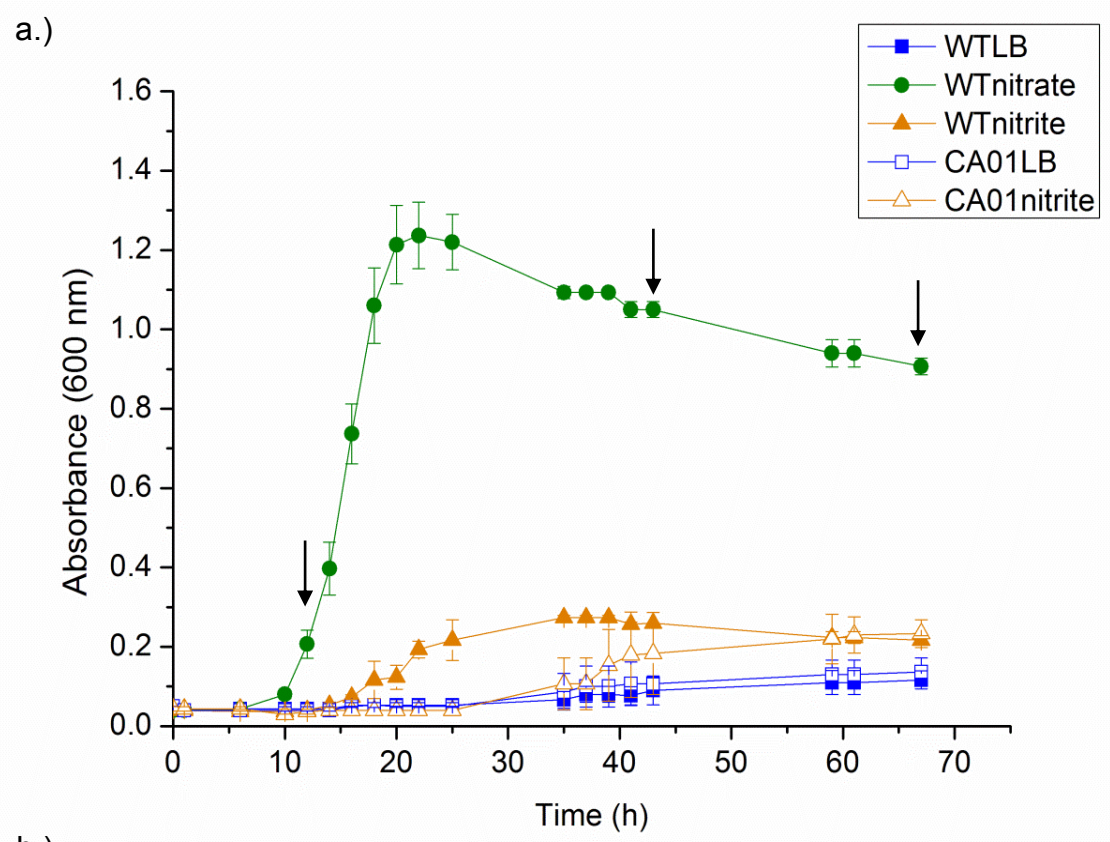
WTLB
WTnitrate
WTnitrite
CA01LB
CA01nitrite
Absorbance (600 nm)
Time (h)
0.0
0.2
0.4
0.6
0.8
1.0
1.2
1.4
1.6
0
10
20
30
40
50
60
70

b.)

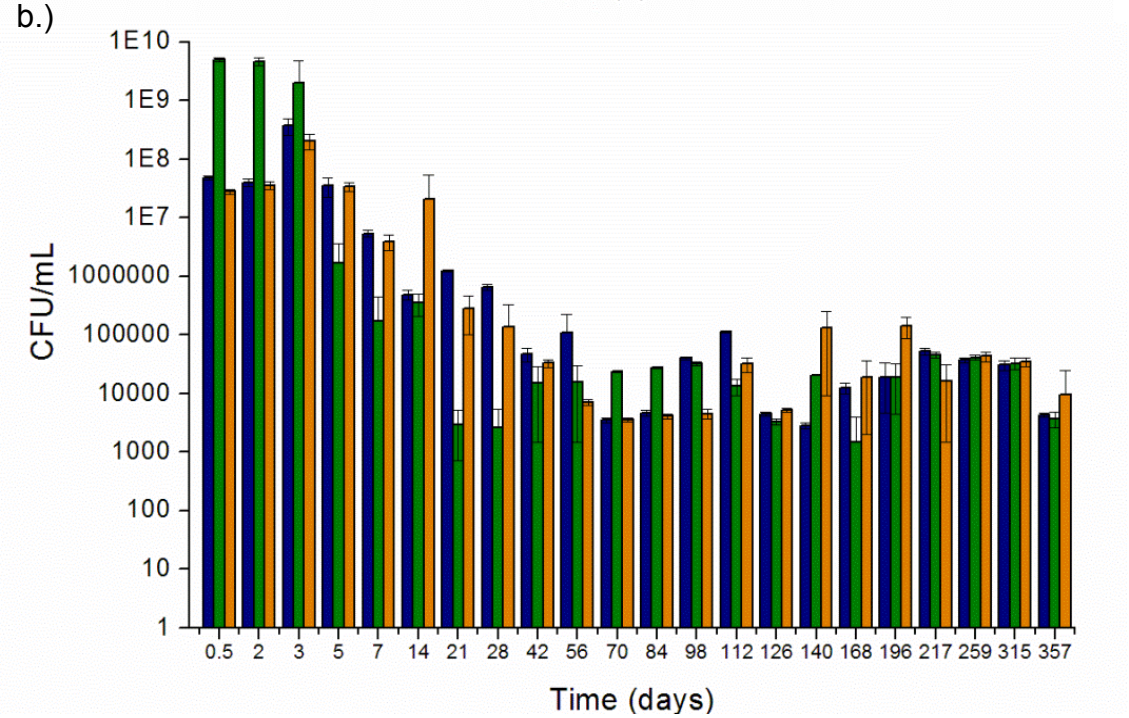
CFU/mL
Time (days)
1E10
1E9
1E8
1E7
1000000
100000
10000
1000
100
10
1
0.5
2
3
5
7
14
21
28
42
56
70
84
98
112
126
140
168
196
217
259
315
357

Figure 4.10 - **Anaerobic viability of *B. thailandensis* E264.** Wild-type *B. thailandensis* E264 and CA01 were grown anaerobically, in medical flat bottomed flasks sparged with nitrogen, in L-broth (LB) supplemented with either 20 mM sodium nitrate or 6 mM sodium nitrite. The viability of these *B. thailandensis* cultures was determined using colony counts (CFU/mL) taken every few weeks for up to one year. a.) Anaerobic growth of wild-type *B. thailandensis* (filled shapes) or CA01 (open shapes) in L-broth; LB only/no electron acceptor (blue squares), LB supplemented with nitrate (green circles), or LB supplemented with nitrite (orange triangles). No significant growth was seen in the absence of any electron acceptor. b.) *B. thailandensis* LB only (blue), *B. thailandensis* LB nitrate (green), CA01 LB only (orange). Viability cell counts (CFU/mL) were taken every few weeks for up to one year. Arrows in (a.) show the times at which the first three CFU counts were taken; 0.5 days, 2 days and 3 days. Similar results were seen for both wild-type *B. thailandensis* and CA01 when incubated with nitrite. Data shown is the average of three biological replicates. All biological replicates had two or three technical replicates used when determining CFU/mL. Error bars ± SD.

4.2.6 BTH_I1704 plays a role in biofilm formation and motility but not virulence in G. mellonella

The ability to form biofilms has often been associated with the capacity to grow under anaerobic conditions. To determine whether disruption of the molybdopterin biosynthetic pathway affects biofilm formation, wild-type *B. thailandensis* and CA01 were grown aerobically or anaerobically in L-broth or minimal media in a 96 well plate supplemented with or without nitrate. The plates were incubated for 3 days and the degree of biofilm formation was assessed using a crystal violet stain. In comparison to the wild-type, CA01 displayed a statistically significant (p-value ≤ 0.05) reduction in biofilm formation under most of the conditions tested (Fig. 4.11). Higher levels of biofilm formation were seen for both wild-type and CA01 when grown in L-broth. CA01 did display an increase in growth after 3 days incubation anaerobically, potentially indicating the induction of BTH_I2200 allowing for growth. This may account for the similar biofilm formation capabilities of CA01 to the wild-type anaerobically in LB medium when supplemented with nitrate.

No significant difference (p-value > 0.01) was seen in growth in L-broth when comparing wild-type *B. thailandensis* and CA01 in the 96 well plate grown under aerobic conditions that would account for the differences in biofilm formation seen between the strains tested. In minimal media a significant difference between growth rates was seen between the wild-type and the mutant, with the mutant displaying a higher growth rate to the wild-type. However, although the mutant displayed a higher growth rate (in terms of OD), the mutant displayed a statistically significant reduction in biofilm formation when compared to the wild-type. Due to the differences in growth seen anaerobically in the presence of nitrate, one cannot discount the possibility that under these conditions the differences in biofilm formation seen between the wild-type and mutant are not due to differences in growth rates. No significant growth was seen for either the wild-type or mutant anaerobically in the absence of nitrate, accounting for the low levels of biofilm formation seen for both strains.

The ability to form biofilms is often dependent on motility. Since CA01 displayed a reduction in biofilm formation it was conceivable that flagella function was affected. CA01 displayed a significant reduction in swimming motility when compared to the wild-type (T-test; p-value ≤ 0.01) (Fig. 4.12). Addition of nitrate to motility media did

not affect degree of motility for either wild-type or mutant (Chapter 8 – Appendix figure 8.2).

G. mellonella have previously been used as an infection model for *B. thailandensis* (Wand *et al.*, 2010). To determine whether CA01 displayed a difference in virulence, ten *G. mellonella* were challenged with either PBS (control), wild-type *B. thailandensis* or CA01 at a 450 – 500 CFU/galleria infectious dose. No significant difference was seen in virulence between the wild-type and mutant CA01 (Two way ANOVA; df =1, f = 5.2, $p > 0.05$) (Fig. 4.13).

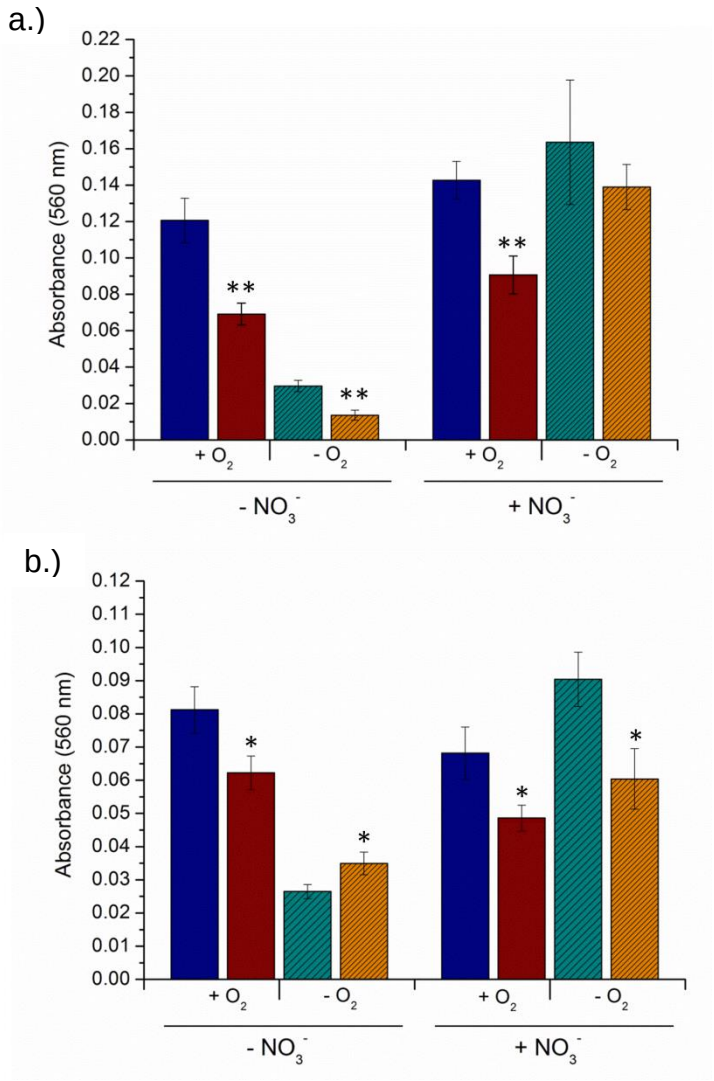

Figure 4.11 - BTH_I1704 plays a role in biofilm formation under aerobic and anaerobic conditions. Both wild-type (WT) *B. thailandensis* E264 and CA01 were grown in L-broth or M9 minimal media supplemented with or without 20 mM sodium nitrate. Biofilm formation was measured using a crystal violet stain following a three day incubation period either aerobically (+ O_2^-) or anaerobically (- O_2^-); WT aerobic (blue), WT anaerobic (cyan with dashed lines), CA01 aerobic (red) and CA01 anaerobic (orange with dashed lines). a.) Average biofilm formation of WT *B. thailandensis* or CA01 in L- broth (LB). b.) Average biofilm formation of WT *B. thailandensis* or CA01 in M9 minimal media supplemented with succinate. No significant growth is seen anaerobically in the absence of NO_3^- for either LB or M9 minimal media. Three biological replicates were used each with 5 technical replicates. Error bars ± SD. Statistically significant results (p-values < 0.05 or < 0.01) are shown with asterisks (*) or (**).

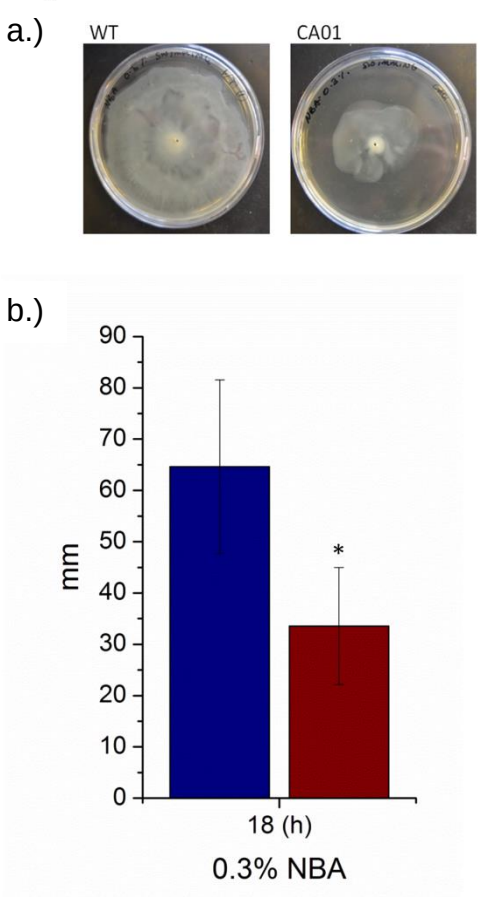

Figure 4.12 - BTH_I1704 plays a role in swimming motility. Motility assays carried out on 0.3 % nutrient broth agar (NBA) supplemented with 0.5% glucose. a.) Representative image of wild-type (WT) and CA01 swimming motility. b.) Degree of motility (mm) for wild-type *B. thailandensis* E264 (blue) and CA01 (red). Measurements (mm) with taken after 18 hours (h) incubation at 37 ^{o}C. Asterisks (*) denotes significant difference (p-value ≤ 0.01) seen between wild-type *B. thailandensis* and CA01. Five biological replicates used each with three technical replicates. Error bars ± SD.

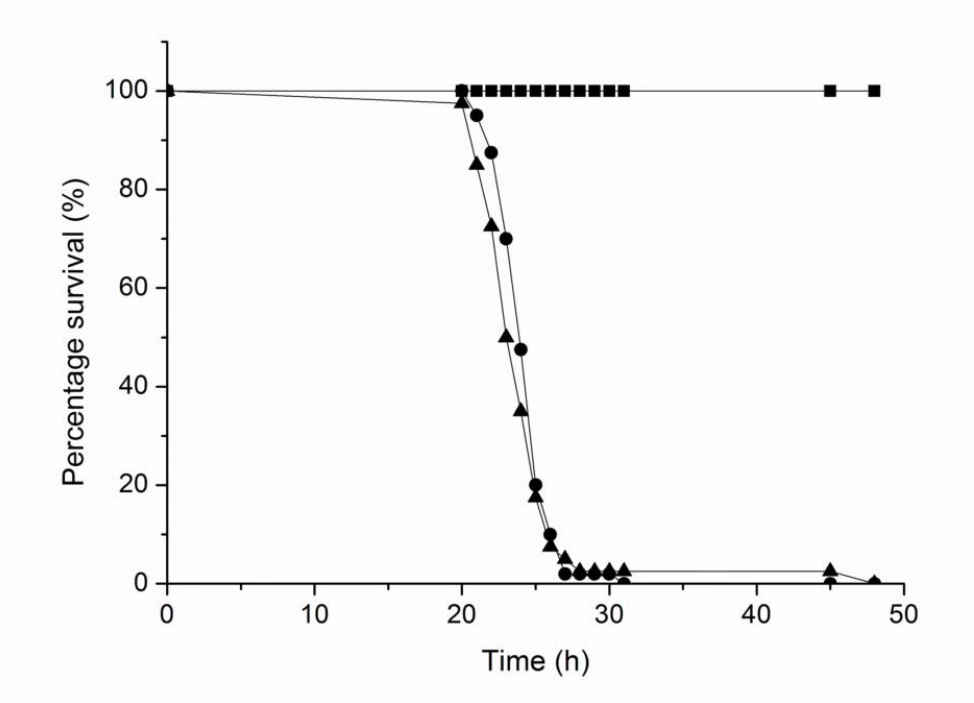

Figure 4.13 – Disruption of BTH_I1704 does not affect virulence in *G. mellonella*. Ten *G. mellonella* were challenged with either PBS (squares), wild-type *B. thailandensis* (circles) or CA01 (triangles). Data shown is the average of four biological replicates with an average infectious dose 450 - 500 CFU/galleria.

4.2.7 CA01 complementation with pDA-17::BTH_I1704 successfully restores anaerobic respiration, NAR activity and biofilm formation

In order to confirm that the phenotypes exhibited by CA01 were due to the disruption of *moeA1,* BTH_I1704 was cloned into the constitutive expression vector pDA-17 encoding a *dhfr* promoter and tetracycline resistance cassette (Fig. 4.14 a). This generated the pDA-17::BTH_I1704 plasmid which was confirmed using PCR and gene sequencing. The pDA-17::BTH_I1704 was then conjugated into CA01 and confirmed with using PCR (Fig. 4.14 b). Complementation of CA01 using pDA-17::BTH_I1704 successfully restored anaerobic growth on nitrate for the mutant in both minimal and rich media and did not adversely affect aerobic growth (Fig. 4.15). All experiments with the mutant complement were performed in the presence of 50 µg/mL tetracycline to ensure the maintenance of pDA-17::BTH_I1704 plasmid.

Once the mutant complement had been successfully created all the experiments showing a difference between wild-type *B. thailandensis* and CA01 were repeated. When the aerobic Griess reaction was repeated the wild-type *B. thailandensis* displayed a 2 hour longer lag phase, accumulating nitrite much earlier on within the growth cycle, when compared to the results presented in figure 4.7 c. Complementation of CA01 with pDA-17::BTH_I1704 was able to restore NAR activity, as seen with an accumulation of nitrite during aerobic growth on minimal media after 16 hours (Fig. 4.16 a). After 24 hours CA01_pDA-17::BTH_I1704 nitrite levels were significantly (T-test; p-value ≤ 0.01) lower (15.5 ± 4 µM) to those seen in the wild-type (21 ± 3 µM). This suggests that the complement may not be able to fully restore nitrate reductase activity to the same extent as that seen in wild-type. In comparison to both the wild-type and the complemented mutant, CA01 nitrite levels only reached 2 ± 0.9 µM after 24 hours growth. Complementation of CA01 with pDA-17::BTH_I1704 was able to successfully restore biofilm formation to the similar extent to that seen in the wild-type aerobically in the presence or absence or nitrate, but not anaerobically in the presence of nitrate (Fig. 4.16 b). The lack of a complete restoration of biofilm formation seen in the complement to wild-type levels, under anaerobic conditions in the presence of nitrate, could potentially be linked the lower levels of nitrite production, and therefore relative NAR activity, seen after 24 hours growth (Fig. 4.15 a). Although complementation did successfully restore anaerobic growth, NAR activity and biofilm formation it could not restore the motility defect seen in CA01 (Fig. 4.16 c).

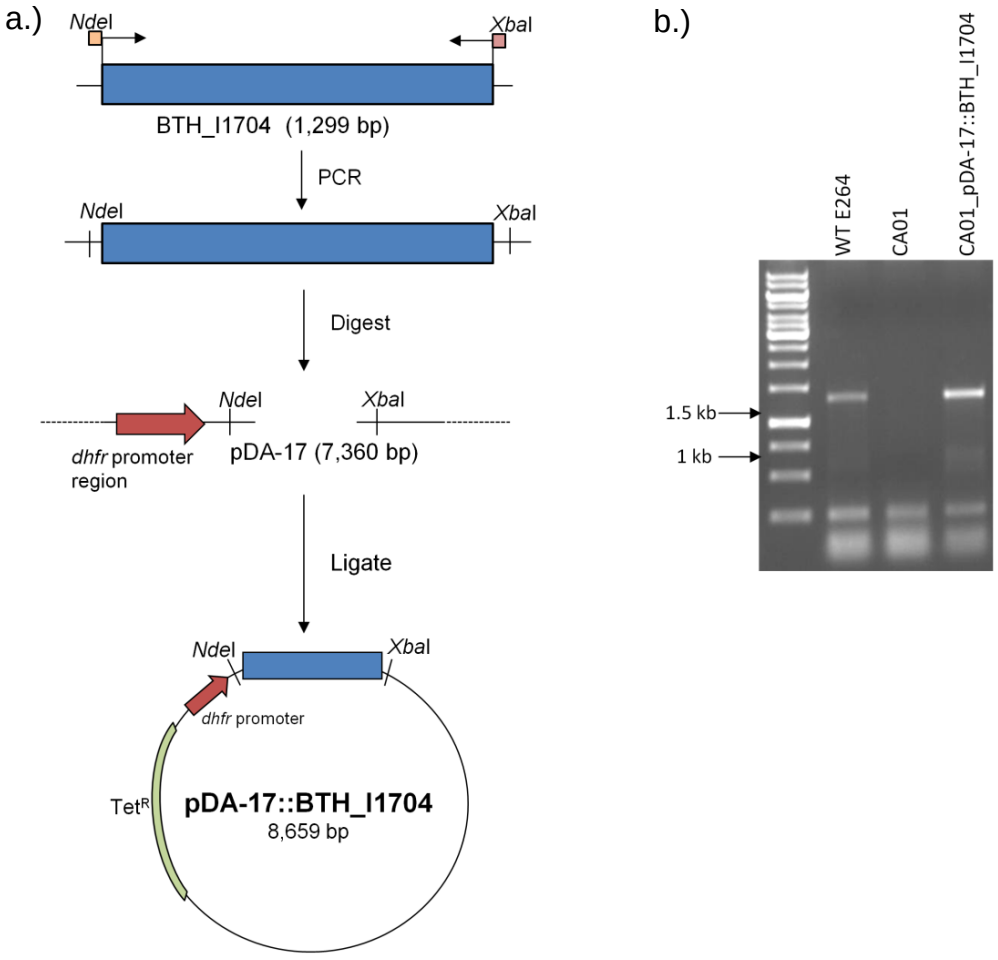

Figure 4.14 – Construction of and validation of pDA-17::BTH_I1704. CA01 was successfully complemented with BTH_I1704 using the pDA-17 constitutive expression vector encoding a *dhfr* promoter and a tetracycline resistance gene cassette. a.) Method work through for creation of the pDA-17::BTH_I1704 vector for complementation of BTH_I1704 (see methods section *2.2.8 Transposon mutant complementation* for more details). b.) PCR confirmation of CA01 pDA-17::BTH_I1704 complement. Primers used to confirm presence of an undisrupted BTH_I1704 were moeA1704_fwd and moeA1704_rv. Lane 1 -1 kb gene ruler ladder; lane 2 - WT E264 gDNA; 3 - CA01 gDNA; lane 4 - CA01_pDA-17::BTH_I1704 PCR lysate.

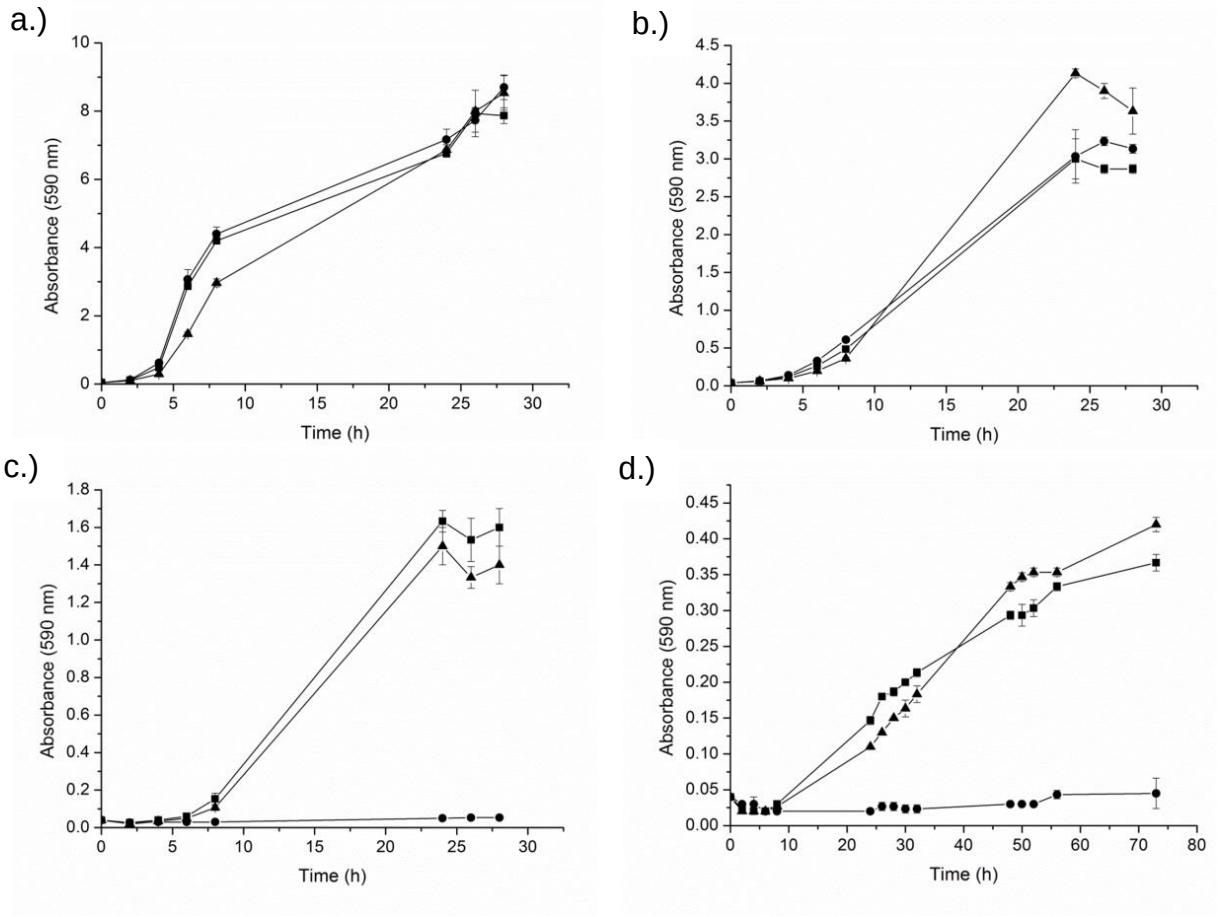

Figure 4.15 – Growth of wild-type *B. thailandensis* E264, CA01 and CA01_pDA-17::BTH_I1704. Wild-type *B. thailandensis* E264 (filled squares), CA01 (filled circles) and CA01_pDA-17::BTH_I1704 (filled triangles) were grown aerobically and anaerobically (in the presence of 20 mM sodium nitrate) in L-broth and M9 minimal medium. a.) Aerobic growth in L-broth; b.) Aerobic growth in M9 minimal media; c.) Anaerobic growth in LB media supplemented with nitrate; d.) Anaerobic growth in M9 minimal media supplemented with nitrate. Data shown is the average of three biological replicates. Error bars ± SD.

As of note when the motility experiment was repeated neither the wild-type or CA01 displayed the same degree of movement through the semi-solid agar, even with an increase in incubation time to 24 hours (see Fig. 4.12). Both motility experiments were repeatable at the time they were performed, with both showing statistically significant differences between wild-type and mutant. The same protocol was followed for all the experiments so the differences seen between experimental replicates could potentially highlight a problem with experimental replication. It is possible that the 0.3 % agar plates, used when performing the experiment with the complement, may have been dried for a little longer to those used previously, resulting in a reduction in *B. thailandensis* motility.

4.3 Discussion

B. thailandensis and *B. pseudomallei* are environmental saprophytes, commonly found in rice paddy fields in Southeast Asia (Inglis & Sagripanti, 2006). Paddy soil becomes hypoxic at a 3 mm depth where nitrate predominates as the major anion, allowing for the colonisation of anaerobic microorganisms (Liesack *et al.*, 2000; Ratering & Schnell, 2001). In the human body nitrate is normally obtained as a dietary source or is produced through the oxidation of nitric oxide, with both nitrate and nitrite found in circulating blood, urine, kidneys, saliva, plasma and in low amounts in the lungs (Kelm, 1999; Lundberg *et al.*, 2004). *B. pseudomallei* has recently been shown to be able to survive and persist within an anaerobic environment for up to one year, and can utilise nitrate as a respiratory substrate (Hamad *et al.*, 2011). Yet despite the obvious availability of nitrogen-oxyanions, the utilization of nitrate by *Burkholderia* spp. as a respiratory substrate to sustain growth either within the environment or during infection has remained poorly studied.

B. pseudomallei, the etiological agent of melioidosis, causes acute, chronic and latent infections, persisting within the human body for up to 62 years (Chua *et al.*, 2003; Currie *et al.*, 2000a). Melioidosis is often misdiagnosed as tuberculosis, as both display similar clinical features such as granulomas, which often display a low oxygen tension (Conejero *et al.*, 2011; Vidyalakshmi *et al.*, 2008). Although currently little is known about the mechanisms of persistence of *B. pseudomallei,* it is possible that the ability to survive under anaerobic conditions will play some role.

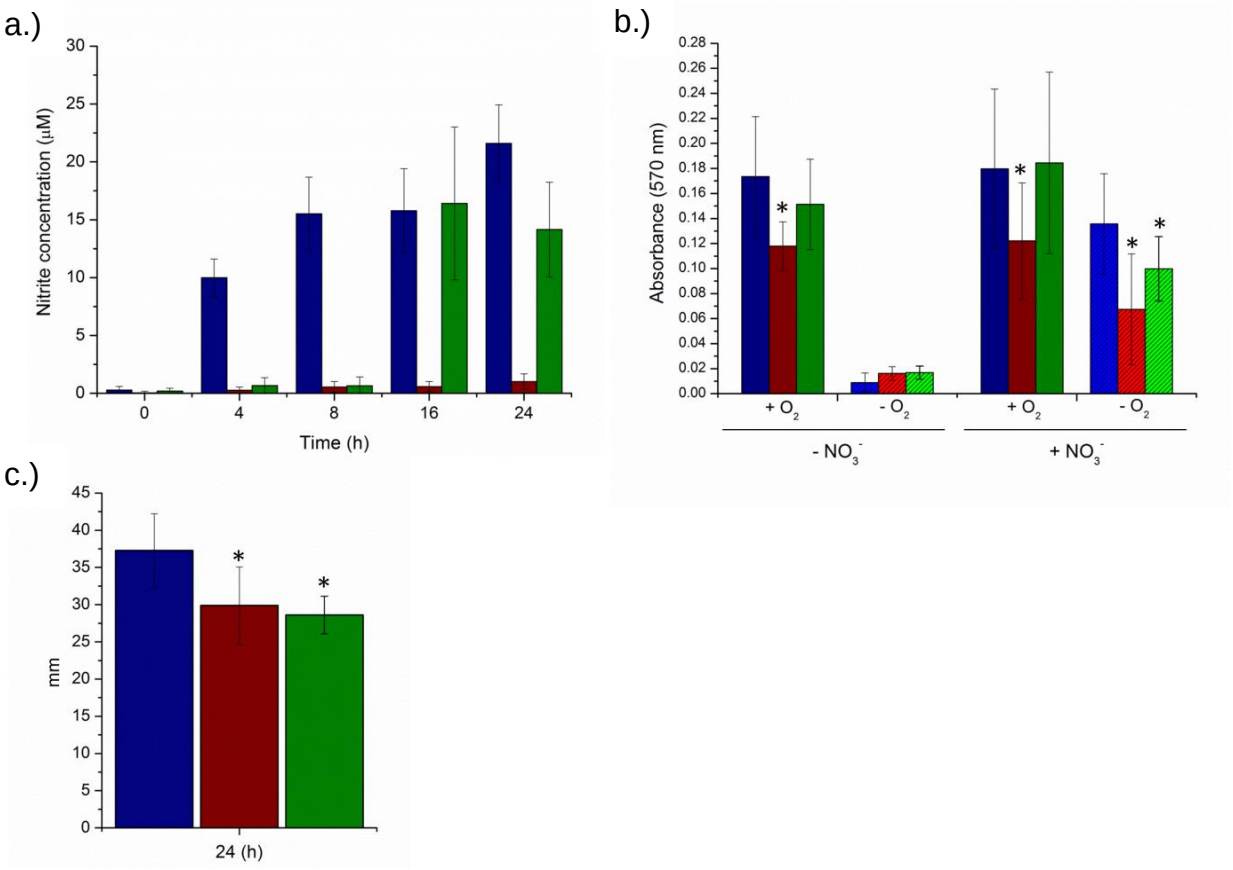

Figure 4.16 - Complementation of CA01 successfully restores NAR activity, biofilm formation but not motility. a.) Nitrite production, measured using the Griess reaction, during aerobic growth in M9 minimal media supplemented with 20 mM sodium nitrate, for WT (blue), CA01 (red) and CA01_pDA-17::BTH_I1704 (green). b.) Biofilm assay was performed in L-broth in the presence or absence of nitrate (NO_3^-) for WT *B. thailandensis* (blue), CA01 (red) and CA01_pDA-17::BTH_I1704 (green). A 96 well plate was incubated for three days aerobically (+ O_2; empty columns) or anaerobically (– O_2; dashed columns), and the degree of biofilm formation was measured using a crystal violet stain. c.) *B. thailandensis* motility on 0.3 % nutrient broth agar after 24 hour incubation. Wild-type (blue), CA01 (red), CA01_pDA-17::BTH_I1704 (green). Three or four independent biological replicates were used each with three or five technical replicates. Statistically significant results (p-values ≤ 0.01), comparing WT and CA01 or WT and CA01_pDA-17::BTH_I1704 are shown with asterisks (*). Error bars ± SD.

B. thailandensis can utilise both nitrate and nitrite as alternative respiratory electron acceptors, powering growth in oxygen limiting environments via the denitrification pathway. *B. thailandensis* encodes two membrane-bound NAR enzymes, both of which require a molybdenum cofactor for their activity. The accumulation of nitrite during late exponential and stationary phase of aerobic growth of wild-type *B. thailandensis,* not seen in CA01, points towards the likely induction of NAR (Fig. 4.7 c), and could indicate a reduction in the oxygen levels of the culture allowing for expression of *narGHJI*. By comparison, nitrite accumulated during the lag phase of growth under anaerobic conditions (Fig. 4.2), declining rapidly at the start of exponential phase. This decline in nitrite levels at the start of exponential phase indicated an induction of the rest of the anaerobic respiratory pathway, allowing for growth and the generation of a PMF.

B. pseudomallei is known to enter a dormant/persistent state under anaerobic conditions, in the absence of a terminal electron acceptor. To test whether the ability to respire under anaerobic conditions affected entry into a dormant state, *B. thailandensis* was grown anaerobically in the presence or absence of nitrate or nitrite. Similar to what was seen for *B. pseudomallei* and *M. smegmatis* (Dick *et al.*, 1998; Hamad *et al.*, 2011) a subpopulation (1×10^5 CFU) of *B. thailandensis* entered a dormant/persistent state under anaerobic conditions, lasting up to one year. This entry into a dormant state occurred regardless of *B. thailandensis* ability to grow under anaerobic conditions, indicating anaerobiosis was sufficient to induce dormancy and entry into a non-replicating persistent (NRP) state (Fig. 4.10). Cells that had entered a dormant/NRP state could be reawakened when transferred to fresh media and incubated aerobically or anaerobically in the presence of nitrate. One could hypothesise that the ability to respire using nitrate as an electron acceptor provides *B. thailandensis,* and potentially *B. pseudomallei,* with a competitive advantage, ensuring its replication once conditions become more favourable.

Creation of a transposon mutant library successfully identified the molybdopterin biosynthetic pathway, specifically *moeA1* (BTH_I1704), to be required for anaerobic nitrate respiration. The molybdopterin biosynthetic pathway is required for the formation of Moco, required for the function of a number of proteins involved in anaerobic respiration and electron transport. Molybdoenzymes fall into two distinct groups, bacterial nitrogenases and pterin-based molybdoenzymes such as the DMSO

reductase family, which includes NAR (Magalon, 2011). *B. thailandensis* and *B. pseudomallei* encode a wide range of different molybdo-proteins (such as formate dehydrogenase, sulfite oxidase, xanthine dehydrogenase, and NarGHI) which share 90 to 99 % sequence identity (Table 4.1) (Holden *et al.*, 2004). A number of molybdoproteins, such as nitrate reductase, DMSO reductase, sulfite oxidase, are known to play roles in anaerobic growth and virulence, and allow for the utilisation of DMSO, nitrate, and sulfite as alternative electron acceptors (Jacobsen *et al.*, 2005; Tareen *et al.*, 2011; Van Alst *et al.*, 2007; Weber *et al.*, 2000). Because the transposon disrupted the function of BTH_I1704, required for molybdopterin cofactor biosynthesis, one cannot be sure that the phenotypes exhibited by CA01 are due to the disruption of nitrate reductase alone, considering formate dehydrogenase and sulfite: cytochrome *c* oxidase have been implicated in motility and biofilm formation in *C. jejuni* (Kassem *et al.*, 2012; Tareen *et al.*, 2011).

The crystal structure for MoeA has been solved to a 2.2 Å resolution, showing it to have a similar structure to MogA (Schrag *et al.*, 2001). MoeA encodes a dimeric protein required for the ligation, along with MogA, of molybdenum to molybdopterin (MPT), generating the molybdenum cofactor (Moco) (Hasona *et al.*, 1998a; Nichols & Rajagopalan, 2005; Schrag *et al.*, 2001). Both *moeA* genes in *B. thailandensis* share around 40 % sequence identity and are both found within gene clusters encoding genes required for the molybdopterin biosynthetic pathway. RT-PCR was performed to determine the expression of BTH_I1704 and BTH_I2200 grown aerobically and anaerobically in the presence of nitrate. In comparison to the housekeeping gene (16S rRNA), BTH_I1704 (*moeA1*) was shown to be constitutively expressed at a low level both aerobically and anaerobically in the presence of nitrate. In contrast, no expression was seen for BTH_I2200 (*moeA2*) under any condition tested (Fig. 4.9). These results indicated that BTH_I1704 to be the main MoeA encoded by *B. thailandensis* E264*.* Although no expression of *moeA2* was seen it is possible that BTH_I2200 may be expressed under different conditions not tested in this study.

In other bacterial species the presence of two *moeA* gene has been suggested to reflect the different requirement for either molybdenum or tungsten metal ions (Bevers *et al.*, 2008; Bevers *et al.*, 2009). Therefore one can speculate that the two *moeA* genes in *B. thailandensis* perform different functions, responding to the presence of either molybdenum or tungsten. For example BTH_I1704 is likely to be

Table 4.1 – Putative molybdoproteins in *B. pseudomallei* and *B. thailandensis*

Name	Gene name(s)[a]	*B. pseudomallei* (K96243)[a]	*B. thailandensis* (E264)[a]	Similarity[b] (%)	Predicted function[c]
Membrane-bound nitrate reductase(s)	*narGHJI* *narZYWV*	BPSL2309-2312 BPSS1156-1159	BTH_I1851-1854 BTH_II1249-1252	90-99	Dissimilatory nitrate reduction
Nitrate reductase	*nasA*	BPSL0510	BTH_I0462	95.5	Assimilatory nitrate reduction
Sulfite oxidase	*yedZY*	BPSL3177-3178	BTH_I3032-3033	89.7-94.1	Oxidation of S- and N-oxides
NAD^+ formate dehydrogenase	*fdsGBAD*	BPSL2528-2531	BTH_I1621-1624	93-96	Formate oxidation
Formate dehydrogenase-N	*fdoGHI*	BPSS1665-1667	BTH_II0707-0710	96-98	Formate oxidation
Xanthine dehydrogenase	*xdhAB*	BPSL2727-2728	BTH_I1408-1409	94-99	Purine metabolism
Putative DMSO reductase	*dmsABC*	BPSS2299-2301	Absent	-	Putative role in anaerobic reduction of DMSO and/or TMAO
MOSC[h] domain-containing protein	*ycbX*[d]	BPSS0707	BTH_II1722	93	Putative role in N-hydroxylaminopurine (HAP) detoxification[d]
MOSC[h] domain-containing protein	*yiiM*	BPSL0935	BTH_I0802	92.5	Putative role in N-hydroxylaminopurine (HAP) detoxification[d]

Bifunctional reductase	-	BPSS1241	BTH_II1172	92.1	Putative nitrate/sulfite reductase[e]
Molybdopterin oxidoreductase	-	BPSL2207	BTH_I1975	93	Unknown function
	-	BPSL3038	BTH_I1105		
	-	BPSS0969	BTH_II1422		
Hypothetical proteins[g]	-	BPSL0733	BTH_I0634	91-93.4	Unknown function
	-	BPSL1294	BTH_I2840		
Sulfite: cytochrome *c* oxidoreductase	-	Absent	BTH_II1622	-	Unknown function

[a] Gene name and locus ID determined using NCBI GenBank database

[b] Similarity of *B. pseudomallei* K96243 genes to those found in *B. thailandensis* E264. Determined using a K.E.G.G. ortholog analysis

[c] Predicted based on known molybdo-protein function in other prokaryotic species

[d] BTH_II1722/BPSS0707 and BTH_I0802/BPSL0935 are predicted orthologs of *E. coli* YcbX and YiiM MOSC domain-containing molybdoenzymes (Kozmin *et al.*, 2008)

[e] BTH_II1172 and BPSS1241share orthology with sulfite reductase (NADH) flavoprotein (according to K.E.G.G.)

[f] BTH_I1067 and BPSL1217 contain a molybdopterin binding signatures

[g] Hypothetical proteins containing SO-family motifs

[h] MOSC - molybdenum cofactor sulfurase C-terminal domain

required for molybdenum ligation to MPT, whereas BTH_I2200 could be required for recognition and ligation of tungsten prior to its incorporation into various metallo-proteins. It is also possible that BTH_I2200 plays no role in Moco biosynthesis, and is redundant in function. Further mutagenesis and biochemical analysis would be required to determine the role of BTH_I2200 in *B. thailandensis* molybdopterin biosynthesis, and whether or not *B. thailandensis* encodes any tungsten containing proteins.

BTH_I2200 is encoded on a putative operon encoding *moaD* and *moaE* (Fig. 4.6 a), required for MPT synthase, an enzyme essential for addition of dithiolene to cPMP to form molybdopterin (Wuebbens & Rajagopalan, 2003). Both *moaD* and *moaE* are essential for molybdopterin biosynthesis. Since no other *moaD* or *moaE* genes are found within *B. thailandensis* it is plausible that BTH_I2201 and BTH_I2202 are under the control of an alternative promoter that does not control BTH_I2200. Preliminary Softberry promoter analysis isolated a putative promoter region within BTH_I2200, which could potentially control the expression of BTH_I2201 and BTH_I2202, however further experimentation would be required to verify this prediction.

To determine whether the phenotypes exhibited by CA01 were due to disruption of BTH_I1704 and transposon insertion into BTH_I1704 did not have any polar effects on expression of BTH_I1705 and BTH_I1706, a mutant complement was constructed using the constitutive expression vector pDA-17 encoding a *dhfr* promoter and tetracycline resistance cassette. BTH_I1704 was cloned into pDA-17 and the pDA-17::BTH_I1704 construct was conjugated into CA01 using triparental mating. The complemented mutant, CA01_pDA-17::BTH_I1704, successfully restored anaerobic growth, NAR activity and biofilm formation but could not restore the motility defect seen in CA01 (Fig. 4.15 and 4.16). This could be due to downstream effects of the over-expression, differential regulation of BTH_I1704, or potentially the loss of the pDA-17::BTH_I1704 plasmid.

Biofilms are associated with virulence in many bacterial pathogens, and have been associated with chronic infection in *N. gonorrhoeae* and *P. aeruginosa* (Falsetta *et al.*, 2010; Hassett *et al.*, 2002; Hill *et al.*, 2005). *B. pseudomallei* and *B. thailandensis* can form biofilms *in vitro* and *in vivo.* Although biofilms are not directly required for virulence of *B. pseudomallei* (Taweechaisupapong *et al.*, 2005) they may play a role

in relapse of infection and antimicrobial resistance. Genes required for the molybdopterin biosynthetic pathway, such as *moeA, moeB* and *moaA,* show a degree of upregulation in biofilms of *Listeria monocytogenes* (Tirumalai, 2012), highlighting the importance of this pathway in biofilms. In *B. thailandensis,* transposon insertion into *moeA1* (CA01) resulted in a reduction in biofilm formation under both aerobic and anaerobic conditions (Fig. 4.11), restored to wild-type levels by complementation with pDA-17::BTH_I1704 (4.16 b). This reduction in biofilm forming capabilities could be linked to the function of NAR, as similar results were seen with *P. aeruginosa,* with a Δ*narGH* mutant demonstrating a thinner biofilm structure to the wild-type (Van Alst *et al.*, 2007). The reduction in biofilm formation may also be due to the disruption of multiple molybdopterin proteins in *B. thailandensis,* and could be linked to the reduction in motility seen in CA01 (Fig. 4.12 and 4.16 c). It is possible that the reduction in biofilm formation and motility seen in CA01 is also due to the lack of NO production as a result of limiting the supply of nitrite by disabling the nitrate reductase. However since other molybdo-proteins have been shown to play a role in motility (Kassem *et al.*, 2012; Tareen *et al.*, 2011) the defect in motility and biofilm formation seen in CA01 may not be due to a reduction in NAR activity alone. Further mutagenesis studies on NAR are required to determine its role in motility and biofilm formation in *B. thailandensis* and/or *B. pseudomallei.*

Flagella are required for virulence and biofilm formation of *B. pseudomallei* (Chua *et al.*, 2003; Sawasdidoln *et al.*, 2010). Swimming and swarming motility are both dependent on flagellar function. Swimming motility is dependent on individual motility, whereas swarming motility requires movement of a group of bacteria over a semi-solid surface (Harshey, 2003). In comparison to wild-type *B. thailandensis*, CA01 exhibited a significant difference in swimming motility (Fig. 4.12). By contrast *P. aeruginosa* Δ*narGH* and Δ*napA* mutants displayed a reduction of swarming but not swimming motility (Van Alst *et al.*, 2007). Mutations within the anaerobic respiratory sulfite oxidoreductase, a molybdopterin containing protein, from *C. jejuni* results in significant reduction in invasion of Caco2 cells, motility and growth in the presence of sodium sulfite (Tareen *et al.*, 2011). The reduction in swimming motility seen with CA01 could indicate a role for the molybdopterin biosynthetic pathway and molybdo-proteins in ATP production required for *B. thailandensis* flagellar function. It is possible that the lack of NAR activity under aerobic conditions may have affected the

restoration of motility in CA01. Considering the motility assay was performed under aerobic conditions it is unlikely that the reduced swimming motility is due to bioenergetic constraints. Transposon insertion into BTH_I1704 is not likely to have directly affected genes required for motility as there are no flagella genes within the gene cluster. The reduction in *P. aeruginosa narGH* mutant swarming motility was due to the reduced formation of NO, a signalling molecule for rhamnolipid production (Van Alst *et al.*, 2007).

Both NAR and the molybdopterin biosynthetic pathway have been implicated in virulence in *P. aeruginosa* and *Mycobacterium* when using *C. elegans* or murine infection models (Filiatrault *et al.*, 2013; Fritz *et al.*, 2002; Van Alst *et al.*, 2007). No difference was seen between wild-type *B. thailandensis* and CA01 in virulence when using *G. mellonella* (Fig. 4.13). It is possible, due to the acute nature of the infection seen when this model organism, that *G. mellonella* may not be the appropriate system for studying the role of anaerobic respiration in virulence of *Burkholderia.* Use of a chronic infection model, allowing for the generation of abscesses or granulomas that may have hypoxic environments, may yet reveal a role for anaerobic respiration and molybdopterin biosynthesis in *B. pseudomallei* pathogenesis.

4.4 Conclusions

Until now, very little was known about the genes required for anaerobic nitrate respiration in *B. thailandensis.* Work presented in this chapter has demonstrated the importance of the molybdopterin biosynthetic pathway in anaerobic respiration, NAR activity, motility and biofilm formation in *B. thailandensis.* This set of work has indicated that NAR may play a role in the pathogenesis of melioidosis. Further work using deletion mutagenesis will be performed to determine the role of the membrane-bound nitrate reductases in virulence and anaerobic respiration in *B. pseudomallei* (see Chapter 5 and 6).

Chapter 5 - Deletion mutagenesis and characterisation of the role of NarGHI in anaerobic respiration

5.1 Introduction

Previous work on *B. thailandensis* (Andreae *et al.*, 2014) (Chapter 4) demonstrated the importance of molybdopterin biosynthesis in anaerobic respiration, NAR activity, biofilm formation and motility. Both *B. thailandensis* E264 and *B. pseudomallei* K96243 encode a variety of molybdoproteins, such as NarGHI, formate dehydrogenase, a putative DMSO reductase, xanthine oxidase and sulfite oxidase (Andreae *et al.*, 2014) (Table 4.1). Considering disruption of the molybdopterin biosynthetic pathway was likely to affect the function of a number of *B. thailandensis* molybdoproteins it was not possible to determine which one was contributing to the phenotype exhibited by CA01. However, it is thought that disruption of NAR was likely to be the main reason for the phenotypes exhibited by CA01.

Members of the DMSO reductase family require a membrane anchor subunit (NarI, DmsC, or FdnI/FdoI) containing heme cofactors and a quinol binding site, electron transfer subunit (NarH, DmsB or FdnH/FdoH) containing [Fe-S] clusters, and a catalytic subunit (NarG, DmsA or FdnG/FdoG) containing an [Fe-S] cluster and Mo-*bis*MGD cofactor (Bertero *et al.*, 2003; Jormakka *et al.*, 2002b; Kisker *et al.*, 1997; McAlpine *et al.*, 1998; Weiner *et al.*, 1992) (see Chapter 1; sections 1.4 and 1.5).

B. pseudomallei encodes two membrane-bound NAR (*narGHJI* and *narZYWV* – Chapter 3 - Table 3.2) predicted to be required either for adaptation to hypoxia or denitrification (Chapter 3 - Fig. 3.11). *B. pseudomallei* NarGHI is part of the D-group of molybdoenzymes, exhibiting a high degree of sequence conservation with NarGHI (NRA) found in *E. coli* (Bertero *et al.*, 2003). The *narGHJI* operon encodes a chaperone protein, NarJ, which specifically recognises the NarG catalytic subunit to aid in folding, assembly and insertion of Mo-*bis*MGD and [Fe-S] cluster into the apo-protein (Blasco *et al.*, 1998; Lanciano *et al.*, 2007; Vergnes *et al.*, 2004; Vergnes *et*

al., 2006). Strains lacking *narJ* have been shown to form an unstable and inactive NarGH complex (Blasco *et al.*, 1998). MogA, MoeA, MobA and MobB are thought to form a complex which, along with the NarJ chaperone protein, is essential for the incorporation of Moco into the apo-nitrate reductase (Vergnes *et al.*, 2004).

NAR and DMSO reductase both catalyse the two electron reduction of their respective substrate (nitrate or DMSO) to either nitrite or DMS, using the Mo-*bis*MGD cofactor (Bertero *et al.*, 2003; Weiner *et al.*, 1992). NAR reaction is shown below. The oxidation state of the Mo ion is known to change during this reaction from Mo (VI) is reduced to Mo (V) and then Mo (IV), allowing for the transfer of electrons. These reactions are key for anaerobic respiration and the generation a PMF, via quinol oxidation.

NAR reaction: $NO_3^- + 2H^+ + 2e^- \rightarrow NO_2^- + H_2O$

Currently little is known about the role different molybdopterin containing proteins play in anaerobic respiration and pathogenesis of melioidosis. The current chapter will outline mutagenesis methods used to create an in-frame *narG* deletion mutant using the pDM4 suicide vector (Logue *et al.*, 2009), and characterise the role of *narG* in denitrification and nitrate reductase activity.

5.2 Results

5.2.1 Anaerobic growth of B. pseudomallei *K96243*

Bioinformatic analysis identified a gene cluster in *B. pseudomallei* K96243 encoding a molybdopterin oxidase (BPSS2299), iron-sulfur cluster protein (BPSS2300) and a hypothetical protein (BPSS2301), exhibiting similarity to *B. cenocepacia* BCAM1176 (a putative DMSO reductase subunit - *dmsC*). This gene cluster is found in pathogenic *Burkholderia* species, such as *B. cenocepacia, B. mallei* and *B. pseudomallei,* but no homolog has been identified in *B. thailandensis* E264*.* Due to the gene arrangement, presence of PFAM motifs required for molybdopterin cofactor and [Fe-S] binding in BPSS2299 and BPSS2300, and similarity to genes annotated as *dmsA, dmsB* and *dmsC,* BPSS2299-2301 is thought to encode a putative DMSO reductase. Further mutagenesis and biochemical characterisation will be required to confirm this prediction.

Preliminary studies on the anaerobic respiratory flexibility were conducted on LB or M9 minimal media agar plates supplemented with nitrate, nitrite and DMSO at a range of concentrations (Table 5.1 and Table 5.2). These anaerobic studies were conducted within an anaerobic box incubated at 37 ^{o}C for two to five days. Like *B. thailandensis, B. pseudomallei* displayed very little growth anaerobically in the absence of an alternative terminal electron acceptor. *B. pseudomallei* K96243 could grow anaerobically using either nitrate or nitrite as alternative electron acceptors, on both LB agar and M9 minimal media supplemented with 20 mM sodium succinate as a sole source of carbon and electrons. No significant growth was seen in the presence of DMSO at any concentration tested, when using LB media or M9 minimal media using succinate as a carbon source.

Previous studies have demonstrated that anaerobic growth in the presence of DMSO requires glycerol or formate to be utilised as a carbon source and energy donor (Bilous & Weiner, 1985a; Bilous & Weiner, 1985b). 0.5 % glycerol was therefore added to LB agar plates, supplemented with a range of DMSO concentrations (5, 10, 20, 40 or 60 mM). *B. pseudomallei* could grow anaerobically in the presence of 10 to 40 mM DMSO, on LB media supplemented with 0.5 % glycerol, after 2 to 4 days incubation at 37 ^{o}C (Table 5.2).

5.2.2 Identification of targets for pDM4 deletion mutagenesis

B. pseudomallei K96243 encodes a wide array of different molybdoproteins, a number of which are likely to function under anaerobic conditions (see Chapter 4 - Table 4.1). Information from transcript datasets obtained from publications (Hamad *et al.*, 2011; Kim *et al.*, 2005; Ooi *et al.*, 2013) were used to identify potential targets for pDM4 deletion mutagenesis (Table 5.3). From this dataset the catalytic subunit of NarGHI (BPSL2309 - *narG*) and the putative DMSO reductase (BPSS2299 - *dmsA*) were selected, as both showed differential regulation under a number of conditions tested, including response to various different *in vitro* stresses and upregulation within a murine infection model (Table 5.3). NarGHI was shown to be upregulated under nutrient deprivation (water), down-regulated under acid stress (pH 4) (Ooi *et al.*, 2013) but showed no difference in regulation under anaerobic conditions; when grown in the absence of an alternative electron acceptor. The NarGHI homolog in *B. mallei* was up-

Table 5.1 - Anaerobic growth of wild-type *B. pseudomallei* on LB or M9 minimal media agar plates

	LB agar	**M9 minimal[a]**
None	+	-
20 mM sodium nitrate	+++	++
5 mM sodium nitrite	++	+
5 mM DMSO	+	-
10 mM DMSO	+	-
20 mM DMSO	+	-
40 mM DMSO	+/-	-

Level of growth indicated with +[b]

+++ = strong growth

++ = medium growth[b]

+ = faint growth[b]

- = no growth

[a] M9 minimal media plates were supplemented with 20 mM sodium succinate as a carbon source.

[b] Compared to level of growth exhibited by wild-type in the presence of nitrate

Plates were incubated anaerobically for 48 hours at 37 ^{o}C

Results are the average of three biological replicates

Table 5.2 - Anaerobic growth of wild-type *B. pseudomallei* on LB agar plates supplemented with 0.5 % glycerol

	2 days[a]	**4 days[a]**
0.5 % Glycerol	+	+
20 mM sodium nitrate	+++	+++
5 mM sodium nitrite	++	+++
10 mM DMSO	++	+++
20 mM DMSO	++	+++
40 mM DMSO	+	++
60 mM DMSO	-	-

Level of growth indicated with +[b]

+++ = strong growth

++ = medium growth[b]

+ = faint growth[b]

- = no growth

[a] Incubation time (days)

[b] Compared to level of growth exhibited by wild-type in the presence of nitrate

Plates were incubated anaerobically at 37 ^{o}C for two to four days.

Results are the average of three biological replicates

regulated in the liver and spleen of murine infection model (Kim *et al.*, 2005). Interestingly the putative DMSO reductase was induced under anaerobic conditions, in the mouse liver and spleen, within BALB/c lungs and under nutrient deprivation conditions (Table 5.3), indicating it to be a potential target for future virulence studies.

Considering previous studies on the *B. thailandensis* E264 molybdopterin biosynthesis pathway mutant revealed a role for molybdoproteins in anaerobic respiration deletion constructs to knockout both the *moeA* genes in *B. pseudomallei* K96243 (BPSL2455 and BPSS1479) were also constructed.

5.2.3 Knockout cassettes for pDM4 mutagenesis were successfully created for in-frame deletion mutagenesis of BPSL2309, BPSS2299, BPSL2455 and BPSL1479

Deletion mutagenesis was carried out using the suicide vector pDM4, encoding a chloramphenicol resistance cassette and *sacB* allowing for efficient sucrose counter-selection (Logue *et al.*, 2009). pDM4 deletion mutagenesis required the creation of a deletion construct containing 600 bp of upstream and downstream flanking regions of the target gene (see methods section 2.4.2 – *pDM4 deletion mutagenesis*), to allow for allelic replacement and generation of an in-frame deletion mutant (Logue *et al.*, 2009). pDM4 knockout cassettes were successfully constructed for BPSL2309 (*narG*), BPSS2299 (putative *dmsA*), BPSL2455 (*moeA1*) and BPSS1479 (*moeA2*), and confirmed with PCR (Fig. 5.1) and DNA sequencing. The pD2309 vector was further confirmed using restriction enzyme digest (Fig. 5.2).

5.2.4 Creation of a BPSL2309 deletion mutant (ΔnarG)

The majority of published work on the role of anaerobic respiration in pathogenesis has focused on nitrate reductase. Although pDM4 deletion constructs for BPSS2299, BPSL2455, and BPSS1479 were successfully created only one deletion mutant (BPSL2309; Δ*narG*) was made and further characterised during the rest of this study, considering previous studies on other pathogenic species have demonstrated a role for *narG* anaerobic respiration, virulence and persistence.

Table 5.3 – Regulation of *B. pseudomallei* K96243 putative molybdoproteins under a range of different conditions

Name	Gene name(s)	Gene ID	Anaerobic[c]	Hypoxia[b]	BALB/c lungs[c]	Mouse spleen and lungs[a]
Membrane-bound nitrate reductase(s)	*narGHJI*	BPSL2309-2312	ND	-[d]	ND	Up (BMA1732)
	narZYWV	BPSS1156-1159	ND	Up	ND	-
Assimilatory nitrate reductase	*nasA*	BPSL0510	ND	-	ND	-
Sulfite oxidase	*yedZY*	BPSL3177-3178	ND	-	ND	-
NAD^+ formate dehydrogenase	*fdsGBAD*	BPSL2528-2531	ND	-	ND	-
Formate dehydrogenase-N	*fdoGHI*	BPSS1665-1667	ND	-	Down	Up (BMA1683)
Xanthine dehydrogenase	*xdhAB*	BPSL2727-2728	ND	-	Down	-
Putative DMSO reductase	*dmsABC*	BPSS2299-2301	Up	-	Up	Up (BMAA2047)
MOSC domain-containing protein	*ycbX*	BPSS0707	ND	-	ND	-
MOSC domain-containing protein	*yiiM*	BPSL0935	ND	-	ND	-
Bifunctional reductase	-	BPSS1241	ND	-	ND	-
Molybdopterin oxidoreductase	-	BPSL2207	ND	-	ND	-
	-	BPSL3038	ND	-	ND	-
	-	BPSS0969	ND	-	ND	-

Hypothetical proteins	-	BPSL0733	ND	-	ND	-
	-	BPSL1294	ND	-	ND	-

[a] Gene regulation of *B. mallei* homologs in mouse liver and spleen (Kim *et al.*, 2005)

[b] Gene regulation after 4 hours in a hypoxic environment (Hamad *et al.*, 2011)

[c] Data taken from (Ooi *et al.*, 2013)

ND – no difference in expression seen

[d] No transcript data available

Table 5.3 continued - Regulation of *B. pseudomallei* K96243 putative molybdoproteins under a range of different conditions

Name	Gene name(s)	Gene ID	Nutrient deprivation (water)[c]	Acid[c]	Human serum (NHS 30 %)[c]	Insulin (11 U/mL)[c]
Membrane-bound nitrate reductase(s)	*narGHJI*	BPSL2309-2312	Up	Down	ND	ND
	narZYWV	BPSS1156-1159	Up	ND	ND	ND
Assimilatory nitrate reductase	*nasA*	BPSL0510	ND	ND	ND	ND
Sulfite oxidase	*yedZY*	BPSL3177-3178	Up	Up	Down	Down
NAD^+ formate dehydrogenase	*fdsGBAD*	BPSL2528-2531	Up	Up	ND	ND
Formate dehydrogenase-N	*fdoGHI*	BPSS1665-1667	Up	ND	ND	ND
Xanthine dehydrogenase	*xdhAB*	BPSL2727-2728	Up	ND	Down	Down
Putative DMSO reductase	*dmsABC*	BPSS2299-2301	Up	ND	Down	Up
MOSC domain-containing protein	*ycbX*[d]	BPSS0707	Down	Down	Up	ND
MOSC domain-containing protein	*yiiM*	BPSL0935	ND	ND	ND	ND
Bifunctional reductase	-	BPSS1241	ND	ND	ND	ND
Molybdopterin oxidoreductase	-	BPSL2207	ND	ND	ND	ND

	-	BPSL3038	ND	ND	ND	ND
	-	BPSS0969	ND	ND	ND	ND
Hypothetical proteins	-	BPSL0733	Up	ND	ND	ND
	-	BPSL1294	ND	ND		ND
				ND		

[a] Gene regulation of *B. mallei* homologs in mouse liver and spleen (Kim *et al.*, 2005)

[b] Gene regulation after 4 hours in a hypoxic environment (Hamad *et al.*, 2011)

[c] Data taken from (Ooi *et al.*, 2013)

ND – no difference in expression seen

[d] No transcript data available

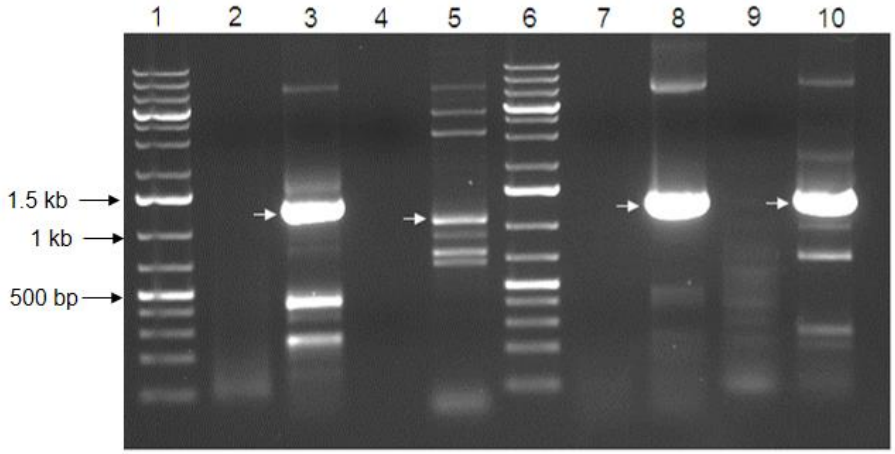

Figure 5.1 - **PCR confirmation of pDM4 knockout cassette construction.** PCR was performed on pD1479, pD2455, pD2309 and pD2299 using primer 1 (p1479_1/p2455_1/p2309_1/p2299_1) and primer 4 (p1479_4/p2455_4/p2309_4/p2299_4), generating a 1.2 kb PCR product (shown with the white arrows). Water was used as a negative control in each PCR reaction. Lane 1 – 1 kb plus DNA ladder; lane 2 – negative control (-ve); lane 3 – pD1479; lane 4 – -ve control; lane 5 – pD2455; lane 6 – DNA ladder; lane 7 – -ve control; lane 8 – pD2309; lane 9 – -ve control; lane 10 – pD2299. PCR was performed using Phusion polymerase and High Fidelity master mix. Use of Phusion polymerase often results in some unspecific binding, as seen in the above gel. This did not affect subsequent cloning steps of the successful construction of a deletion mutant.

A BPSL2309 deletion mutant (Δ*narG*) was successfully constructed by conjugation of pD2309 into wild-type *B. pseudomallei* K96243. This mutant was confirmed using two separate PCR reactions using primers binding outside the target gene and primers binding within the wild-type gene (Fig. 5.3). Use of the pDM4 suicide vector for deletion mutagenesis is known to result in either reversion to the wild-type copy of the gene, or removal of the target gene (Logue *et al.*, 2009). A number of potential second cross-overs (sucrose resistant and chloramphenicol sensitive) were initially screened with an initial PCR reaction using primers binding to a 300 bp internal region of the BPSL2309 (Fig. 5.3 a and b). Successful deletion mutants lacking this 300 bp band are marked with asterisks in figure 5.3 (b.). The BPSL2309 deletion mutant (Δ*narG*) was further confirmed by a second PCR using primers that bind 300 bp up and downstream of BPSL2309 to give a 600 bp band in the mutant and a much larger band (over 3.5 kb) in the wild-type (Fig. 5.3 c). The larger wild-type band was not detected under the PCR conditions used in this study. However the absence of a wild-type band and presence of a 600 bp PCR product in the mutant was considered enough to indicate successful in-frame deletion of BPSL2309 (*narG*).

5.2.5 Deletion of BPSL2309 (ΔnarG) *prevents anaerobic growth on nitrate and significantly reduces NAR activity*

To confirm that deletion of BPSL2309 does not affect aerobic growth both wild-type *B. pseudomallei* K96243 and the Δ*narG* mutant were grown aerobically in L-broth (Fig. 5.4) or M9 minimal media supplemented with 20 mM sodium succinate. No difference was seen between the wild-type and the mutant in terms of growth under aerobic conditions. Anaerobic growth experiments were carried out using the BD GasPak anaerobic container system. Due to constraints when working in the BSL3 lab (which did not have an anaerobic chamber or permit use any glassware or syringes), all anaerobic growth studies were conducted within a BD GasPak anaerobic box, using two anaerobic sachets. Considering the anaerobic experiments were conducted within the BD GasPak EZ anaerobic box system, generating a hypoxic environment within 2 hours, only one point could be taken when performing a growth experiment. The anaerobic growth experiments were therefore conducted using end point cell counts in 24 well plates containing 1 mL of L-broth or M9 minimal media supplemented with

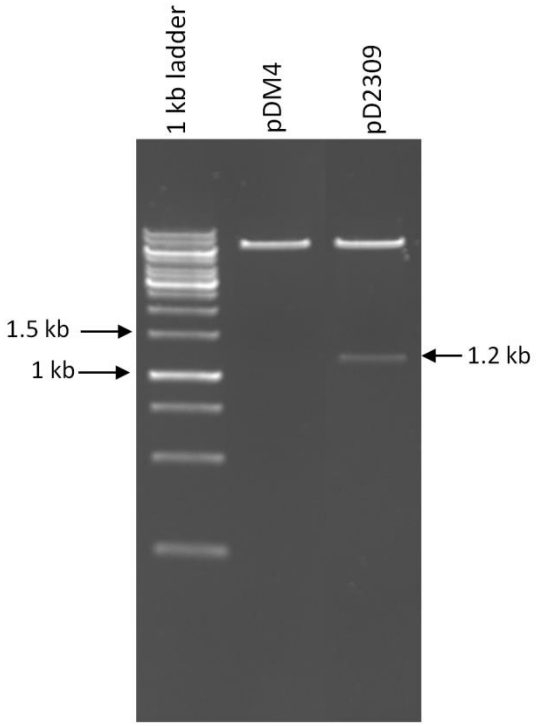

Figure 5.2 – Restriction enzyme digest of pD2309 using *Xba*I and *Nhe*I. Successful ligation of the BPSL2309 knockout cassette (1.2 kb) into the suicide vector pDM4 was confirmed using *Xba*I and *Nhe*I restriction enzymes. Lane 1 – 1 kb DNA ladder; lane 2 – digested pDM4; lane 3 digested pD2309.

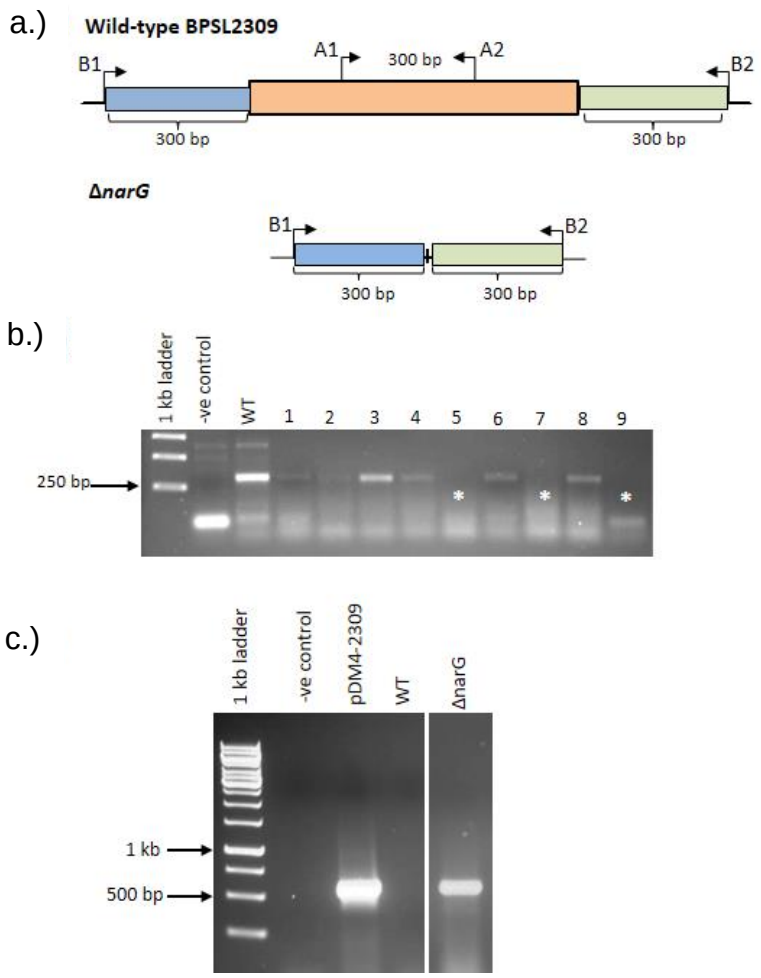

Figure 5.3 – PCR confirmation of the *B. pseudomallei* BPSL2309 deletion mutant (Δ*narG*). a.) Schematic diagram showing primer binding sites for BPSL2309 deletion mutant (Δ*narG*) confirmation. Top – primer binding sites in wild-type (WT) *B. pseud*omallei K96243; A1 and A2 denote primers 2309-check_fwd/2309 check_rv binding within BPSL2309 to give a 300 bp band for the WT and absent in the deletion mutant; B1 and B2 refer to primers 2309_fwd1 and 2309_rv2 respectively, binding outside of BPSL2309 giving a 600 bp product for the mutant but not the WT (see Chapter 2 Table 2.4 for primer sequences). b.) PCR using primers A1 and A2 to identify successful second crossovers. Lane 1 – 1 kb DNA ladder; lane 2 – negative control (-ve) (pDM4-2309); lane 3 – WT gDNA; lane 4 to 12 – potential Δ*narG* second crossover colony lysates. Successful second crossovers (marked with asterisk) were identified by a lack of 300 bp band, as seen in lanes 5, 7 and 9. c.) Confirmation of deletion mutant PCR using primers B1 and B2. Lane 1 – 1 kb DNA ladder; lane 2 – negative control (H_2O); lane 3 – pDM4-2309; lane 4 – WT colony lysate; lane 5 – Δ*narG* colony lysate. Lack of a WT band and presence of 600 bp band for Δ*narG* confirms the deletion of BPSL2309.

or without 20 mM sodium nitrate. Only wild-type *B. pseudomallei* displayed significant anaerobic growth when cultured with nitrate, with no growth seen for Δ*narG* (Fig. 5.5). No significant anaerobic growth on nitrate was seen for Δ*narG* in either M9 minimal media or L-broth.

Like *B. thailandensis* E264*, B. pseudomallei* K96243 encodes two NARs, one sharing homology with the cryptic NarZVY found in *E. coli* and *Salmonella.* Since deletion of BPSL2309 prevented growth under anaerobic conditions, it is very likely that this is the main NAR encoded by *B. pseudomallei.* To confirm this hypothesis a Griess reaction was performed on wild-type and the Δ*narG* mutant grown aerobically in M9 minimal media supplemented with 20 mM sodium nitrate. No difference was seen between wild-type and mutant in terms of aerobic growth (Fig. 5.6 a). Only the wild-type started to accumulate significant amounts of nitrite after 8 hours of growth under aerobic conditions (Fig. 5.6). After 24 hours wild-type *B. pseudomallei* accumulated around 256 µM nitrite whereas the Δ*narG* mutant accumulated only 7 µM nitrite (Fig. 5.6 b. and c). This indicates the BPSL2309-2312 (*narGHJI*) encodes the main nitrate reductase in *B. pseudomallei,* which may function under aerobic as well as anaerobic conditions. Previous literature on other prokaryotic species has stated that NarGHI is expressed under anaerobic conditions in the presence of nitrate, and not under aerobic conditions. It is entirely possible that the cultures became micro-aerobic during the growth cycle, which may have resulted in an increased in expression of *narGHJI* resulting in a high level of nitrate reductase activity is seen in the wild-type. Considering *B. pseudomallei narGHJI* is likely to be under control of NarXL it is also possible that the presence of nitrate in the culture medium resulted in the expression of the operon under aerobic conditions. Further experiments would be required to confirm this prediction.

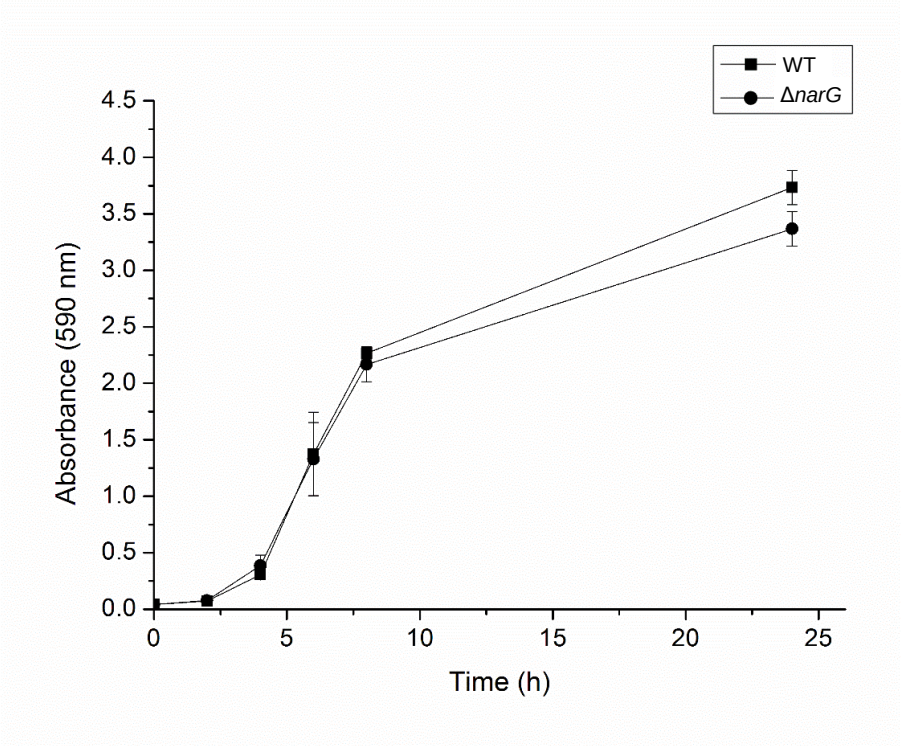

Figure 5.4 - Aerobic growth of wild-type *B. pseudomallei* and the Δ*narG* mutant in rich media. Wild-type *B. pseudomallei* (filled squares) and the Δ*narG* mutant (filled circles) were grown aerobically in L-broth for 24 hours. Experiment performed using three independent biological replicates. Error bars ± SD.

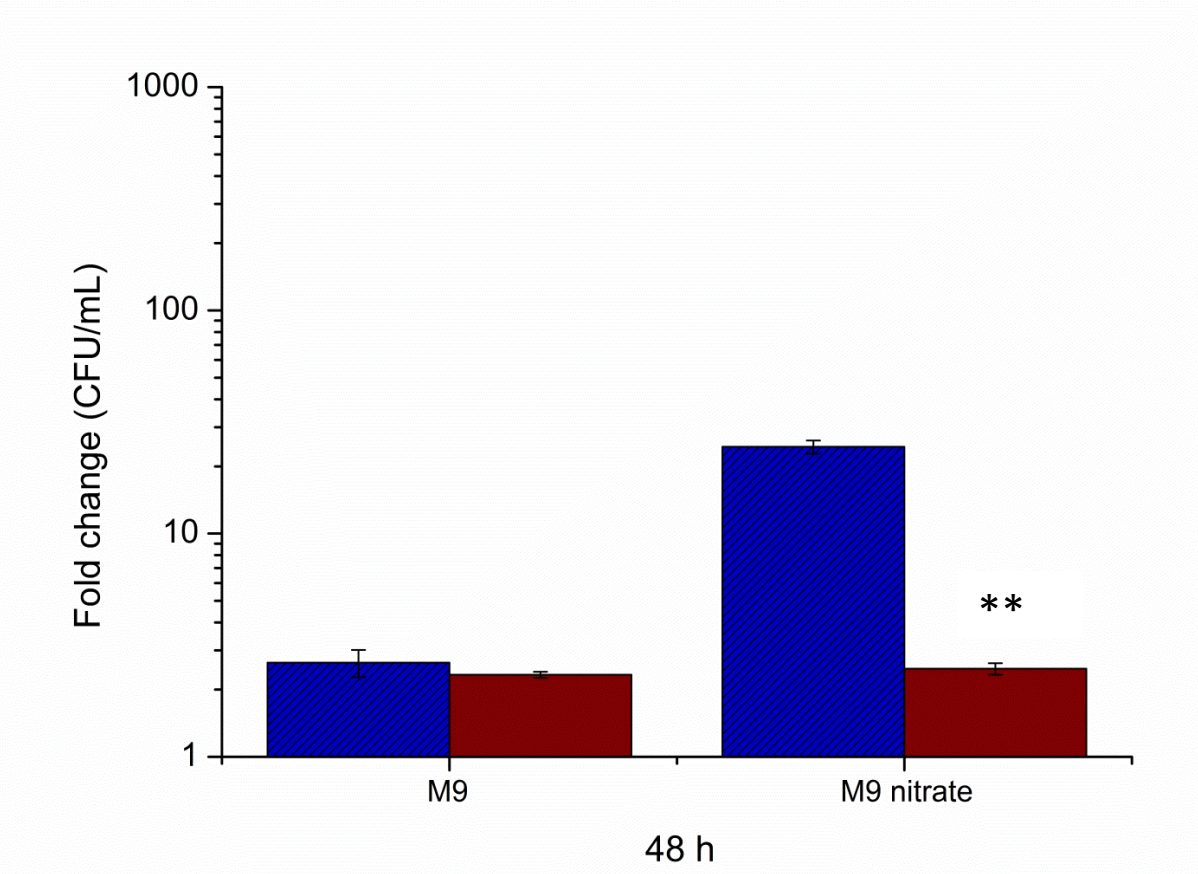

Figure 5.5 - Anaerobic growth of *B. pseudomallei* K96243 in the presence or absence of nitrate. Wild-type *B. pseudomallei* (blue) and Δ*narG* (red) were grown in an anaerobic box for 48 hours (h) in M9 minimal media, supplemented with 20 mM sodium succinate, in the presence or absence of 20 mM sodium nitrate. Three independent biological replicates were used, each with two technical replicates. Error bars indicate ± SD. Asterisks (**) denote statistically significant difference between WT and Δ*narG* (Two tailed T-test assuming equal variance; p-value < 0.01).

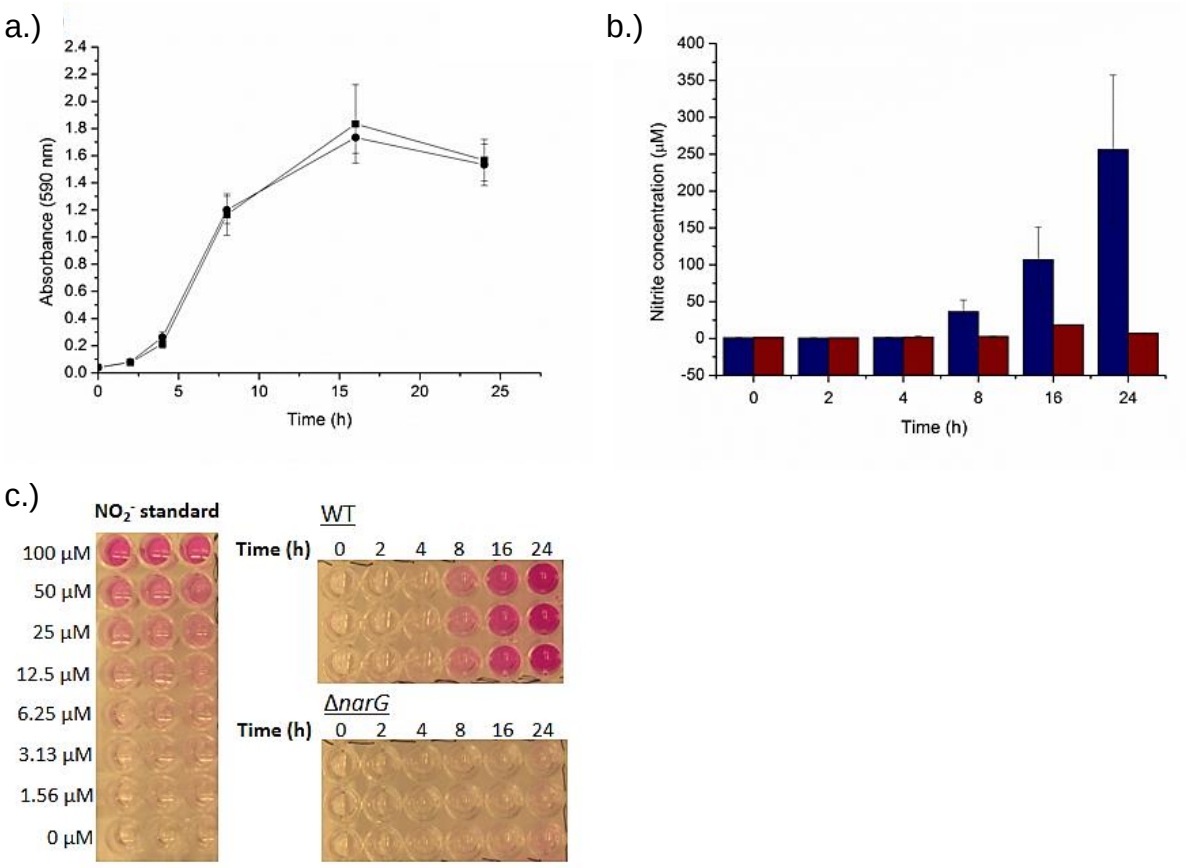

Figure 5.6 - Aerobic nitrate reductase activity exhibited by wild-type *B. pseudomallei* and the Δ*narG* deletion mutant. *B. pseudomallei* K96243 cultures were grown aerobically in M9 minimal media supplemented with 20 mM sodium succinate and 20 mM sodium nitrate for up to 24 hours. a.) Aerobic growth in M9 minimal media for wild-type (WT) *B. pseudomallei* (squares) and the Δ*narG* mutant (circles). 1 mL samples were taken throughout the growth curve and frozen at –80 ^{o}C prior to performing the Griess reaction. b.) Concentration of nitrite (NO_2^-) produced during aerobic growth for the WT (blue) or Δ*narG* (red), determine using the Griess reaction. c.) Representative image for the Griess reaction and nitrite standard curve use to determined NO_2^- concentration of the experimental samples. The experiment was performed using three independent biological replicates, each with three technical replicates used when performing the Griess reaction. Error bars ± SD.

5.2.6 NarGHI is not required for the assimilation of nitrate in B. pseudomallei *K96243*

A study on *M. tuberculosis* has highlighted a novel role for NarGHI in the assimilation of nitrate, as well as the dissimilation of nitrate and anaerobic growth (Malm *et al.*, 2009). To determine whether *B. pseudomallei* NarGHI was involved in nitrate assimilation, nitrogen-free M9 minimal salts were made up, omitting NH_4Cl from the recipe. The nitrogen free M9 minimal media containing succinate as a carbon source, was solidified using 1.5 % bacteriological agar and supplemented with either 20 mM sodium nitrate, 5 mM sodium nitrite or 5 mM ammonium chloride. Wild-type *B. pseudomallei* and Δ*narG* were streaked out, in triplicate, on to all the M9 minimal agar plates (Table 5.4). Little growth for either the wild-type or mutant was seen on M9 minimal media plates supplemented with succinate alone. No difference was seen in growth between the wild-type and the Δ*narG* mutant when grown on M9 minimal plates supplemented with nitrate, nitrite or ammonium. These results indicate that, unlike the *M. tuberculosis* NarGHI, the *B. pseudomallei* NarGHI is not required for the assimilation nitrate, when grown on media containing nitrate as a sole source of nitrogen.

*5.2.7 Complementation of the Δ*narG *mutant using BPSL2309* (narG) *with its native promoter*

In order to ensure that the phenotypes seen in Δ*narG* were due to the deletion of BPSL2309 a complement was created using pBHR-MCS-1 vector encoding chloramphenicol resistance cassette, multiple cloning site and *lacZ* gene. This vector was selected for complementation as it would allow for use of the predicted native promoter and blue/white screening. Softberry promoter analysis was used to predict the position of the promoter, found to be approximately 250 bp upstream of the start of BPSL2309. BPSL2309 with its native promoter (3,996 bp) was amplified by PCR and successfully cloned into the pBHR-MCS-1 vector, via *Bam*HI and *Xba*I restriction sites. This generated the plasmid construct pBHR::BPSL2309native, which was confirmed with PCR (Fig. 5.7) and DNA sequencing and maintained in DH5α competent cells.

The pBHR::BPSL2309native was conjugated into Δ*narG* and selected for based on chloramphenicol resistance, giving Δ*narG*_pBHR::BPSL2309native (Fig. 5.8). This

Table 5.4 – Growth of *B. pseudomallei* K96243 on M9 minimal media agar supplemented with different nitrogen sources

	Control[a]	**Nitrate[b] (NO_3^-)**	**Nitrite[c] (NO_2^-)**	**Ammonium chloride[d] (NH_4Cl)**
Wild-type	+	+++	+++	+++
Δ*narG*	+	+++	+++	+++

+ - little growth

+++ - strong growth

[a] – M9 minimal media supplemented with succinate only, no nitrogen source

[b] – 20 mM $NaNO_3$

[c] – 5 mM $NaNO_2$

[d] – 5 mM NH_4Cl

All M9 minimal media agar plates were supplemented with 20 mM sodium succinate, and incubated aerobically at 37 ^oC overnight

Results are the average of two biological replicates

complement displayed no difference in growth under aerobic conditions, compared to the mutant and the wild-type. Unfortunately complementation with BPSL2309 with its native promoter did not restore growth under anaerobic conditions in the presence of nitrate (Fig. 5.9). It is possible that the lack of *narG* in the mutant could have affect the expression of *narH* and the rest of the operon, as it has been shown to be expressed as one transcriptional unit.

Considering strong hydrogen bond links are seen between NarG and NarH subunits in the *E. coli* NarGHI (Bertero *et al.*, 2003) it is possible that the expression of NarG on its own may have resulted in improper subunit folding of the enzyme. It is also likely that the entire *narGHJI* operon, which including the NarJ chaperone protein, needs to be expressed as one transcriptional unit to ensure proper folding and assembly of the protein. *B. pseudomallei* NarG shares 67.8 % sequence identity with *E. coli* NarG. *B. pseudomallei* BPSL2309 (NarG) was modelled against the *E. coli* NarGHI (PDB: 1Q16), using the I-TASSER service, in order to determine the degree of structural homology. As expected the structure of *B. pseudomallei* NarG was almost identical to that seen in *E. coli* NarG (see Chapter 3 Fig. 3.4), both displaying a loop required for binding to the NarH subunit.

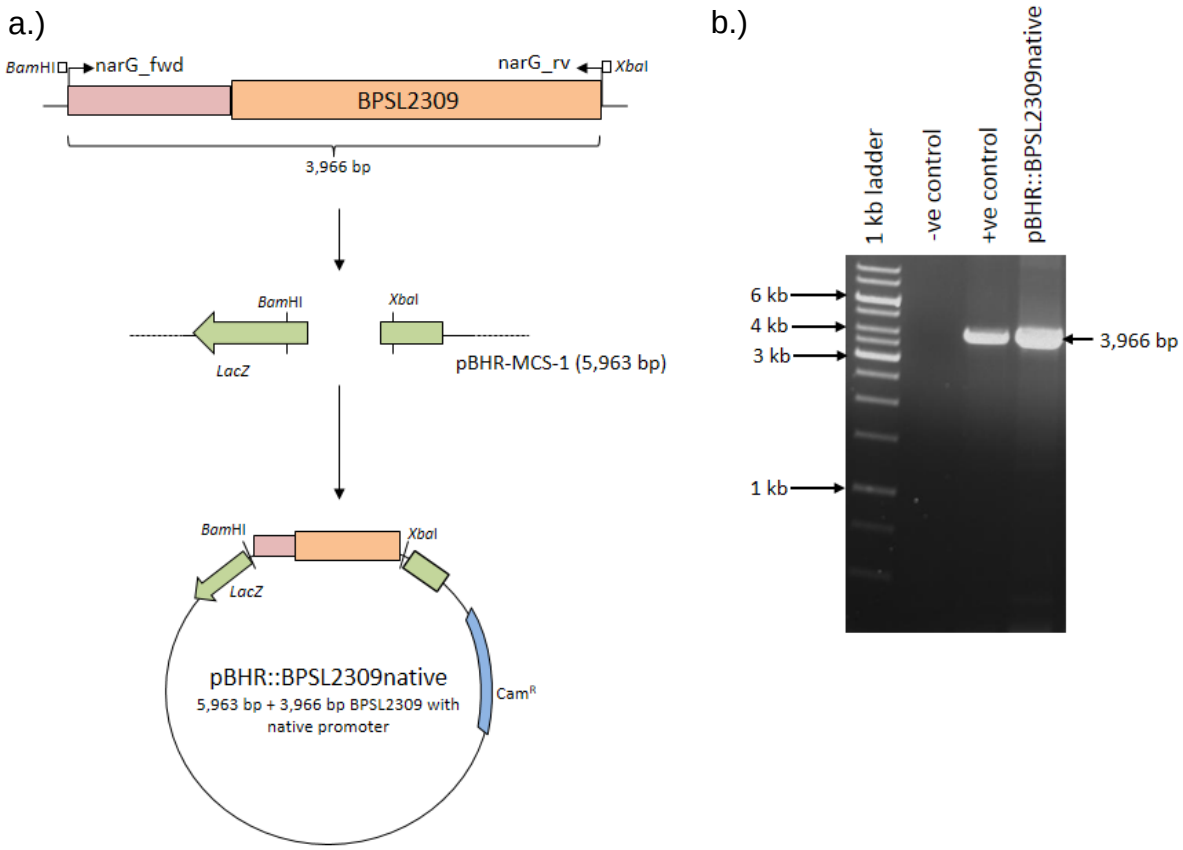

Figure 5.7 - Construction and PCR confirmation of pBHR::BPSL2309native. a.) BPSL2309 was PCR amplified with its predicted native promoter and cloned into pBHR-MCS-1 vector via *Bam*HI and *Xba*I restriction sites and transformed into DH5α competent cells (see methods section 2.4.5 *Complementation using pBHR-MCS-1*). b.) PCR confirmation of a successful pBHR::BPSL2309native construct using primers amplifying BPSL2309 with its native promoter (3,966 bp). Lane 1 – 1 kb DNA ladder; lane 2 – negative (-ve) control (water); lane 3 – positive (+ve) control (wild-type *B. pseudomallei* gDNA); lane 4 – pBHR::BPSL2309native plasmid DNA.

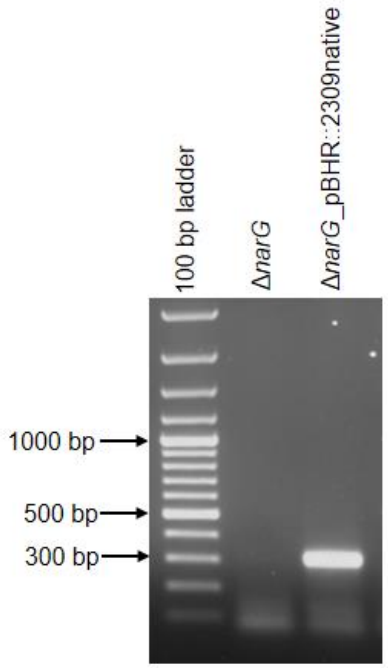

Figure 5.8 – PCR confirmation of pBHR::BPSL2309native in Δ*narG.* The pBHR::BPSL2309native plasmid was successfully conjugated into the BPSL2309 deletion mutant (Δ*narG*) using tri-parental mating. PCR was performed using 2309check_fwd and 2309check_rv primers, binding to a 300 bp internal region of BPSL2309. Lane 1 – 100 bp plus DNA ladder; lane 2 – Δ*narG* boiled PCR lysate; lane 3 - Δ*narG*_pBHR-BPSL2309native boiled lysate.

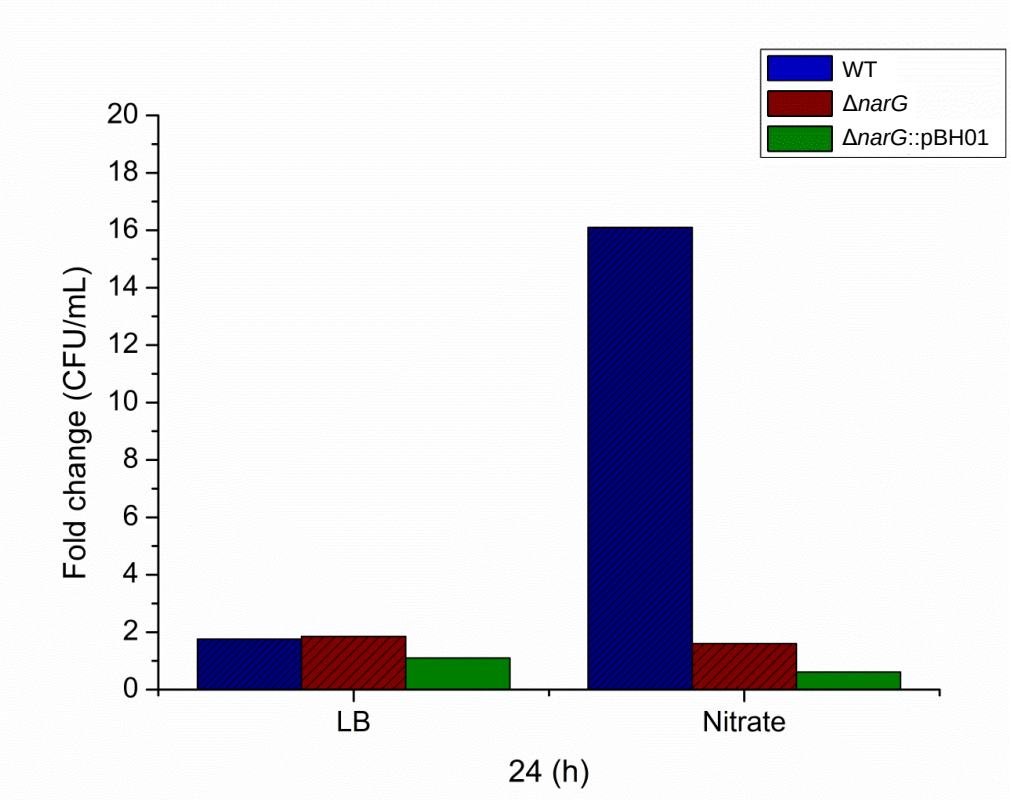

Figure 5.9 – Complementation of Δ*narG* with pBHR::BPSL2309native does not restore anaerobic growth. Wild-type (blue), Δ*narG* (red), and Δ*narG*_pBHR::2309native (green) were grown anaerobically in L-broth supplemented with or without 20 mM sodium nitrate. No growth restoration was observed for Δ*narG*_pBHR::2309native. Results shown are the average of one biological replicate, performed with two technical replicates.

*5.2.8 Complementation of Δ*narG *using the* narGHJI *operon with its native promoter*

The majority of published work on *narG* or *narGH* deletion mutants have complemented the phenotype with the entire *narGHJI* operon, either via chromosomal insertion using mini-Tn5 transposable elements or use of a cosmid library (Van Alst *et al.*, 2007; Weber *et al.*, 2000). The *B. pseudomallei narGHJI* operon (BPSL2309-2312) is a four gene cluster of 6,634 bp, including its native promoter. Initial attempts to PCR this large operon using conventional *Taq* polymerases proved difficult, even after repeated attempts at optimisation. Eventually the operon was successfully amplified as one PCR fragment using KOD Xtreme polymerase, which is specific for the amplification of GC rich and long DNA sequences. Creation of pBHR-MCS::BPSL2309native was successfully achieved by directly cloning the PCR fragment, after restriction digest, into the digested pBHR-MCS-1 vector. Initial and repeated attempts of direct cloning of the BPSL2309-2312native PCR product straight into pBHR-MCS-1 proved unsuccessful, with most clones containing empty vector or an incomplete PCR product. To try to overcome this issue BPSL2309-2312native was cloned into pJET1.2/blunt (Thermo-Scientific), giving pJET::BPSL2309-2312native (pJ01) (see figure 5.10 for cloning protocol). pJ01 was then transformed into High Efficiency 5α competent cells (NEB) as previous transformation attempts using alternative cell lines such as JM109 and DH5α had proved unsuccessful. Successful pJ01 clones were confirmed using DNA sequencing, restriction digest and PCR (Fig. 5.11)

Sub-cloning of BPSL2309-2312native (6,634 bp) into pBHR-MCS-1 (5,963 bp) again proved difficult but after repeated attempts a pBHR::BPSL2309-2312native (pBH01) construct was successfully created and maintained in *E. coli* High Efficiency 5α competent cells. Potential pBH01 constructs were initially screened using a PCR reaction using primers generating a 300 bp band internal to BPSL2309 (Fig. 5.12 a). Any successful constructs were then further confirmed using a restriction enzyme digest, sequencing and PCR to amplifying BPSL2309-2312native product in pBHR-MCS-1 using KOD Xtreme polymerase and narG_fwd(2) and comp_rv(2) primers (Fig. 5.12).

Next pBH01 was conjugated into Δ*narG* using triparental mating. Any colonies were re-streaked onto LB agar plates containing 100 µg/mL chloramphenicol to select

for the pBH01 vector, and several colonies were screened by PCR using 2309_check(fwd) and 2309_check(rv) primers (Fig. 5.13 a). The Δ*narG* mutant complement (Δ*narG*::pBH01), was grown on media supplemented with 50 µg/mL chloramphenicol, to maintain selection for the resistance cassette in pBH01 Complementation of Δ*narG* with pBH01 was able to successfully restore anaerobic growth of the Δ*narG* mutant on LB agar plates supplemented with nitrate, but only to wild-type levels when grown in the presence of chloramphenicol (Fig. 5.13 b). In comparison no anaerobic growth restoration was seen for the complemented mutant (Δ*narG*::pBH01) after 48 hours incubation in 1 mL M9 minimal media (Fig. 5.13 c), even with addition of chloramphenicol (50 µg/mL) to both the culture media and agar plates. It is possible during the 48 hour anaerobic incubation period the chloramphenicol activity may have reduced or become degraded, resulting in the loss of pBH01 plasmid from *ΔnarG*::pBH01 and a reversion back to the mutant (Δ*narG*) phenotype. After 48 hours Δ*narG*::pBH01 was plated out on to LB agar plates containing chloramphenicol at 50 µg/mL. A slight decrease (less than one log) in colony forming units was seen for the 'complement' after 48 hour anaerobic incubation, when comparing it to the input CFU/mL count. This reduction in CFU/mL for the complemented mutant was thought to be due to a reversion back to the mutant phenotype, resulting in the bacterial culture becoming susceptible to chloramphenicol.

It was thought that perhaps the lack of anaerobic growth restoration in M9 minimal media for the complemented mutant was due to a loss of the pBH01 plasmid. To test the stability of pBH01 in the Δ*narG* mutant, Δ*narG*::pBH01 was cultured overnight in L-broth containing 50 µg/mL chloramphenicol. The next day 100 µL of the Δ*narG*::pBH01 overnight culture was spread onto a LB agar plate (no antibiotic) and incubated overnight at 37 ^{o}C, prior resuspension in 4 mL of L-broth, serial dilution and spot plating on LB agar plates supplemented with or without 50 µg/mL chloramphenicol. No difference in CFU/mL counts was seen for Δ*narG*::pBH01 when grown on LB agar plates supplemented with or without chloramphenicol. This indicated that the pBH01 plasmid can remain stable within the Δ*narG* mutant when grown absence of antibiotic selection in LB media under aerobic conditions.

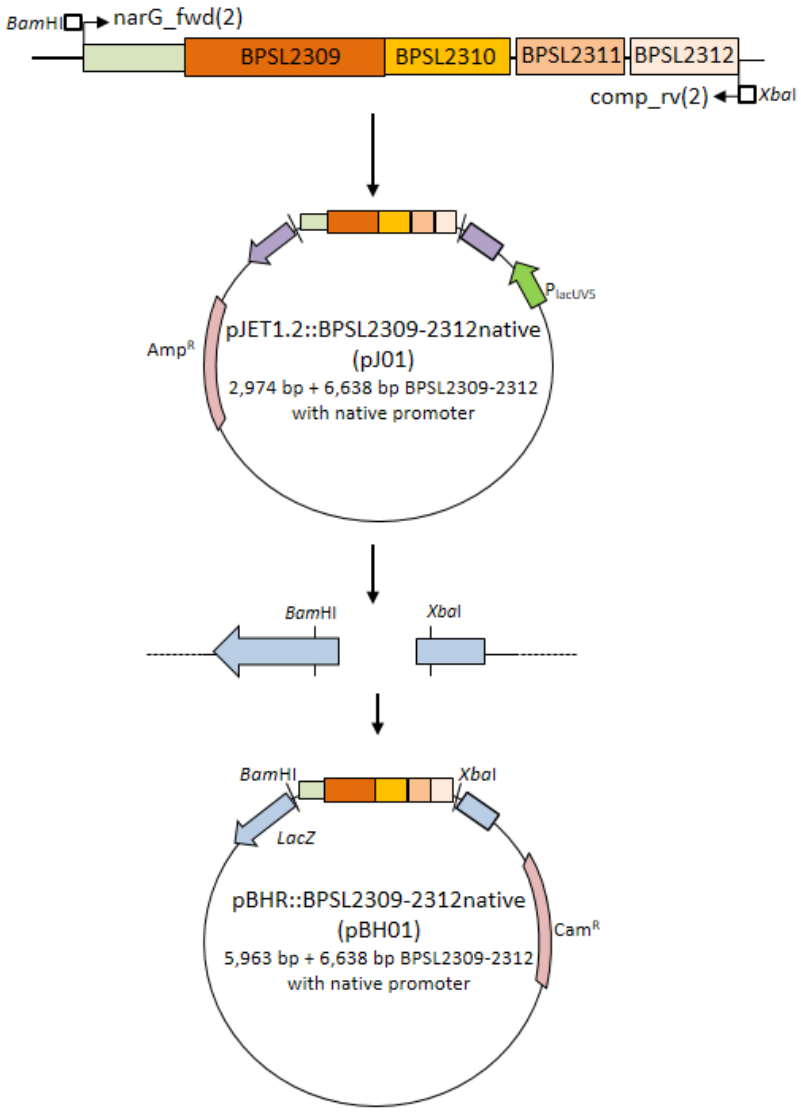

Figure 5.10 – Schematic representation of cloning work through for creation of a pBHR-MCS-1 vector containing *B. pseudomallei narGHJI* (BPSL2309-2312) operon with its native promoter. BPSL2309-2312 (BPSL2309 – orange; BPSL2310 – yellow; BPSL2311 – pink; BPSL2312 – light pink) with its native promoter (green) was amplified by PCR using narG_fwd(2) and comp_rv(2) primers prior to ligation into the pJET1.2/blunt cloning vector, generating pJ01. Both BPSL2309-2312native and the pBHR-MCS-1 vector were digested using *Bam*HI and *Xba*I, ligated together to create pBH01. Both pJ01 and pBH01 were maintained in High Efficiency 5α competent cells.

a.) b.)

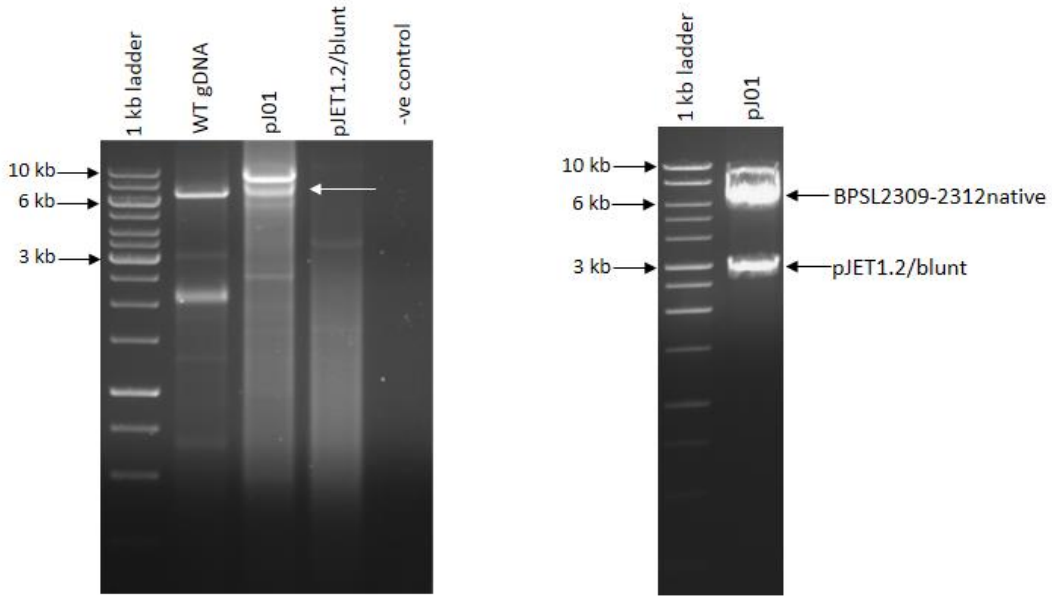

Figure 5.11 – Confirmation of a pJET1.2/blunt containing BPSL2309-2312 with its native promoter (pJ01). a.) PCR confirmation of pJ01 using narG_fwd(2) and comp_rv(2) using KOD Xtreme DNA polymerase. Lane 1 – 1 kb DNA ladder; lane 2 – Wild-type K96243 gDNA; lane 3 – pJ01; lane 4 – pJET1.2/blunt; lane 5 – negative control (H_2O). b.) Restriction enzyme digest of pJ01 using *Bam*HI and *Xba*I. Lane 1 – 1 kb DNA ladder; lane 2 – digested pJ01.

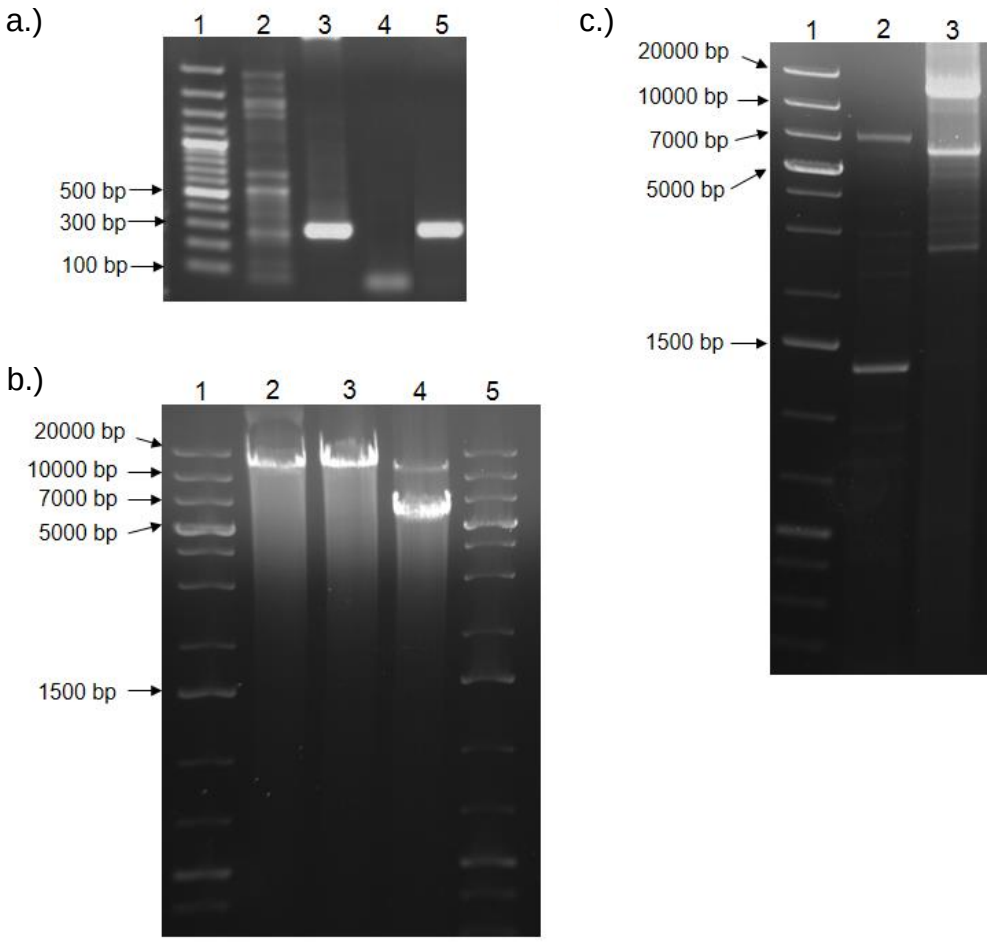

Figure 5.12 – Cloning of BPSL2309-2312native into pBHR-MCS-1 and confirmation using PCR and restriction digest. a.) Colony PCR using 2309check_fwd and 2309check_rv primers of potential pBH01 *E. coli* transformants. Lane 1 – 100 bp plus DNA ladder; 2 – wild-type *B. pseudomallei* K96243 gDNA; 3 – pJ01; pBHR-MCS-1; lanes 4 – unsuccessful ligation of pBHR-MCS-1 and BPSL2309-2312native; lane 5 – successful pBH01 transformant. b.) Restriction enzyme digest of pBH01. Lane 1 – 1 kb plus DNA ladder; lane 2 – *Xba*I digested potential pBH01; lane 3 - *Bam*HI digested potential pBH01; lane 4 – *Xba*I and *Bam*HI digested potential pBH01; lane 5 – 1 kb plus DNA ladder. c.) PCR using KOD Xtreme polymerase using narG_fwd(2) and comp_rv(2). Lane 1 – 1 kb plus DNA ladder; lane 2 – WT gDNA; lane 3 – pBH01.

a.)

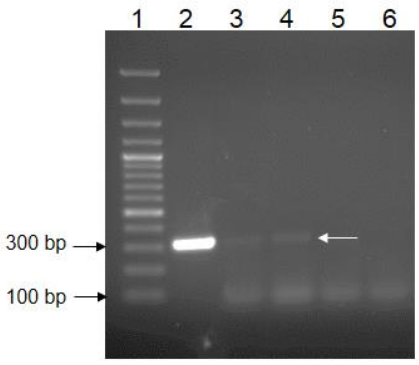
1 2 3 4 5 6
300 bp
100 bp

b.)

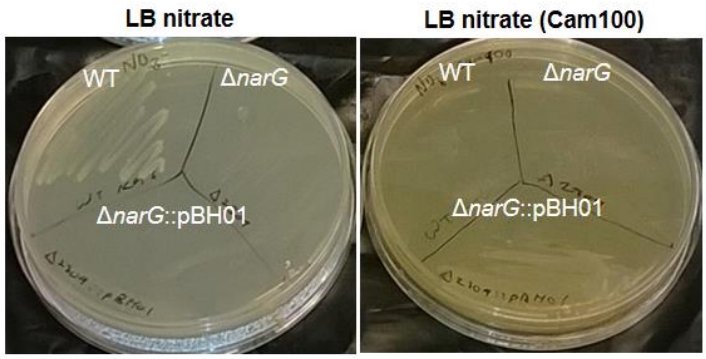
LB nitrate
LB nitrate (Cam100)
WT
ΔnarG
ΔnarG::pBH01
WT
ΔnarG
ΔnarG::pBH01

c.)

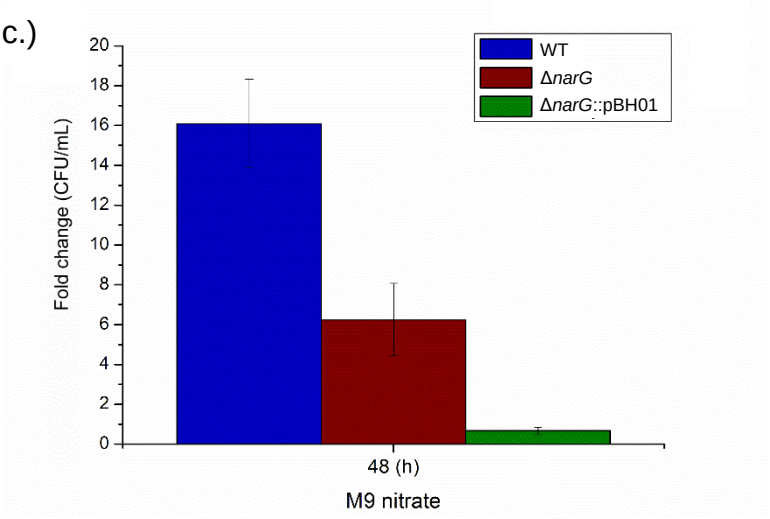
WT
ΔnarG
ΔnarG::pBH01
Fold change (CFU/mL)
0
2
4
6
8
10
12
14
16
18
20
48 (h)
M9 nitrate

Figure 5.13 – Complementation of Δ*narG* with pBH01 successfully restores anaerobic growth on nitrate on LB agar but not in M9 minimal media. a.) PCR of potential Δ*narG*::pBH01 complement lysates. PCR was performed using 2309check_fwd and 2309check_rv primers and pBH01 plasmid extract as a positive control. Lane 1 – 100 bp plus DNA ladder; 2 to 5 – potential Δ*narG*::pBH01 colony lysates; 6 – negative control (H_2O). Arrow denotes successful conjugation of pBH01 into Δ*narG,* as shown with a 300 bp PCR product. b.) Wild-type *B. pseudomallei,* Δ*narG* and Δ*narG*::pBH01 were sub-cultured onto LB agar plates containing 20 mM sodium nitrate and incubated anaerobically for 48 hours. The LB agar plates were supplemented with or without chloramphenicol (100 µg/mL) to ensure selection of the pBH01 in Δ*narG*::pBH01. The pBH01 plasmid containing BPSL2309-2312 (*narGHJI*) with its native promoter successfully restored anaerobic growth of the mutant but only when grown in the presence of chloramphenicol. c.) Anaerobic growth in M9 minimal media supplemented with 20 mM sodium succinate and 20 mM sodium nitrate for wild-type *B. pseudomallei* (blue), Δ*narG* (red), and Δ*narG*::pBH01 (green). No growth restoration of the complement was seen when incubated for 48 hours in M9 minimal media supplemented with 20 mM sodium nitrate and 50 µg/mL chloramphenicol. Results for the 48 hour anaerobic M9 minimal media (20 mM sodium nitrate) growth experiment are the average of two biological replicates each with two technical replicates. Error bars ± SD. Chloramphenicol (50 µg/mL) was added to the media, both liquid culture and plates to ensure selection of the pBHR-MCS-1 plasmid containing BPSL2309-2312native and chloramphenicol resistance cassette.

5.3 Discussion

B. pseudomallei, like *B. thailandensis,* can respire anaerobically using nitrate and nitrite as terminal electron acceptors. Initial studies have indicated that *B. pseudomallei* K96243 may also respire anaerobically using DMSO as a terminal electron acceptor, when grown in the presence of glycerol. Anaerobic respiration using DMSO as a terminal electron acceptor requires glycerol, formate or hydrogen to be used as electron donors to allow for sufficient generation of a PMF (Bilous & Weiner, 1985a; Bilous & Weiner, 1985b). *B. pseudomallei* K96243 encodes multiple different primary dehydrogenases, including glycerol-3-phosphate dehydrogenase (Table 3.1 - Chapter 3) which may be used to couple electron transfer to the putative DMSO reductase (encoded by BPSS2299-2301) to allow for anaerobic growth using DMSO as a terminal electron acceptor (Weiner *et al.*, 1992). Further mutagenesis and biochemical characterisation of BPSS2299-2301 will be required to determine whether this hypothesis is correct and whether or not the gene cluster encodes a putative DMSO reductase.

A *B. pseudomallei narG* (BPSL2309) deletion mutant was successfully made using the pDM4 suicide vector. This mutant (Δ*narG*) displayed no growth deficiency when grown aerobically (Fig. 5.4 and 5.6 a) in either rich or minimal media supplemented with nitrate. In comparison to the wild-type, the Δ*narG* mutant could not grow under anaerobic conditions in the presence of nitrate and displayed a significant reduction in its ability to reduce nitrate to nitrite (Fig. 5.5 and Fig. 5.6).

Complementation of anaerobic growth in the presence of nitrate for Δ*narG* was unsuccessful when using *narG* on its own, likely due to a need for *narGHJI* to be transcribed together to ensure proper folding and assembly of the enzyme. Cloning of the *narGHJI* operon with its native promoter into pBHR-MCS-1 was able to restore the anaerobic growth deficiency exhibited by the Δ*narG* mutant on LB agar supplemented with nitrate (Fig. 5.13 b). In comparison, no anaerobic growth restoration was seen for the complement when grown for 48 hours in M9 minimal media supplemented with nitrate (Fig. 5.13 c). Because the pBH01 plasmid was shown to remain stable within Δ*narG* in the absence of antibiotic selection, it is not completely understood why anaerobic growth was not restored when using M9 minimal media, but was when using LB agar.

Like *E. coli*, *B. pseudomallei* encodes two NAR enzymes; NarGHI and NarZYV. In *E. coli* NarGHI (NRA) is expressed under anaerobic conditions in the presence of nitrate and performs around 90 % of all NAR activity (Blasco *et al.*, 1990; Bonnefoy & Demoss, 1994). In comparison NarZYV (NRZ) is constitutively expressed and is not directly affected by anaerobiosis or nitrate (Blasco *et al.*, 1990; Bonnefoy & Demoss, 1994; Chang *et al.*, 1999). Under aerobic conditions *E. coli* exhibits NAR activity during early stationary phase of growth. Deletion of *E. coli* NRA (in a $NRA^{-}NRZ^{+}$ mutant) causes an almost a complete loss of NAR activity, with only a small amount of nitrite accumulation seen, due to NRZ activity (Chang *et al.*, 1999). This is very similar to what was seen in *B. pseudomallei* cultures grown aerobically in the presence of nitrate. Under these growth conditions only wild-type *B. pseudomallei* accumulated significant amounts of nitrite during late exponential/early stationary phase. Deletion of *B. pseudomallei narG* (BPSL2309) resulted in almost a complete loss of NAR activity, with the Δ*narG* mutant only accumulating 7.4 µM NO_2^- after 24 hours growth, compared to 256 µM NO_2^- seen in the wild-type (Fig. 5.6). This indicated BPSL2309-2312 (*narGHJI*) to encode the main NAR required for denitrification, with BPSS1156-1159 (*narZYWV*) likely to play accessory role in adaptation to hypoxia.

Expression of *E. coli narG* during aerobic respiration increased on entry into stationary phase, thought to be attributed to a reduction in oxygen levels in denser cultures, with a significant increase in expression seen when the medium was supplemented with nitrate (Chang *et al.*, 1999). It is likely that *B. pseudomallei* K96243 expresses *narGHJI* (BPSL2309-2312) during aerobic growth as a hedge betting strategy to ensure its continued survival and growth in potentially oxygen limiting environments. Many prokaryotes possess the ability to reduce nitrate under aerobic conditions, normally using the periplasmic Nap, indicating there to be an alternative role other than the generation of a PMF (Berks *et al.*, 1995a).

B. pseudomallei BPSS1159 (*narZ*) has recently been shown to be induced after 4 hours exposure to hypoxia when grown in L-broth supplemented with glucose (no nitrate) (Hamad *et al.*, 2011). In comparison no genes required for *B. pseudomallei* denitrification (*narGHI, aniA, nor* and *nos*) were induced under hypoxic conditions. However, genes encoding proteins required for the arginine deiminase pathway and electron transfer to high-oxygen-affinity cytochrome *c* oxidases and *c*-type

cytochromes were induced after 4 hours exposure to oxygen limiting conditions (Hamad *et al.*, 2011).

Recently *B. pseudomallei narGHJI, arcDABC* and *paaABCDE* gene clusters have been shown to exhibit dynamic regulation across 66 *in vitro* conditions. Interestingly none of these were related to growth in oxygen limiting environments, with the gene clusters being induced in response to temperature, ultra-violet exposure and oxidative stress (Ooi *et al.*, 2013) (see Table 5.3 for examples). Not only did *narGHJI* operon exhibit expression under various *in vitro* stress conditions the BPSL2309-2312 gene cluster was shown to be upregulated after 3 hours aerobic growth in L-broth (Ooi *et al.*, 2013). The expression of *narGHJI* under a range of different conditions tested in this study suggests that this gene cluster is constitutively expressed in response to a range of different stress conditions and may play alternative roles to just being required for anaerobic respiration.

Under aerobic conditions nitrate can be assimilated into biomolecules via its conversion to ammonia using the assimilatory nitrate reductase (Nas) and NADH-dependent nitrite reductase (NADH-NIR) (Berks *et al.*, 1995a). Aerated *M. tuberculosis* cultures have been shown to reduce nitrate to nitrite at a logarithmic rate corresponding to the log increase bacilli growth (Wayne & Hayes, 1998). *M. tuberculosis* does not encode a Nas even though its genome contains an assimilatory nitrite reductase (Sohaskey & Wayne, 2003). Growth of a *M. tuberculosis narG* mutant in minimal media using nitrate as a sole carbon source revealed NarGHI play a role in assimilation of nitrate along with NirBD (Malm *et al.*, 2009). The *B. pseudomallei* Δ*narG* mutant was shown to be able to utilise nitrate as a sole nitrogen source, indicating, that unlike the NarGHI from *M. tuberculosis,* the *B. pseudomallei* NarGHI does not perform an assimilatory function. *B. pseudomallei,* in comparison to *M. tuberculosis,* encodes a putative assimilatory nitrate reductase (BPSL0510) likely to be involved in the assimilation of nitrate to ammonia, along with NirBD (BPSL0511-0512).

Microarray analysis has revealed the upregulation of genes required for anaerobic respiration (nitrate reductase, outer-membrane nitrite reductase, and formate dehydrogenase) in the liver and spleen of mice infected with *B. mallei,* suggesting a role for anaerobic respiration in these organs (Kim *et al.*, 2005). Another

molybdopterin containing oxidoreductase family protein (BMAA2047) also showed an increase in expression in mouse liver and spleens. This gene exhibits some homology to *dmsA* found in other bacterial species, such as *R. capsulatus,* and is also found in *B. pseudomallei* but not its avirulent relative *B. thailandensis*. The upregulation of nitrate reductase, formate dehydrogenase and putative *dmsA* in *B. mallei* infected mouse liver and spleens implicates molybdopterin containing proteins to play a role in pathogenesis of *Burkholderia.* The putative DMSO reductase in *B. pseudomallei* was also shown to be induced under anaerobic conditions and within the lungs of BALB/c infected mice (see Table 5.3). Further work is required to determine the roles of these genes *in vivo*.

5.4 Conclusion

B. pseudomallei K96243 can respire anaerobically on a range of different terminal electron acceptors, such as nitrate, nitrite and potentially DMSO. Deletion of BPSL2309 encoding *narG* resulted in the lack of growth anaerobically and a significant reduction in NAR activity under aerobic conditions indicating BPSL2309-2312 to encode the main NarGHI. Further characterisation of this mutant will be performed to determine the role of NarGHI in virulence of *B. pseudomallei* (see Chapter 6).

Chapter 6 – A role for nitrate reductase in pathogenesis of melioidosis

6.1 Introduction

B. pseudomallei causes acute, chronic and latent infections and can relapse after several months or years after initial presentation. The ability for *B. pseudomallei* to survive within the host for extended periods of time is thought to be linked to its ability to survive under anaerobic conditions.

Nitrate is a strong electron acceptor able to generate a PMF upon its reduction to nitrite, by NarGHI. Not only does nitrate reductase play a significant role in respiration and bioenergetics, it has been shown to contribute to virulence, motility, intracellular survival and resistance to acid and acidified nitrite stress (Kohler *et al.*, 2002; Tan *et al.*, 2010; Van Alst *et al.*, 2007). Disruption of the molybdopterin biosynthetic pathway in *B. thailandensis* has been shown to cause a disruption of flagella motility (Andreae *et al.*, 2014) (Chapter 4). Flagella are known to play a role in virulence of *B. pseudomallei* (Chua *et al.*, 2003). Considering the *B. thailandensis moeA1* transposon mutant (CA01) displayed a reduction in motility, along with an inability to respire anaerobically on nitrate, it was hypothesised that a lack of nitrate reductase activity was also somehow contributing to the decrease in motility seen in this mutant.

The role of NarGHI in virulence is controversial and seems to depend on the infection model used and site of infection. Mutations in *P. aeruginosa* or *Mycobacterium* spp. *narGHI* have been shown to result in avirulence when using *C. elegans* (Van Alst *et al.*, 2007) and immune-competent BALB/c mice as infection models (Fritz *et al.*, 2002). However, when immune-deficient SCID mice were challenged with *M. bovis* BCG Δ*narG* mutant the mice succumbed to infection after 37 weeks, rather than 14 weeks as seen with the wild-type. This indicated that the disruption of *narG* did not affect the capacity to cause a chronic infection within SCID mice (Fritz *et al.*, 2002). Similarly a *M. tuberculosis* Δ*narG* mutant strain displaying lack of anaerobic persistence *in vitro,* displayed characteristic growth patterns within the lungs of infected C57BL/6 mice, with both mutant and wild-type infected mice

succumbing to infection after 400 days (Aly *et al.*, 2006). The differences in virulence levels seen for the Δ*narG* mutants is thought to be partially due to differences in oxygen status of infected organs. For example the lungs of infected C57BL/6 mice challenged with *M. tuberculosis* have been shown to display reduced oxygen levels but not to the levels of hypoxia (Aly *et al.*, 2006). This difference in role of nitrate reductase in pathogenesis is likely to depend on tissue specificity, oxygen concentration and levels of nitrate within infected organs.

Survival of *B. pseudomallei* within the host is likely to depend on it having various mechanisms to resist killing by reactive oxygen species (ROS) and reactive nitrogen intermediates (RNI). Both RNI and ROS are produced by the immune system in response to invading bacteria. *B. pseudomallei* is susceptible to killing by nitrite, produced as a consequence of iNOS activation, when internalised within IFN-γ stimulated macrophages (Miyagi *et al.*, 1997). The intracellular environment is known to be highly acidic. Under acidic conditions nitrite (NO_2^-) can be spontaneously converted to the toxic nitric oxide (NO). Aerobic and anaerobic *B. pseudomallei* are known to be susceptible to the antimicrobial action of NO, with a marked reduction in culturable cells seen when grown in the presence of 50 µM $NaNO_2$ in acidified minimal media (pH 5) (Jones-Carson *et al.*, 2012; Miyagi *et al.*, 1997). Nitrate respiration and NAR activity in *M. tuberculosis* has been shown to play a protective role in acid tolerance and survival under NO stress, two conditions encountered during infection (Tan *et al.*, 2010).

A recent study on *C. jejuni* has demonstrated a role of various respiratory proteins in survival when in the presence of oxidative stress, with Δ*napA* and Δ*fdhA* mutants displaying an increased susceptibility to hydrogen peroxide. This suggested a role for these respiratory proteins in bacterial homeostasis and redox balancing (Kassem *et al.*, 2012).

One of the problems facing the treatment of bacterial infections is partially due to the acquisition of antibiotic resistance genes, and the formation of persister cells. Persister cells have been characterised as a subpopulation of a bacterial culture, distinct from exponential and stationary phase cells that exhibit multidrug tolerance, a lower rate of protein turnover and reduced metabolic activity (Keren *et al.*, 2004b; Lewis, 2010; Shah *et al.*, 2006). The number of cells becoming persisters within a

bacterial population increases with the age of the culture, reaching its peak during stationary phase (Keren *et al.*, 2004a). Recently bacterial persistence has been shown to be due to halted protein synthesis, and a reduction in ATP synthesis (Kwan *et al.*, 2013), both likely to be experienced in a stationary phase culture and during dormancy. In contrast to popular belief it has been proposed that persisters do not form a distinct subpopulation in stationary phase, but simply reflect differences in awakening from dormancy (Joers *et al.*, 2010). This study showed that when grown in rich media (LB) *E. coli* showed a faster exit from dormancy whereas those grown in MOPS (MOPS- 3-(N-morpholino) propanesulfonic acid) minimal media exhibited a delayed exit from dormancy, increasing their ability to withstand antibiotic treatment (Joers *et al.*, 2010).

B. pseudomallei is able to persist within the body for extended periods of time, even after antibiotic treatment. Relapse of infection often occurs due to poor adherence to antibiotic treatment, and is thought to be partially due to the formation of persister cells. Both *B. thailandensis* and *B. pseudomallei* are known form persister cells after treatment with ceftazidime or ciprofloxacin, with a higher persister frequency seen with stationary phase cultures compared to exponential phase cultures (Hemsley *et al.* unpublished data) (Butt *et al.*, 2014). The formation of *Burkholderia* persister cells is thought to involve a switch towards an anaerobic metabolic state. However, currently little is known as to what role anaerobic respiration and NAR will play in persister cell formation.

One of the major contributing factors to the formation of persister cells is the regulation and expression of toxin-antitoxin (TA) modules, such as *hipA* (Keren *et al.*, 2004b; Lewis, 2010). Recently the HicAB TA system from *B. pseudomallei* has been shown to play a role in persister cell formation, with a Δ*hicAB* mutant displaying reduced persister frequencies when compared to the wild-type when cultured with ciprofloxacin, but not ceftazidime (Butt *et al.*, 2014). A reduction in persister frequency was also seen with a *M. tuberculosis* Δ*hicAB* mutant. Transcript profiling of *M. tuberculosis* persister cells has indicated that a small number of genes upregulated within persister cells, including TA systems, display the same degree of regulation in an *in vitro* dormancy model, whereas those genes required for energy and metabolic pathways were downregulated (Keren *et al.*, 2011).

The role of NarGHI in pathogenesis of melioidosis has yet to be characterised, although it has been speculated that it will play some role in motility, virulence and persistence. The current chapter will outline work into determining the role of NarGHI in pathogenesis of melioidosis. The role of Δ*narG* in susceptibility to hydrogen peroxide and acidified nitrite stress, motility, intracellular survival and virulence and persister cell formation will be assessed using a range of different *in vitro* and *in vivo* assays.

6.2 Results

6.2.1 Response of wild-type B. pseudomallei *K96243 and the* ΔnarG *mutant to acidified nitrite and hydrogen peroxide stress*

Macrophages often produce both ROS and RNI as a part of the immune response to invading bacteria. *C. jejuni* respiratory proteins, such as NapA, have been shown to play a role in susceptibility to hydrogen peroxide (H_2O_2) stress (Kassem *et al.*, 2012). The periplasmic nitrate reductase (NapA) was thought to play a role in response to H_2O_2 stress due to its role in redox balancing within the periplasm. In comparison to NapA, the catalytic subunit of NarGHI (NarG) is cytoplasmically orientated so it was hypothesised that *B. pseudomallei* NarGHI would play no role in redox balancing. To confirm this prediction wild-type *B. pseudomallei* K96243 or mutant (Δ*narG*) cultures were treated with a range of different H_2O_2 concentrations for 15 minutes. *B. pseudomallei* was shown to be highly sensitive to H_2O_2 at concentrations above 2.5 mM, with a dramatic reduction in survival rate seen for both the wild-type and the mutant. As predicted no difference in survival in response to H_2O_2 was observed between the wild-type and mutant (Fig. 6.1).

M. tuberculosis nitrate respiration has been shown to protect against acidified nitrite stress (Tan *et al.*, 2010). In order to determine whether NarGHI plays a role in response to acidified nitrite stress, wild-type *B. pseudomallei* and Δ*narG* were grown in acidified L-broth (pH 5) at a range of nitrite concentrations. Cell counts were taken after 6 and 24 hours growth in the acidified nitrite medium (Fig. 6.2). After 6 hours incubation both wild-type *B. pseudomallei* and the Δ*narG* mutant showed a reduced growth rate in the presence of over 0.1 mM nitrite (Fig. 6.2 a). After 24 hours, both cultures displayed an increase in growth at all nitrite concentrations tested, although

the cultures exposed to 2 and 4 mM acidified nitrite still displayed a reduction in growth when compared to the L-broth controls (Fig. 6.2 b). Although the Δ*narG* mutant displayed a slightly better growth rate to wild-type *B. pseudomallei,* no significant difference was seen between the wild-type and mutant in response to acidified nitrite stress.

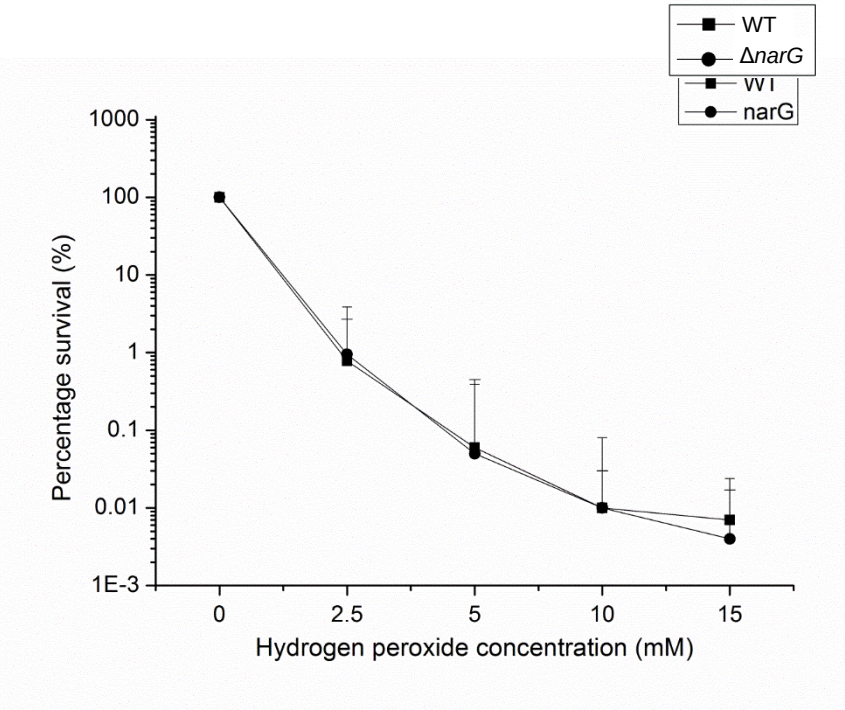

Figure 6.1 - Response of *B. pseudomallei* K96243 to hydrogen peroxide (H_2O_2) stress. Wild-type *B. pseudomallei* (filled squares) and Δ*narG* mutant (filled circles) overnight cultures were standardised to 1 x 10^8 CFU/mL prior to a 15 minute exposure to varying concentrations (0 to 15 mM) of H_2O_2. Three independent biological replicates were used. Error bars ± SD.

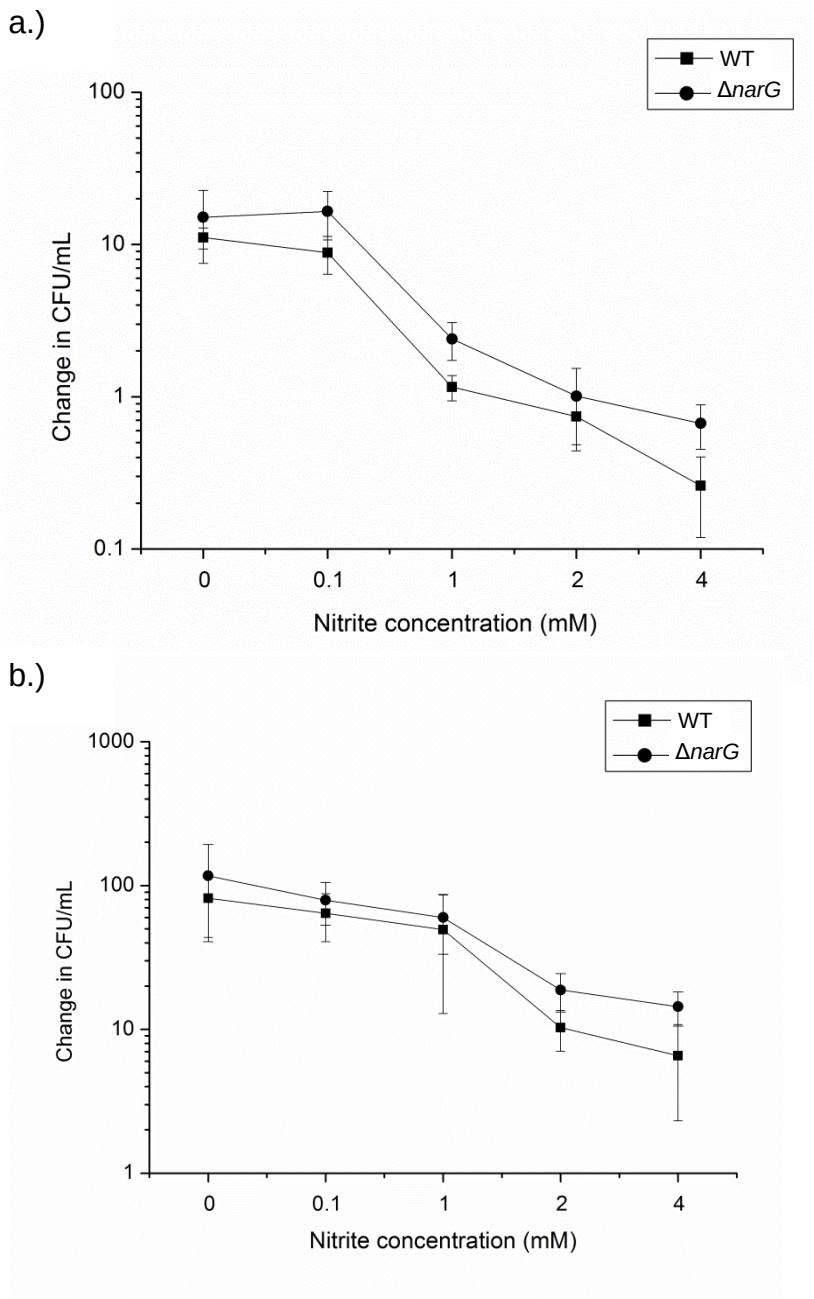

Figure 6.2 - Response of *B. pseudomallei* to acidified (pH 5) nitrite stress. Wild-type *B. pseudomallei* (filled squares) and the Δ*narG* mutant (filled circles) were grown aerobically at 37 ºC in acidified (pH 5) L-broth supplemented with varying concentrations of sodium nitrite (0 – 4 mM). Cell counts were performed to determine the number of surviving bacteria/change in CFU/mL after either a.) 6 hours or b.) 24 hours treatment. Experiment was performed using three independent biological replicates. Error bars ± SD.

6.2.2 Deletion of narG *causes a defect in motility in rich but not minimal media*

Disruption of the molybdopterin biosynthesis pathway lead to a reduction in motility in *B. thailandensis,* thought to be due to a reduction in NAR activity. To determine whether NarGHI in *B. pseudomallei* plays a role in motility various assays were performed using rich or minimal media solidified with 0.3 % bacteriological agar.

Initial studies were performed using nutrient broth supplemented with glucose, following the same protocol used for *B. thailandensis* (Chapter 4) (Andreae *et al.*, 2014). The Δ*narG* deletion mutant displayed a significant reduction in motility on nutrient broth agar (Fig. 6.3). To test what effect nitrate addition had on *B. pseudomallei* motility, 20 mM sodium nitrate was added to the motility medium. In contrast to what was seen with *B. thailandensis* (Chapter 4 – section 4.2.6), the addition of nitrate caused a significant reduction in wild-type *B. pseudomallei* motility, but did not affect the general motility defect exhibited by the mutant (Fig. 6.3).

The majority of work presented in this study has been performed using either L-broth or M9 minimal media. In order to avoid any potential differences in gene expression due to the media used the motility assays were repeated using either L-broth or M9 minimal media solidified 0.3 % bacteriological agar. M9 minimal media was also used as *B. pseudomallei* is likely to experience more of a nutrient limiting environment *in vivo.*

In LB media the Δ*narG* mutant displayed a significant reduction in motility when compared to the wild-type. Considering addition of nitrate caused a reduction in motility for the wild-type *B. pseudomallei* it was reasoned that this could be due to its reduction to nitrite, which may be having an inhibitory effect on *B. pseudomallei* motility. To confirm this hypothesis 5 mM sodium nitrite was added to the motility media (Fig. 6.4 a). As predicted the addition of nitrite resulted in a significant reduction in wild-type motility, to a similar extent to that seen with nitrate addition. In contrast,

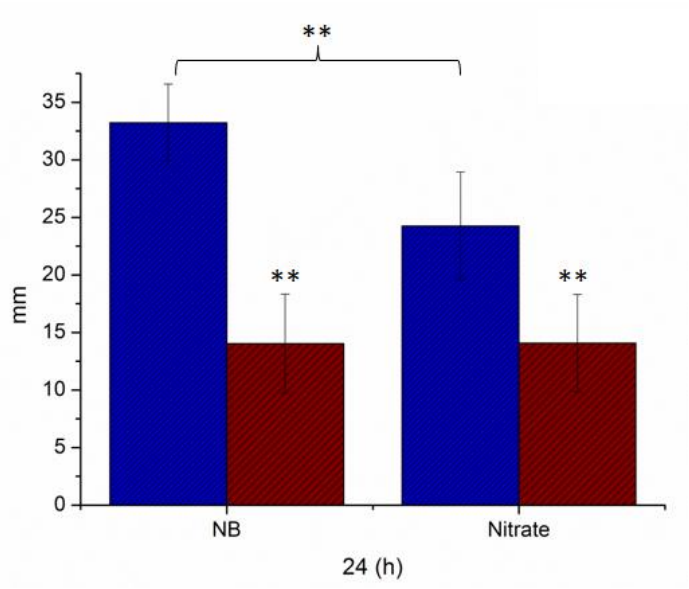

Figure 6.3 - The Δ*narG* mutant displays altered motility on nutrient broth (NB) 0.3 % agar media. Standardised wild-type *B. pseudomallei* and Δ*narG* cultures were inoculated into the centre of semi-solid (0.3 %) NB motility agar plates, supplemented with or without 20 mM sodium nitrate. Plates were incubated for 24 hours in a 37 ^{o}C incubator. Asterisks (**) denote significant differences between WT (blue) and Δ*narG* (red) (two tailed T-test p-value < 0.01). Brackets with asterisks identify significant differences between wild-type motility when treated with nitrate. Two to three independent biological replicates were used each with three technical replicates. Error bars ± SD.

neither the addition of nitrate or nitrite to the LB agar motility media had any effect on the general motility defect seen for the Δ*narG* mutant (Fig. 6.4).

In contrast to what was seen when using LB and nutrient broth motility plates, no motility defect was seen for the Δ*narG* mutant when using M9 minimal media. Both nitrate and nitrite addition still resulted in a decrease in motility seen for the wild-type. In comparison only nitrite resulted in a significant decreased motility seen in the Δ*narG* mutant, similar to that seen in the wild-type (Fig. 6.4 b).

Since the Δ*narG* mutant did not display a motility defect when using minimal media, it was hypothesised that the mutant still had flagella. To confirm this hypothesis both wild-type *B. pseudomallei* and Δ*narG* were grown overnight in L-broth and imaged using transmission electron microscopy (TEM). Bacterial cultures were fixed using a final concentration of 4 % formaldehyde and the cells were washed in distilled water prior to fixation on a TEM grid. Fifteen different images, taken from three separate TEM grids, were used to get an overall picture of whether the Δ*narG* mutant still possessed flagella. A number of flagella had broken off during treatment of the both the wild-type and mutant cultures, but overall the majority of the cells possessed one or more flagella, confirming that the motility defect seen for Δ*narG* mutant is not due to a lack of flagella (Fig. 6.5).

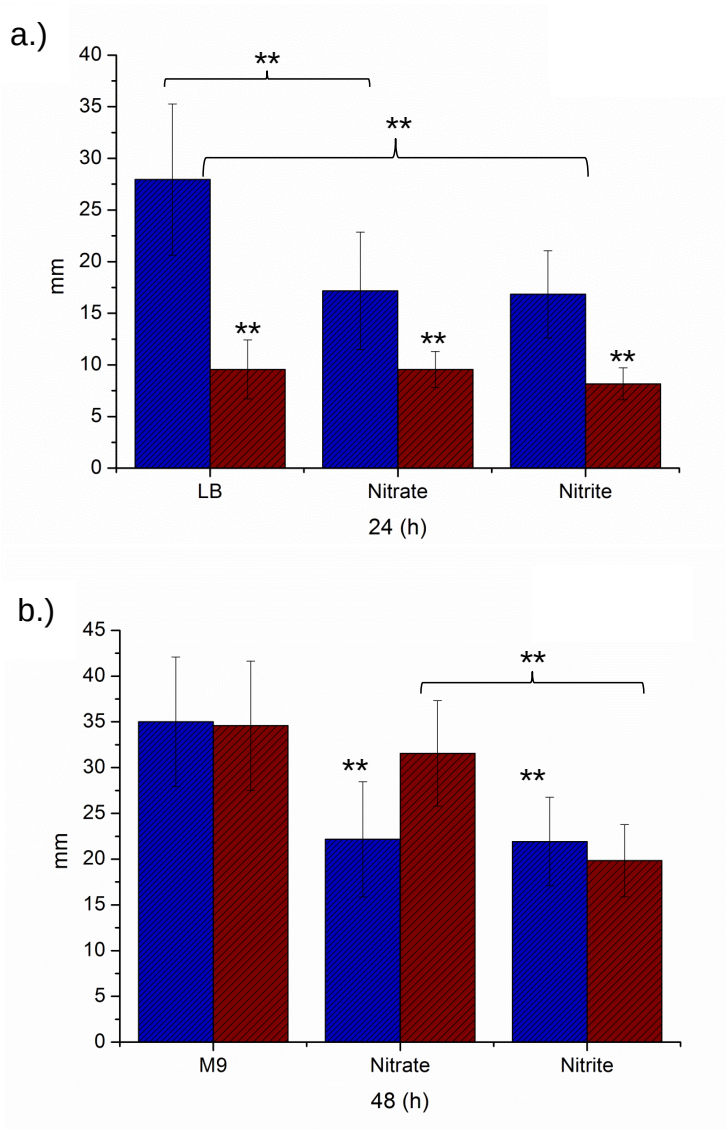

Figure 6.4 – Deletion of BPSL2309 (Δ*narG*) effects *B. pseudomallei* K96243 motility in LB but not in M9 minimal motility media. Standardised wild-type *B. pseudomallei* and Δ*narG* cultures were inoculated into the center of semi-solid (0.3 %) agar (a.) LB or (b.) M9 minimal motility agar plates, supplemented with either 20 mM sodium nitrate or 5 mM sodium nitrite. All M9 minimal media motility plates were supplemented with 20 mM sodium succinate as a carbon source. Plates were incubated for 24 or 48 hours in a 37 ^{o}C incubator. Asterisks (**) denote significant differences between wild-type *B. pseudomallei* (blue) and the Δ*narG* mutant (red) (two tailed T-test p-value < 0.01). Brackets with asterisks identify significant differences between wild-type or Δ*narG* mutant motility when treated with nitrate or nitrite. Two to four independent biological replicates were used each with three technical replicates. Error bars ± SD.

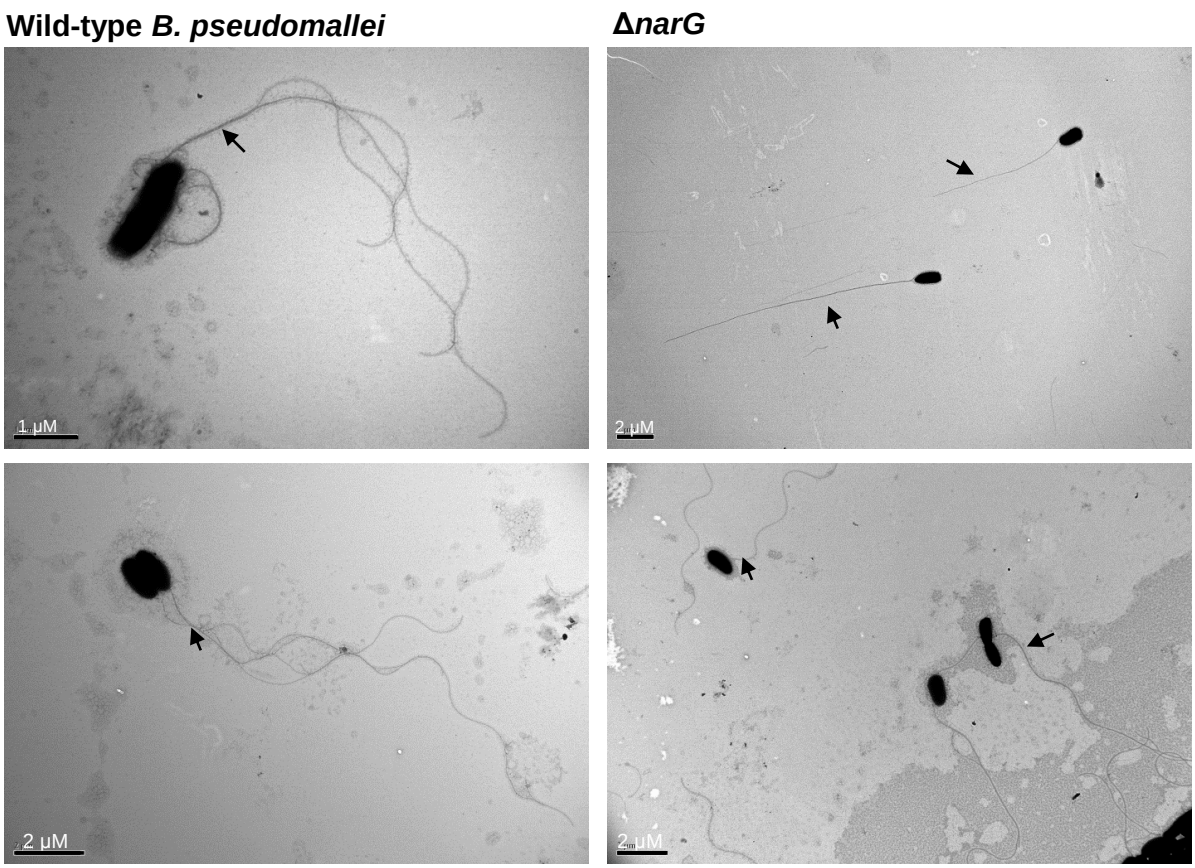

Figure 6.5 – Reduction in motility seen for the Δ*narG* mutant is not due to a lack of flagella. TEM microscopy was performed, with the aid of Peter Splatt, on wild-type *B. pseudomallei* K96243 and Δ*narG* cells taken from an L-broth overnight culture, fixed using 4 % formaldehyde and washed with distilled water. Fifteen images were taken from three separate TEM grids. Scale bar for top left hand image denote 1 µM. Scale bars for all other images denote 2 µM. The above images are the representative of what was seen for both the wild-type and mutant.

*6.2.3 No virulence defect is seen for the Δ*narG *mutant when using* G. mellonella *as an infection model*

To determine whether *B. pseudomallei* NarGHI played a role in virulence, *G. mellonella* were challenged with wild-type, Δ*narG* or PBS. No death was seen after challenge with PBS. Ten *Galleria* were challenged with 1,300 to 1,400 CFU/galleria of either wild-type or the Δ*narG* mutant (Fig. 6.6). No difference was observed in the time to death of *Galleria* infected with either wild-type *B. pseudomallei* K96243 or the Δ*narG* mutant. Similar results were seen when using a higher infection dose of 1 x 10^4 bacteria. This is unsurprising considering no virulence defect was observed for the *moeA* (CA01) *B. thailandensis* transposon mutant (Chapter 4 – Fig. 4.13).

6.2.4 NarGHI is not required for intracellular replication

Murine J774A.1 macrophages were used to determine whether the deletion of *narG* (BPSL2309) affected intracellular replication (Wand *et al.*, 2010). J774A.1 macrophages were seeded at a multiplicity of infection of 10:1 and infected with 1 x 10^6 CFU/mL of either wild-type *B. pseudomallei* or the Δ*narG* mutant. The infected macrophages were then incubated at 37 ^oC for 2 hours to allow for adherence and internalisation of extracellular bacteria. After 2 hours 1 mg/mL of kanamycin was added to suppress the growth of any extracellular bacteria and to ensure that the cell counts for the next time points (4 to 8 hours) would only be the number of intracellular bacteria. No growth of wild-type *B. pseudomallei* was seen in the presence of 1 mg/mL kanamycin. Intracellular growth was measured after cell lysis by a 10 fold serial dilution and spot plating. An initial decline in the number of CFU/mL was noted for the first two time points; 0 hours measuring the total number of cells in the assay, and 2 hours measuring intracellular and adhered bacteria. Both wild-type and mutant CFU/mL cell counts increased after 4 hours post infection indicating an increase in intracellular replication. No difference in intracellular replication at any time point (0, 2, 4, 6 or 8 hours) was seen for Δ*narG* when compared to the wild-type (Fig. 6.7), indicating NarGHI does not play a role in intracellular replication in this model system.

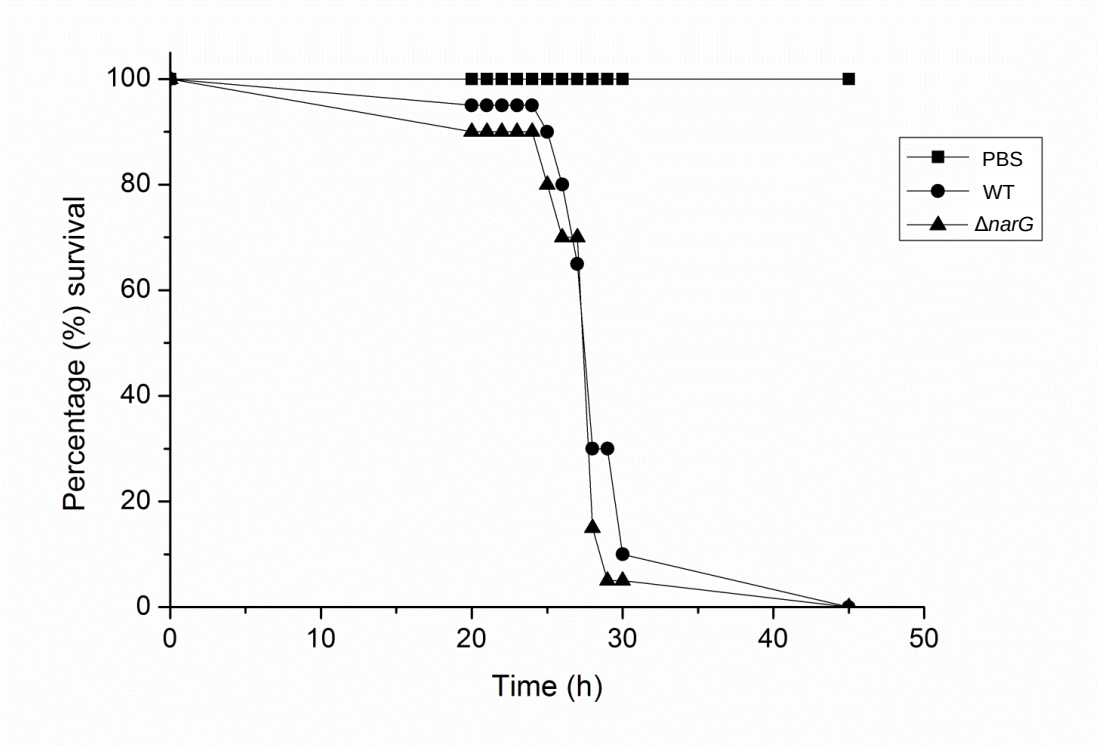

Figure 6.6 - Deletion of BPSL2309 does not affect virulence in *G. mellonella.* Ten *G. mellonella* larvae were each challenged with 1,300 to 1,400 CFU of wild-type *B. pseudomallei* K96243 (filled circles) or Δ*narG* mutant (filled triangles). No difference in virulence was seen between the wild-type and mutant. PBS was used as an infection control (filled squares). Results are the average of two independent challenges each with 10 galleria per challenge.

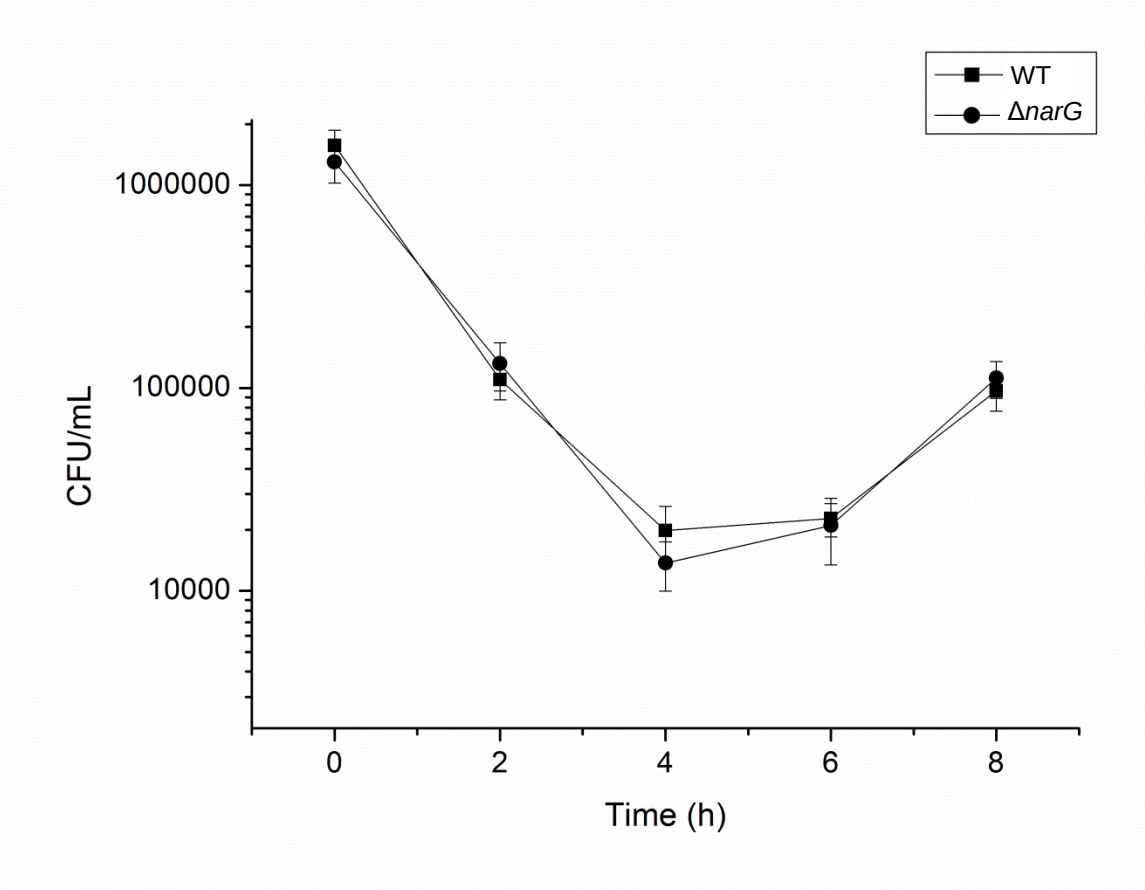

Figure 6.7 – The Δ*narG* mutant does not exhibit a difference in intracellular replication in murine J774A.1 macrophages. J774A.1 murine macrophages were exposed to wild-type *B. pseudomallei* (filled squares) or the Δ*narG* mutant (filled circles) at an MOI of 10 and the number of intracellular bacteria was determine at 0 (input CFU) 2, 4, 6 or 8 hours post infection. 1 mg/mL kanamycin was added after 2 hours to suppress the growth of any extracellular bacteria. Any extracellular bacteria were killed off 2 hours post infection using 1 mg/mL kanamycin. Results shown are the average of one biological replicate performed in triplicate. Error bars ± SD.

6.2.5 Role of B. pseudomallei *anaerobic respiration in a murine model of infection*

Preliminary studies have been conducted, in collaboration with Dr. Gregory Bancroft's group at the London School of Hygiene & Tropical Medicine, to determine the role of NarGHI in virulence of *B. pseudomallei*. C56BL/6 mice were challenged with two different CFU of wild-type *B. pseudomallei* K96243 or the Δ*narG* deletion mutant. Two different CFU were used, either 200 CFU or 4,000 CFU, to achieve either a chronic (low dose) or acute (high dose) infection (Fig. 6.8). In the chronic infection model 90 % of the Δ*narG* infected mice were alive after around 150 days post infection, whereas no mice were dead in those infected with the wild-type (Fig. 6.8 a). After 55 days post infection in the acute model only 10 % of wild-type challenged C56BL/6 mice were alive, compared to 50 % in those challenged with the Δ*narG* mutant (Fig. 6.8 b). Unfortunately the effective dose administered to the mice in both the chronic (Fig. 6.8 a) and acute (Fig. 6.8 b) infection models for the wild-type *B. pseudomallei* (K96243) and Δ*narG* are far too different to draw any real conclusion from the dataset (see tables in Fig. 6.8). For example, the reduction in virulence seen for Δ*narG* in the acute infection model may simply be due to the fact that the challenge dose for the Δ*narG* mutant (2,600 CFU) was almost half that of the wild-type (4,700 CFU). This makes it very difficult to say whether or not deletion of *narG* (BPSL2309) affects the *B. pseudomallei* virulence in a murine infection model. The experiments are currently still on going.

6.2.6 No difference is seen between the wild-type and mutant in susceptibility to antimicrobials

To determine whether or not deletion of BPSL2309 would alter *B. pseudomallei* K96243 susceptibility to antibiotics a minimal inhibitory concentration (MIC) experiment was performed on wild-type *B. pseudomallei* and Δ*narG* mutant cultures. Wild-type and mutant cultures were standardised and exposed to a number of antibiotics (chloramphenicol, ceftazidime, trimethoprim, and ciprofloxacin) at a range of different concentrations. The MIC was performed statically in L-broth in a 96 well plate incubated aerobically overnight at 37 ^{o}C. Nitrate was added to both wild-type and mutant cultures to determine whether or not it would have an effect on antibiotic efficiency. No difference was seen between wild-type *B. pseudomallei* or the Δ*narG*

a.)

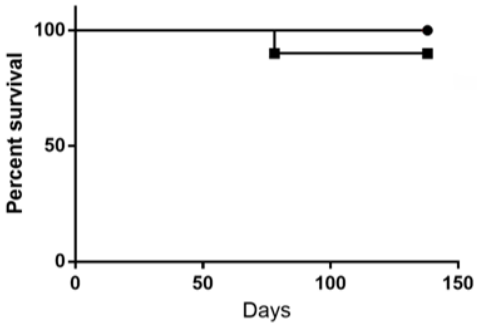

	CFU intended	Counting/effective dose	Number of mice challenged
Wild-type K96243	200	60	10
Δ*narG*	200	220	10

b.)

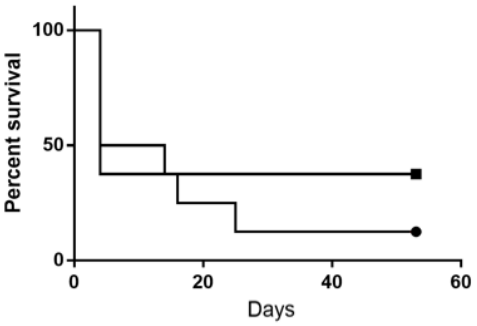

	CFU intended	Counting/effective dose	Number of mice challenged
Wild-type K96243	4000	4700	8
Δ*narG*	4000	2600	8

Figure 6.8 – Preliminary study of the survival of C56BL/6 mice after challenge with wild-type *B. pseudomallei* K96243 or the Δ*narG* mutant. a.) Chronic infection model. C56BL/6 mice were challenged with an intended dose of 200 CFU, or either wild-type *B. pseudomallei* K96243 (circles) or the Δ*narG* mutant (squares). b.) Acute infection model. C56BL/6 mice were challenged with an intended infectious dose of 4,000 CFU, or either wild-type *B. pseudomallei* (circles) or the Δ*narG* mutant (squares). Intended CFU dose and the actual effective dose varied dramatically between the wild-type and mutant (see tables on the right side of the figure) for both acute and chronic infections. The number of mice used in this preliminary study are also indicated in each table. Work conducted by Dr. Gregory Bancroft's research group with the London School of Hygiene & Tropical Medicine (results obtained from Felipe Cia).

mutant in their susceptibility to any of the antibiotics tested, in either L-broth or L-broth supplemented with nitrate (Table 6.1). As of note, the MIC for ceftazidime for the wild-type *B. pseudomallei* K96243 used in this study is much higher to that previously published (Hamad *et al.*, 2011). This higher MIC for ceftazidime may contribute to the high percentage of persister cells seen in Fig. 6.9 (see next section).

6.2.7 Persister cell transcriptome highlights the importance of anaerobic respiration in persister cell formation

A study on *B. thailandensis* E264 was conducted by Dr. Claudia Hemsley in order to identify genes that are differentially regulated in persister cells. In this study mRNA was extracted from *B. thailandensis* cultures grown to mid-log phase, stationary phase and ceftazidime persister cells (Hemsley *et al.*, unpublished work). To generate persisters *B. thailandensis* cultures were treated with 100 x MIC ceftazidime (400 µg/mL) for 24 hours. All genes required for anaerobic respiration, including both nitrate reductases, showed a degree of upregulation when comparing mRNA extracted from mid-log phase and ceftazidime persister cells. On the other hand, when comparing RNA extracted from stationary phase cultures and ceftazidime persisters, the cryptic nitrate reductase (*narZYWV*), second putative Cu-Nir (BTH_II0944) and BTH_II0945 were down-regulated, whereas all other genes for the main anaerobic respiratory pathway still showed a degree of upregulation. Those genes required for aerobic respiration, such as NADH dehydrogenase and some cytochrome *c* oxidases were shown to exhibit a degree of down-regulation in this same study. This study highlighted the potential importance for NarGHI and anaerobic respiration in persister cell formation, pointing towards a switch to anaerobic metabolism in *Burkholderia* persister cells on treatment with ceftazidime.

Table 6.1 – *B. pseudomallei* and Δ*narG* mutant antibiotic MIC

	Wild-type K96243	**Δ*narG***
Ceftazidime	128 µg/mL	128 µg/mL
Ciprofloxacin	< 1 µg/mL	< 1 µg/mL
Trimethoprim	32 µg/mL	32 µg/mL
Chloramphenicol	8 µg/mL	8 µg/mL

Addition of nitrate does not affect MIC for either the wild-type or Δ*narG* mutant

Results are the average of two independent biological replicates.

Experiment was performed statically in a 96 well plate using L-broth and a 1 in 100 dilution of OD 0.1 (absorbance 600 nm) standardised bacterial cultures

Table 6.2 – *B. thailandensis* persister cell transcriptome dataset relating to those genes required for denitrification

Gene ID	Gene name	Ratio persisters/LBML	Ratio persisters/LBS
Nitrate reductase			
BTH_I1851-1854	*narGHJI*	Up (5.45 – 12.89)	Up (6.51 - 16.63)
BTH_I1849-1850	*narXL*	Up (7.62 – 11.69)	Up (16.27 – 20.65)
BTH_I1855-1856	*narK1K2*	Up (1.83 – 4.78)	Up (1.97 – 2.14)
BTH_II1249-1252	*narZYWV*	Up (2.29 – 3.41)	Down (0.09 – 0.11)
BTH_II1254	*narK*	Up (1.21)	Down (0.5)
Nitrite reductase			
BTH_II0881	*aniA*	Up (2.37)	Up (3.28)
BTH_II0944	*cu-nir2*	Up (3.09)	Down (0.03)
Nitric oxide reductase			
BTH_I1813	*norZ*	Up (8.61)	Up (3.65)
BTH_I0945	*norZ*	Up (1.83)	Down (0.03)
Nitrous oxide reductase			
BTH_I2325	*nosZ*	Up (22.37)	Up (4.25)

Data obtained and presented, with permission, from work by Dr. Claudia Hemsley (unpublished dataset)

Numbers represent fold change in expression of the respective gene or gene cluster (p-value < 0.001)

Genes that were upregulated in ceftazidime persisters are highlighted in green and those that were down-regulated in red.

6.2.8 Addition of nitrate to B. pseudomallei *K96243 persister cells increases susceptibility to ceftazidime*

To test whether anaerobic respiration plays a role in persister cell formation both wild-type *B. pseudomallei* and the Δ*narG* mutant were treated with 400 µg/mL ceftazidime for 24 hours. The persister cell experiment was performed aerobically using L-broth supplemented with or without 20 mM sodium nitrate (Fig. 6.9 a). Initial persister cell studies were conducted on late exponential/stationary phase bacterial cultures grown overnight in L-broth. The persister assay was performed statically in a 24 well plate, in order to mimic slow growing and oxygen limiting conditions seen *in vivo* (Hemsley *et al.* unpublished data). The cultures were standardised to give 2 x 10^8 CFU/mL and diluted 1:1 in a 24 well plate with L-broth containing 800 µg/mL ceftazidime. This gave a final antibiotic concentration of 400 µg/mL ceftazidime and cell density of 1 x 10^8 CFU/mL. The 24 well plate was then incubated overnight at 37 ^oC in a static incubator and input and output cell counts were conducted using a 10-fold dilution series with the cells enumerated on LB agar plates. In L-broth alone no difference was seen in persister cell formation for stationary phase *B. pseudomallei* wild-type or Δ*nar*G mutant, with around 10 % of the population entering a persistent state after 24 hours. However a significant difference was seen when incubated with nitrate, with the wild-type exhibiting a decline in the persister frequency, with only 1 % of the population surviving ceftazidime treatment. By contrast the Δ*narG* mutant displayed the same level of percentage survival (around 10 % persisters) as those persisters cells incubated in L-broth alone (Fig. 6.9 b). This indicated that nitrate reductase activity played a role in *B. pseudomallei* susceptibility to ceftazidime.

Considering wild-type *B. pseudomallei* exhibits NAR activity after 8 hours aerobic growth (Chapter 5 – Fig. 5.6) it was hypothesised that part of the overnight culture had entered an anaerobic metabolic state, inducing genes required for anaerobic respiration. To determine whether log phase persister cells, exhibit the same susceptibility to ceftazidime, when incubated with nitrate, *B. pseudomallei* cultures grown overnight and sub-cultured into fresh L-broth and incubation for 6 hours aerobically. After 6 hours growth the log phase bacterial cultures were standardised and treated with ceftazidime in L-broth supplemented with and without nitrate. In comparison to those stationary phase cultures treated with ceftazidime, only around 2

a.)

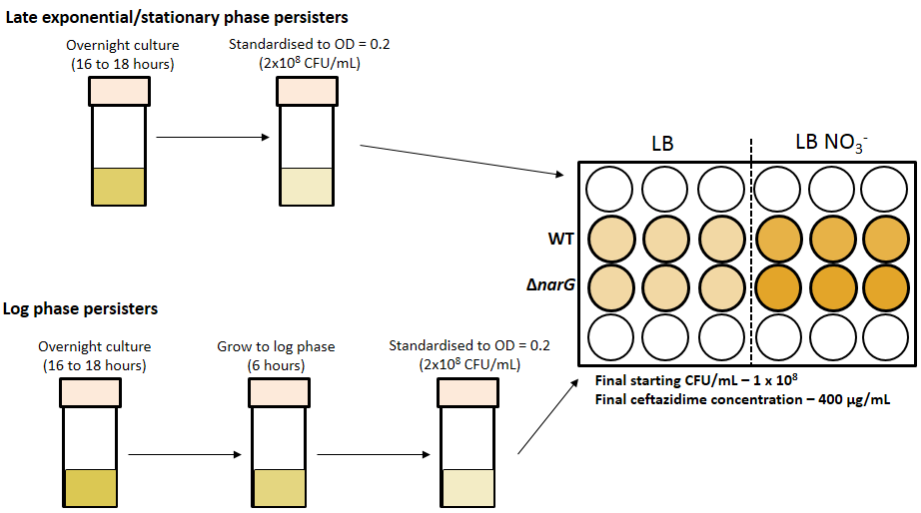

b.)

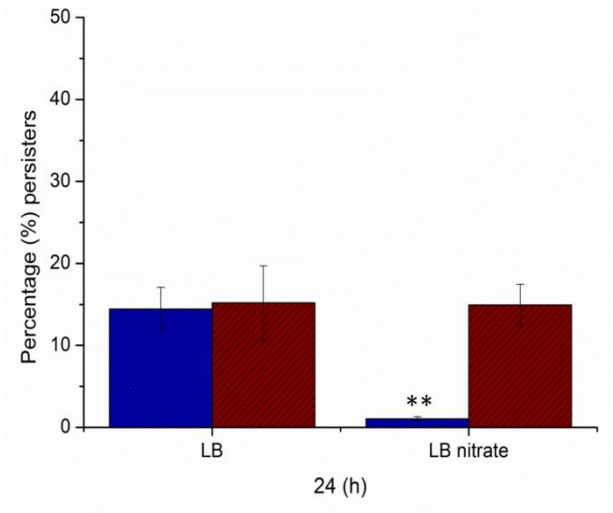

c.)

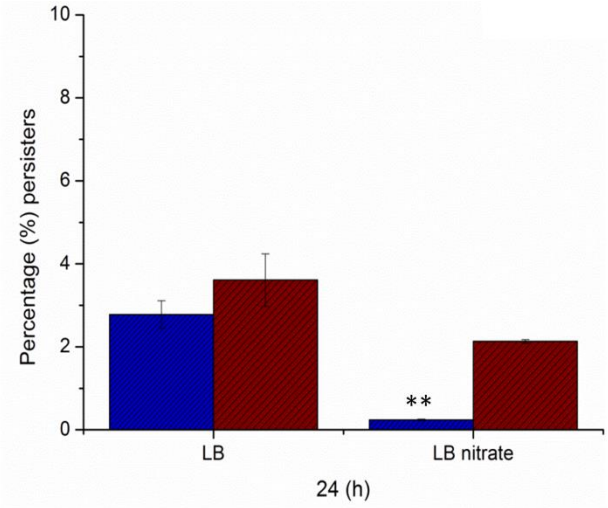

Figure 6.9 - Addition of nitrate significantly increases wild-type, but not the Δ*narG* mutants, susceptibility to ceftazidime. Wild-type *B. pseudomallei* K96243 and Δ*narG* were grown to late exponential/stationary phase (16 to 18 hours) or log phase (6 hours) in L-broth medium, prior to treatment with 400 µg/mL ceftazidime. The persister assay was performed using LB medium supplemented with or without 20 mM sodium nitrate. a.) Persister cell assay protocol. See Chapter 2 section 2.5.6 *Persister cell assay* for more details. Wild-type *B. pseudomallei* (blue) and Δ*narG* mutant (red) persister cell frequency was determined for either b.) Late exponential/stationary phase (16 to 18 hours) or c.) Log phase (6 hours) bacterial cultures. Three independent biological replicates were used each with three technical replicates. Error bars ± SD. Asterisks (**) denote significant differences between WT (blue) and Δ*narG* (red) (T-test, p-value < 0.01).

to 4 % of both wild-type *B. pseudomallei* and Δ*narG* mutant formed persister cells in L-broth (Fig. 6.9 c). Again the addition of nitrate significantly increased wild-type persister cells susceptibility to ceftazidime, not seen in the Δ*narG* deletion mutant.

To confirm that the *B. pseudomallei* had formed persister cells, exhibiting tolerance but not resistance to antibiotic treatment, those cells forming colonies on the LB agar plates after 24 hour treatment were streaked out onto LB agar plates and LB agar plates supplemented with 400 µg/mL ceftazidime. Subculture of the persister cells on to LB agar plates supplemented with ceftazidime resulted in a reversion of *B. pseudomallei* persisters to an antibiotic susceptible phenotype. Growth of *B. pseudomallei* persister cells was only seen in the absence of ceftazidime, confirming the formation of persister cells exhibiting tolerance but not resistance to antibiotic action. This was the same as what was seen for *B. pseudomallei* prior to treatment with ceftazidime.

6.2.9 *Biphasic kill curve of wild-type* B. pseudomallei *K96243 in the presence or absence of nitrate*

To determine the point at which nitrate addition increased susceptibility of wild-type *B. pseudomallei* to ceftazidime the persister cell assay was repeated with cell counts taken every few hours (0, 2, 4, 6, 8, 10, 24 and 30 hours). As previously seen (Butt *et al.*, 2014) treatment of *B. pseudomallei* with ceftazidime results in biphasic killing, with initial killing seen after the first two hours of treatment. This was followed by a plateau and further killing after 10 hours incubation with the antibiotic, with a greater killing seen in the presence of nitrate (Fig. 6.10). A slight increase in CFU/mL was seen after 6 hours incubation indicating a potential resumption of growth/replication after initial killing. After 10 hours a further killing was seen for both *B. pseudomallei* persister cells cultured in either L-broth or L-broth supplemented with nitrate, with a plateau seen after 24 hours treatment. A greater degree of killing was seen for the wild-type after 10 to 24 hours ceftazidime treatment when cultured with nitrate, likely due to NarGHI activity resulting in increased antibiotic susceptibility.

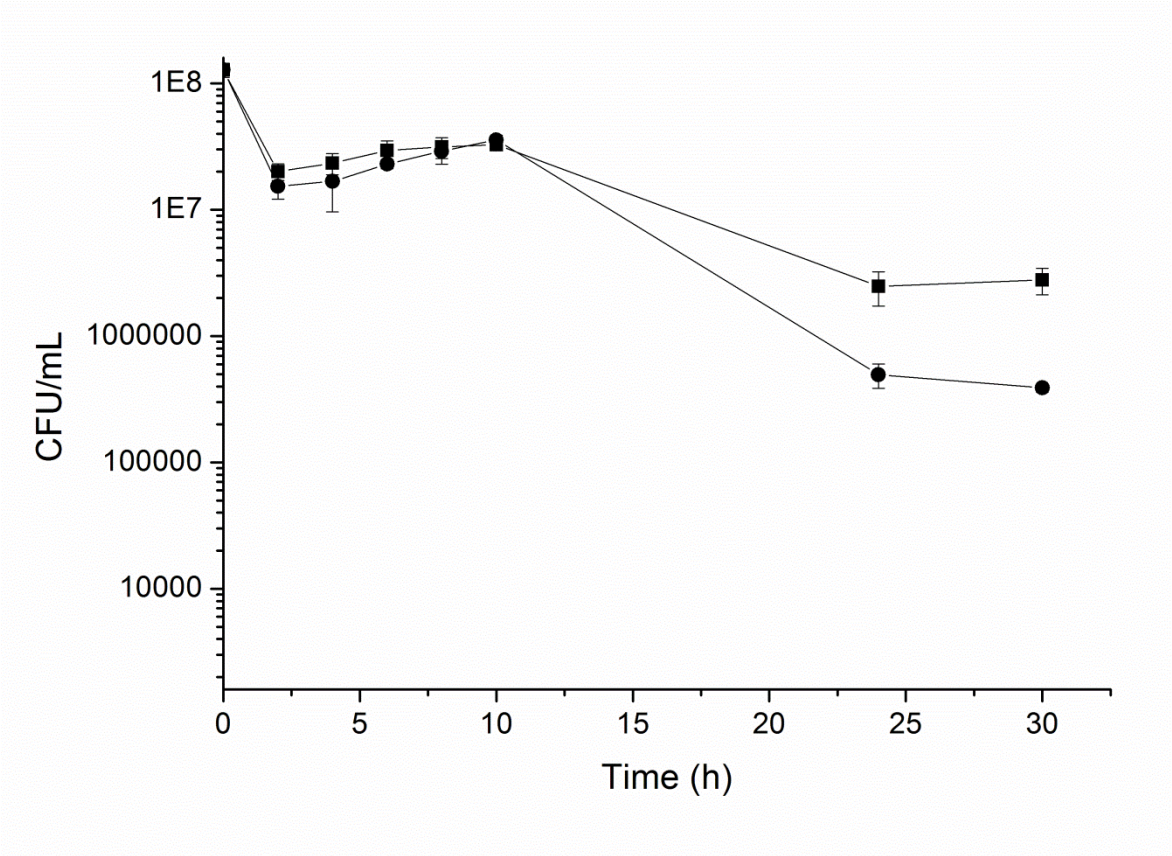

Figure 6.10 – Addition of nitrate to *B. pseudomallei* K96243 persister cells enhances killing after 24 hours incubation with ceftazidime. Wild-type *B. pseudomallei* cultures were grown to stationary phase overnight prior to treatment with 400 µg/mL ceftazidime. Antibiotic killing was monitored every few hours, with the number of surviving CFU/mL determined after washing in fresh L-broth. The persister assay was performed using LB medium supplemented with (filled circles) or without (filled squares) 20 mM sodium nitrate. Two independent biological replicates were used each with two technical replicates. Error bars ± SD.

6.3 Discussion

The role of respiratory proteins in survival and persistence of bacterial pathogens has recently become more of interest. Building on work previously conducted on *B. thailandensis,* the role of NarGHI in *B. pseudomallei* K96243 in virulence and persistence was characterised using a Δ*narG* deletion mutant.

Respiratory proteins in *C. jejuni,* a pathogenic bacteria and causative agent of food-born gastroenteritis, have recently been demonstrated to be play a role in motility, response to H_2O_2 stress and biofilm formation (Kassem *et al.*, 2012). In relation to anaerobic respiration the periplasmic nitrate reductase, NapA, was shown to play a role in tolerance to H_2O_2, thought to be due to its role in cellular homeostasis. In comparison, and unsurprisingly, the *B. pseudomallei* Δ*narG* mutant did not display any difference in susceptibility to H_2O_2 stress when compared to the wild-type. The differences in role of the different types of nitrate reductases in response to oxidative stress is likely to be partially due to the differences in their cellular location. NapA is found within the periplasm which may allow it to play a more direct role in redox balancing, whereas NarGHI is bound to the inner-membrane with its catalytic subunit cytoplasmically orientated and is generally only required for the generation of PMF (Bertero *et al.*, 2003; Gonzalez *et al.*, 2006).

Nitrate respiration has been shown to play a role in protection against acid and acidified nitrite stress, both of which are experienced *in vivo* by *M. tuberculosis* (Tan *et al.*, 2010). When cultured microaerobically or anaerobically in the absence of nitrate, *M. tuberculosis* was shown to be sensitive to acid and acidified nitrite stress, attributed to the breakdown of PMF and lack of ATP generation. In comparison, the addition of nitrate allowed anaerobic *M. tuberculosis* cells to resist acid-mediated killing, due to the renewed ability for the cells to generate a PMF and maintain a good redox balance (Tan *et al.*, 2010). This ability to resist acid mediated killing was shown to be due to NarGHI activity. To determine whether this was true for *B. pseudomallei* NarGHI, both the wild-type and *ΔnarG* mutant were subjected to different concentrations of nitrite in acidified L-broth under aerobic conditions. No difference was seen between *B. pseudomallei* and Δ*narG* when subjected to acidified (pH 5) nitrite stress (Fig. 6.2), after either 6 or 24 hours incubation. An increase in growth was seen after 24 hours treatment with acidified (pH 5) nitrite, for both the wild-type and mutant indicating that there may have been an induction of detoxification mechanisms or change in pH of

the culture medium. Whether or not anaerobic nitrate respiration protects against acidified nitrite stress for *B. pseudomallei* under anaerobic conditions remains to be determined.

Disruption of the molybdopterin biosynthetic pathway in *B. thailandensis* caused a reduction in motility, thought to be partly due to a reduction in NAR activity (Chapter 4). The *B. pseudomallei* Δ*narG* mutant displayed a significant reduction in motility, in rich but not minimal media. TEM microscopy confirmed the presence of flagella in both the wild-type and mutant, indicating the motility defect seen in the Δ*narG* mutant was due to alternative mechanism, other than the absence of flagella (Fig. 6.5). The difference in motility displayed by the mutant in rich or minimal media could potentially be due to differences in gene regulation. Flagella and chemotaxis proteins in *E. coli* have been shown to be down-regulated in an *rpoS* mutant in minimal media, corresponding with a decrease in motility seen in the mutant (Dong & Schellhorn, 2009). *B. pseudomallei* genes required for motility and chemotaxis have been shown to be upregulated after 4 hours hypoxia in L-broth supplemented glucose (Hamad *et al.*, 2011). It is possible, in rich media, the lack of NarG causes a reduction in motility due to decrease in energy generation, altered gene transcription or change in bioenergetics. It is likely that the expression of genes associated with motility varies depending on the surrounding environmental conditions. In minimal media one could speculate that alternative regulatory mechanisms are induced to ensure the bacteria can disseminate to environments more nutrient rich. An induction of different mechanism to ensure flagella function in minimal media would therefore compensate for the loss of a functional NarGHI, as seen with comparable wild-type *B. pseudomallei* and Δ*narG* mutant motility in M9 minimal media solidified with 0.3 % bacteriological agar.

It was initially assumed that the addition of nitrate to the motility medium would result in increase in motility, due to an increase in NarGHI activity, as seen in *P. aeruginosa* (Van Alst *et al.*, 2007). However this was not the case, and the addition of either nitrate or nitrite caused a reduction in wild-type in all media tested.

S. typhimurium and *E. coli* are known to exhibit electron acceptor taxis, in response to the presence of alternative terminal electron acceptors (Taylor *et al.*, 1979). Electron acceptor taxis requires the presence of a functioning electron transport

chain and allows bacteria to sense changes in the external environment and PMF to alter their motility, in response to oxygen, nitrate, or nitrite (Taylor *et al.*, 1979). Anaerobically grown *S. typhimurium,* lacking a functional nitrate reductase, exhibited altered motility in response to nitrate, highlighting the importance of NAR in the chemotaxis (Taylor *et al.*, 1979). Electron acceptor chemotaxis in *Shewanella putrefacians,* in comparison to both *E. coli* and *S. typhimurium,* does not appear to require the presence of a functional electron transport system and PMF, with mutants incapable of nitrate or nitrite reduction still showing normal tactic responses towards nitrate and nitrite (Nealson *et al.*, 1995).

It is tempting to speculate that the reduction in motility seen for the wild-type *B. pseudomallei* K96243 in the presence of nitrate and nitrite (Figs. 6.3, 6.4 and 6.5) is due to a change in chemotactic behaviour, and more specifically electron acceptor taxis. It is possible, in wild-type *B. pseudomallei,* the presence of either nitrate or nitrite allowed for the generation of a PMF via the denitrification pathway, decreasing the need for the bacteria to seek out alternative forms of energy, resulting in a reduced movement through the semi-solid (0.3 %) agar. In M9 minimal media the Δ*narG* mutant exhibited similar motility levels as seen for the wild-type when in the absence of either nitrate or nitrite. However, in comparison to the wild-type, addition of nitrate did not affect the Δ*narG* mutant's motility. This lack of a response to nitrate may be due to the lack of a functional NarGHI, required for the reduction of nitrate to nitrite. The reduction in motility in the presence of nitrite, seen for both the wild-type and mutant (in M9 minimal media), indicates nitrite, and not nitrate, is responsible for the reduction/inhibition of motility seen for *B. pseudomallei*. On the other hand, although less likely, the presence of nitrite could potentially allow the bacteria to generate a PMF via the reduction of nitrite (e.g. by AniA), reducing the need to seek out alternative energy sources. This is all purely speculative and further work to determine the chemotactic response of *B. pseudomallei* to various electron acceptors will be required to determine whether this prediction is correct.

An alternative explanation is that nitrate and nitrite may be acting as chemorepellents. The gene operon encoding *narGHJI* also encodes a two component system NarXL known to play a role in the regulation of *E. coli* NarGHI, anaerobically in the presence of nitrate (Stewart, 2003). An *E. coli* NarX-Tar chimera, joining the

NarX sensor kinase transmembrane and linker domains to the signalling and adaptation domains of the Tar chemoreceptor, has been shown to mediate repellent responses to both nitrate and nitrite (Ward *et al.*, 2002). It is possible that *B. pseudomallei* NarXL is partially responsible for the wild-type motility response to the presence of nitrate or nitrite within the motility media, resulting in a transcriptional response and finally reduction in motility. This however does not explain the phenotype exhibited by the mutant.

The ability to survive intracellularly, in some bacterial species, has been shown to require a functional anaerobic respiratory pathway. Nitrate reductase has been shown to be required for intracellular survival of both *M. tuberculosis* (Jung *et al.*, 2013) and *B. suis* (Kohler *et al.*, 2002), with mutations in *narG* causing an attenuation of intracellular growth, but not persistence within macrophages. A recent study on the role of *M. tuberculosis* NarG in intracellular survival has been conducted using a *narG* mutant that displayed similar virulence levels to a wild-type strain (Aly *et al.*, 2006; Cunningham-Bussel *et al.*, 2013). This study added nitrate to the media that had been omitted from previous studies, and performed the assay under non-toxic hypoxic conditions. *M. tuberculosis* is expected to encounter hypoxia *in vivo*, for example within a granuloma, so the convention of performing cell culture experiments under laboratory conditions aerobically in the absence of nitrate was brought into question. This study revealed that the intracellular accumulation of nitrite (25 µM) was due to *M. tuberculosis* nitrate respiration, rather than nitrite production by iNOS activation (Cunningham-Bussel *et al.*, 2013). Similarly narG-dependent accumulation of nitrite was seen when the same experiment was performed using 21 % oxygen when culturing infected macrophages (Cunningham-Bussel *et al.*, 2013). This study pointed towards a role for *M. tuberculosis narG* in intracellular growth and survival.

B. pseudomallei infected macrophages accumulate significantly higher levels of nitrite (200 to 250 µM), attributed to the activation of iNOS by IFN-γ (Miyagi *et al.*, 1997). In comparison, in the absence of IFN-γ stimulation, only low levels of nitrite (20 – 25 µM) are produced when infected with *B. pseudomallei.* This low level of nitrite production may be due to *B. pseudomallei* NarGHI activity, as seen in *M. tuberculosis.* Further studies are required to determine whether NarGHI is active within

macrophages if the experiment is performed in a similar manner to that used for *M. tuberculosis* in Cunnington-Bussel *et al*. (2013).

A study into the transcriptional changes of *B. pseudomallei* when internalised into macrophages revealed that 22 % of the genome shows significant transcriptional adaptation (Chieng *et al.*, 2012). *B. pseudomallei* once internalised downregulated many different genes including those required for motility, metabolism, amino acid and ion transport. In comparison those genes required for anaerobic metabolism showed a degree of upregulation (Chieng *et al.*, 2012). However, none of the anaerobic respiratory genes showed a difference in expression intracellularly, with only BPSL2311 (*narJ*) and BPSL2312 (*narI*) showing a degree of upregulation. The lack of expression of the denitrification pathway, along with the fact that the Δ*narG* mutant displayed the same level of intracellular replication as wild-type *B. pseudomallei* (Fig. 6.7) indicates that the ability to respire anaerobically is not required for intracellular survival.

Ceftazidime, a third generation cephalosporin and β-lactam antibiotic (inhibiting cell wall biosynthesis), is the frontline treatment for melioidosis. Poor adherence to antimicrobial therapy in patients with melioidosis has been linked to an increase rate of relapse (see Chapter 1 – sections *1.1.4 Recurrent melioidosis* and *1.1.5 Treatment and antibiotic resistance*). *B. pseudomallei* has been shown to form persister cells in the presence of ceftazidime under *in vitro* experimental conditions (Fig. 6.9) (Butt *et al.*, 2014). This study tested the effect of nitrate respiration on persister cell formation in the presence of 400 µg/mL ceftazidime, using both log and stationary phase *B. pseudomallei* cultures.

Persister cell formation is thought to be a hedge-betting strategy, generating phenotypic heterogeneity in order to cope with changes within the surrounding environment (Lewis, 2010; Luidalepp *et al.*, 2011). Persister frequency is known to be highly dependent on the age of the inoculum, with cells in the later stages of the growth cycle, e.g. stationary phase, exhibiting an increased number of cells entering a dormant/persistent state (Luidalepp *et al.*, 2011). This was seen with *B. pseudomallei* with a lower number of persister cells seen when using a log phase culture (around 2 to 4 % - Fig. 6.9 c) when compared to a late exponential/stationary phase culture (around 10 % - Fig. 6.9 b). Stationary phase cultures are likely to already have a

proportion of their population that have entered a low metabolic/dormant state, and so contain a greater number of cells that are likely to become persister cells. On re-culturing *B. pseudomallei* persister cells revert to an antibiotic susceptible form, confirming the survival seen after ceftazidime treatment is due to increase in tolerance rather than the acquisition of resistance mechanisms.

Antibiotic killing, for example with ciprofloxacin or ceftazidime, of *B. thailandensis* and *B. pseudomallei* is known to exhibit a biphasic pattern, with the greatest killing in the first few hours of treatment (Hemsley *et al.* unpublished data, (Butt *et al.*, 2014) and Fig. 6.10). *E. coli* cells treated with antibiotics targeting protein synthesis (e.g. amikacin), results in a rapid decline in the number of culturable cells within the first few hours. In comparison, those antibiotics that target cell wall synthesis (β-lactams; e.g. ampicillin or norfloxacin) display a much smaller decline in number of culturable cells, as seen with a shallower biphasic kill curve (Luidalepp *et al.*, 2011). *E. coli* treated with antibiotics exhibiting a shallow kill curve were shown to cause the formation of persister cells that was dependent on the age of inoculum, not seen when treated with amikacin (Luidalepp *et al.*, 2011). Treatment of *B. pseudomallei* with ceftazidime results in a shallow kill curve, with a one or two log drop in CFU/mL seen in the first two hours of treatment (Fig. 6.10), similar to that exhibited by *E. coli* treated with ampicillin (Luidalepp *et al.*, 2011). This slower kill rate of bacterial cells on treatment with antibiotics that target cell wall synthesis (such as ceftazidime or ampicillin), may allow for a greater proportion of the bacterial cells to enter a dormant/persistent state, and thus become more tolerant to antimicrobial treatment. A slight increase in *B. pseudomallei* CFU/mL was seen after 6 hours treatment with ceftazidime, indicating a potential resumption of growth/replication. This slight resumption of growth may have allowed for an increase in ceftazidime killing seen after 10 hours treatment. Ceftazidime killing treatment was further increased in the presence of nitrate, potentially due to an increase in PMF generation (Fig. 6.10).

Persister cells are thought to be a subpopulation of a bacterial population exhibiting a low level of metabolic activity, translation and protein turn-over (Allison *et al.*, 2011; Shah *et al.*, 2006). A recent study has demonstrated that the addition of metabolites, such as glucose, fructose and mannitol, have a synergistic effect on aminoglycoside antibiotic activity (Allison *et al.*, 2011). The addition of these metabo-

a.)

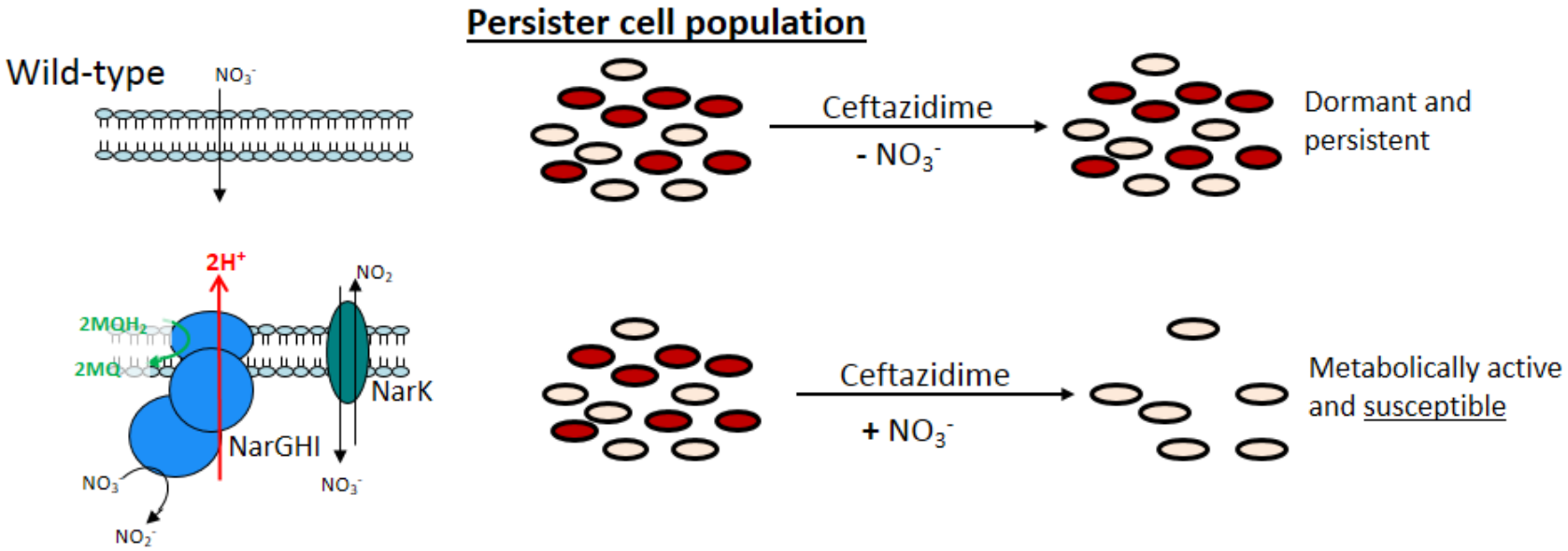
Wild-type
NO_3^-
2H+
NO_2
2MQH2
2MQ
NarK
NarGHI
NO_3^-
NO_3^-
NO_2^-
Persister cell population
Ceftazidime
- NO_3^-
Dormant and persistent
Ceftazidime
+ NO_3^-
Metabolically active and susceptible

b.)

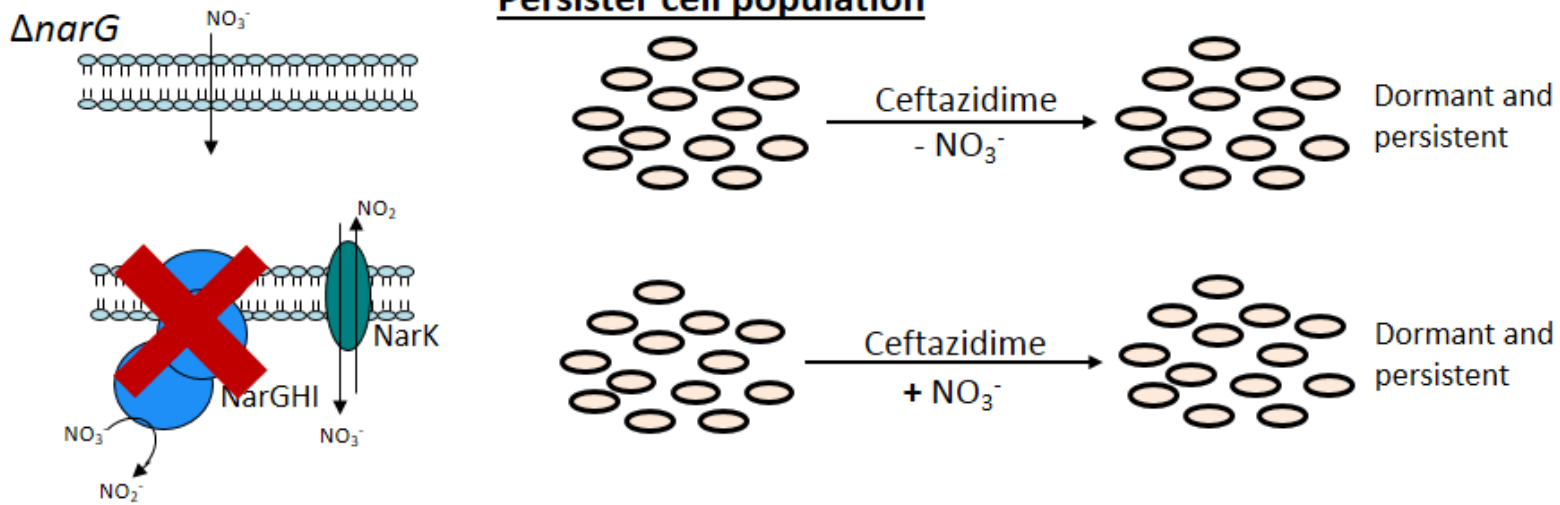
ΔnarG
NO_3^-
NO_2
NarK
NarGHI
NO_3^-
NO_3^-
NO_2^-
Persister cell population
Ceftazidime
- NO_3^-
Dormant and persistent
Ceftazidime
+ NO_3^-
Dormant and persistent

Figure 6.11 – Illustration highlighting the predicted role of nitrate reductase in persister cell formation, on the addition of nitrate. a.) Function of nitrate reductase in wild-type persister cells. NarGHI reduces nitrate to nitrite generating a proton motive force, releasing protons (H^+) into the periplasmic compartment (shown on the left). Both log phase and stationary phase cultures are predicted to contain a proportion of cells that have induced genes required for anaerobic respiration (shown in red), allowing for generation of a PMF in the presence of nitrate. In the absence of nitrate those cells that have entered a persistent state prior to ceftazidime treatment remain dormant, tolerating high levels of antibiotic. In the presence of nitrate those cells that have induced genes required for anaerobic respiration (red) become metabolically active (due to NarGHI activity) and therefore become more susceptible to ceftazidime treatment. Only those cells that are truly dormant (yellow) remain in a dormant/persistent state. b.) The Δ*narG* mutant does not have a functioning NarGHI so cannot generate a PMF to the same extent as the wild-type in the presence of nitrate. It is known that *narGHJI* is not expressed in the mutant. Therefore the addition of nitrate to the persister assay does not affect the persister cell formation, with all cells in the Δ*narG* culture remaining in a dormant and persistent state. Cells represented in red – NarGHI active; in yellow – dormant/persistent. Diagram on the previous page. See text for more details.

lites potentiated aminoglycoside activity due to their action, via the glycolytic pathway, increasing PMF generation when in the presence of glucose, mannitol and fructose (Allison *et al.*, 2011). In relation to this study the addition of nitrate to *B. pseudomallei* persister cells resulted in an increase susceptibility of wild-type to ceftazidime, for both log and stationary phase cultures, not seen in the Δ*narG* mutant (Fig. 6.9). The frequency of persister cell formation in *E. coli,* has been demonstrated to reflect differences in wake up kinetics, with those cells in the culture that are rapidly growing exhibiting increased susceptibility to antibiotic treatment (Joers *et al.*, 2010).

It is thought that a proportion of the *B. pseudomallei* population (prior to ceftazidime treatment), entered a dormant/persistent state in both stationary and log phase cultures, with this subpopulation being revealed on the addition of high concentration of ceftazidime. Increase susceptibility of the wild-type to ceftazidime in the presence of nitrate is thought to be due to the generation of a PMF by NarGHI, increasing metabolic activity and resulting in increased killing by ceftazidime and likely reawakening from dormancy (Fig. 6.11). In the absence of nitrate or a functional NarGHI, in the Δ*narG* mutant, *B. pseudomallei* is thought to remain in a persistent/dormant state, more tolerant to antibiotic treatment due to a reduction in metabolic activity. Considering nitrate was only added to the persister cell assay (added the same time as the addition of 400 µg/mL ceftazidime), it is likely that the increase in susceptibility of wild-type persister cells is due to an altered metabolic state of the drug tolerant/persister cells, due to NarGHI, rather than nitrate reducing persister cell numbers. These results indicate that *B. pseudomallei* NarGHI plays a role in antibiotic resistance when in the presence of nitrate.

To support the argument that NarGHI plays a role in antibiotic tolerance, due to its role in the generation of a PMF, the addition of nitrate has been shown to increase susceptibility of both *E. coli* and *P. aeruginosa* biofilms to antimicrobial action (Allison *et al.*, 2011; Borriello *et al.*, 2006). Along with this a recent ceftazidime *B. thailandensis* persister cell transcriptome analysis has revealed an upregulation of those genes required for anaerobic respiration (Table 6.2 – Hemsley *et al.* unpublished data). More recently a low abundance of *E. coli* NarGH has been linked to resistance of multiple different aminoglycosides and cephalosporins including ceftazidime (CAZ), tetracyclin (TET), gentamycin (GEN), and streptomycin (SM) (Ma *et al.*, 2013). In this study *narG* and *narH* mutants were shown to exhibit increased resistance to CAZ, GEN and SM.

Authors speculated that the low abundance of NarGHI resulted in a lower PMF limiting aminoglycoside uptake resulting in an increased antibiotic resistance (Ma *et al.*, 2013) as seen in Allison and colleagues (2011) with metabolite enable potentiation of aminoglycoside activity. Unlike aminoglycosides, ceftazidime acts to inhibit cell wall biosynthesis, so its antibiotic action is unlikely to require increased antibiotic uptake. It is currently unknown why the addition of nitrate increases susceptibility of *B. pseudomallei* to ceftazidime. However it is thought to be due to an increase in PMF generation due to NarGHI activity, considering nitrate addition did not affect the persister frequency in the Δ*narG* mutant.

6.4 Conclusion

This chapter has highlighted a role for NarGHI in pathogenesis of melioidosis. Deletion of *narG* (BPSL2309) resulted in a reduction in motility seen when using rich but not minimal media and caused a significant difference in persister cell susceptibility to ceftazidime when in the presence of nitrate. No difference in virulence or intracellular survival was observed between the Δ*narG* mutant and wild-type *B. pseudomallei* when using *G. mellonella* and J7441.A murine macrophages, indicating anaerobic respiration is not required for survival within these model systems. Work into determine the role of NarGHI in virulence in a murine infection model is still on going.

Chapter 7 – Final discussion and future work

7.1 B. thailandensis *E264 and* B. pseudomallei *K96243 encode a wide range of proteins required for aerobic and anaerobic respiration*

The ability to utilise a range of electron acceptors such as oxygen, nitrate, nitrite and DMSO/TMAO provides facultative anaerobes with a distinct advantage. Bioinformatic analysis identified a range of primary dehydrogenases and terminal oxidases required for aerobic and anaerobic respiration and genes required for molybdopterin biosynthesis in *B. pseudomallei* K96243*, B. thailandensis* E264 and *B. mallei* ATCC 23344 (Table 3.1, 3.2 and 3.3). Differences in the variety and number of aerobic and anaerobic respiratory genes seen between *B. thailandensis, B. pseudomallei* and *B. mallei* is thought to reflect differences the ability for the species to survive within the environment and/or within the host.

B. thailandensis E264, *B. pseudomallei* K96243 and *B. mallei* ATCC 23344 encode a full denitrification pathway, required for utilisation of nitrate or nitrite as alternative terminal electron acceptors. Unlike *B. thailandensis*, both *B. pseudomallei* and *B. mallei* encode a putative DMSO reductase, upregulated during anaerobic growth and within a murine infection model (Kim *et al.*, 2005; Ooi *et al.*, 2013). Preliminary growth analysis indicated *B. pseudomallei* K96243 to respire using DMSO as an electron acceptor and glycerol as an electron donor (Table 5.2). This supports the idea that BPSS2299-2301 encodes a putative DMSO reductase, not found in *B. thailandensis.* Further work in to the characterisation of this gene cluster and determination of its role in virulence could be used to expand what is currently known about respiratory flexibility in *B. pseudomallei* K96243.

Creation of a *B. thailandensis* transposon mutant library identified *moeA1* (BTH_I1704) to be required for anaerobic respiration, NAR activity, biofilm formation, and motility (Andreae *et al.*, 2014). Bioinformatic analysis identified two putative *moeA* gene encoded in both *B. thailandensis* E264 and *B. pseudomallei* K96243 (*moeA1* - BTH_I1704/BPSL2455 and *moeA2* – BTH_I2200/BPSL1479). Only *B. thailandensis moeA1* (BTH_I1704) was expressed under both aerobic and anaerobic conditions (Fig. 4.9). This indicated that *moeA1* is required for ligation of Mo to MPT, whereas *moeA2* is likely to be either redundant in function or expressed under other conditions not tested in this study.

The expression of *E. coli moeA* is molybdate independent and exhibits a low level of transcription under aerobic conditions (Hasona *et al.*, 2001). Expression of *moeA* is enhanced under hypoxic conditions in the presence of nitrate, DMSO and TMAO, linking in with an increased demand for the production of molybdoenzymes required for anaerobic respiration (Hasona *et al.*, 2001). Like *narGHJI,* the expression of *E. coli moeA* is regulated by NarXL in response to nitrate, and Arc and FNR which acts as negative regulators to maintain a basal level of *moeA* expression (Hasona *et al.*, 2001). This pointed towards an intimate link between the expression of *moeA* and NAR, considering both NarXL and FNR are also responsible for controlling the switch from aerobic to anaerobic respiration (Bouchal *et al.*, 2010; Egan & Stewart, 1990; Fink *et al.*, 2007; Stewart, 1993). The transcription of *narGHJI* and *hyc* (formate hydrogenlyase) has also been shown to be dependent on the ModE-molybdate (a repressor of *modABCD*) and MoeA, with a *E. coli moeA modE* double mutant failing to produce either NarGHI or formate hydrogenlyase proteins (Hasona *et al.*, 1998b).

B. thailandensis E264 and *B. pseudomallei* K96243 encode both the NarXL and FNR likely to be required for the regulation of anaerobic respiratory genes. Work into determining the regulatory network required for the expression of *B. thailandensis* and *B. pseudomallei* anaerobic respiratory genes, and potential links between the expression of *moeA* and *narGHJI* could provide interesting avenues of research.

B. thailandensis E264 and *B. pseudomallei* K96243 encode two membrane-bound nitrate reductases; *narGHJI* and *narZYWV*. Deletion of *B. pseudomallei narG* (BPSL2309) prevented anaerobic growth and significantly reduced NAR activity. This confirmed the prediction that *narGHJI* encodes the main NAR required for denitrification (Fig. 5.5 and 5.6), with the second cryptic *narZYWV* likely to play an accessory function similar to that seen in *E. coli* and *Salmonella* (Fig. 3.11).

Different *Mycobacterium* species are known to display varying levels of NAR activity. *M. tuberculosis* is the most efficient denitrifier exhibiting the highest levels of NAR activity, when compared to other *Mycobacterium* species, such as *M. bovis* BCG which displays reduced NAR activity due to a single nucleotide polymorphism within the *narGHJI* gene cluster (Khan & Sarkar, 2012). In relation to this study the accumulation of nitrite was significantly higher in *B. pseudomallei* K96243 cultures (accumulating up to 256 µM NO_2^-) (Fig. 5.6) when compared to *B. thailandensis* E264, which accumulated around 21 µM NO_2^- (Fig. 4.7) (Andreae *et al.*, 2014) after 24 hours aerobic growth. This potentially indicates that *B. pseudomallei* is a more efficient

denitrifier compared to *B. thailandensis.* However, even though the experiments were performed using the same media and time points, *B. pseudomallei* and *B. thailandensis* were cultured slightly differently. For example *B. thailandensis* cultures were grown in 30 mL medium in 250 mL volumetric flasks, and *B. pseudomallei* cultures being grown in 4 mL medium in 25 mL universal tubes. Because of the way each species were cultured it is possible that the *B. thailandensis* cultures were better aerated compared to *B. pseudomallei* cultures, potentially resulting in a reduced expression/activity of *narGHJI*. To determine whether or not the differences in nitrite accumulation seen during aerobic growth are not simply due to the degree of oxygenation of the cultures it would be worth repeating the experiment for both wild-type *B. thailandensis* and *B. pseudomallei,* using the same culture conditions. Further studies using real time PCR could also be used to determine when and to what extent *narGHJI* and *narZYWV* are expressed during aerobic and anaerobic growth.

B. thailandensis E264 and *B. pseudomallei* K96243 are thought to encode two putative copper nitrite reductases, annotated as multicopper oxidase containing proteins. BTH_II0881 and BPSS1487 display structural homology to the *Neisseria* AniA, possessing all key residues for binding to both type I and type II copper ligands and transmembrane helices potentially allowing for it to be bound to the outer-membrane (Fig. 3.4, 3.6 a and 3.7). In comparison the second putative Cu-Nir (BTH_II0944 and BPSS1452) displayed little homology to any published nitrite reductases and several *B. pseudomallei* and *B. mallei* strains possessed an amino acid replacement in a key residue required for copper binding, indicating it might not function as a NIR (Fig. 3.5). Future work into determining whether or not the replacement of the key His residue, predicted to be required for copper binding (seen in *B. pseudomallei* BPSS1452, but not *B. thailandensis* BTH_II0944), alters NIR activity is required to determine the function of BPSS1452. Preliminary work has been conducted by project students under my supervision on the cloning and overexpression of BTH_II0944 and BPSS1452, using a His-tagged protein lacking its signal peptide. This unfortunately has been unsuccessful and only yielded protein in the insoluble fraction (data not shown).

7.2 The Burkholderia *molybdopterin biosynthetic pathway and nitrate reductase plays a role in motility and biofilm formation*

Chronic bacterial infections are often characterised by the formation of biofilms (Costerton *et al.*, 1999), and are known to play a role in virulence in *N. gonorrhoeae* and *P. aeruginosa* (Falsetta *et al.*, 2010; Hassett *et al.*, 2002; Hill *et al.*, 2005). In comparison, the formation of biofilms by *B. pseudomallei* is not associated with infection in BALB/c mice (Taweechaisupapong *et al.*, 2005). Nevertheless the formation of biofilms in *B. pseudomallei* has been implicated in the survival of *B. pseudomallei* within the host. It has been proposed that relapse may be due to a reactivation of *B. pseudomallei* ability to form biofilms, considering it provides the bacteria with a mechanism to resist to antimicrobials (Sawasdidoln *et al.*, 2010). Recent evidence has revealed that the formation of biofilms *in vitro* by primary infecting isolates is associated with patients presenting with relapse of melioidosis (Limmathurotsakul *et al.*, 2014a). The association of biofilm formation with relapse was independent of any other risk factor including choice and length of oral antimicrobial therapy (Limmathurotsakul *et al.*, 2014a).

Biofilms are highly organised structures known to be relatively oxygen and nutrient limiting, and often display increased antibiotic resistance due to low antibiotic penetration or a reduced metabolism (Costerton *et al.*, 1999). Biofilms exhibit a steep oxygen gradient with the substratum being relatively anaerobic, requiring anaerobic respiration, via *narG* or *aniA,* for survival and maintenance of the mature structure (Falsetta *et al.*, 2010; Van Alst *et al.*, 2007). Disruption of the molybdopterin biosynthesis pathway in *B. thailandensis* (CA01) resulted in a reduction in biofilm formation, restored on complementation with pDA-17::BTH_I1704 (Andreae *et al.*, 2014) (Fig. 4.11 and Fig. 4.16). In *P. aeruginosa* disruption of *narGH* resulted in a thinner biofilm structure to the wild-type, attributed by the inability for the mutant to dissimilate nitrate (Van Alst *et al.*, 2007). It is tempting to speculate that due to the inability of *B. thailandensis* CA01 to reduce nitrate, the reduction in biofilm formation was due to the lack of NAR activity. To test this the biofilm assay was carried out on wild-type *B. pseudomallei* and the Δ*narG* mutant, using a similar assay to that used with *B. thailandensis,* modified only by use of a peg plate rather than a 96 well micro-titre plate. Unfortunately, no biofilm was detected on the pegs after a three day incubation period (data not shown). It is possible that the biofilms ‘fell off’ the pegs

during incubation at 37 ^{o}C. Shorter incubation periods and further optimisation of the biofilm assay under containment level three conditions will be required to determine whether or not *B. pseudomallei* NarGHI plays a role in biofilm formation.

The formation of biofilms is dependent on bacterial motility, requiring flagella and type IV pili for initial attachment and dispersal (Pratt & Kolter, 1998). Flagella are required for virulence, adhesion, virulence factor secretion and modulation of the host immune response (Adler *et al.*, 2009; Chua *et al.*, 2003; Duan *et al.*, 2012a; Inglis *et al.*, 2003). Recently it has been shown that *B. thailandensis* (strain CDC2721121) alters the transcription of flagella and chemotactic genes in response to temperature and oxygen status, with a down-regulation seen in response to 37 ^{o}C and anoxia (Peano *et al.*, 2014). It was reasoned that because *B. thailandensis* CA01 displayed a biofilm defect it was possible that the reduction in biofilm formation was due to a reduction in motility as well as an inability to respire anaerobically. This prediction was confirmed using a *B. pseudomallei* Δ*narG* deletion mutant, which displayed a significant reduction in motility when using rich media (NB or L-broth), but not minimal media (Fig. 6.3 and 6.4). Unfortunately complementation of Δ*narG* with pBH01 could not restore the motility defect seen when using LB medium solidified with 0.3 % bacteriological agar (see Chapter 8 - Appendix Fig. 8.3).

Addition of nitrate or nitrite caused a significant decrease in motility for wild-type *B. pseudomallei* K96243 but did not affect the motility defect seen for the Δ*narG* mutant in rich media (LB or nutrient broth) (Fig 6.3 and 6.4 a). In comparison, in M9 minimal media the Δ*narG* mutant displayed comparable wild-type motility levels, and only the addition of nitrite caused reduction in the mutant's motility (Fig. 6.4 b). The lack of a response to nitrate addition in the *B. pseudomallei* Δ*narG* mutant in M9 minimal media indicates the potential need for a functioning NarGHI and anaerobic electron transport chain in the aerotaxic/chemotaxic response to nitrate. It is likely that the presence of nitrite, either due to direct addition to the motility media or its reduction from nitrate by NarGHI, is the cause of the decrease in motility seen for *B. pseudomallei*. Further work into determining whether nitrate or nitrite affect *B. pseudomallei* chemotaxis/aerotaxis or act as chemorepellents are required to confirm whether the predicted hypotheses are correct. The use of *B. pseudomallei* flagella and chemotaxis mutants and mutant complementation would help to further explain the results seen in these studies.

In comparison to what was seen for *B. pseudomallei* the addition of nitrate to *B. thailandensis* motility media did not significantly affect either wild-type of CA01 motility (Chapter 8 – Appendix Fig. 8.2). Of note the motility defect seen with CA01 was not as severe as that seen with *B. pseudomallei* Δ*narG* when using rich media. These differences could be due to species differences or potentially differences in NAR activity exhibited by *B. thailandensis* and *B. pseudomallei.*

Initial anaerobic studies using LB agar plates pointed towards a successful restoration of anaerobic growth for Δ*narG* complemented with the BPSL2309-2312 operon containing its native promoter. However further studies did not show an anaerobic growth restoration when using M9 minimal media supplemented with nitrate (Fig. 5.13). Further work complementation of Δ*narG* and repetition of the motility assays will be required in order to confirm that the significant reduction in motility seen for the Δ*narG* mutant is due to the lack of a functional NarGHI.

7.3 B. thailandensis *and* B. pseudomallei *can enter a dormant/non-replicating persistent state, affecting antibiotic treatment and persister cell formation*

Understanding the mechanisms of bacterial persistence has been the subject of much discussion, due to the implications it has on the treatment of chronic and latent infections. *B. pseudomallei,* like *M. tuberculosis,* is known to cause latent infections, with both bacterial species surviving within the host for extended periods of time.

B. pseudomallei genome is known to remain relatively stable during infection, and a relapse of infection is often due to the same strain rather than reinfection (Currie *et al.*, 2000a; Maharjan *et al.*, 2005; Vadivelu *et al.*, 1998). However, a recent within-host evolution analysis of *B. pseudomallei* 12 year chronic carriage has revealed a substantial genome wide reduction and positive selection on genes required for antibiotic resistance and evasion of the immune response (Price *et al.*, 2013). *B. pseudomallei* within-host reductive evolution resulted a loss of non-essential genes, not required for persistence within the host. A number of *B. pseudomallei* genes lost during the 12 year chronic carriage have also been lost during the evolution of *B. mallei,* including the *narZYWV* operon, type III secretion system and a number of others encoded on chromosome 2 (Price *et al.*, 2013). The deleted genes are mainly

thought to be required for secondary metabolite pathways, pathogenesis and those required for environmental survival.

Both tuberculosis and melioidosis infections are known to present with granulomas, likely to be limiting in oxygen. *M. tuberculosis* forms granulomas within the lungs (Saunders & Britton, 2007), whereas *B. pseudomallei* forms granulomas within various organs, including the lungs, during both mice and human infections (Conejero *et al.*, 2011; Currie *et al.*, 2010a; Limmathurotsakul & Peacock, 2011). Currently little is known about the mechanisms in which *B. pseudomallei* enters this persistent state, however much work has been done to understand non-replicating persistence in *Mycobacterium* species. Due to the similarities in disease progression of both chronic melioidosis and tuberculosis it is likely that the mechanisms of persistence used by *M. tuberculosis* are similar to what may be used by *B. pseudomallei.*

Entry into a non-replicating persistent (NRP) state is thought to have implications in treatment of chronic or latent infections. *M. tuberculosis* has multiple mechanisms to ensure its survival and persistence within the host. These include *pcaA,* which aids in resistance to RNIs and ROS (Honer zu Bentrup & Russell, 2001), isocitrate lyase (McKinney *et al.*, 2000), stress related proteins, metabolic enzymes (Honer zu Bentrup & Russell, 2001), and genes involved in the enduring hypoxic response (Rustad *et al.*, 2008).

Isocitrate lyase is an enzyme in the glyoxylate shunt pathway, and has been shown to be required for persistence, and virulence in various intracellular pathogenic bacteria, such as *M, tuberculosis, Salmonella, P. aeruginosa* and *B. pseudomallei* (Fang *et al.*, 2005; Lindsey *et al.*, 2008; van Schaik *et al.*, 2009). Isocitrate lyase is required for intracellular survival and persistence, with the majority of bacteria entering a vegetative state, not undergoing replication (Honer zu Bentrup & Russell, 2001). Along with isocitrate lyase, NAR and the nitrate-nitrite exclusion protein (NarK) have been implicated in persistence and virulence of *Mycobacterium* species (Boshoff & Barry, 2005; Honer zu Bentrup & Russell, 2001; Munoz-Elias & McKinney, 2005; Weber *et al.*, 2000).

The ability to utilise various carbon sources, via the gluconeogenesis pathway, glycolysis, fermentation, TCA cycle and the glyoxylate shunt are important for

intracellular survival and virulence (Eisenreich *et al.*, 2010). Genes for β-oxidation pathway and those for alternative respiratory pathways, including fumarate reductase and nitrate reductase, are induced in *M. tuberculosis* surviving within macrophages. During microaerophilic growth, it is speculated that nitrate reductase is required to restore redox balance intracellularly during growth on fatty acids (Boshoff & Barry, 2005).

Exposure to low oxygen conditions and nitric oxide signals the induction of the dormancy regulon, causing *M. tuberculosis* to enter a NRP and latent state (Boshoff & Barry, 2005; Voskuil *et al.*, 2003). The dormancy regulon is known to involve the induction of 48 genes, expressing similar genes to that seen during NRP-1, such as the narK2-narX operon and the cytochrome *bd* oxidase (Boshoff & Barry, 2005). A study has shown a proportion of internalised *S. typhimurium* cells to enter a non-replicating but viable state within macrophages, highlighting the importance of bacterial dormancy in intracellular survival as a potential reservoir for persistent bacteria (Helaine *et al.*, 2010). This hypothesis has recently been proven with non-replicating persisters seen in mouse organs following infection and internalised within macrophages (Helaine *et al.*, 2014). Internalisation was the only prerequisite for macrophage induced persister cell formation, with macrophage-induced persisters exhibiting tolerance to a range of antibiotics (Helaine *et al.*, 2014).

Development of the Wayne's model enabled much study to be done on latency and persistence *in vitro.* The Wayne's model of hypoxic shift down allows for the gradual acclimatisation to anaerobic environment; characterised by two stages NRP; NRP-1 and NRP-2 (Wayne & Hayes, 1996). A reduction in oxygen concentration and exposure to non-toxic concentrations of nitric oxide are known to trigger entry into dormancy/NRP, resulting in the induction of the dormancy regulon (DosR/DosS) (Dick *et al.*, 1998; Voskuil *et al.*, 2003). Cells that have entered NRP/dormancy can be reawakened on exposure to oxygen rich medium, triggering cell division and replication. *M. tuberculosis* DosR is essential for long term survival during anaerobic dormancy and is known to be required for the shift away from aerobic respiration and the maintenance of a redox balance and energy levels (Leistikow *et al.*, 2010).

The Wayne's model was used to study anaerobic adaptation and antibiotic tolerance in *B. pseudomallei* (Hamad *et al.*, 2011). Initial growth of *B. pseudomallei*

seen in this model was likely due to the presence of dissolved oxygen in the culture medium, the gradual depletion of which resulted in a cessation of growth and likely entry in to NRP-2 (Hamad *et al.*, 2011), as seen with *M. tuberculosis. B. pseudomallei* was shown to enter a NRP surviving for up to one year under anaerobic conditions, with no change in survival kinetics seen after one month (Hamad *et al.*, 2011). Like *B. pseudomallei,* a subpopulation of *B. thailandensis* E264 was able to enter a NRP state, when grown anaerobically in the presence or absence of an alternative terminal electron acceptor (Fig. 4.10). This subpopulation of *B. thailandensis* anaerobic dormant cells could be reawakened on transfer to fresh media and growth aerobically or anaerobically in the presence of nitrate. Results of this study and Hamad *et al.* (2011) indicate that *Burkholderia* is likely to enter a dormant/NRP state due to the presence of an oxygen limiting environment, which is not affected by the ability to respire anaerobically. *B. pseudomallei* and *B. thailandensis,* like *M. tuberculosis,* may encode a yet unidentified dormancy regulon that may aid in adaptation and maintenance of a NRP state within an anaerobic environment.

The transcriptional response of *B. pseudomallei* to hypoxic conditions (grown for 4 hours in the shaking Wayne's model) has been determined and shown an induction of genes for arginine and pyruvate fermentation (arginine deiminase pathway), electron transport (cytochrome *bd* oxidase, ubiquinol oxidase and various *c*-type cytochromes and *narZ*), ATP synthase, motility and chemotaxis proteins, and those genes required for stress-related functions (Hamad *et al.*, 2011). Genes required for molybdopterin biosynthesis were also induced under hypoxic conditions. No induction of genes required for denitrification were seen in this study, which is unsurprising considering *B. pseudomallei* was not respiring via nitrate respiration under the conditions tested.

Entry of *B. pseudomallei* into a NRP state, after one-months incubation under anaerobic conditions, resulted in an increased tolerance to multiple different antimicrobials, such as ceftazidime (targeting cell wall synthesis), trimethoprim-sulfamethoxazole (targets DNA synthesis), chloramphenicol (targeting protein synthesis) and metronidazole which acts specifically on anaerobic bacteria (Hamad *et al.*, 2011). It is possible that this increased tolerance to antibiotic action is due to a lack of respiratory action and lowered metabolic activity leading to the formation of persister cells.

Persister cells are a sub-population that exhibit a lowered metabolic activity and increased tolerance but not resistance to antibiotics, later switching back to a susceptible form on transfer to fresh media (Lewis, 2010). The formation of persister cells is thought to be part of a bacterial population's heterogeneity, aiding survival in a changing environment (Balaban *et al.*, 2004). Persister cells are thought to be dormant cells, exhibiting a distinct physiological state to the rest of a bacterial culture with a significant reduction in protein and ATP synthesis (Kwan *et al.*, 2013; Lewis, 2010; Shah *et al.*, 2006). Although cells exhibiting a reduced replication rate and low metabolic activity (considered to be metabolically dormant) are more likely to form persisters, a proportion displaying high reductase activity (more metabolically active) can still form persisters. This indicated that dormancy is not necessary or sufficient for persister cell formation (Orman & Brynildsen, 2013).

A recent *Burkholderia* persister cell transcriptome, revealed some similarities between those genes induced during hypoxia and in persister cells, both showing an induction of genes for the arginine deiminase pathway and stress response and a decrease in expression of genes required for cell division and DNA replication (Hemsley *et al.* unpublished results). In comparison to the genes induced during hypoxia *Burkholderia* ceftazidime persisters showed an upregulation of genes required for denitrification (*narGHJI, aniA, nos* and *nor*) (Table 6.2). Similar to the *Burkholderia* persister transcriptome, *Mycobacteria* persister cells exhibit a down-regulation of genes required for energy metabolism (e.g. genes require for glycolysis, respiration and electron transport) and biosynthesis pathways, consistent with entry into dormancy, and the induction of several toxin-antitoxin systems (Keren *et al.*, 2011).

The induction of genes required for denitrification in *Burkholderia* persister cells (Hemsley *et al.* unpublished data), implicated anaerobic respiration, and NarGHI in persister cell formation. Because of this it was postulated that deletion of *narG* in *B. pseudomallei* would affect persister cell formation. To test this both wild-type *B. pseudomallei* and Δ*narG* mutant log and stationary phase cultures were treated with 400 µg/mL ceftazidime, in L-broth supplemented with or without nitrate. The persister assay was performed under conditions thought to mimic oxygen limiting conditions seen *in vivo*. Addition of nitrate to wild-type *B. pseudomallei* persister cells resulted in an increased susceptibility to ceftazidime for both log and stationary phase cultures

(Fig. 6.9). The increased susceptibility of wild-type *B. pseudomallei* cells to ceftazidime on nitrate addition was not seen in the Δ*narG* mutant. A similar result was seen in a preliminary study with wild-type *B. thailandensis* and CA01 persister cells, where nitrate addition resulted in a decrease in persister frequency for wild-type but not CA01. In comparison the addition of nitrite to either *B. thailandensis* or CA01 persister cells did not significantly affect persister frequency, with the same number forming persister cells when incubated with nitrite as that seen when in L-broth alone (see Chapter 8 Appendix - Fig. 8.4).

It is thought that the increase in susceptibility on the addition of nitrate is due to the generation of a PMF by NarGHI, resulting in an increase in metabolic activity and sensitivity to ceftazidime. Previous studies have implicated the generation of PMF, by addition of metabolites such as nitrate, in alteration of persister frequencies and antibiotic susceptibility (Allison *et al.*, 2011; Borriello *et al.*, 2006). Recently a low abundance of NarGH in *E. coli* has been linked to aminoglycoside and cephalosporin (including ceftazidime) resistance, thought to be due to a lowered PMF (Ma *et al.*, 2013). In support of the argument that an increase in susceptibility of persister cells to ceftazidime is due to the generation of a PMF, increased aeration during the persister assay resulted in a decrease *B. thailandensis* in persister frequency (Hemsley *et al.,* unpublished data). The results together suggest that activation of an electron transport, either via denitrification or oxidative phosphorylation, renders *Burkholderia* susceptible to ceftazidime action. Therefore one could argue that the absence of a functioning respiratory system (e.g. in the Δ*narG* mutant), is advantageous for the maintenance (but not generation) of persister cells, as it allows them to remain in a dormant state and thus remain tolerant to ceftazidime action. The increase in susceptibility of *Burkholderia* persister cells seen in when in the presence of oxygen or nitrate could have implications on treatment of chronic melioidosis infections, through the elevation of respiratory activity (Hemsley *et al.* unpublished work). Further work into characterisation of the role of nitrate and *B. pseudomallei* NarGHI in persister cell formation in response to other antibiotics (e.g. metronidazole and ciprofloxacin) would help aid in the understanding of the role of anaerobic respiration in persister cells.

A screening system based on determining nitrate reductase activity (using the Griess reaction) has been used to identify dormant and latent bacilli of tuberculosis

infected patients, considering NarGHI is induced during dormancy in *Mycobacterium* (Khan & Sarkar, 2008). Detection of NAR activity has been shown to be a robust and inexpensive assay to determine *Mycobacterium* sensitivity to antibiotics (Coban *et al.*, 2014). For example those *Mycobacterium* strains exhibiting NAR activity were associated with resistance to rifampicin and isoniazid, with susceptible strains losing the capacity to reduce nitrate (Martin *et al.*, 2008). Whether or not the NarGHI in *B. pseudomallei* is induced during dormancy or whether it could be used as an assay for antibiotic resistance remains to be determined. Further work into determining whether NarGHI or NarK is expressed during dormancy could provide interesting avenues for treatment of melioidosis.

7.4 Role of nitrate reductase and anaerobic adaptation in pathogenesis

Use of *G. mellonella* larvae infection model has shown no role for the molybdopterin biosynthetic pathway or nitrate reductase in virulence of either *B. thailandensis* (Andreae et al., 2014) or *B. pseudomallei.* This may be due to the fact that *G. mellonella* is not an appropriate model for determination of the role of anaerobic respiration in virulence considering it is quite likely that the larvae are not limiting in oxygen due to their size. Use of a different infection model, e.g. a murine infection model, may help better determine a role for NarGHI in pathogenesis of melioidosis.

A mouse infection with tuberculosis never truly gives a latent stage of infection as bacilli have been shown to be continuously replicating, and granulomas have been shown, in comparison to other mammalian and non-human primate models, not to be hypoxic (Aly *et al.*, 2006; Rustad *et al.*, 2009; Tsai *et al.*, 2006). Induction of genes required for the enduring hypoxic response along with the DosR regulon are likely to be required during latent and chronic infections, ensuring the maintenance of viable cells in NRP, and survival during respiratory, nitrosative or redox stress (Rustad *et al.*, 2009). Whether or not similar mechanisms exist in *B. pseudomallei* is currently not known but research into this may provide a better understanding of how *B. pseudomallei* remains latent within the body prior to causing a relapse of infection.

Change in the oxygen status of tuberculosis infected organs is thought to play a role in relapse of infection (Rustad *et al.*, 2009). This change in oxygen status of infected organs, in tuberculosis patients, may implicate the induction of respiratory

pathways in relapse of infection. Relapse cases of melioidosis normally present with pneumonia, liver and splenic abscesses (Limmathurotsakul *et al.*, 2009). The idea that a change in oxygen status of infected organs prior to relapse in tuberculosis potentially could be applied to relapse cases of melioidosis. Perhaps this idea also correlates with the observation that increased aeration or nitrate addition to *Burkholderia* persister cells caused an increased susceptibility to antibiotic action, thought to be due to the induction or respiration/electron transport pathway.

The *B. thailandensis* clinical isolate CDC2721121, encoding a *B. pseudomallei* CPS-like cluster (Deshazer, 2007), has recently been shown to produce exopolysaccharides (EPS) and lipopolysaccharides (LPS) in response to oxygen limitation (Peano *et al.*, 2014). The production of EPS/LPS in response to anaerobic conditions is thought to have implications on virulence of *B. thailandensis* CDC2772112. Growth under oxygen limiting conditions resulted in increased resistance to phagocytosis and a strong induction of an inflammatory cytokine response by murine macrophages (Peano *et al.*, 2014).

The role of nitrate reductase in virulence has been well described for *Mycobacterium* species, seeming to vary depending on tissue specificity, infection model used, level of oxygen in the lungs and immune status of the host (Aly *et al.*, 2006; Fritz *et al.*, 2002; Weber *et al.*, 2000). Preliminary infection studies comparing wild-type *B. pseudomallei* (K96243) and the Δ*narG*, performed in collaboration with the London School of Hygiene & Tropical Medicine, have been conducted using C56BL/6 mice. Unfortunately, due to differences in cell counts for both the acute and chronic infection model, no conclusions can currently be drawn from the current set so the role of *B. pseudomallei* in NarGHI in virulence in this model is currently unknown (Fig. 6.8). However, disruption of the molybdopterin pathway in *B. pseudomallei* (strain E8) has been shown to cause a reduction in NAR activity, anaerobic growth, motility, and cause a significant reduction in virulence in chronic murine infection model (C56BL/6) (personal communication with Professor Ivo Steinmetz's group; unpublished results). Disruption of the molybdopterin biosynthetic pathway although affecting virulence but did not cause a reduction in cellular invasion or intracellular survival (personal communication with Professor Ivo Steinmetz). The results obtained by Professor Ivo Steinmetz group correspond with the phenotype exhibited by my *B.*

pseudomallei Δ*narG* mutant and highlight a potential role for molybdoproteins and nitrate reductase in virulence.

It is currently unclear where *B. pseudomallei* resides during chronic infection. However, a recent study has shown the GI tract to be the primary site of colonisation during a persistent infection (Goodyear *et al.*, 2012). The GI tract is known to be primarily colonised by anaerobic bacteria and both nitrate reductase and fumarate reductase have been shown to provide *E. coli* with a distinct colonisation advantage (Jones *et al.*, 2011). Considering the GI tract is likely to be limiting in oxygen it is possible that the ability for *B. pseudomallei* to survive and replicate under anaerobic conditions will provide it with a survival advantage enabling colonisation and survival within the GI tract.

7.5 Concluding comments

Before completion of my thesis little was known about the respiratory flexibility exhibited by *B. thailandensis* and *B. pseudomallei,* and nothing was known about the role anaerobic respiratory proteins would play in the pathogenesis of melioidosis. This study has highlighted the importance of NarGHI in anaerobic respiration, motility, biofilm formation and persister cell formation. Further work into characterisation of other anaerobic respiratory proteins involvement in survival and virulence would be advantageous to further understand their implications in the pathogenesis of melioidosis.

Chapter 8 – Appendix

8.1 - Figures

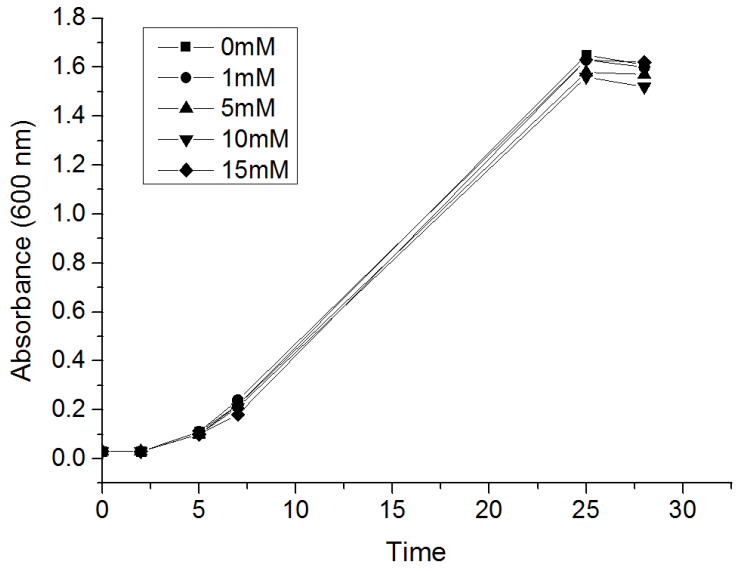

Figure 8.1 - Aerobic growth of *B. thailandensis* E264 in the presence of sodium tungstate. Aerobic growth of *B. thailandensis* in M9 minimal media supplemented with 20 mM sodium succinate and 20 mM sodium nitrate and varying concentrations of sodium tungstate (Na_2WO_4) - 0 mM (squares), 1 mM (circles), 5 mM (triangles) 10 mM (inverted pyramid). Addition of sodium tungstate did not affect aerobic growth of *B. thailandensis.* Results are of one biological replicate.

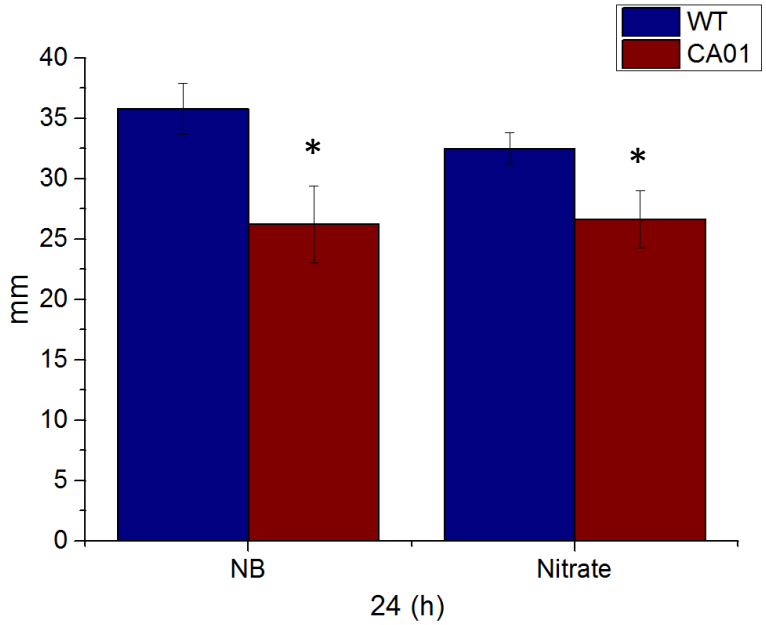

Figure 8.2 - *B. thailandensis* and CA01 motility is not significantly altered by the addition of nitrate. Motility assays carried out on 0.3 % nutrient broth agar plates, supplemented with 0.5 % glucose, in the presence or absence of 20 mM sodium nitrate. Addition of nitrate has no significant effect on the degree of swimming motility for either *B. thailandensis* (blue) or CA01 (red) after 24 hour incubation at 37 ^{o}C. The mutant still shows a reduction in motility when compared to the wild-type. Asterisk indicate significant p-value of ≥ 0.01 (T-test assuming; equal variance). Three independent biological replicates each with three technical replicates. Error bars ± SD.

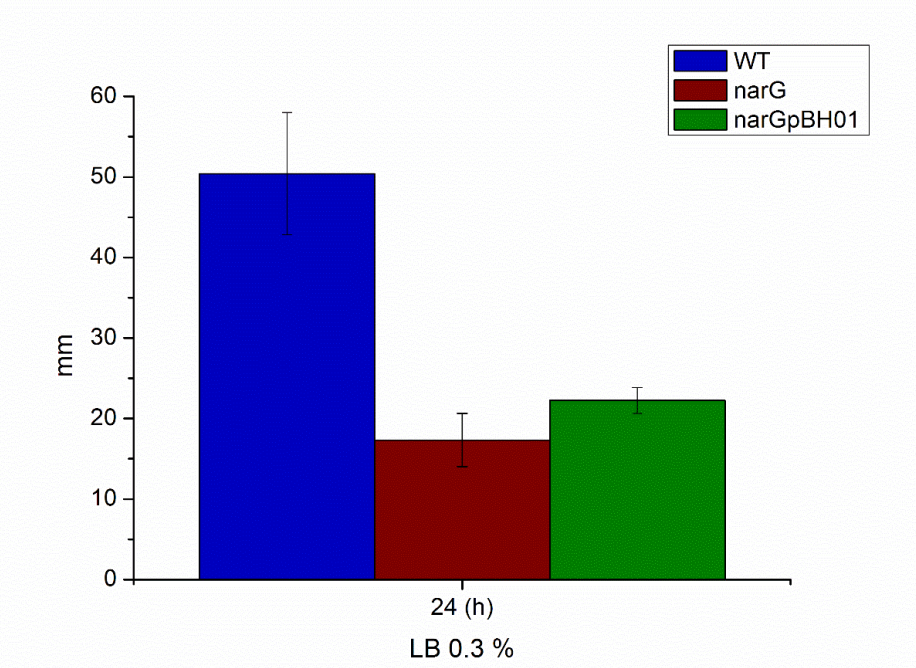

Figure 8.3 – Preliminary motility studies with *B. pseudomallei* Δ*narG*::pBHO1. Wild-type *B. pseudomallei* (blue), the Δ*narG* mutant (red) and mutant complement Δ*narG*::pBH01 (green) cultures were grown overnight in L-broth prior to standardisation and inoculation into LB agar plates solidified with 0.3 % bacteriological agar. Chloramphenicol (50 µg/mL) was added to both the complement overnight cultures and the motility agar plates in the hopes of maintaining selection of pBH01. Results are the average of two biological replicates, each with three technical replicates. Error bars ± SD.

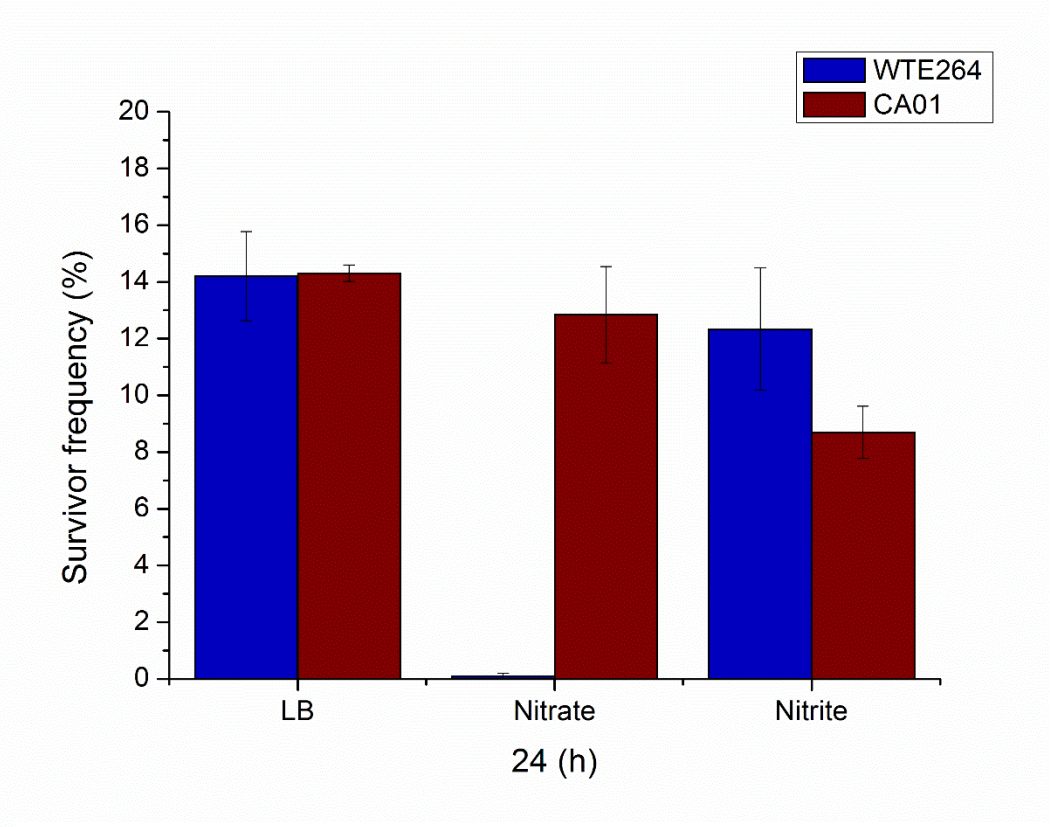

Figure 8.4 – Addition of nitrate, but not nitrite, significantly increases *B. thailandensis* E264 persister cell susceptibility to ceftazidime. Data is the result of a preliminary persister cell assay performed on wild-type *B. thailandensis* (blue) and the molybdopterin biosynthesis mutant (CA01 - red). Wild-type *B. thailandensis* and CA01 (*moeA*1 - transposon mutant) were grown aerobically overnight prior to standardisation and treatment with 400 µg/mL ceftazidime. The persister cell assay was performed statically in L-broth supplemented with either 20 mM sodium nitrate or 5 mM sodium nitrite. Results are the average of two biological replicates, each with three technical replicates. Error bars ± SD.

Persister frequency seen here correlates with what has been seen with *B. pseudomallei* (see Chapter 6), but is significantly higher (10 % rather than 1 %) then what has been seen in other studies (data not shown). Addition of nitrate significantly reduced persister frequency in the wild-type but not the mutant, which is unable to utilise nitrate as an alternative terminal electron acceptor. Addition of nitrite to the persister cell study did not affect the persister cell frequencies for either the wild-type or the mutant, likely because nitrite is not as efficient as nitrate at generating a PMF under oxygen limiting conditions. Results correlate with what was seen for *B. pseudomallei.*

Table 8.1 – Preliminary bioinformatic analysis on the identification of putative *c*-type cytochromes and cytochrome *c* family proteins predicted to be required for electron transport in *B. thailandensis* and *B. pseudomallei*

Annotation[a]	**Gene ID**	
	***B. thailandensis* (E264)**	***B. pseudomallei* (K96243)**
Chromosome 1		
Cytochrome b_{561}	BTH_I0073	BPSL0072
	BTH_I1271	BPSL2876
Cytochrome *c* family protein	BTH_I0608	BPSL0696
	BTH_I0826	BPSL0968
	BTH_I0967	BPSL1100
	BTH_I2318	BPSL1600
	BTH_I2873	BPSL1261
	BTH_I2877	BPSL1257
	BTH_I3145	BPSL3271
Putative cytochrome c_4	BTH_I0609	BPSL0697
	BTH_I2878	BPSL1256
Putative cytochrome c_5	BTH_I3261	BPSL3354
Cytochrome *c*	BTH_I0966	BPSL1099
		BPSL3181
Chromosome 2		
Cytochrome b_{561}, putative	BTH_II0636	BPSS1744
	BTH_I1084	BPSS1340
Cytochrome *c* family protein	BTH_II0457	-[b]
	BTH_II0652	BPSS1729
	BTH_II1414	BPSS0977
	BTH_II1779	-
Cytochrome *c*	BTH_II0653	BPSS1729
	BTH_II1778	-

Table shows results of a preliminary bioinformatic analysis identifying putative *c*-type cytochromes and cytochrome family proteins predicted to be required for electron transport in *B. thailandensis* (E264) and the gene orthologs in *B. pseudomallei* (K96243).

[a] Correspond to the *B. thailandensis* gene annotation

[b] Ortholog not identified

Information from genome search only using NCBI and K.E.G.G.

8.2 – Growth medium and Buffers

LB media

10 g/L - Bacto-Tryptone

5 g/L - Bacto-Yeast extract

5 g/L – Sodium chloride (NaCl)

Add 1.5 % Bacteriological Agar No. 2 when required

Autoclave at 121 ^{o}C for 20 minutes

SOB media

20 g/L - Bacto-Tryptone

5 g/L - Bacto-Yeast extract

0.58 g/L - NaCl (anhydrous)

0.1875 g/L – Potassium chloride (KCl) (anhydrous)

2 g/L – Magnesium chloride hexahydrate ($MgCl_2.6H_20$)

2.5 g/L – Magnesium sulfate heptahydrate ($MgSO_4.7H_20$)

Autoclave at 121 ^{o}C for 20 minutes

Nutrient broth

1 g/L – D-glucose

15 g/L – Peptone

6 g/L – NaCl

3 g/L – Yeast extract

M9 5x Salts

85.5 g/L – Disodium phosphate anhydrous ($Na_2HPO_4.12H_2O$)

15 g/L – Potassium phosphate monobasic (KH_2PO_4)

2.5 g/L - NaCl

5 g/L – Ammonium chloride (NH_4Cl)

Make up to 1 L using ddH_2O (distilled water) and autoclave at 121 ^oC for 20 minutes

TFB1 per 100mL

0.25 g - Sodium acetate ($C_2H_3O_2Na$)

0.14 g – Calcium chloride ($CaCl_2$)

0.99 g – Manganese chloride ($MnCl_2$)

1.21 g – Rubidium chloride ($RbCl_2$)

15 mL - Glycerol

pH to 5.8 using 1 M acetic acid and autoclave

Store at 4 ^oC

M9 minimal media

390 mL – Distilled water (ddH_2O)

100 mL – 5 x M9 Salts

Autoclave at 121 ^oC for 20 minutes, then add;

1 mL – 1 M Magnesium sulfate ($MgSO_4$) to give a 2 mM final concentration

50 µL – 1 M $CaCl_2$ to give a 0.1 mM final concentration

TFB2 per 100 mL

1 mL – MOPs (1 M stock)

1.07 g – $CaCl_2$

0.12 g – $RbCl_2$

15 mL - Glycerol

-pH to 6.5 using 1 M KOH and autoclave

-Stored at 4 ^oC

Phosphate buffer –pH 7.5 (200mL)

A = 0.2 M KH_2PO_4

B = 0.2 M K_2HPO_4

Mix A (16 mL) and B (84 mL) together in the appropriate volumes and dilute to 200 mL with ddH_2O, adjust pH to 7.5 and autoclave at 121 ^oC for 20 minutes.

Motility media

NBA 0.3 %

400 mL - Nutrient broth

0.5 % (w/v) – Glucose

0.3 % - Bacteriological Agar

LB agar 0.3 %

400 mL – Luria Bertani broth

0.3 % - Bacteriological agar No. 2

M9 minimal media 0.3 %

390 mL – ddH_2O

100 mL – 5x M9 Salts

20 mM – Sodium succinate

0.3 % - Bacteriological agar No. 2

Motility agar media autoclaved at 121 ^oC for 20 minutes

20 mL 0.3 % agar used per plate

Ensure plates are dry before use.

Antibiotic stocks

100 mg/mL – Ampicillin – dissolved in water

100 mg/mL – Gentamicin sulfate – dissolved in water

50 mg/mL – Chloramphenicol – dissolved in 70 % ethanol

50 mg/mL – Tetracyclin – dissolved in 70 % ethanol

50 mg/mL – Kanamycin sulfate – dissolved in water

50 mg/mL – Trimethoprim – dissolved in 50 % DMSO

10 mg/mL – Ceftazidime hydrate – dissolved in 0.1 M NaOH

10 mg/mL – Ciprofloxacin – dissolved in 0.1 M NaOH

References

Abaibou, H., Pommier, J., Benoit, S., Giordano, G. & Mandrand-Berthelot, M. A. (1995). Expression and characterization of the *Escherichia coli fdo* locus and a possible physiological role for aerobic formate dehydrogenase. *J Bacteriol* **177**, 7141-7149.

Abraham, Z. H., Lowe, D. J. & Smith, B. E. (1993). Purification and characterization of the dissimilatory nitrite reductase from *Alcaligenes xylosoxidans* subsp. *xylosoxidans* (N.C.I.M.B. 11015): evidence for the presence of both type 1 and type 2 copper centres. *Biochem J* **295 (Pt 2)**, 587-593.

Adler, N. R., Govan, B., Cullinane, M., Harper, M., Adler, B. & Boyce, J. D. (2009). The molecular and cellular basis of pathogenesis in melioidosis: how does *Burkholderia pseudomallei* cause disease? *FEMS Microbiol Rev* **33**, 1079-1099.

Adman, E. T., Godden, J. W. & Turley, S. (1995). The structure of copper-nitrite reductase from *Achromobacter cycloclastes* at five pH values, with NO_2^- bound and with type II copper depleted. *J Biol Chem* **270**, 27458-27474.

Ahmed, K., Enciso, H. D., Masaki, H., Tao, M., Omori, A., Tharavichikul, P. & Nagatake, T. (1999). Attachment of *Burkholderia pseudomallei* to pharyngeal epithelial cells: a highly pathogenic bacteria with low attachment ability. *Am J Trop Med Hyg* **60**, 90-93.

Allison, K. R., Brynildsen, M. P. & Collins, J. J. (2011). Metabolite-enabled eradication of bacterial persisters by aminoglycosides. *Nature* **473**, 216-220.

Aly, S., Wagner, K., Keller, C., Malm, S., Malzan, A., Brandau, S., Bange, F. C. & Ehlers, S. (2006). Oxygen status of lung granulomas in *Mycobacterium tuberculosis*-infected mice. *J Pathol* **210**, 298-305.

Anand, R. D., Sertil, O. & Lowry, C. V. (2004). Restriction digestion monitors facilitate plasmid construction and PCR cloning. *Biotechniques* **36**, 982-985.

Andreae, C. A., Titball, R. W. & Butler, C. S. (2014). Influence of the molybdenum cofactor biosynthesis on anaerobic respiration, biofilm formation and motility in *Burkholderia thailandensis*. *Res Microbiol* **165**, 41-49.

Antonyuk, S. V., Han, C., Eady, R. R. & Hasnain, S. S. (2013). Structures of protein-protein complexes involved in electron transfer. *Nature* **496**, 123-126.

Arjcharoen, S., Wikraiphat, C., Pudla, M., Limposuwan, K., Woods, D. E., Sirisinha, S. & Utaisincharoen, P. (2007). Fate of a *Burkholderia pseudomallei* lipopolysaccharide mutant in the mouse macrophage cell line RAW 264.7: possible role for the O-antigenic polysaccharide moiety of lipopolysaccharide in internalization and intracellular survival. *Infect Immun* **75**, 4298-4304.

Arnoux, P., Sabaty, M., Alric, J., Frangioni, B., Guigliarelli, B., Adriano, J. M. & Pignol, D. (2003). Structural and redox plasticity in the heterodimeric periplasmic nitrate reductase. *Nat Struct Biol* **10**, 928-934.

Ashdown, L. R. & Koehler, J. M. (1990). Production of hemolysin and other extracellular enzymes by clinical isolates of *Pseudomonas pseudomallei*. *J Clin Microbiol* **28**, 2331-2334.

Baker, S. C., Saunders, N. F., Willis, A. C., Ferguson, S. J., Hajdu, J. & Fulop, V. (1997). Cytochrome cd_1 structure: unusual haem environments in a nitrite reductase and analysis of factors contributing to beta-propeller folds. *J Mol Biol* **269**, 440-455.

Balaban, N. Q., Merrin, J., Chait, R., Kowalik, L. & Leibler, S. (2004). Bacterial persistence as a phenotypic switch. *Science* **305**, 1622-1625.

Baltes, N., Hennig-Pauka, I., Jacobsen, I., Gruber, A. D. & Gerlach, G. F. (2003). Identification of dimethyl sulfoxide reductase in *Actinobacillus pleuropneumoniae* and its role in infection. *Infect Immun* **71**, 6784-6792.

Baltes, N., N'Diaye, M., Jacobsen, I. D., Maas, A., Buettner, F. F. & Gerlach, G. F. (2005). Deletion of the anaerobic regulator HlyX causes reduced colonization and persistence of *Actinobacillus pleuropneumoniae* in the porcine respiratory tract. *Infect Immun* **73**, 4614-4619.

Bamford, V. A., Angove, H. C., Seward, H. E., Thomson, A. J., Cole, J. A., Butt, J. N., Hemmings, A. M. & Richardson, D. J. (2002). Structure and spectroscopy of the periplasmic cytochrome *c* nitrite reductase from *Escherichia coli*. *Biochemistry* **41**, 2921-2931.

Barnes, K. B., Steward, J., Thwaite, J. E. & other authors (2013). Trimethoprim/sulfamethoxazole (co-trimoxazole) prophylaxis is effective against acute murine inhalational melioidosis and glanders. *Int J Antimicrob Agents* **41**, 552-557.

Barth, K. R., Isabella, V. M. & Clark, V. L. (2009). Biochemical and genomic analysis of the denitrification pathway within the genus *Neisseria*. *Microbiology* **155**, 4093-4103.

Benkert, B., Quack, N., Schreiber, K., Jaensch, L., Jahn, D. & Schobert, M. (2008). Nitrate-responsive NarX-NarL represses arginine-mediated induction of the *Pseudomonas aeruginosa* arginine fermentation *arcDABC* operon. *Microbiology* **154**, 3053-3060.

Benkert, P., Biasini, M. & Schwede, T. (2011). Toward the estimation of the absolute quality of individual protein structure models. *Bioinformatics* **27**, 343-350.

Benoit, S., Abaibou, H. & Mandrand-Berthelot, M. A. (1998). Topological analysis of the aerobic membrane-bound formate dehydrogenase of *Escherichia coli*. *J Bacteriol* **180**, 6625-6634.

Berks, B. C., Ferguson, S. J., Moir, J. W. & Richardson, D. J. (1995a). Enzymes and associated electron transport systems that catalyse the respiratory reduction of nitrogen oxides and oxyanions. *Biochim Biophys Acta* **1232**, 97-173.

Berks, B. C., Richardson, D. J., Reilly, A., Willis, A. C. & Ferguson, S. J. (1995b). The *napEDABC* gene cluster encoding the periplasmic nitrate reductase system of *Thiosphaera pantotropha*. *Biochem J* **309 (Pt 3)**, 983-992.

Berks, B. C., Sargent, F. & Palmer, T. (2000). The Tat protein export pathway. *Mol Microbiol* **35**, 260-274.

Bertero, M. G., Rothery, R. A., Palak, M., Hou, C., Lim, D., Blasco, F., Weiner, J. H. & Strynadka, N. C. (2003). Insights into the respiratory electron transfer pathway from the structure of nitrate reductase A. *Nat Struct Biol* **10**, 681-687.

Bevers, L. E., Hagedoorn, P. L., Santamaria-Araujo, J. A., Magalon, A., Hagen, W. R. & Schwarz, G. (2008). Function of MoaB proteins in the biosynthesis of the molybdenum and tungsten cofactors. *Biochemistry* **47**, 949-956.

Bevers, L. E., Hagedoorn, P. L. & Hagen, W. R. (2009). The bioinorganic chemistry of tungsten. *Coord Chem Rev* **253**, 269–290.

Bilous, P. T. & Weiner, J. H. (1985a). Proton translocation coupled to dimethyl sulfoxide reduction in anaerobically grown *Escherichia coli* HB101. *J Bacteriol* **163**, 369-375.

Bilous, P. T. & Weiner, J. H. (1985b). Dimethyl sulfoxide reductase activity by anaerobically grown *Escherichia coli* HB101. *J Bacteriol* **162**, 1151-1155.

Blasco, F., Iobbi, C., Ratouchniak, J., Bonnefoy, V. & Chippaux, M. (1990). Nitrate reductases of *Escherichia coli*: sequence of the second nitrate reductase and comparison with that encoded by the *narGHJI* operon. *Mol Gen Genet* **222**, 104-111.

Blasco, F., Dos Santos, J. P., Magalon, A., Frixon, C., Guigliarelli, B., Santini, C. L. & Giordano, G. (1998). NarJ is a specific chaperone required for molybdenum cofactor assembly in nitrate reductase A of *Escherichia coli*. *Mol Microbiol* **28**, 435-447.

Boddey, J. A., Day, C. J., Flegg, C. P., Ulrich, R. L., Stephens, S. R., Beacham, I. R., Morrison, N. A. & Peak, I. R. (2007). The bacterial gene *lfpA* influences the potent induction of calcitonin receptor and osteoclast-related genes in *Burkholderia pseudomallei*-induced TRAP-positive multinucleated giant cells. *Cell Microbiol* **9**, 514-531.

Bohmer, N., Hartmann, T. & Leimkuhler, S. (2014). The chaperone FdsC for *Rhodobacter capsulatus* formate dehydrogenase binds the *bis*-molybdopterin guanine dinucleotide cofactor. *FEBS Lett* **588**, 531-537.

Bonnefoy, V. & Demoss, J. A. (1994). Nitrate reductases in *Escherichia coli*. *Antonie Van Leeuwenhoek* **66**, 47-56.

Bordoli, L., Kiefer, F., Arnold, K., Benkert, P., Battey, J. & Schwede, T. (2009). Protein structure homology modeling using SWISS-MODEL workspace. *Nature Protoc* **4**, 1-13.

Bordoli, L. & Schwede, T. (2012). Automated protein structure modeling with SWISS-MODEL Workspace and the Protein Model Portal. *Methods Mol Biol* **857**, 107-136.

Borriello, G., Richards, L., Ehrlich, G. D. & Stewart, P. S. (2006). Arginine or nitrate enhances antibiotic susceptibility of *Pseudomonas aeruginosa* in biofilms. *Antimicrob Agents Chemother* **50**, 382-384.

Boshoff, H. I. & Barry, C. E. (2005). Tuberculosis - metabolism and respiration in the absence of growth. *Nat Rev Microbiol* **3**, 70-80.

Bosse, J. T., Janson, H., Sheehan, B. J., Beddek, A. J., Rycroft, A. N., Kroll, J. S. & Langford, P. R. (2002). *Actinobacillus pleuropneumoniae*: pathobiology and pathogenesis of infection. *Microbes Infect* **4**, 225-235.

Bouchal, P., Struharova, I., Budinska, E. & other authors (2010). Unraveling an FNR based regulatory circuit in *Paracoccus denitrificans* using a proteomics-based approach. *Biochim Biophys Acta* **1804**, 1350-1358.

Boulanger, M. J. & Murphy, M. E. (2002). Crystal structure of the soluble domain of the major anaerobically induced outer membrane protein (AniA) from pathogenic *Neisseria*: a new class of copper-containing nitrite reductases. *J Mol Biol* **315**, 1111-1127.

Brett, P. J., DeShazer, D. & Woods, D. E. (1998). *Burkholderia thailandensis* sp. nov., a *Burkholderia pseudomallei*-like species. *Int J Syst Bacteriol* **48 Pt 1**, 317-320.

Brokx, S. J., Rothery, R. A., Zhang, G., Ng, D. P. & Weiner, J. H. (2005). Characterization of an *Escherichia coli* sulfite oxidase homologue reveals the role of a conserved active site cysteine in assembly and function. *Biochemistry* **44**, 10339-10348.

Brown, K., Tegoni, M., Prudencio, M., Pereira, A. S., Besson, S., Moura, J. J., Moura, I. & Cambillau, C. (2000). A novel type of catalytic copper cluster in nitrous oxide reductase. *Nat Struct Biol* **7**, 191-195.

Buc, J., Santini, C. L., Giordani, R., Czjzek, M., Wu, L. F. & Giordano, G. (1999). Enzymatic and physiological properties of the tungsten-substituted molybdenum TMAO reductase from *Escherichia coli*. *Mol Microbiol* **32**, 159-168.

Burgess, B. K. & Lowe, D. J. (1996). Mechanism of Molybdenum Nitrogenase. *Chem Rev* **96**, 2983-3012.

Burtnick, M. N., Brett, P. J., Harding, S. V. & other authors (2011). The cluster 1 type VI secretion system is a major virulence determinant in *Burkholderia pseudomallei*. *Infect Immun* **79**, 1512-1525.

Butler, C. S., Debieux, C. M., Dridge, E. J., Splatt, P. & Wright, M. (2012). Biomineralization of selenium by the selenate-respiring bacterium *Thauera selenatis*. *Biochem Soc Trans* **40**, 1239-1243.

Butler, D. (2012). Viral research faces clampdown. *Nature* **490**, 456.

Butt, A., Higman, V. A., Williams, C., Crump, M. P., Hemsley, C. M., Harmer, N. & Titball, R. W. (2014). The HicA toxin from *Burkholderia pseudomallei* has a role in persister cell formation. *Biochem J* **459**, 333-344.

Cardinale, J. A. & Clark, V. L. (2000). Expression of AniA, the major anaerobically induced outer membrane protein of *Neisseria gonorrhoeae*, provides protection against killing by normal human sera. *Infect Immun* **68**, 4368-4369.

Cerqueira, N. M., Fernandes, P. A., Gonzalez, P. J., Moura, J. J. & Ramos, M. J. (2013). The sulfur shift: an activation mechanism for periplasmic nitrate reductase and formate dehydrogenase. *Inorg Chem* **52**, 10766-10772.

Chandler, J. R., Duerkop, B. A., Hinz, A., West, T. E., Herman, J. P., Churchill, M. E., Skerrett, S. J. & Greenberg, E. P. (2009). Mutational analysis of *Burkholderia thailandensis* quorum sensing and self-aggregation. *J Bacteriol* **191**, 5901-5909.

Chang, C. & Stewart, R. C. (1998). The two-component system. Regulation of diverse signaling pathways in prokaryotes and eukaryotes. *Plant Physiol* **117**, 723-731.

Chang, L., Wei, L. I., Audia, J. P., Morton, R. A. & Schellhorn, H. E. (1999). Expression of the *Escherichia coli* NRZ nitrate reductase is highly growth phase dependent and is controlled by RpoS, the alternative vegetative sigma factor. *Mol Microbiol* **34**, 756-766.

Chantratita, N., Rholl, D. A., Sim, B. & other authors (2011). Antimicrobial resistance to ceftazidime involving loss of penicillin-binding protein 3 in *Burkholderia pseudomallei*. *Proc Natl Acad Sci U S A* **108**, 17165-17170.

Chaowagul, W., White, N. J., Dance, D. A., Wattanagoon, Y., Naigowit, P., Davis, T. M., Looareesuwan, S. & Pitakwatchara, N. (1989). Melioidosis: a major cause of community-acquired septicemia in Northeastern Thailand. *J Infect Dis* **159**, 890-899.

Chaowagul, W., Suputtamongkol, Y., Dance, D. A., Rajchanuvong, A., Pattara-arechachai, J. & White, N. J. (1993). Relapse in melioidosis: incidence and risk factors. *J Infect Dis* **168**, 1181-1185.

Chaowagul, W., Simpson, A. J., Suputtamongkol, Y., Smith, M. D., Angus, B. J. & White, N. J. (1999). A comparison of chloramphenicol, trimethoprim-sulfamethoxazole, and

doxycycline with doxycycline alone as maintenance therapy for melioidosis. *Clin Infect Dis* **29**, 375-380.

Charoensap, J., Utaisincharoen, P., Engering, A. & Sirisinha, S. (2009). Differential intracellular fate of *Burkholderia pseudomallei* 844 and *Burkholderia thailandensis* UE5 in human monocyte-derived dendritic cells and macrophages. *BMC Immunol* **10**, 20.

Chen, K., Sun, G. W., Chua, K. L. & Gan, Y. H. (2005). Modified virulence of antibiotic-induced *Burkholderia pseudomallei* filaments. *Antimicrob Agents Chemother* **49**, 1002-1009.

Cheng, A. C. & Currie, B. J. (2005). Melioidosis: epidemiology, pathophysiology, and management. *Clin Microbiol Rev* **18**, 383-416.

Cheng, V. W., Rothery, R. A., Bertero, M. G., Strynadka, N. C. & Weiner, J. H. (2005). Investigation of the environment surrounding iron-sulfur cluster 4 of *Escherichia coli* dimethylsulfoxide reductase. *Biochemistry* **44**, 8068-8077.

Chieng, S., Carreto, L. & Nathan, S. (2012). *Burkholderia pseudomallei* transcriptional adaptation in macrophages. *BMC Genomics* **13**, 328.

Chua, K. L., Chan, Y. Y. & Gan, Y. H. (2003). Flagella are virulence determinants of *Burkholderia pseudomallei*. *Infect Immun* **71**, 1622-1629.

Clarke, T. A., Mills, P. C., Poock, S. R. & other authors (2008). *Escherichia coli* cytochrome *c* nitrite reductase NrfA. *Methods Enzymol* **437**, 63-77.

Coban, A. Y., Deveci, A., Sunter, A. T. & Martin, A. (2014). Nitrate reductase assay for rapid detection of isoniazid, rifampin, ethambutol, and streptomycin resistance in *Mycobacterium tuberculosis*: a systematic review and meta-analysis. *J Clin Microbiol* **52**, 15-19.

Coenye, T., Mahenthiralingam, E., Henry, D., LiPuma, J. J., Laevens, S., Gillis, M., Speert, D. P. & Vandamme, P. (2001). *Burkholderia ambifaria* sp. nov., a novel member of

the *Burkholderia cepacia* complex including biocontrol and cystic fibrosis-related isolates. *Int J Syst Evol Microbiol* **51**, 1481-1490.

Cole, J. (1996). Nitrate reduction to ammonia by enteric bacteria: redundancy, or a strategy for survival during oxygen starvation? *FEMS Microbiol Lett* **136**, 1-11.

Conejero, L., Patel, N., de Reynal, M., Oberdorf, S., Prior, J., Felgner, P. L., Titball, R. W., Salguero, F. J. & Bancroft, G. J. (2011). Low-dose exposure of C57BL/6 mice to *Burkholderia pseudomallei* mimics chronic human melioidosis. *Am J Pathol* **179**, 270-280.

Costerton, J. W., Stewart, P. S. & Greenberg, E. P. (1999). Bacterial biofilms: a common cause of persistent infections. *Science* **284**, 1318-1322.

Cramm, R., Siddiqui, R. A. & Friedrich, B. (1997). Two isofunctional nitric oxide reductases in *Alcaligenes eutrophus* H16. *J Bacteriol* **179**, 6769-6777.

Craske, A. & Ferguson, S. J. (1986). The respiratory nitrate reductase from *Paracoccus denitrificans*. Molecular characterisation and kinetic properties. *Eur J Biochem* **158**, 429-436.

Cuccui, J., Easton, A., Chu, K. K., Bancroft, G. J., Oyston, P. C., Titball, R. W. & Wren, B. W. (2007). Development of signature-tagged mutagenesis in *Burkholderia pseudomallei* to identify genes important in survival and pathogenesis. *Infect Immun* **75**, 1186-1195.

Cunningham-Bussel, A., Bange, F. C. & Nathan, C. F. (2013). Nitrite impacts the survival of *Mycobacterium tuberculosis* in response to isoniazid and hydrogen peroxide. *Microbiology Open* **2**, 901-911.

Currie, B. J., Fisher, D. A., Anstey, N. M. & Jacups, S. P. (2000a). Melioidosis: acute and chronic disease, relapse and re-activation. *Trans R Soc Trop Med Hyg* **94**, 301-304.

Currie, B. J., Fisher, D. A., Howard, D. M., Burrow, J. N., Selvanayagam, S., Snelling, P. L., Anstey, N. M. & Mayo, M. J. (2000b). The epidemiology of melioidosis in Australia and Papua New Guinea. *Acta Trop* **74**, 121-127.

Currie, B. J. (2003). Melioidosis: an important cause of pneumonia in residents of and travellers returned from endemic regions. *Eur Respir J* **22**, 542-550.

Currie, B. J., Jacups, S. P., Cheng, A. C., Fisher, D. A., Anstey, N. M., Huffam, S. E. & Krause, V. L. (2004). Melioidosis epidemiology and risk factors from a prospective whole-population study in northern Australia. *Trop Med Int Health* **9**, 1167-1174.

Currie, B. J., Dance, D. A. & Cheng, A. C. (2008). The global distribution of *Burkholderia pseudomallei* and melioidosis: an update. *Trans R Soc Trop Med Hyg* **102 Suppl 1**, S1-4.

Currie, B. J., Ward, L. & Cheng, A. C. (2010a). The Epidemiology and Clinical Spectrum of Melioidosis: 540 Cases from the 20 Year Darwin Prospective Study. *PLoS Negl Trop Dis* **4**, e900.

Currie, B. J., Ward, L. & Cheng, A. C. (2010b). The epidemiology and clinical spectrum of melioidosis: 540 cases from the 20 year Darwin prospective study. *PLoS Negl Trop Dis* **4**, e900.

Cuypers, H., Berghofer, J. & Zumft, W. G. (1995). Multiple *nosZ* promoters and anaerobic expression of *nos* genes necessary for *Pseudomonas stutzeri* nitrous oxide reductase and assembly of its copper centers. *Biochim Biophys Acta* **1264**, 183-190.

Dalsing, B. L. & Allen, C. (2014). Nitrate assimilation contributes to *Ralstonia solanacearum* root attachment, stem colonization, and virulence. *J Bacteriol* **196**, 949-960.

Dance, D. A. (2000). Ecology of *Burkholderia pseudomalle*i and the interactions between environmental *Burkholderia* spp. and human-animal hosts. *Acta Trop* **74**, 159-168.

de Lorenzo, V., Herrero, M., Jakubzik, U. & Timmis, K. N. (1990). Mini-Tn5 transposon derivatives for insertion mutagenesis, promoter probing, and chromosomal insertion of cloned DNA in gram-negative eubacteria. *J Bacteriol* **172**, 6568-6572.

Dejsirilert, S., Kondo, E., Chiewsilp, D. & Kanai, K. (1991). Growth and survival of *Pseudomonas pseudomallei* in acidic environments. *Jpn J Med Sci Biol* **44**, 63-74.

Deng, M., Moureaux, T. & Caboche, M. (1989). Tungstate, a molybdate analog inactivating nitrate reductase, deregulates the expression of the nitrate reductase structural gene. *Plant Physiol* **91**, 304-309.

DeShazer, D., Brett, P. J. & Woods, D. E. (1998). The type II O-antigenic polysaccharide moiety of *Burkholderia pseudomallei* lipopolysaccharide is required for serum resistance and virulence. *Mol Microbiol* **30**, 1081-1100.

DeShazer, D., Brett, P. J., Burtnick, M. N. & Woods, D. E. (1999). Molecular characterization of genetic loci required for secretion of exoproducts in *Burkholderia pseudomallei*. *J Bacteriol* **181**, 4661-4664.

Deshazer, D. (2007). Virulence of clinical and environmental isolates of *Burkholderia oklahomensis* and *Burkholderia thailandensis* in hamsters and mice. *FEMS Microbiol Lett* **277**, 64-69.

Dias, J. M., Than, M. E., Humm, A. & other authors (1999). Crystal structure of the first dissimilatory nitrate reductase at 1.9 Å solved by MAD methods. *Structure* **7**, 65-79.

Dick, T., Lee, B. H. & Murugasu-Oei, B. (1998). Oxygen depletion induced dormancy in *Mycobacterium smegmatis*. *FEMS Microbiol Lett* **163**, 159-164.

Dong, T. & Schellhorn, H. E. (2009). Control of RpoS in global gene expression of *Escherichia coli* in minimal media. *Mol Genet Genomics:* **281**, 19-33.

Douglas, M. W., Lum, G., Roy, J., Fisher, D. A., Anstey, N. M. & Currie, B. J. (2004). Epidemiology of community-acquired and nosocomial bloodstream infections in tropical Australia: a 12-month prospective study. *Trop Med Int Health* **9**, 795-804.

Dow, J. M., Grahl, S., Ward, R., Evans, R., Byron, O., Norman, D. G., Palmer, T. & Sargent, F. (2014). Characterization of a periplasmic nitrate reductase in complex with its biosynthetic chaperone. *FEBS J* **281**, 246-260.

Duan, Q., Zhou, M., Zhu, L. & Zhu, G. (2012a). Flagella and bacterial pathogenicity. *J Basic Microbiol*.

Duan, Q., Zhou, M., Zhu, X. & other authors (2012b). The flagella of F18ab *Escherichia coli* is a virulence factor that contributes to infection in a IPEC-J2 cell model in vitro. *Vet Microbiol* **160**, 132-140.

Duarte, A. G., Cordas, C. M., Moura, J. J. & Moura, I. (2014). Steady-state kinetics with nitric oxide reductase (NOR): new considerations on substrate inhibition profile and catalytic mechanism. *Biochim Biophys Acta* **1837**, 375-384.

Dutta, N. K., Mehra, S., Didier, P. J. & other authors (2010). Genetic requirements for the survival of tubercle bacilli in primates. *J Infect Dis* **201**, 1743-1752.

Edwards, J., Quinn, D., Rowbottom, K. A., Whittingham, J. L., Thomson, M. J. & Moir, J. W. (2012). *Neisseria meningitidis* and *Neisseria gonorrhoeae* are differently adapted in the regulation of denitrification: single nucleotide polymorphisms that enable species-specific tuning of the aerobic-anaerobic switch. *Biochem J* **445**, 69-79.

Egan, S. M. & Stewart, V. (1990). Nitrate regulation of anaerobic respiratory gene expression in *narX* deletion mutants of *Escherichia coli* K-12. *J Bacteriol* **172**, 5020-5029.

Eisenreich, W., Dandekar, T., Heesemann, J. & Goebel, W. (2010). Carbon metabolism of intracellular bacterial pathogens and possible links to virulence. *Nat Rev Microbiol* **8**, 401-412.

Ellington, M. J., Sawers, G., Sears, H. J., Spiro, S., Richardson, D. J. & Ferguson, S. J. (2003). Characterization of the expression and activity of the periplasmic nitrate reductase of *Paracoccus pantotrophus* in chemostat cultures. *Microbiology* **149**, 1533-1540.

Essex-Lopresti, A. E., Boddey, J. A., Thomas, R. & other authors (2005). A type IV pilin, PilA, contributes to adherence of *Burkholderia pseudomallei* and virulence in vivo. *Infect Immun* **73**, 1260-1264.

Falsetta, M. L., McEwan, A. G., Jennings, M. P. & Apicella, M. A. (2010). Anaerobic metabolism occurs in the substratum of gonococcal biofilms and may be sustained in part by nitric oxide. *Infect Immun* **78**, 2320-2328.

Fang, F. C., Libby, S. J., Castor, M. E. & Fung, A. M. (2005). Isocitrate lyase (AceA) is required for *Salmonella* persistence but not for acute lethal infection in mice. *Infect Immun* **73**, 2547-2549.

Fedor, J. G., Rothery, R. A., Giraldi, K. S. & Weiner, J. H. (2014). Q-Site Occupancy Defines Heme Heterogeneity in *Escherichia coli* Nitrate Reductase A (NarGHI). *Biochemistry* **53**, 1733-1741.

Fenhalls, G., Stevens, L., Moses, L., Bezuidenhout, J., Betts, J. C., Helden Pv, P., Lukey, P. T. & Duncan, K. (2002). *In situ* detection of *Mycobacterium tuberculosis* transcripts in human lung granulomas reveals differential gene expression in necrotic lesions. *Infect Immun* **70**, 6330-6338.

Field, S. J., Thornton, N. P., Anderson, L. J. & other authors (2005). Reductive activation of nitrate reductases. *Dalton Trans*, 3580-3586.

Filiatrault, M. J., Tombline, G., Wagner, V. E., Van Alst, N., Rumbaugh, K., Sokol, P., Schwingel, J. & Iglewski, B. H. (2013). *Pseudomonas aeruginosa* PA1006, which plays a role in molybdenum homeostasis, is required for nitrate utilization, biofilm formation, and virulence. *PLoS One* **8**, e55594.

Fink, R. C., Evans, M. R., Porwollik, S., Vazquez-Torres, A., Jones-Carson, J., Troxell, B., Libby, S. J., McClelland, M. & Hassan, H. M. (2007). FNR is a global regulator of virulence and anaerobic metabolism in *Salmonella* enterica serovar *Typhimurium* (ATCC 14028s). *J Bacteriol* **189**, 2262-2273.

Flannagan, R. S., Aubert, D., Kooi, C., Sokol, P. A. & Valvano, M. A. (2007). Burkholderia cenocepacia requires a periplasmic HtrA protease for growth under thermal and osmotic stress and for survival in vivo. *Infect Immun* **75**, 1679-1689.

Flannagan, R. S., Cosio, G. & Grinstein, S. (2009). Antimicrobial mechanisms of phagocytes and bacterial evasion strategies. *Nat Rev Microbiol* **7**, 355-366.

Flock, U., Reimann, J. & Adelroth, P. (2006). Proton transfer in bacterial nitric oxide reductase. *Biochem Soc Trans* **34**, 188-190.

Frangoulidis, D., Schwab, D., Scholz, H., Tomaso, H., Hogardt, M., Meyer, H., Splettstoesser, W. D. & Pohle, F. K. (2008). 'Imported' melioidosis in Germany: relapse after 10 years. *Trans R Soc Trop Med Hyg* **102 Suppl 1**, S40-41.

French, C. T., Toesca, I. J., Wu, T. H. & other authors (2011). Dissection of the *Burkholderia* intracellular life cycle using a photothermal nanoblade. *Proc Natl Acad Sci U S A* **108**, 12095-12100.

Fritz, C., Maass, S., Kreft, A. & Bange, F. C. (2002). Dependence of *Mycobacterium bovis* BCG on anaerobic nitrate reductase for persistence is tissue specific. *Infect Immun* **70**, 286-291.

Galyov, E. E., Brett, P. J. & DeShazer, D. (2010). Molecular insights into *Burkholderia pseudomallei* and *Burkholderia mallei* pathogenesis. *Annu Rev Microbiol* **64**, 495-517.

Gamage, A. M., Shui, G., Wenk, M. R. & Chua, K. L. (2011). N-Octanoylhomoserine lactone signalling mediated by the BpsI-BpsR quorum sensing system plays a major role in biofilm formation of *Burkholderia pseudomallei*. *Microbiology* **157**, 1176-1186.

Garcia-Horsman, J. A., Barquera, B., Rumbley, J., Ma, J. & Gennis, R. B. (1994). The superfamily of heme-copper respiratory oxidases. *J Bacteriol* **176**, 5587-5600.

Gates, A. J., Hughes, R. O., Sharp, S. R. & other authors (2003). Properties of the periplasmic nitrate reductases from *Paracoccus pantotrophus* and *Escherichia coli* after growth in tungsten-supplemented media. *FEMS Microbiol Lett* **220**, 261-269.

Gates, A. J., Luque-Almagro, V. M., Goddard, A. D., Ferguson, S. J., Roldan, M. D. & Richardson, D. J. (2011). A composite biochemical system for bacterial nitrate and nitrite assimilation as exemplified by *Paracoccus denitrificans*. *Biochem J* **435**, 743-753.

Giffin, M. M., Raab, R. W., Morganstern, M. & Sohaskey, C. D. (2012). Mutational analysis of the respiratory nitrate transporter NarK2 of *Mycobacterium tuberculosis*. *PLoS One* **7**, e45459.

Glass, M. B., Gee, J. E., Steigerwalt, A. G. & other authors (2006). Pneumonia and septicemia caused by *Burkholderia thailandensis* in the United States. *J Clin Microbiol* **44**, 4601-4604.

Godoy, D., Randle, G., Simpson, A. J., Aanensen, D. M., Pitt, T. L., Kinoshita, R. & Spratt, B. G. (2003). Multilocus sequence typing and evolutionary relationships among the causative agents of melioidosis and glanders, *Burkholderia pseudomallei* and *Burkholderia mallei*. *J Clin Microbiol* **41**, 2068-2079.

Gonzalez, P. J., Correia, C., Moura, I., Brondino, C. D. & Moura, J. J. (2006). Bacterial nitrate reductases: Molecular and biological aspects of nitrate reduction. *J Inorg Biochem* **100**, 1015-1023.

Goodyear, A., Kellihan, L., Bielefeldt-Ohmann, H., Troyer, R., Propst, K. & Dow, S. (2009). Protection from pneumonic infection with *Burkholderia* species by inhalational immunotherapy. *Infect Immun* **77**, 1579-1588.

Goodyear, A., Bielefeldt-Ohmann, H., Schweizer, H. & Dow, S. (2012). Persistent gastric colonization with *Burkholderia pseudomallei* and dissemination from the gastrointestinal tract following mucosal inoculation of mice. *PLoS One* **7**, e37324.

Grimaldi, S., Schoepp-Cothenet, B., Ceccaldi, P., Guigliarelli, B. & Magalon, A. (2013). The prokaryotic Mo/W-*bis*PGD enzymes family: a catalytic workhorse in bioenergetic. *Biochim Biophys Acta* **1827**, 1048-1085.

Groll, M., Schellenberg, B., Bachmann, A. S., Archer, C. R., Huber, R., Powell, T. K., Lindow, S., Kaiser, M. & Dudler, R. (2008). A plant pathogen virulence factor inhibits the eukaryotic proteasome by a novel mechanism. *Nature* **452**, 755-758.

Grunden, A. M. & Shanmugam, K. T. (1997). Molybdate transport and regulation in bacteria. *Arch Microbiol* **168**, 345-354.

Gudmundsdottir, T., Asgeirsson, H., Hardarson, H. S. & Thorisdottir, A. S. (2014). [Melioidosis, first four cases in Iceland]. *Laeknabladid* **100**, 85-89.

Haltia, T., Brown, K., Tegoni, M., Cambillau, C., Saraste, M., Mattila, K. & Djinovic-Carugo, K. (2003). Crystal structure of nitrous oxide reductase from *Paracoccus denitrificans* at 1.6 Å resolution. *Biochem J* **369**, 77-88.

Hamad, M. A., Austin, C. R., Stewart, A. L., Higgins, M., Vazquez-Torres, A. & Voskuil, M. I. (2011). Adaptation and antibiotic tolerance of anaerobic *Burkholderia pseudomallei*. *Antimicrob Agents Chemother* **55**, 3313-3323.

Haraga, A., West, T. E., Brittnacher, M. J., Skerrett, S. J. & Miller, S. I. (2008). *Burkholderia thailandensis* as a model system for the study of the virulence-associated type III secretion system of *Burkholderia pseudomallei*. *Infect Immun* **76**, 5402-5411.

Harshey, R. M. (2003). Bacterial motility on a surface: many ways to a common goal. *Annu Rev Microbiol* **57**, 249-273.

Hartig, E., Schiek, U., Vollack, K. U. & Zumft, W. G. (1999). Nitrate and nitrite control of respiratory nitrate reduction in denitrifying *Pseudomonas stutzeri* by a two-component regulatory system homologous to NarXL of *Escherichia coli*. *J Bacteriol* **181**, 3658-3665.

Hartmann, T. & Leimkuhler, S. (2013). The oxygen-tolerant and NAD^+-dependent formate dehydrogenase from *Rhodobacter capsulatus* is able to catalyze the reduction of CO_2 to formate. *FEBS J* **280**, 6083-6096.

Hasona, A., Ray, R. M. & Shanmugam, K. T. (1998a). Physiological and genetic analyses leading to identification of a biochemical role for the *moeA* (molybdate metabolism) gene product in *Escherichia coli*. *J Bacteriol* **180**, 1466-1472.

Hasona, A., Self, W. T., Ray, R. M. & Shanmugam, K. T. (1998b). Molybdate-dependent transcription of *hyc* and *nar* operons of *Escherichia coli* requires MoeA protein and ModE-molybdate. *FEMS Microbiol Lett* **169**, 111-116.

Hasona, A., Self, W. T. & Shanmugam, K. T. (2001). Transcriptional regulation of the *moe* (molybdate metabolism) operon of *Escherichia coli*. *Arch Microbiol* **175**, 178-188.

Hassan, M. R., Pani, S. P., Peng, N. P., Voralu, K., Vijayalakshmi, N., Mehanderkar, R., Aziz, N. A. & Michael, E. (2010). Incidence, risk factors and clinical epidemiology of melioidosis: a complex socio-ecological emerging infectious disease in the Alor Setar region of Kedah, Malaysia. *BMC Infect Dis* **10**, 302.

Hassett, D. J., Cuppoletti, J., Trapnell, B. & other authors (2002). Anaerobic metabolism and quorum sensing by *Pseudomonas aeruginosa* biofilms in chronically infected cystic fibrosis airways: rethinking antibiotic treatment strategies and drug targets. *Adv Drug Deliv Rev* **54**, 1425-1443.

Haussler, S., Rohde, M., von Neuhoff, N., Nimtz, M. & Steinmetz, I. (2003). Structural and functional cellular changes induced by *Burkholderia pseudomallei* rhamnolipid. *Infect Immun* **71**, 2970-2975.

Helaine, S., Thompson, J. A., Watson, K. G., Liu, M., Boyle, C. & Holden, D. W. (2010). Dynamics of intracellular bacterial replication at the single cell level. *Proc Natl Acad Sci U S A* **107**, 3746-3751.

Helaine, S., Cheverton, A. M., Watson, K. G., Faure, L. M., Matthews, S. A. & Holden, D. W. (2014). Internalization of *Salmonella* by macrophages induces formation of nonreplicating persisters. *Science* **343**, 204-208.

Hendriks, J., Warne, A., Gohlke, U., Haltia, T., Ludovici, C., Lubben, M. & Saraste, M. (1998). The active site of the bacterial nitric oxide reductase is a dinuclear iron center. *Biochemistry* **37**, 13102-13109.

Hensel, M., Hinsley, A. P., Nikolaus, T., Sawers, G. & Berks, B. C. (1999). The genetic basis of tetrathionate respiration in *Salmonella typhimurium*. *Mol Microbiol* **32**, 275-287.

Higgins, D. G., Thompson, J. D. & Gibson, T. J. (1996). Using CLUSTAL for multiple sequence alignments. *Methods Enzymol* **266**, 383-402.

Hill, D., Rose, B., Pajkos, A. & other authors (2005). Antibiotic susceptabilities of *Pseudomonas aeruginosa* isolates derived from patients with cystic fibrosis under aerobic, anaerobic, and biofilm conditions. *J Clin Microbiol* **43**, 5085-5090.

Hille, R. (1996). The Mononuclear Molybdenum Enzymes. *Chem Rev* **96**, 2757-2816.

Hille, R. (2002). Molybdenum and tungsten in biology. *Trends Biochem Sci* **27**, 360-367.

Hino, T., Matsumoto, Y., Nagano, S., Sugimoto, H., Fukumori, Y., Murata, T., Iwata, S. & Shiro, Y. (2010). Structural basis of biological N_2O generation by bacterial nitric oxide reductase. *Science* **330**, 1666-1670.

Hoehn, G. T. & Clark, V. L. (1992). The major anaerobically induced outer membrane protein of *Neisseria gonorrhoeae,* Pan 1, is a lipoprotein. *Infect Immun* **60**, 4704-4708.

Holden, M. T., Titball, R. W., Peacock, S. J. & other authors (2004). Genomic plasticity of the causative agent of melioidosis, *Burkholderia pseudomallei*. *Proc Natl Acad Sci U S A* **101**, 14240-14245.

Holland, D. J., Wesley, A., Drinkovic, D. & Currie, B. J. (2002). Cystic Fibrosis and *Burkholderia pseudomallei* Infection: An Emerging Problem? *Clin Infect Dis* **35**, e138-140.

Honer zu Bentrup, K. & Russell, D. G. (2001). Mycobacterial persistence: adaptation to a changing environment. *Trends Microbiol* **9**, 597-605.

Hopper, A., Tovell, N. & Cole, J. (2009). A physiologically significant role in nitrite reduction of the CcoP subunit of the cytochrome oxidase cbb_3 from *Neisseria gonorrhoeae*. *FEMS Microbiol Lett* **301**, 232-240.

Hopper, A. C., Li, Y. & Cole, J. A. (2013). A critical role for the *cccA* gene product, cytochrome c_2, in diverting electrons from aerobic respiration to denitrification in *Neisseria gonorrhoeae*. *J Bacteriol* **195**, 2518-2529.

Horton, R. E., Morrison, N. A., Beacham, I. R. & Peak, I. R. (2012). Interaction of *Burkholderia pseudomallei* and *Burkholderia thailandensis* with human monocyte-derived dendritic cells. *J Med Microbiol* **61**, 607-614.

Householder, T. C., Fozo, E. M., Cardinale, J. A. & Clark, V. L. (2000). Gonococcal nitric oxide reductase is encoded by a single gene, *norB*, which is required for anaerobic growth and is induced by nitric oxide. *Infect Immun* **68**, 5241-5246.

Hu, B. L., Shen, L. D., Xu, X. Y. & Zheng, P. (2011). Anaerobic ammonium oxidation (anammox) in different natural ecosystems. *Biochem Soc Trans* **39**, 1811-1816.

Inglis, T. J., Robertson, T., Woods, D. E., Dutton, N. & Chang, B. J. (2003). Flagellum-mediated adhesion by *Burkholderia pseudomallei* precedes invasion of *Acanthamoeba astronyxis*. *Infect Immun* **71**, 2280-2282.

Inglis, T. J. & Sagripanti, J. L. (2006). Environmental factors that affect the survival and persistence of *Burkholderia pseudomallei*. *Appl Environ Microbiol* **72**, 6865-6875.

Inglis, T. J., Merritt, A., Montgomery, J., Jayasinghe, I., Thevanesam, V. & McInnes, R. (2008). Deployable laboratory response to emergence of melioidosis in central Sri Lanka. *J Clin Microbiol* **46**, 3479-3481.

Inoue, T., Gotowda, M., Deligeer, Kataoka, K., Yamaguchi, K., Suzuki, S., Watanabe, H., Gohow, M. & Kai, Y. (1998). Type 1 Cu structure of blue nitrite reductase from *Alcaligenes xylosoxidans* GIFU 1051 at 2.05 Å resolution: comparison of blue and green nitrite reductases. *J Biochem* **124**, 876-879.

Iobbi-Nivol, C. & Leimkuhler, S. (2013). Molybdenum enzymes, their maturation and molybdenum cofactor biosynthesis in *Escherichia coli*. *Biochim Biophys Acta* **1827**, 1086-1101.

Jacobsen, I., Hennig-Pauka, I., Baltes, N., Trost, M. & Gerlach, G. F. (2005). Enzymes involved in anaerobic respiration appear to play a role in *Actinobacillus pleuropneumoniae* virulence. *Infect Immun* **73**, 226-234.

Jacques, J. G., Fourmond, V., Arnoux, P. & other authors (2014). Reductive activation in periplasmic nitrate reductase involves chemical modifications of the Mo-cofactor beyond the first coordination sphere of the metal ion. *Biochim Biophys Acta* **1837**, 277-286.

Jeddeloh, J. A., Fritz, D. L., Waag, D. M., Hartings, J. M. & Andrews, G. P. (2003). Biodefense-driven murine model of pneumonic melioidosis. *Infect Immun* **71**, 584-587.

Jepson, B. J., Anderson, L. J., Rubio, L. M., Taylor, C. J., Butler, C. S., Flores, E., Herrero, A., Butt, J. N. & Richardson, D. J. (2004). Tuning a nitrate reductase for function. The first spectropotentiometric characterization of a bacterial assimilatory nitrate reductase reveals novel redox properties. *J Biol Chem* **279**, 32212-32218.

Jepson, B. J., Mohan, S., Clarke, T. A., Gates, A. J., Cole, J. A., Butler, C. S., Butt, J. N., Hemmings, A. M. & Richardson, D. J. (2007). Spectropotentiometric and structural analysis of the periplasmic nitrate reductase from *Escherichia coli*. *J Biol Chem* **282**, 6425-6437.

Joers, A., Kaldalu, N. & Tenson, T. (2010). The frequency of persisters in *Escherichia coli* reflects the kinetics of awakening from dormancy. *J Bacteriol* **192**, 3379-3384.

Johnston, E. M., Dell'Acqua, S., Ramos, S., Pauleta, S. R., Moura, I. & Solomon, E. I. (2014). Determination of the active form of the tetranuclear copper sulfur cluster in nitrous oxide reductase. *J Am Chem Soc* **136**, 614-617.

Jones-Carson, J., Laughlin, J. R., Stewart, A. L., Voskuil, M. I. & Vázquez-Torres, A. (2012). Nitric oxide-dependent killing of aerobic, anaerobic and persistent *Burkholderia pseudomallei*. *Nitric oxide*.

Jones, A. L., Beveridge, T. J. & Woods, D. E. (1996). Intracellular survival of *Burkholderia pseudomallei*. *Infect Immun* **64**, 782-790.

Jones, C. M., Stres, B., Rosenquist, M. & Hallin, S. (2008). Phylogenetic analysis of nitrite, nitric oxide, and nitrous oxide respiratory enzymes reveal a complex evolutionary history for denitrification. *Mol Biol Evol* **25**, 1955-1966.

Jones, R. W. & Garland, P. B. (1977). Sites and specificity of the reaction of bipyridylium compounds with anaerobic respiratory enzymes of *Escherichia coli.* Effects of permeability barriers imposed by the cytoplasmic membrane. *Biochem J* **164**, 199-211.

Jones, S. A., Gibson, T., Maltby, R. C., Chowdhury, F. Z., Stewart, V., Cohen, P. S. & Conway, T. (2011). Anaerobic respiration of *Escherichia coli* in the mouse intestine. *Infect Immun* **79**, 4218-4226.

Jormakka, M., Tornroth, S., Abramson, J., Byrne, B. & Iwata, S. (2002a). Purification and crystallization of the respiratory complex formate dehydrogenase-N from *Escherichia coli*. *Acta Crystallogr D Biol Crystallogr* **58**, 160-162.

Jormakka, M., Tornroth, S., Byrne, B. & Iwata, S. (2002b). Molecular basis of proton motive force generation: structure of formate dehydrogenase-N. *Science* **295**, 1863-1868.

Jormakka, M., Byrne, B. & Iwata, S. (2003). Formate dehydrogenase - a versatile enzyme in changing environments. *Curr Opin Struct Biol* **13**, 418-423.

Jormakka, M., Richardson, D., Byrne, B. & Iwata, S. (2004). Architecture of NarGH reveals a structural classification of Mo-*bis*MGD enzymes. *Structure* **12**, 95-104.

Jung, J. Y., Madan-Lala, R., Georgieva, M., Rengarajan, J., Sohaskey, C. D., Bange, F. C. & Robinson, C. M. (2013). The intracellular environment of human macrophages that produce nitric oxide promotes growth of mycobacteria. *Infect Immun* **81**, 3198-3209.

Kartal, B., Maalcke, W. J., de Almeida, N. M. & other authors (2011). Molecular mechanism of anaerobic ammonium oxidation. *Nature* **479**, 127-130.

Kassem, II, Khatri, M., Esseili, M. A., Sanad, Y. M., Saif, Y. M., Olson, J. W. & Rajashekara, G. (2012). Respiratory proteins contribute differentially to *Campylobacter jejuni*'s survival and in vitro interaction with hosts' intestinal cells. *BMC Microbiol* **12**, 258.

Kelm, M. (1999). Nitric oxide metabolism and breakdown. *Biochim Biophys Acta* **1411**, 273-289.

Kemp, G. L., Clarke, T. A., Marritt, S. J., Lockwood, C., Poock, S. R., Hemmings, A. M., Richardson, D. J., Cheesman, M. R. & Butt, J. N. (2010). Kinetic and thermodynamic resolution of the interactions between sulfite and the pentahaem cytochrome NrfA from *Escherichia coli*. *Biochem J* **431**, 73-80.

Keren, I., Kaldalu, N., Spoering, A., Wang, Y. & Lewis, K. (2004a). Persister cells and tolerance to antimicrobials. *FEMS Microbiol Lett* **230**, 13-18.

Keren, I., Shah, D., Spoering, A., Kaldalu, N. & Lewis, K. (2004b). Specialized persister cells and the mechanism of multidrug tolerance in *Escherichia coli*. *J Bacteriol* **186**, 8172-8180.

Keren, I., Minami, S., Rubin, E. & Lewis, K. (2011). Characterization and Transcriptome Analysis of *Mycobacterium tuberculosis* Persisters. *MBio* **2**.

Kern, M. & Simon, J. (2009). Electron transport chains and bioenergetics of respiratory nitrogen metabolism in *Wolinella succinogenes* and other Epsilon proteobacteria. *Biochim Biophys Acta* **1787**, 646-656.

Kespichayawattana, W., Rattanachetkul, S., Wanun, T., Utaisincharoen, P. & Sirisinha, S. (2000). *Burkholderia pseudomallei* induces cell fusion and actin-associated membrane protrusion: a possible mechanism for cell-to-cell spreading. *Infect Immun* **68**, 5377-5384.

Khan, A. & Sarkar, D. (2008). A simple whole cell based high throughput screening protocol using *Mycobacterium bovis* BCG for inhibitors against dormant and active tubercle bacilli. *J Microbiol Methods* **73**, 62-68.

Khan, A. & Sarkar, D. (2012). Nitrate reduction pathways in mycobacteria and their implications during latency. *Microbiology* **158**, 301-307.

Kim, H. S., Schell, M. A., Yu, Y., Ulrich, R. L., Sarria, S. H., Nierman, W. C. & DeShazer, D. (2005). Bacterial genome adaptation to niches: divergence of the potential virulence genes in three *Burkholderia* species of different survival strategies. *BMC Genomics* **6**, 174.

Kishikawa, J., Kabashima, Y., Kurokawa, T. & Sakamoto, J. (2010). The cytochrome *bcc-aa*$_3$-type respiratory chain of *Rhodococcus rhodochrous*. *J Biosci Bioeng* **110**, 42-47.

Kisker, C., Schindelin, H. & Rees, D. C. (1997). Molybdenum-cofactor-containing enzymes: structure and mechanism. *Annu Rev Biochem* **66**, 233-267.

Kohler, S., Foulongne, V., Ouahrani-Bettache, S., Bourg, G., Teyssier, J., Ramuz, M. & Liautard, J. P. (2002). The analysis of the intramacrophagic virulome of *Brucella suis* deciphers the environment encountered by the pathogen inside the macrophage host cell. *Proc Natl Acad Sci U S A* **99**, 15711-15716.

Korbsrisate, S., Tomaras, A. P., Damnin, S., Ckumdee, J., Srinon, V., Lengwehasatit, I., Vasil, M. L. & Suparak, S. (2007). Characterization of two distinct phospholipase C enzymes from *Burkholderia pseudomallei*. *Microbiology* **153**, 1907-1915.

Kozmin, S. G., Leroy, P., Pavlov, Y. I. & Schaaper, R. M. (2008). YcbX and YiiM, two novel determinants for resistance of *Escherichia coli* to N-hydroxylated base analogues. *Mol Microbiol* **68**, 51-65.

Krogh, A., Larsson, B., von Heijne, G. & Sonnhammer, E. L. (2001). Predicting transmembrane protein topology with a hidden Markov model: application to complete genomes. *J Mol Biol* **305**, 567-580.

Kukimoto, M., Nishiyama, M., Murphy, M. E., Turley, S., Adman, E. T., Horinouchi, S. & Beppu, T. (1994). X-ray structure and site-directed mutagenesis of a nitrite reductase from *Alcaligenes faecalis* S-6: roles of two copper atoms in nitrite reduction. *Biochemistry* **33**, 5246-5252.

Kumar, A., Majid, M., Kunisch, R., Rani, P. S., Qureshi, I. A., Lewin, A., Hasnain, S. E. & Ahmed, N. (2012). *Mycobacterium tuberculosis* DosR regulon gene Rv0079 encodes a putative, 'dormancy associated translation inhibitor (DATIN)'. *PLoS One* **7**, e38709.

Kvitko, B. H., Goodyear, A., Propst, K. L., Dow, S. W. & Schweizer, H. P. (2012). *Burkholderia pseudomallei* known siderophores and hemin uptake are dispensable for lethal murine melioidosis. *PLoS Negl Trop Dis* **6**, e1715.

Kwan, B. W., Valenta, J. A., Benedik, M. J. & Wood, T. K. (2013). Arrested protein synthesis increases persister-like cell formation. *Antimicrob Agents Chemother* **57**, 1468-1473.

Lanciano, P., Vergnes, A., Grimaldi, S., Guigliarelli, B. & Magalon, A. (2007). Biogenesis of a respiratory complex is orchestrated by a single accessory protein. *J Biol Chem* **282**, 17468-17474.

Lee, N., Wu, J. L., Lee, C. H. & Tsai, W. C. (1985). *Pseudomonas pseudomallei* infection from drowning: the first reported case in Taiwan. *J Clin Microbiol* **22**, 352-354.

Leelarasamee, A. (1998). *Burkholderia pseudomallei*: the unbeatable foe? *Southeast Asian J Trop Med Public Health* **29**, 410-415.

Leimkuhler, S., Wuebbens, M. M. & Rajagopalan, K. V. (2011). The History of the Discovery of the Molybdenum Cofactor and Novel Aspects of its Biosynthesis in Bacteria. *Coord Chem Rev* **255**, 1129-1144.

Leistikow, R. L., Morton, R. A., Bartek, I. L., Frimpong, I., Wagner, K. & Voskuil, M. I. (2010). The *Mycobacterium tuberculosis* DosR regulon assists in metabolic homeostasis and enables rapid recovery from nonrespiring dormancy. *J Bacteriol* **192**, 1662-1670.

Lewis, K. (2010). Persister cells. *Annu Rev Microbiol* **64**, 357-372.

Liesack, W., Schnell, S. & Revsbech, N. P. (2000). Microbiology of flooded rice paddies. *FEMS Microbiol Rev* **24**, 625-645.

Limmathurotsakul, D., Chaowagul, W., Chierakul, W., Stepniewska, K., Maharjan, B., Wuthiekanun, V., White, N. J., Day, N. P. & Peacock, S. J. (2006). Risk factors for recurrent melioidosis in Northeast Thailand. *Clin Infect Dis* **43**, 979-986.

Limmathurotsakul, D., Chaowagul, W., Chantratita, N., Wuthiekanun, V., Biaklang, M., Tumapa, S., White, N. J., Day, N. P. & Peacock, S. J. (2008). A simple scoring system to differentiate between relapse and re-infection in patients with recurrent melioidosis. *PLoS Negl Trop Dis* **2**, e327.

Limmathurotsakul, D., Chaowagul, W., Day, N. P. & Peacock, S. J. (2009). Patterns of organ involvement in recurrent melioidosis. *Am J Trop Med Hyg* **81**, 335-337.

Limmathurotsakul, D., Wongratanacheewin, S., Teerawattanasook, N., Wongsuvan, G., Chaisuksant, S., Chetchotisakd, P., Chaowagul, W., Day, N. P. & Peacock, S. J. (2010).

Increasing incidence of human melioidosis in Northeast Thailand. *Am J Trop Med Hyg* **82**, 1113-1117.

Limmathurotsakul, D. & Peacock, S. J. (2011). Melioidosis: a clinical overview. *Br Med Bull* **99**, 125-139.

Limmathurotsakul, D., Dance, D. A., Wuthiekanun, V. & other authors (2013a). Systematic review and consensus guidelines for environmental sampling of *Burkholderia pseudomallei*. *PLoS Negl Trop Dis* **7**, e2105.

Limmathurotsakul, D., Kanoksil, M., Wuthiekanun, V., Kitphati, R., deStavola, B., Day, N. P. & Peacock, S. J. (2013b). Activities of daily living associated with acquisition of melioidosis in northeast Thailand: a matched case-control study. *PLoS Negl Trop Dis* **7**, e2072.

Limmathurotsakul, D., Paeyao, A., Wongratanacheewin, S. & other authors (2014a). Role of *Burkholderia pseudomallei* biofilm formation and lipopolysaccharide in relapse of melioidosis. *Clin Microbiol Infect*. *Epub ahead of print.*

Limmathurotsakul, D., Wongsuvan, G., Aanensen, D. & other authors (2014b). Melioidosis caused by *Burkholderia pseudomallei* in drinking water, Thailand, 2012. *Emerg Infect Dis* **20**, 265-268.

Lin, J. T., Goldman, B. S. & Stewart, V. (1994). The *nasFEDCBA* operon for nitrate and nitrite assimilation in *Klebsiella pneumoniae* M5al. *J Bacteriol* **176**, 2551-2559.

Lin, J. T. & Stewart, V. (1998). Nitrate assimilation by bacteria. *Adv Microb Physiol* **39**, 1-30, 379.

Lindsey, T. L., Hagins, J. M., Sokol, P. A. & Silo-Suh, L. A. (2008). Virulence determinants from a cystic fibrosis isolate of *Pseudomonas aeruginosa* include isocitrate lyase. *Microbiology* **154**, 1616-1627.

Ling, J. M., Moore, R. A., Surette, M. G. & Woods, D. E. (2006). The *mviN* homolog in *Burkholderia pseudomallei* is essential for viability and virulence. *Can J Microbiol* **52**, 831-842.

Logue, C. A., Peak, I. R. & Beacham, I. R. (2009). Facile construction of unmarked deletion mutants in *Burkholderia pseudomallei* using *sacB* counter-selection in sucrose-resistant and sucrose-sensitive isolates. *J Microbiol Methods* **76**, 320-323.

Lonetto, M. A., Rhodius, V., Lamberg, K., Kiley, P., Busby, S. & Gross, C. (1998). Identification of a contact site for different transcription activators in region 4 of the *Escherichia coli* RNA polymerase sigma70 subunit. *J Mol Biol* **284**, 1353-1365.

Lorenzi, M., Sylvi, L., Gerbaud, G. & other authors (2012). Conformational selection underlies recognition of a molybdoenzyme by its dedicated chaperone. *PLoS One* **7**, e49523.

Loschi, L., Brokx, S. J., Hills, T. L., Zhang, G., Bertero, M. G., Lovering, A. L., Weiner, J. H. & Strynadka, N. C. (2004). Structural and biochemical identification of a novel bacterial oxidoreductase. *J Biol Chem* **279**, 50391-50400.

Luidalepp, H., Joers, A., Kaldalu, N. & Tenson, T. (2011). Age of inoculum strongly influences persister frequency and can mask effects of mutations implicated in altered persistence. *J Bacteriol* **193**, 3598-3605.

Lundberg, J. O., Weitzberg, E., Cole, J. A. & Benjamin, N. (2004). Nitrate, bacteria and human health. *Nat Rev Microbiol* **2**, 593-602.

Luque-Almagro, V. M., Lyall, V. J., Ferguson, S. J., Roldan, M. D., Richardson, D. J. & Gates, A. J. (2013). Nitrogen oxyanion-dependent dissociation of a two-component complex that regulates bacterial nitrate assimilation. *J Biol Chem* **288**, 29692-29702.

Ma, Y., Guo, C., Li, H. & Peng, X. X. (2013). Low abundance of respiratory nitrate reductase is essential for *Escherichia coli* in resistance to aminoglycoside and cephalosporin. *J Proteomics* **87**, 78-88.

MacGurn, J. A. & Cox, J. S. (2007). A genetic screen for *Mycobacterium tuberculosis* mutants defective for phagosome maturation arrest identifies components of the ESX-1 secretion system. *Infect Immun* **75**, 2668-2678.

Magalon, A., Asso, M., Guigliarelli, B., Rothery, R. A., Bertrand, P., Giordano, G. & Blasco, F. (1998). Molybdenum cofactor properties and [Fe-S] cluster coordination in *Escherichia coli* nitrate reductase A: investigation by site-directed mutagenesis of the conserved His-50 residue in the NarG subunit. *Biochemistry* **37**, 7363-7370.

Magalon, A., Fedor, J. G., Walburger, A., Weiner, J. H. (2011). Molybdenum enzymes in bacteria and their maturation. *Coord Chem Rev* **255**, 1159-1178.

Maharjan, B., Chantratita, N., Vesaratchavest, M., Cheng, A., Wuthiekanun, V., Chierakul, W., Chaowagul, W., Day, N. P. & Peacock, S. J. (2005). Recurrent melioidosis in patients in northeast Thailand is frequently due to reinfection rather than relapse. *J Clin Microbiol* **43**, 6032-6034.

Malm, S., Tiffert, Y., Micklinghoff, J. & other authors (2009). The roles of the nitrate reductase NarGHJI, the nitrite reductase NirBD and the response regulator GlnR in nitrate assimilation of *Mycobacterium tuberculosis*. *Microbiology* **155**, 1332-1339.

Martin, A., Panaiotov, S., Portaels, F., Hoffner, S., Palomino, J. C. & Angeby, K. (2008). The nitrate reductase assay for the rapid detection of isoniazid and rifampicin resistance in *Mycobacterium tuberculosis*: a systematic review and meta-analysis. *J Antimicrob Chemother* **62**, 56-64.

Martinez-Espinosa, R. M., Dridge, E. J., Bonete, M. J., Butt, J. N., Butler, C. S., Sargent, F. & Richardson, D. J. (2007). Look on the positive side! The orientation, identification and bioenergetics of 'Archaeal' membrane-bound nitrate reductases. *FEMS Microbiol Lett* **276**, 129-139.

May, H. D., Patel, P. S. & Ferry, J. G. (1988). Effect of molybdenum and tungsten on synthesis and composition of formate dehydrogenase in *Methanobacterium formicicum*. *J Bacteriol* **170**, 3384-3389.

McAlpine, A. S., McEwan, A. G. & Bailey, S. (1998). The high resolution crystal structure of DMSO reductase in complex with DMSO. *J Mol Biol* **275**, 613-623.

McGuire, A. M., Weiner, B., Park, S. T. & other authors (2012). Comparative analysis of *Mycobacterium* and related *Actinomycetes* yields insight into the evolution of *Mycobacterium tuberculosis* pathogenesis. *BMC Genomics* **13**, 120.

McKinney, J. D., Honer zu Bentrup, K., Munoz-Elias, E. J. & other authors (2000). Persistence of *Mycobacterium tuberculosis* in macrophages and mice requires the glyoxylate shunt enzyme isocitrate lyase. *Nature* **406**, 735-738.

Mellies, J., Jose, J. & Meyer, T. F. (1997). The *Neisseria gonorrhoeae* gene *aniA* encodes an inducible nitrite reductase. *Mol Gen Genet* **256**, 525-532.

Mills, P. C., Rowley, G., Spiro, S., Hinton, J. C. & Richardson, D. J. (2008). A combination of cytochrome *c* nitrite reductase (NrfA) and flavorubredoxin (NorV) protects *Salmonella* enterica serovar *Typhimurium* against killing by NO in anoxic environments. *Microbiology* **154**, 1218-1228.

Minch, K., Rustad, T. & Sherman, D. R. (2012). Mycobacterium tuberculosis growth following aerobic expression of the DosR regulon. *PLoS One* **7**, e35935.

Miyagi, K., Kawakami, K. & Saito, A. (1997). Role of reactive nitrogen and oxygen intermediates in gamma interferon-stimulated murine macrophage bactericidal activity against *Burkholderia pseudomallei*. *Infect Immun* **65**, 4108-4113.

Moir, J. W. (2011a). Nitrogen Cycling in Bacteria: Molecular Analysis. First edition. Norfolk, UK. *Caister Academic Press*.

Moir, J. W. (2011b). A snapshot of a pathogenic bacterium mid-evolution: *Neisseria meningitidis* is becoming a nitric oxide-tolerant aerobe. *Biochem Soc Trans* **39**, 1890-1894.

Moore, R. A., Tuanyok, A. & Woods, D. E. (2008). Survival of *Burkholderia pseudomallei* in water. *BMC Res Notes* **1**, 11.

Moreno-Vivian, C., Cabello, P., Martinez-Luque, M., Blasco, R. & Castillo, F. (1999). Prokaryotic nitrate reduction: molecular properties and functional distinction among bacterial nitrate reductases. *J Bacteriol* **181**, 6573-6584.

Muller, C. M., Conejero, L., Spink, N., Wand, M. E., Bancroft, G. J. & Titball, R. W. (2012). Role of RelA and SpoT in *Burkholderia pseudomallei* virulence and immunity. *Infect Immun* **80**, 3247-3255.

Munoz-Elias, E. J. & McKinney, J. D. (2005). *Mycobacterium tuberculosis* isocitrate lyases 1 and 2 are jointly required for in vivo growth and virulence. *Nat Med* **11**, 638-644.

Murphy, L. M., Dodd, F. E., Yousafzai, F. K., Eady, R. R. & Hasnain, S. S. (2002). Electron donation between copper containing nitrite reductases and cupredoxins: the nature of protein-protein interaction in complex formation. *J Mol Biol* **315**, 859-871.

Murphy, M. E., Turley, S., Kukimoto, M., Nishiyama, M., Horinouchi, S., Sasaki, H., Tanokura, M. & Adman, E. T. (1995). Structure of *Alcaligenes faecalis* nitrite reductase and a copper site mutant, M150E, that contains zinc. *Biochemistry* **34**, 12107-12117.

Myers, J. D. & Kelly, D. J. (2005). A sulphite respiration system in the chemoheterotrophic human pathogen *Campylobacter jejuni*. *Microbiology* **151**, 233-242.

Nakano, M. M. & Zuber, P. (1998). Anaerobic growth of a "strict aerobe" (*Bacillus subtilis*). *Annu Rev Microbiol* **52**, 165-190.

Nealson, K. H., Moser, D. P. & Saffarini, D. A. (1995). Anaerobic electron acceptor chemotaxis in *Shewanella putrefaciens*. *Appl Environ Microbiol* **61**, 1551-1554.

Nelson, M., Dean, R. E., Salguero, F. J., Taylor, C., Pearce, P. C., Simpson, A. J. & Lever, M. S. (2011). Development of an acute model of inhalational melioidosis in the common marmoset (*Callithrix jacchus*). *Int J Exp Pathol* **92**, 428-435.

Ngauy, V., Lemeshev, Y., Sadkowski, L. & Crawford, G. (2005). Cutaneous melioidosis in a man who was taken as a prisoner of war by the Japanese during World War II. *J Clin Microbiol* **43**, 970-972.

Ngugi, S. A., Ventura, V. V., Qazi, O. & other authors (2010). Lipopolysaccharide from *Burkholderia thailandensis* E264 provides protection in a murine model of melioidosis. *Vaccine* **28**, 7551-7555.

Nichols, J. D. & Rajagopalan, K. V. (2005). *In vitro* molybdenum ligation to molybdopterin using purified components. *J Biol Chem* **280**, 7817-7822.

Nicke, T., Schnitzer, T., Munch, K. & other authors (2013). Maturation of the cytochrome cd_1 nitrite reductase NirS from *Pseudomonas aeruginosa* requires transient interactions between the three proteins NirS, NirN and NirF. *Biosci Rep* **33** (3).

Nierman, W. C., DeShazer, D., Kim, H. S. & other authors (2004). Structural flexibility in the *Burkholderia mallei* genome. *Proc Natl Acad Sci U S A* **101**, 14246-14251.

Nieves, W., Petersen, H., Judy, B. M., Blumentritt, C. A., Russell-Lodrigue, K., Roy, C. J., Torres, A. G. & Morici, L. A. (2014). A *Burkholderia pseudomallei* outer membrane vesicle vaccine provides protection against lethal sepsis. *Clin Vaccine Immunol*. *Epub ahead of print (Mar 26)*

Nishimura, T., Teramoto, H., Toyoda, K., Inui, M. & Yukawa, H. (2010). Regulation of nitrate reductase operon *narKGHJI* by cyclic AMP-dependent regulator GlxR in *Corynebacterium glutamicum. Microbiology*. **157** (Pt 1): 21-8

Nojiri, M., Xie, Y., Inoue, T. & other authors (2007). Structure and function of a hexameric copper-containing nitrite reductase. *Proc Natl Acad Sci U S A* **104**, 4315-4320.

Ooi, W. F., Ong, C., Nandi, T. & other authors (2013). The condition-dependent transcriptional landscape of *Burkholderia pseudomallei*. *PLoS Genet* **9**, e1003795.

Orman, M. A. & Brynildsen, M. P. (2013). Dormancy is not necessary or sufficient for bacterial persistence. *Antimicrob Agents Chemother* **57**, 3230-3239.

Palmer, K. L., Brown, S. A. & Whiteley, M. (2007). Membrane-bound nitrate reductase is required for anaerobic growth in cystic fibrosis sputum. *J Bacteriol* **189**, 4449-4455.

Palmer, T., Santini, C. L., Iobbi-Nivol, C., Eaves, D. J., Boxer, D. H. & Giordano, G. (1996). Involvement of the *narJ* and *mob* gene products in distinct steps in the biosynthesis of the molybdoenzyme nitrate reductase in *Escherichia coli*. *Mol Microbiol* **20**, 875-884.

Peano, C., Chiaramonte, F., Motta, S. & other authors (2014). Gene and Protein Expression in Response to Different Growth Temperatures and Oxygen Availability in *Burkholderia thailandensis*. *PLoS One* **9**, e93009.

Philippot, L. (2002). Denitrifying genes in bacterial and Archaeal genomes. *Biochim Biophys Acta* **1577**, 355-376.

Pitcher, R. S. & Watmough, N. J. (2004). The bacterial cytochrome cbb_3 oxidases. *Biochim Biophys Acta* **1655**, 388-399.

Poock, S. R., Leach, E. R., Moir, J. W., Cole, J. A. & Richardson, D. J. (2002). Respiratory detoxification of nitric oxide by the cytochrome *c* nitrite reductase of *Escherichia coli*. *J Biol Chem* **277**, 23664-23669.

Potter, L., Angove, H., Richardson, D. & Cole, J. (2001). Nitrate reduction in the periplasm of gram-negative bacteria. *Adv Microb Physiol* **45**, 51-112.

Pratt, L. A. & Kolter, R. (1998). Genetic analysis of *Escherichia coli* biofilm formation: roles of flagella, motility, chemotaxis and type I pili. *Mol Microbiol* **30**, 285-293.

Price, E. P., Sarovich, D. S., Mayo, M. & other authors (2013). Within-Host Evolution of *Burkholderia pseudomallei* over a Twelve-Year Chronic Carriage Infection. *Mbio* **4** (4):e00388-13

Prudencio, M., Eady, R. R. & Sawers, G. (1999). The blue copper-containing nitrite reductase from *Alcaligenes xylosoxidans*: cloning of the *nirA* gene and characterization of the recombinant enzyme. *J Bacteriol* **181**, 2323-2329.

Pruekprasert, P. & Jitsurong, S. (1991). Case report: septicemic melioidosis following near drowning. *Southeast Asian J Trop Med Public Health* **22**, 276-278.

Pruksachartvuthi, S., Aswapokee, N. & Thankerngpol, K. (1990). Survival of *Pseudomonas pseudomallei* in human phagocytes. *J Med Microbiol* **31**, 109-114.

Puthucheary, S. D. & Nathan, S. A. (2006). Comparison by electron microscopy of intracellular events and survival of *Burkholderia pseudomallei* in monocytes from normal subjects and patients with melioidosis. *Singapore Med J* **47**, 697-703.

Rachman, H., Strong, M., Ulrichs, T., Grode, L., Schuchhardt, J., Mollenkopf, H., Kosmiadi, G. A., Eisenberg, D. & Kaufmann, S. H. (2006). Unique transcriptome signature of *Mycobacterium tuberculosis* in pulmonary tuberculosis. *Infect Immun* **74**, 1233-1242.

Radoul, M., Barak, Y., Rinaldo, S., Cutruzzola, F., Pecht, I. & Goldfarb, D. (2012). Solvent accessibility in the distal heme pocket of the nitrosyl d_1-heme complex of *Pseudomonas stutzeri* cd_1 nitrite reductase. *Biochemistry* **51**, 9192-9201.

Rajchanuvong, A., Chaowagul, W., Suputtamongkol, Y., Smith, M. D., Dance, D. A. & White, N. J. (1995). A prospective comparison of co-amoxiclav and the combination of chloramphenicol, doxycycline, and co-trimoxazole for the oral maintenance treatment of melioidosis. *Trans R Soc Trop Med Hyg* **89**, 546-549.

Ralph, A., McBride, J. & Currie, B. J. (2004). Transmission of *Burkholderia pseudomallei* via breast milk in northern Australia. *Pediatr Infect Dis J* **23**, 1169-1171.

Ramaswamy, K. S., Endley, S. & Golden, J. W. (1996). Nitrate reductase activity and heterocyst suppression on nitrate in *Anabaena* sp. strain PCC 7120 require *moeA*. *J Bacteriol* **178**, 3893-3898.

Ratering, S. & Schnell, S. (2001). Nitrate-dependent iron(II) oxidation in paddy soil. *Environ Microbiol* **3**, 100-109.

Ray, N., Oates, J., Turner, R. J. & Robinson, C. (2003). DmsD is required for the biogenesis of DMSO reductase in Escherichia coli but not for the interaction of the DmsA signal peptide with the Tat apparatus. *FEBS Lett* **534**, 156-160.

Reckseidler, S. L., DeShazer, D., Sokol, P. A. & Woods, D. E. (2001). Detection of bacterial virulence genes by subtractive hybridization: identification of capsular polysaccharide of *Burkholderia pseudomallei* as a major virulence determinant. *Infect Immun* **69**, 34-44.

Rholl, D. A., Papp-Wallace, K. M., Tomaras, A. P., Vasil, M. L., Bonomo, R. A. & Schweizer, H. P. (2011). Molecular investigations of PenA-mediated beta-lactam resistance in *Burkholderia pseudomallei*. *Front Microbiol* **2**, 139.

Richardson, D. & Sawers, G. (2002). Structural biology. PMF through the redox loop. *Science* **295**, 1842-1843.

Richardson, D. J. (2000). Bacterial respiration: a flexible process for a changing environment. *Microbiology* **146 (Pt 3)**, 551-571.

Richardson, D. J., Berks, B. C., Russell, D. A., Spiro, S. & Taylor, C. J. (2001). Functional, biochemical and genetic diversity of prokaryotic nitrate reductases. *Cell Mol Life Sci* **58**, 165-178.

Richter, O. M. & Ludwig, B. (2009). Electron transfer and energy transduction in the terminal part of the respiratory chain - lessons from bacterial model systems. *Biochim Biophys Acta* **1787**, 626-634.

Rinaldo, S., Arcovito, A., Giardina, G., Castiglione, N., Brunori, M. & Cutruzzola, F. (2008). New insights into the activity of *Pseudomonas aeruginosa* cd_1 nitrite reductase. *Biochem Soc Trans* **36**, 1155-1159.

Robertson, J., Levy, A., Sagripanti, J. L. & Inglis, T. J. (2010). The survival of *Burkholderia pseudomallei* in liquid media. *Am J Trop Med Hyg* **82**, 88-94.

Romao, M. J., Archer, M., Moura, I., Moura, J. J., LeGall, J., Engh, R., Schneider, M., Hof, P. & Huber, R. (1995). Crystal structure of the xanthine oxidase-related aldehyde oxido-reductase from *Desulfovibrio gigas*. *Science* **270**, 1170-1176.

Rothery, R. A., Bertero, M. G., Cammack, R., Palak, M., Blasco, F., Strynadka, N. C. & Weiner, J. H. (2004). The catalytic subunit of *Escherichia coli* nitrate reductase A contains a novel [4Fe-4S] cluster with a high-spin ground state. *Biochemistry* **43**, 5324-5333.

Roychoudhury, A. N. (2004). Sulphate metabolism among thermophiles and hyperthermophiles in natural aquatic systems. *Biochem Soc Trans* **32**, 172-174.

Rustad, T. R., Harrell, M. I., Liao, R. & Sherman, D. R. (2008). The enduring hypoxic response of *Mycobacterium tuberculosis*. *PLoS One* **3**, e1502.

Rustad, T. R., Sherrid, A. M., Minch, K. J. & Sherman, D. R. (2009). Hypoxia: a window into *Mycobacterium tuberculosis* latency. *Cell Microbiol* **11**, 1151-1159.

Sambasivarao, D. & Weiner, J. H. (1991). Dimethyl sulfoxide reductase of *Escherichia coli*: an investigation of function and assembly by use of *in vivo* complementation. *J Bacteriol* **173**, 5935-5943.

Sarkar-Tyson, M., Thwaite, J. E., Harding, S. V., Smither, S. J., Oyston, P. C., Atkins, T. P. & Titball, R. W. (2007). Polysaccharides and virulence of Burkholderia pseudomallei. *J Med Microbiol* **56**, 1005-1010.

Sarkar-Tyson, M., Smither, S. J., Harding, S. V., Atkins, T. P. & Titball, R. W. (2009). Protective efficacy of heat-inactivated *B. thailandensis, B. mallei* or *B. pseudomallei* against experimental melioidosis and glanders. *Vaccine* **27**, 4447-4451.

Sarovich, D. S., Price, E. P., Limmathurotsakul, D., Cook, J. M., Von Schulze, A. T., Wolken, S. R., Keim, P., Peacock, S. J. & Pearson, T. (2012). Development of ceftazidime resistance in an acute *Burkholderia pseudomallei* infection. *Infect Drug Resist* **5**, 129-132.

Sato, N., Ishii, S., Sugimoto, H., Hino, T., Fukumori, Y., Sako, Y., Shiro, Y. & Tosha, T. (2013). Structures of reduced and ligand-bound nitric oxide reductase provide insights into functional differences in respiratory enzymes. *Proteins*. Epub ahead of print (Dec 13)

Saunders, B. M. & Britton, W. J. (2007). Life and death in the granuloma: immunopathology of tuberculosis. *Immunol Cell Biol* **85**, 103-111.

Sawasdidoln, C., Taweechaisupapong, S., Sermswan, R. W., Tattawasart, U., Tungpradabkul, S. & Wongratanacheewin, S. (2010). Growing Burkholderia pseudomallei in biofilm stimulating conditions significantly induces antimicrobial resistance. *PLoS One* **5**, e9196.

Schrag, J. D., Huang, W., Sivaraman, J., Smith, C., Plamondon, J., Larocque, R., Matte, A. & Cygler, M. (2001). The crystal structure of *Escherichia coli* MoeA, a protein from the molybdopterin synthesis pathway. *J Mol Biol* **310**, 419-431.

Schreiber, K., Krieger, R., Benkert, B., Eschbach, M., Arai, H., Schobert, M. & Jahn, D. (2007). The anaerobic regulatory network required for *Pseudomonas aeruginosa* nitrate respiration. *J Bacteriol* **189**, 4310-4314.

Schwarz, G., Mendel, R. R. & Ribbe, M. W. (2009). Molybdenum cofactors, enzymes and pathways. *Nature* **460**, 839-847.

Seefeldt, L. C., Hoffman, B. M. & Dean, D. R. (2009). Mechanism of Mo-dependent nitrogenase. *Annu Rev Biochem* **78**, 701-722.

Seki-Chiba, S. & Ishimoto, M. (1977). Studies on nitrate reductase of *Clostridium perfringens.* Purification, some properties, and effect of tungstate on its formation. *J Biochem* **82**, 1663-1671.

Sevcenco, A. M., Bevers, L. E., Pinkse, M. W., Krijger, G. C., Wolterbeek, H. T., Verhaert, P. D., Hagen, W. R. & Hagedoorn, P. L. (2010). Molybdenum incorporation in tungsten aldehyde oxidoreductase enzymes from *Pyrococcus furiosus*. *J Bacteriol* **192**, 4143-4152.

Shah, D., Zhang, Z., Khodursky, A., Kaldalu, N., Kurg, K. & Lewis, K. (2006). Persisters: a distinct physiological state of *E. coli*. *BMC Microbiol* **6**, 53.

Shewell, L. K., Ku, S. C., Schulz, B. L., Jen, F. E., Mubaiwa, T. D., Ketterer, M. R., Apicella, M. A. & Jennings, M. P. (2013). Recombinant truncated AniA of pathogenic *Neisseria* elicits a non-native immune response and functional blocking antibodies. *Biochem Biophys Res Commun* **431**, 215-220.

Silvestrini, M. C., Falcinelli, S., Ciabatti, I., Cutruzzola, F. & Brunori, M. (1994). *Pseudomonas aeruginosa* nitrite reductase (or cytochrome oxidase): an overview. *Biochimie* **76**, 641-654.

Sim, B. M., Chantratita, N., Ooi, W. F. & other authors (2010). Genomic acquisition of a capsular polysaccharide virulence cluster by non-pathogenic *Burkholderia* isolates. *Genome Biol* **11**, R89.

Simon, J. (2002). Enzymology and bioenergetics of respiratory nitrite ammonification. *FEMS Microbiol Rev* **26**, 285-309.

Simon, J., van Spanning, R. J. & Richardson, D. J. (2008). The organisation of proton motive and non-proton motive redox loops in prokaryotic respiratory systems. *Biochim Biophys Acta* **1777**, 1480-1490.

Smart, J. P., Cliff, M. J. & Kelly, D. J. (2009). A role for tungsten in the biology of *Campylobacter jejuni*: tungstate stimulates formate dehydrogenase activity and is transported

via an ultra-high affinity ABC system distinct from the molybdate transporter. *Mol Microbiol* **74**, 742-757.

Smith, M. D., Angus, B. J., Wuthiekanun, V. & White, N. J. (1997). Arabinose assimilation defines a nonvirulent biotype of *Burkholderia pseudomallei*. *Infect Immun* **65**, 4319-4321.

Sodeman, W. A., Jr. (1994). Sherlock Holmes and tropical medicine: a centennial appraisal. *Am J Trop Med Hyg* **50**, 99-101.

Sohaskey, C. D. & Wayne, L. G. (2003). Role of *narK2X* and *narGHJI* in hypoxic upregulation of nitrate reduction by *Mycobacterium tuberculosis*. *J Bacteriol* **185**, 7247-7256.

Sohaskey, C. D. (2008). Nitrate enhances the survival of *Mycobacterium tuberculosis* during inhibition of respiration. *J Bacteriol* **190**, 2981-2986.

Sonnhammer, E. L., von Heijne, G. & Krogh, A. (1998). A hidden Markov model for predicting transmembrane helices in protein sequences. *Proc Int Conf Intell Syst Mol Biol* **6**, 175-182.

Spector, M. P., Garcia del Portillo, F., Bearson, S. M., Mahmud, A., Magut, M., Finlay, B. B., Dougan, G., Foster, J. W. & Pallen, M. J. (1999). The *rpoS*-dependent starvation-stress response locus *stiA* encodes a nitrate reductase (*narZYWV*) required for carbon-starvation-inducible thermotolerance and acid tolerance in *Salmonella typhimurium*. *Microbiology* **145 (Pt 11)**, 3035-3045.

Stanley, N. R., Sargent, F., Buchanan, G., Shi, J., Stewart, V., Palmer, T. & Berks, B. C. (2002). Behaviour of topological marker proteins targeted to the Tat protein transport pathway. *Mol Microbiol* **43**, 1005-1021.

Stefanelli, P., Colotti, G., Neri, A., Salucci, M. L., Miccoli, R., Di Leandro, L. & Ippoliti, R. (2008). Molecular characterization of nitrite reductase gene (*aniA*) and gene product in *Neisseria meningitidis* isolates: Is *aniA* essential for meningococcal survival? *IUBMB Life* **60**, 629-636.

Stevens, M. P., Wood, M. W., Taylor, L. A., Monaghan, P., Hawes, P., Jones, P. W., Wallis, T. S. & Galyov, E. E. (2002). An Inv/Mxi-Spa-like type III protein secretion system in *Burkholderia pseudomallei* modulates intracellular behaviour of the pathogen. *Mol Microbiol* **46**, 649-659.

Stewart, L. J., Bailey, S., Bennett, B., Charnock, J. M., Garner, C. D. & McAlpine, A. S. (2000). Dimethylsulfoxide reductase: an enzyme capable of catalysis with either molybdenum or tungsten at the active site. *J Mol Biol* **299**, 593-600.

Stewart, V. (1993). Nitrate regulation of anaerobic respiratory gene expression in *Escherichia coli*. *Mol Microbiol* **9**, 425-434.

Stewart, V., Lu, Y. & Darwin, A. J. (2002). Periplasmic nitrate reductase (NapABC enzyme) supports anaerobic respiration by *Escherichia coli* K-12. *J Bacteriol* **184**, 1314-1323.

Stewart, V. (2003). Biochemical Society Special Lecture. Nitrate- and nitrite-responsive sensors NarX and NarQ of proteobacteria. *Biochem Soc Trans* **31**, 1-10.

Sullivan, M. J., Gates, A. J., Appia-Ayme, C., Rowley, G. & Richardson, D. J. (2013). Copper control of bacterial nitrous oxide emission and its impact on vitamin B12-dependent metabolism. *Proc Natl Acad Sci U S A* **110**, 19926-19931.

Suputtamongkol, Y., Chaowagul, W., Chetchotisakd, P. & other authors (1999). Risk factors for melioidosis and bacteremic melioidosis. *Clin Infect Dis* **29**, 408-413.

Tan, G. Y., Liu, Y., Sivalingam, S. P., Sim, S. H., Wang, D., Paucod, J. C., Gauthier, Y. & Ooi, E. E. (2008). *Burkholderia pseudomallei* aerosol infection results in differential inflammatory responses in BALB/c and C57Bl/6 mice. *J Med Microbiol* **57**, 508-515.

Tan, M. P., Sequeira, P., Lin, W. W. & other authors (2010). Nitrate respiration protects hypoxic *Mycobacterium tuberculosis* against acid and reactive nitrogen species stresses. *PLoS One* **5**, e13356.

Tang, H., Rothery, R. A., Voss, J. E. & Weiner, J. H. (2011). Correct assembly of iron-sulfur cluster FS0 into *Escherichia coli* dimethyl sulfoxide reductase (DmsABC) is a prerequisite for molybdenum cofactor insertion. *J Biol Chem* **286**, 15147-15154.

Tang, H., Rothery, R. A. & Weiner, J. H. (2013). A variant conferring cofactor-dependent assembly of *Escherichia coli* dimethylsulfoxide reductase. *Biochim Biophys Acta* **1827**, 730-737.

Tareen, A. M., Dasti, J. I., Zautner, A. E., Gross, U. & Lugert, R. (2011). Sulphite: cytochrome *c* oxidoreductase deficiency in *Campylobacter jejuni* reduces motility, host cell adherence and invasion. *Microbiology* **157**, 1776-1785.

Tavares, P., Pereira, A. S., Moura, J. J. & Moura, I. (2006). Metalloenzymes of the denitrification pathway. *J Inorg Biochem* **100**, 2087-2100.

Taweechaisupapong, S., Kaewpa, C., Arunyanart, C., Kanla, P., Homchampa, P., Sirisinha, S., Proungvitaya, T. & Wongratanacheewin, S. (2005). Virulence of *Burkholderia pseudomallei* does not correlate with biofilm formation. *Microb Pathog* **39**, 77-85.

Taylor, B. L., Miller, J. B., Warrick, H. M. & Koshland, D. E., Jr. (1979). Electron acceptor taxis and blue light effect on bacterial chemotaxis. *J Bacteriol* **140**, 567-573.

Taylor, B. L. & Zhulin, I. B. (1999). PAS domains: internal sensors of oxygen, redox potential, and light. *Microbiol Mol Biol Rev* **63**, 479-506.

Teixido, L., Cortes, P., Bigas, A., Alvarez, G., Barbe, J. & Campoy, S. (2010). Control by Fur of the nitrate respiration regulators NarP and NarL in *Salmonella enterica*. *Int Microbiol* **13**, 33-39.

ter Beek, J., Krause, N., Reimann, J., Lachmann, P. & Adelroth, P. (2013). The nitric-oxide reductase from *Paracoccus denitrificans* uses a single specific proton pathway. *J Biol Chem* **288**, 30626-30635.

Timkovich, R., Dhesi, R., Martinkus, K. J., Robinson, M. K. & Rea, T. M. (1982). Isolation of *Paracoccus denitrificans* cytochrome cd_1: comparative kinetics with other nitrite reductases. *Arch Biochem Biophys* **215**, 47-58.

Tirumalai, P. S., Prakash, S., (2012). Time-dependent gene expression pattern of *Listeria monocytogenes* J0161 in biofilms. *Adv Genomics Genet* **2**, 1-18.

Titball, R. W., Russell, P., Cuccui, J. & other authors (2008). *Burkholderia pseudomallei*: animal models of infection. *Trans R Soc Trop Med Hyg* **102 Suppl 1**, S111-116.

Toyofuku, M., Nomura, N., Fujii, T., Takaya, N., Maseda, H., Sawada, I., Nakajima, T. & Uchiyama, H. (2007). Quorum sensing regulates denitrification in *Pseudomonas aeruginosa* PAO1. *J Bacteriol* **189**, 4969-4972.

Toyofuku, M., Nomura, N., Kuno, E., Tashiro, Y., Nakajima, T. & Uchiyama, H. (2008). Influence of the *Pseudomonas* quinolone signal on denitrification in *Pseudomonas aeruginosa*. *J Bacteriol* **190**, 7947-7956.

Tribuddharat, C., Moore, R. A., Baker, P. & Woods, D. E. (2003). *Burkholderia pseudomallei* class a beta-lactamase mutations that confer selective resistance against ceftazidime or clavulanic acid inhibition. *Antimicrob Agents Chemother* **47**, 2082-2087.

Trunk, K., Benkert, B., Quack, N. & other authors (2010). Anaerobic adaptation in *Pseudomonas aeruginosa*: definition of the Anr and Dnr regulons. *Environ Microbiol* **12**, 1719-1733.

Tsai, M. C., Chakravarty, S., Zhu, G., Xu, J., Tanaka, K., Koch, C., Tufariello, J., Flynn, J. & Chan, J. (2006). Characterization of the tuberculous granuloma in murine and human lungs: cellular composition and relative tissue oxygen tension. *Cell Microbiol* **8**, 218-232.

Tsuda, A., Ishikawa, R., Koteishi, H., Tange, K., Fukuda, Y., Kobayashi, K., Inoue, T. & Nojiri, M. (2013). Structural and mechanistic insights into the electron flow through protein for cytochrome *c*-tethering copper nitrite reductase. *J Biochem* **154**, 51-60.

Tuanyok, A., Tom, M., Dunbar, J. & Woods, D. E. (2006). Genome-wide expression analysis of *Burkholderia pseudomallei* infection in a hamster model of acute melioidosis. *Infect Immun* **74**, 5465-5476.

Ulrich, R. L., Deshazer, D., Brueggemann, E. E., Hines, H. B., Oyston, P. C. & Jeddeloh, J. A. (2004). Role of quorum sensing in the pathogenicity of *Burkholderia pseudomallei*. *J Med Microbiol* **53**, 1053-1064.

Unden, G. & Bongaerts, J. (1997). Alternative respiratory pathways of *Escherichia coli*: energetics and transcriptional regulation in response to electron acceptors. *Biochim Biophys Acta* **1320**, 217-234.

Utaisincharoen, P., Tangthawornchaikul, N., Kespichayawattana, W., Chaisuriya, P. & Sirisinha, S. (2001). *Burkholderia pseudomallei* interferes with inducible nitric oxide synthase (iNOS) production: a possible mechanism of evading macrophage killing. *Microbiol Immunol* **45**, 307-313.

Utaisincharoen, P., Anuntagool, N., Limposuwan, K., Chaisuriya, P. & Sirisinha, S. (2003). Involvement of beta interferon in enhancing inducible nitric oxide synthase production and antimicrobial activity of *Burkholderia pseudomallei*-infected macrophages. *Infect Immun* **71**, 3053-3057.

Utaisincharoen, P., Arjcharoen, S., Limposuwan, K., Tungpradabkul, S. & Sirisinha, S. (2006). *Burkholderia pseudomallei* RpoS regulates multinucleated giant cell formation and inducible nitric oxide synthase expression in mouse macrophage cell line (RAW 264.7). *Microb Pathog* **40**, 184-189.

Vadivelu, J., Puthucheary, S. D., Drasar, B. S., Dance, D. A. & Pitt, T. L. (1998). Stability of strain genotypes of *Burkholderia pseudomallei* from patients with single and recurrent episodes of melioidosis. *Trop Med Int Health* **3**, 518-521.

Valade, E., Thibault, F. M., Gauthier, Y. P., Palencia, M., Popoff, M. Y. & Vidal, D. R. (2004). The PmlI-PmlR quorum-sensing system in *Burkholderia pseudomallei* plays a key role in virulence and modulates production of the MprA protease. *J Bacteriol* **186**, 2288-2294.

Van Alst, N. E., Picardo, K. F., Iglewski, B. H. & Haidaris, C. G. (2007). Nitrate sensing and metabolism modulate motility, biofilm formation, and virulence in *Pseudomonas aeruginosa*. *Infect Immun* **75**, 3780-3790.

Van Alst, N. E., Sherrill, L. A., Iglewski, B. H. & Haidaris, C. G. (2009). Compensatory periplasmic nitrate reductase activity supports anaerobic growth of *Pseudomonas aeruginosa* PAO1 in the absence of membrane nitrate reductase. *Can J Microbiol* **55**, 1133-1144.

Van Schaik, E. J., Tom, M. & Woods, D. E. (2009). Burkholderia pseudomallei isocitrate lyase is a persistence factor in pulmonary melioidosis: implications for the development of isocitrate lyase inhibitors as novel antimicrobials. *Infect Immun* **77**, 4275-4283.

Van Zandt, K. E., Tuanyok, A., Keim, P. S., Warren, R. L. & Gelhaus, H. C. (2012). An objective approach for *Burkholderia pseudomallei* strain selection as challenge material for medical countermeasures efficacy testing. *Front Cell Infect Microbiol* **2**, 120.

Vergnes, A., Gouffi-Belhabich, K., Blasco, F., Giordano, G. & Magalon, A. (2004). Involvement of the molybdenum cofactor biosynthetic machinery in the maturation of the *Escherichia coli* nitrate reductase A. *J Biol Chem* **279**, 41398-41403.

Vergnes, A., Pommier, J., Toci, R., Blasco, F., Giordano, G. & Magalon, A. (2006). NarJ chaperone binds on two distinct sites of the aponitrate reductase of *Escherichia coli* to coordinate molybdenum cofactor insertion and assembly. *J Biol Chem* **281**, 2170-2176.

Via, L. E., Lin, P. L., Ray, S. M. & other authors (2008). Tuberculous granulomas are hypoxic in guinea pigs, rabbits, and nonhuman primates. *Infect Immun* **76**, 2333-2340.

Vidyalakshmi, K., Chakrapani, M., Shrikala, B., Damodar, S., Lipika, S. & Vishal, S. (2008). Tuberculosis mimicked by melioidosis. *Int J Tuberc Lung Dis ISO* **12**, 1209-1215.

Voskuil, M. I., Schnappinger, D., Visconti, K. C., Harrell, M. I., Dolganov, G. M., Sherman, D. R. & Schoolnik, G. K. (2003). Inhibition of respiration by nitric oxide induces a *Mycobacterium tuberculosis* dormancy program. *J Exp Med* **198**, 705-713.

Wagley, S., Hemsley, C., Thomas, R. & other authors (2013). The twin arginine translocation system is essential for aerobic growth and full virulence of *Burkholderia thailandensis*. *J Bacteriol*. **196** (2): 407-416

Wand, M. E., Muller, C. M., Titball, R. W. & Michell, S. L. (2010). Macrophage and *Galleria mellonella* infection models reflect the virulence of naturally occurring isolates of *B. pseudomallei, B. thailandensis* and *B. oklahomensis*. *BMC Microbiol* **11**, 11.

Warawa, J. & Woods, D. E. (2005). Type III secretion system cluster 3 is required for maximal virulence of *Burkholderia pseudomallei* in a hamster infection model. *FEMS Microbiol Lett* **242**, 101-108.

Warawa, J. M., Long, D., Rosenke, R., Gardner, D. & Gherardini, F. C. (2009). Role for the *Burkholderia pseudomallei* capsular polysaccharide encoded by the *wcb* operon in acute disseminated melioidosis. *Infect Immun* **77**, 5252-5261.

Ward, S. M., Delgado, A., Gunsalus, R. P. & Manson, M. D. (2002). A NarX-Tar chimera mediates repellent chemotaxis to nitrate and nitrite. *Mol Microbiol* **44**, 709-719.

Watmough, N. J., Field, S. J., Hughes, R. J. & Richardson, D. J. (2009). The bacterial respiratory nitric oxide reductase. *Biochem Soc Trans* **37**, 392-399.

Wayne, L. G. & Hayes, L. G. (1996). An in vitro model for sequential study of shiftdown of *Mycobacterium tuberculosis* through two stages of nonreplicating persistence. *Infect Immun* **64**, 2062-2069.

Wayne, L. G. & Hayes, L. G. (1998). Nitrate reduction as a marker for hypoxic shiftdown of *Mycobacterium tuberculosis*. *Tuber Lung Dis* **79**, 127-132.

Weber, I., Fritz, C., Ruttkowski, S., Kreft, A. & Bange, F. C. (2000). Anaerobic nitrate reductase (*narGHJI*) activity of *Mycobacterium bovis* BCG in vitro and its contribution to virulence in immunodeficient mice. *Mol Microbiol* **35**, 1017-1025.

Weiner, J. H., Rothery, R. A., Sambasivarao, D. & Trieber, C. A. (1992). Molecular analysis of dimethylsulfoxide reductase: a complex iron-sulfur molybdoenzyme of *Escherichia coli*. *Biochim Biophys Acta* **1102**, 1-18.

West, T. E., Frevert, C. W., Liggitt, H. D. & Skerrett, S. J. (2008). Inhalation of *Burkholderia thailandensis* results in lethal necrotizing pneumonia in mice: a surrogate model for pneumonic melioidosis. *Trans R Soc Trop Med Hyg* **102 Suppl 1**, S119-126.

White, N. J. (2003). Melioidosis. *Lancet* **361**, 1715-1722.

Whitehead, R. N. & Cole, J. A. (2006). Different responses to nitrate and nitrite by the model organism *Escherichia coli* and the human pathogen *Neisseria gonorrhoeae*. *Biochem Soc Trans* **34**, 111-114.

Whitmore A, K. C. (1912). An account of the discovery of a hitherto undescribed infective disease occurring among the population of Rangoon. *Indian Med Gaz* **92**.

Wiersinga, W. J., van der Poll, T., White, N. J., Day, N. P. & Peacock, S. J. (2006). Melioidosis: insights into the pathogenicity of *Burkholderia pseudomallei*. *Nat Rev Microbiol* **4**, 272-282.

Wiersinga, W. J., Wieland, C. W., Dessing, M. C. & other authors (2007). Toll-like receptor 2 impairs host defense in gram-negative sepsis caused by Burkholderia pseudomallei (Melioidosis). *PLoS Med* **4**, e248.

Wiersinga, W. J., Wieland, C. W., Roelofs, J. J. & Van der Poll, T. (2008). MyD88 dependent signaling contributes to protective host defense against *Burkholderia pseudomallei*. *PLoS One* **3**, e3494.

Wiersinga, W. J., Currie, B. J. & Peacock, S. J. (2012). Melioidosis. *N Engl J Med* **367**, 1035-1044.

Wikraiphat, C., Charoensap, J., Utaisincharoen, P., Wongratanacheewin, S., Taweechaisupapong, S., Woods, D. E., Bolscher, J. G. & Sirisinha, S. (2009). Comparative *in vivo* and *in vitro* analyses of putative virulence factors of *Burkholderia pseudomallei* using lipopolysaccharide, capsule and flagellin mutants. *FEMS Immunol Med Microbiol* **56**, 253-259.

Williams, M. J., Kana, B. D. & Mizrahi, V. (2011). Functional Analysis of Molybdopterin Biosynthesis in Mycobacteria Identifies a Fused Molybdopterin Synthase in *Mycobacterium tuberculosis*. *J Bacteriol* **193**, 98-106.

Winsor, G. L., Khaira, B., Van Rossum, T., Lo, R., Whiteside, M. D. & Brinkman, F. S. (2008). The *Burkholderia* Genome Database: facilitating flexible queries and comparative analyses. *Bioinformatics* **24**, 2803-2804.

Winstone, T. M., Tran, V. A. & Turner, R. J. (2013). The hydrophobic region of the DmsA twin-arginine leader peptide determines specificity with chaperone DmsD. *Biochemistry* **52**, 7532-7541.

Woodman, M. E., Worth, R. G. & Wooten, R. M. (2012). Capsule influences the deposition of critical complement C3 levels required for the killing of *Burkholderia pseudomallei* via NADPH-oxidase induction by human neutrophils. *PLoS One* **7**, e52276.

Wuebbens, M. M. & Rajagopalan, K. V. (2003). Mechanistic and mutational studies of *Escherichia coli* molybdopterin synthase clarify the final step of molybdopterin biosynthesis. *J Biol Chem* **278**, 14523-14532.

Xi, H., Schneider, B. L. & Reitzer, L. (2000). Purine catabolism in *Escherichia coli* and function of xanthine dehydrogenase in purine salvage. *J Bacteriol* **182**, 5332-5341.

Yang, H., Kooi, C. D. & Sokol, P. A. (1993). Ability of *Pseudomonas pseudomallei* malleobactin to acquire transferrin-bound, lactoferrin-bound, and cell-derived iron. *Infect Immun* **61**, 656-662.

Zakian, S., Lafitte, D., Vergnes, A., Pimentel, C., Sebban-Kreuzer, C., Toci, R., Claude, J. B., Guerlesquin, F. & Magalon, A. (2010). Basis of recognition between the NarJ chaperone and the N-terminus of the NarG subunit from *Escherichia coli* nitrate reductase. *FEBS J* **277**, 1886-1895.

Zhang, Y. (2008). I-TASSER server for protein 3D structure prediction. *BMC Bioinformatics* **9**, 40.

Zheng, H., Wisedchaisri, G. & Gonen, T. (2013). Crystal structure of a nitrate/nitrite exchanger. *Nature* **497**, 647-651.

Zumft, W. G., Viebrock-Sambale, A. & Braun, C. (1990). Nitrous oxide reductase from denitrifying *Pseudomonas stutzeri*. Genes for copper-processing and properties of the deduced products, including a new member of the family of ATP/GTP-binding proteins. *Eur J Biochem* **192**, 591-599.

Zumft, W. G. (2005). Biogenesis of the bacterial respiratory CuA, Cu-S enzyme nitrous oxide reductase. *J Mol Microbiol Biotechnol* **10**, 154-166.